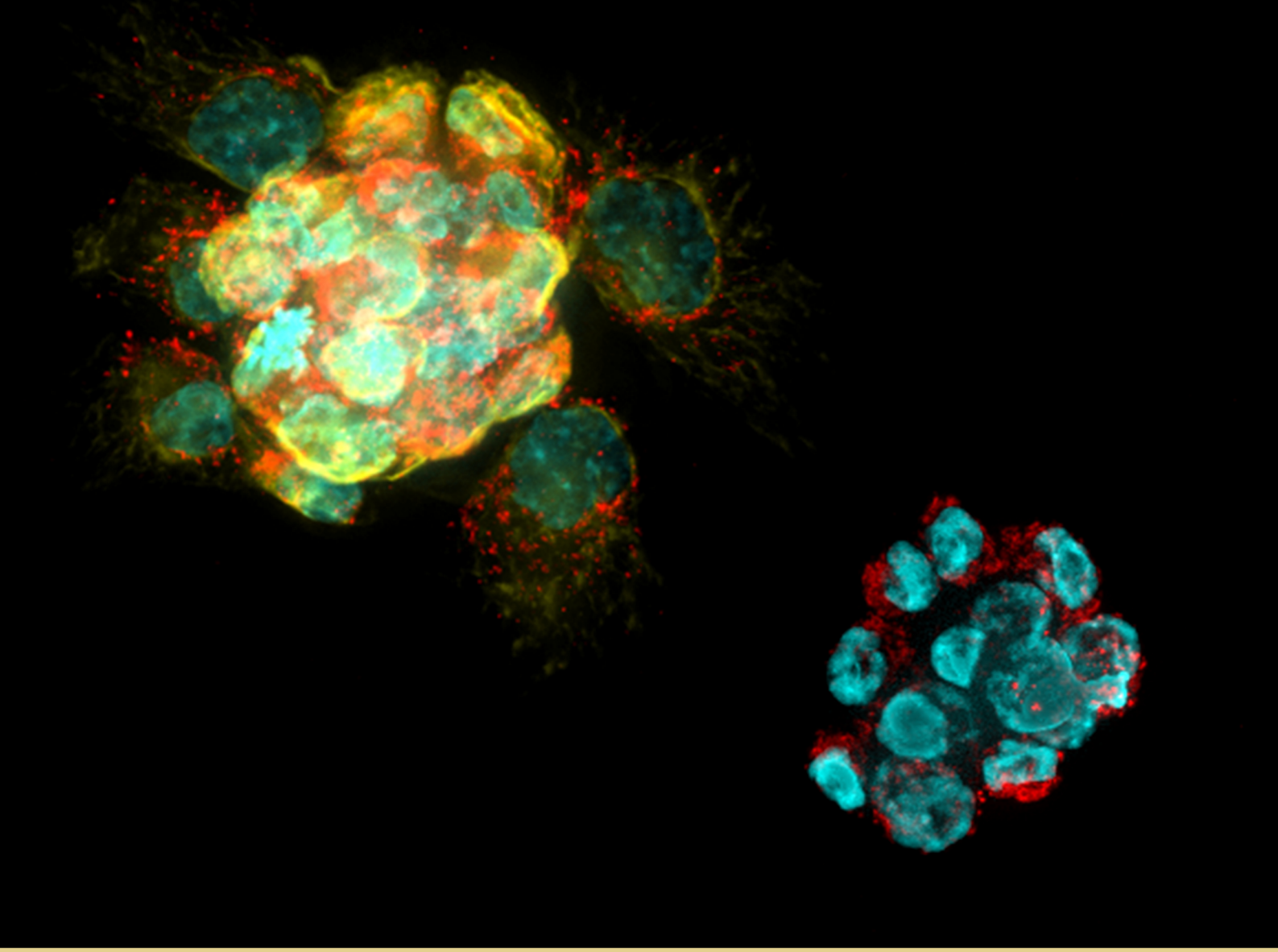

Joana Balça Pinheiro da Costa e Silva

Molecular Mechanisms Of Glioblastoma Resistance: Glioma Stem-Like And Non-Stem-Like Cells Specific Targets

Doctoral Thesis of the Inter-University Doctoral Program in Aging and Chronic Diseases,
supervised by Professor Doctor Maria Celeste Fernandes Lopes, Professor Doctor Ana Bela Sarmento Antunes Cruz Ribeiro
and Professor Doctor Vivaldo Moura Neto, and presented to the Faculty of Medicine of the University of Coimbra

August 2017

· U C ·

Universidade de Coimbra

Joana Balça Pinheiro da Costa e Silva

Molecular Mechanisms Of Glioblastoma Resistance: Glioma Stem-Like And Non-Stem-Like Cells Specific Targets

Doctoral Thesis of the Inter-University Doctoral Program in Aging and Chronic Diseases, supervised by Professor Doctor Maria Celeste Fernandes Lopes, Professor Doctor Ana Bela Sarmento Antunes Cruz Ribeiro and Professor Doctor Vivaldo Moura Neto, and presented to the Faculty of Medicine of the University of Coimbra

August 2017

· U C ·

UNIVERSIDADE DE COIMBRA

Cover:
Immunofluorescence staining of Cx46 (red), vimentin (yellow) and dapi (cyan) in the serum-free GBM cells (OB1-SF), using a DMi8 advanced fluorescence microscope (Leica Microsystems, Germany) equipped with a 63x oil-immersion objective.

INSTITUTIONS AND FUNDING

This work was conducted at the Faculty of Medicine, University of Coimbra, Portugal and at the Instituto Estadual do Cérebro Paulo Niemeyer (IECPN) - Secretaria de Estado de Saúde, Rio de Janeiro, Brazil.

The presented work was supported by PhD fellowship (SFRH / BD / 51993 / 2012) from the Portuguese Foundation for Science and Technology (FCT) awarded to the author; and by the project PEst-C/SAU/LA0001/2013-2014. Adicional funding was granted by FEDER/COMPETE/ FCT PTDC/EBB-EBI/120634/2010 and PDTC/QUI-BIQ/120652/2010; by the Conselho Nacional de Desenvolvimento Tecnológico (CNPq), Brazil, Coordenação de Aperfeiçoamento de Pessoal de Nível Superior (CAPES), Brazil, Fundação Carlos Chagas Filho de Amparo à Pesquisa do Estado do Rio de Janeiro (FAPERJ) and Pró-Saúde - Associação Beneficente de Assistência Social e Hospitalar, Brazil.

The research work presented in this thesis involved the following institutions:

PUBLICATIONS

Part of the results presented in this dissertation have been published in international peer-reviewed scientific journals:

- Original articles –

Joana, Balça-Silva; Diana, Matias; Anália, do Carmo; Henrique, Girão; Vivaldo, Moura-Neto; Ana Bela, Sarmento-Ribeiro; Maria Celeste, Lopes. 2015. Tamoxifen in combination with temozolomide induce a synergistic inhibition of PKC-pan in GBM cell lines. *Biochimica et Biophysica Acta (BBA) - General Subjects*. 1850 (4), 722-732. doi:10.1016/j.bbagen.2014.12.022;

Joana, Balça-Silva; Diana, Matias; Anália, do Carmo; Luiz Gustavo, Dubois; Ana Cristina, Gonçalves; Henrique, Girão; Nathalie Henriques, Silva Canedo; Ana Helena, Correia; Jorge, Marcondes de Souza; Ana Bela, Sarmento-Ribeiro; Maria Celeste, Lopes; Vivaldo, Moura Neto. 2017. Glioblastoma entities express subtle differences in molecular composition and response to treatment. *Oncology Reports*. 38 (3), 1341-1352. doi: 10.3892/or.2017.5799;

Joana, Balça-Silva; Diana, Matias; Luiz Gustavo, Dubois; Brenno, Carneiro; Anália, do Carmo; Henrique, Girão; Fernanda, Ferreira; Valéria, Pereira Ferrer; Leila, Chimelli; Paulo, Niemeyer Filho; Hermínio, Tão; Olinda, Rebelo; Marcos, Barbosa; Ana Bela, Sarmento-Ribeiro; Maria Celeste, Lopes; Vivaldo, Moura-Neto. 2017. The expression of connexins and SOX2 reflects the plasticity of glioma stem-like cells. *Translational Oncology*. 10 (4), 555-569. doi:10.1016/j.tranon.2017.04.005.

- Abstracts -

Joana, Balça-Silva; Diana, Matias; Anália, do Carmo; Ana Bela, Sarmento-Ribeiro; Maria Celeste, Lopes. 2012. Evaluation of the role of temozolomide on glioma cell line. In: 1º congresso do CIMAGO, Coimbra. *Suplemento da Acta Médica Portuguesa*. 18-18. (Abstract).

Joana, Balça-Silva; Diana, Matias; Anália, do Carmo; Ana Bela, Sarmento-Ribeiro; Maria Celeste, Lopes. 2013. PKC as therapeutic target in glioblastoma. In: European Cancer Congress, Amsterdam. *European Journal of Cancer*. Elsevier. 49, S130-S130. doi:10.1016/S0959-8049(13)70060-1 (Abstract);

Joana, Balça-Silva; Anália, do Carmo; Ana Bela, Sarmento-Ribeiro; Vivaldo, Moura-Neto; Maria Celeste, Lopes; João Nuno, Moreira. 2016. Nucleolin overexpression in glioblastoma stem-like cells enables targeted intracellular delivery and improves cytotoxicity. In: 41st FEBS Congress, Molecular and Systems Biology for a Better Life, At Ephesus/Kuşadasi, Turkey. *The FEBS Journal*. 283 (Suppl. 1), 129–417. doi: 10.1111/febs.2016.283.issue-S1 (Abstract).

Note: The results presented in this dissertation, included in Chapter 3, 4, and 5 are formatted according to the style of the journal where the papers were published, with minor modifications. The chapter 6 of this dissertation is formatted according to the style of the journal where the manuscript will be submitted.

The following publications in international peer-reviewed scientific journals were also published under the scope of the present dissertation:

- Original articles –

Diana, Matias; **Joana, Balça-Silva**; Luiz Gustavo, Dubois; Bruno, Pontes; Valéria, Pereira Ferrer; Luciane, Rosário; Anália, do Carmo; Juliana, Echevarria-Lima; Ana Bela, Sarmento-Ribeiro; Maria Celeste, Lopes; Vivaldo, Moura-Neto. 2017. Dual treatment with shikonin and temozolomide reduces glioblastoma tumor growth, migration and epithelial-mesenchymal transition. *Cellular Oncology*. 40 (3), 247-261. doi: 10.1007/s13402-017-0320-1

- Review Articles -

Anália, do Carmo; **Joana, Balça-Silva**; Diana, Matias; Maria Celeste, Lopes. PKC signalling in glioblastoma. 2014. *Cancer Biology & Therapy*. 14 (4), 287-294. doi:10.4161/cbt.23615;

Luiz Gustavo, Dubois; Loraine, Campanati; Cassia, Righy; Isabella, D'Andrea-Meira; Tania Cristina, Leite de Sampaio E Spohr; Isabel, Porto-Carreiro; Cláudia, Maria Pereira; **Joana, Balça-Silva**; Suzana, Assad Kahn; Marcos, F. Dos Santos; Marcela, de Almeida Rabello Oliveira; Adriana, Ximenes-da-Silva; Maria Celeste, Lopes; Eduardo, Faveret; Emerson, Gasparetto; Vivaldo, Moura-Neto. 2014. Gliomas and the vascular fragility of the blood brain barrier. *Frontiers in Cellular Neuroscience.* 8 (418), 1-13. doi:10.3389/fncel.2014.00418.

- Chapters from Book -

Vivaldo, Moura-Neto; Loraine, Campanati; Diana, Matias; Claudia Maria, Pereira; Catarina; Freitas; Juliana M, Coelho-Aguiar; Tania Cristina, Leite de Sampaio e Spohr; Ana Lucia, Tavares-Gomes; Diego, Pinheiro-Aguiar; Suzana Assad, Kahn; **Joana, Silva-Balça**; Bruno, Pontes; Isabel, Porto-Carreiro; Jane, Faria; Rodrigo Alves Portela, Martins; Sílvia, Lima-Costa; Maria de Fátima, Dias-Costa; Maria Celeste, Lopes; Flavia Regina, Souza Lima. 2014. In book: Glioma Cell Biology. Chapter II: *Glioblastomas and the Special Role of Adhesion Molecules in Their Invasion*. Publisher: Springer Vienna. Editors: Aleksi Sedo, Rolf Mentlein. 293-315. doi:10.1007/978-3-7091-1431-5_11

Juliana, de Mattos Coelho-Aguiar; Felipe Andreiuolo; Henrike, Gebhardt; Luiz Henrique, Geraldo; Bruno, Pontes; Diana Isabel, Lourenço Matias; **Joana, Balça-Silva**; Diego, Pinheiro Aguiar; Anália, do Carmo; Maria Celeste, Lopes; Rolf, Mentlein; Vivaldo, Moura-Neto. 2015. In book: The Cytoskeleton in Health and Disease. Chapter: 4: *The Role of the Cytoskeleton in Cell Migration, Its Influence on Stem Cells and the Special Role of GFAP in Glial Functions*. Publisher: Springer. Editors: Heide Schatten. 87-119. doi:10.1007/978-1-4939-2904-7.

"One thing I have learned in a long life: That all our science, measured against reality, is primitive and childlike — and yet it is the most precious thing we have."

Albert Einstein

ACKNOWLEDGMENTS

To Professor Maria Celeste, thank you very much. Thank you for concern, for caring, for the presence. Thank you for reminding me that the road, no matter how hard it may be, is ahead. Thank you for recognizing me and accompanying along the way.

To Professor Ana Bela, thank you very much. Thank you for the patience, for the scientific rigor and respect. Thank you for having accompanied me over the years and a few more before that with commitment and concern.

To Professor Vivaldo, thank you very much. Thank you for your sincerity, for the scientific and emotional teaching. Thank you for receiving me with open arms on the other side of the ocean and always made me feel like I've never been away from home. Thank you for believe in me. Thank you for the unforgettable opportunity to listen to you and, above all, thank you for provoking me: defying me, as science does every day.

To Analia, thank you very much. Thank you for the immensity of time, the answers, the understanding, the questions and even the hesitations. Thank you for teaching, for the wonderful example and for caring. There are people who inspire us and make us believe that it is possible, is not it? ... Thank you for that legacy…

To Professor João Nuno Moreira and to the whole group, thank you very much. Thank you for the opportunity to work in your group, challenging me to risk learning outside my comfort zone, persisting and insisting.

To Professor Henrique Girão, thank you very much. Thank you for the complicity, for the recognition, for teaching me along the way. Thank you for believing that I have something similar to what is expected. Thank you for applauding every little step of mine along these years.

To Professor Marcos Barbosa, Dr. Olinda Rebelo and Dr. Hermínio Tão, thank you very much. Thank you for the constancy and opportunity, for believing and arguing, for questioning and contributing, and for teaching me along the way.

To Professor Paulo Niemeyer Filho, thank you very much. Thank you for receiving me in Instituto Estadual do Cérebro, Rio de Janeiro. Thank you for the support and the amazing opportunity.

To Professor Leila Chimelli, thank you very much. Thank you for listen, for teach me, for patiently answer. Thank you for the amazing opportunity to listen to you.

To Diana, my partner in science, and to Gustavo, my scientific inspiration, thank you very much. Thank you both for making me laugh, cry, and look upward over and over again. Thank you for provoking, hearing and believing in me. Thank you for being there: from morning to night ..., for those endless hours around a small believe that I bring with pride, today. Thank you for the complicity and the smile. Thank you for making far so close. Although nothing worthwhile is easy to have, Rio de Janeiro would have a world of stories to tell if he could. Either way, I'll bring them all; for life... Thank you both for that immensity.

To Isabel Nunes, thank you very much. Thank you for your patience, for sincerity and certainty and for the persistence. Thank you for the time thinking of science by my side.

To those who walked alongside the course with more or less similar objectives, more or less parallel courses, and more or less the same wishes, thank you very much: Vanessa, Mafalda, Cátia, Raquel, Cristina, Joana Crisóstomo, Margarida, Mónica, Isabel, Joana Liberal, Ana Rufino, Ana Silva, 'Joãos', Bruno, Madalena, Susana, Carla, Joana Verdasca, Tânia, Teresa, Steve and Carla. Also to those that are around the world and still made it count for my course: Ana Silva, Diogo, Inês, Mariana, Joana Santos, and Susana. Thank you all for the understanding, for complicity, for friendship, for those words, for laugh and, above all, for the particular moments. Thank you for making me feel in the right place at the right time with the right purpose.

To those scientists who walked beside me on the other side of the ocean, thank you very much: Tânia, Ana Bon, Lucy, Bruno, Brenno, Geralda, Juliana, Valéria, Anna, Luciana and Claúdia. Thank you for making me feel at home and, as they say of the wonderful city, to have welcomed me with open arms and with a so characteristic warm smile…

…And thank you to those who are part of a world of mine that I will not enumerate here for the certainty of having guaranteed that they received my smile along the way, along the step, in the exact moment, during life, in each measure for each one. From family to friends, to the special people in my life and to the countless pieces of me that I'm making a point of leaving marked. To those who know how to identify themselves when they read this paragraph. To those who, lucky enough to be more but not too much, know me by heart. And to those who take a little of me and who, without a doubt, made me Be. Thank you for the fullness and the sensible design of a simple strategy until today.

Still, in particular, because it would not make sense otherwise, to Mana. Thank you for being my person. Thank you for the immensity of the course you do because you are and you must be. Thank you for the certainty, for the wisdom of the trick that life made you and for inspiring me every step of the way. Thank you for the unequaled complicity; the unforgettable determination; for the incomparable sense of knowing me, without which I would certainty not be writing the final paragraphs of this work today. Thank you for that infinity…

TABLE OF CONTENTS

ABBREVIATIONS

A

ABC ATP-binding cassette
ATCC American Type Culture Collection
ATP Adenosine Triphosphate
ATRX alpha-thalassemia/mental retardation syndrome X-linked
AV Annexin V

B

BBB blood-brain barrier
BBBD blood brain barrier disruption
BBTB blood–brain tumor barrier
BCRP breast cancer-resistance protein

C

CNS central nervous system
CDKN2B cyclin-dependent kinase inhibitor 2B
CHECK2 checkpoint kinase 2 gene
CT Computed tomography
CSF cerebrospinal fluid
CP choroid plexus
CDKN2A cyclin-dependent kinase inhibitor 2A
CDK cyclin D-dependent protein kinases
CCC cation-chloride co-transporter
CSCs Cancer stem-like cells
Cer ceramides
CHEMS cholesteryl hemisuccinate
Cx connexin

D

DAB diaminobenzidine
DAG diacylglycerol
DMSO Dimethyl sulfoxide
DNEM Dulbecco's modified Eagle's medium
DOPE fusogenic lipid 1,2-dioleoyl-sn-glycero-3-phosphoethanol-amine
DXR doxorubicin

E

EBRT External Beam Radiation Therapy
ECM external cellular matrix
ECs endothelial cells
EdU 5-ethynyl-2'-deoxyuridine
EGF endothelial growth factor
EGFR epidermal growth factor receptor
EMT epithelial-mesenchymal transition
EPR permeability and retention effect
ER estrogen receptor
ERK extracellular signal-regulated kinase
ESCs embryonic stem cells
EZT Enzastaurin

F

FAKs focal adhesion kinases
FBS fetal bovine serum
FDA Food and Drug Administration
FGF basic fibroblast growth factor
FITC Fluorescein isothiocyanate
FLAIR fluid-attenuated inversion recovery

G

GBM Glioblastoma
GBM-SF Glioblastoma-serum free
Gd gadolinium
GFAP glial fibrillary acidic protein
GSCs glioma stem-like cells

H

H&E Haematoxylin-eosin staining
HD-CTx high-dose chemotherapy

I

IC50 half maximal inhibitory concentration (50%)
ICGJ intercellular communication through gap junctions
ICP intracranial pressure
IDH Isocitrate dehydrogenase
IF immunofluorescence

J

JAK janus kinase

K

KPS Karnofsky Performance Scale

L

L1CAM L1 cell-adhesion molecule

LOH loss of heterozygosity

LUV large unilamellar vesicles

M

MAPK Mitogen activated-protein kinase

MAPK mitogen-activated protein kinase

MDR multidrug resistance–associated protein

MGMT *O*6-methylguanine DNA methyltransferase

MLV multilamellar vesicles

MRI magnetic resonance imaging

MRP multi-drug-resistance protein

MTIC (5-(3-dimethyl-1-triazenyl) imidazole-4-carboxamide)

MTT 3-(4,5-dimethylthiazol-2-yl)-2,5-diphenyl tetrazolium bromide

N

NANOG homeobox

NCL nucleolin

NHE-1 sodium-hydrogen exchanger isoform 1

NKCC-1 sodium-potassium-chloride co-transporter isoform 1

NOS nitric-oxide synthase

NS Non-sense

NS34 supplemented neurobasal medium

NSCs Normal stem cells

NT non-targeted

Non-SCCs non-stem cancer cells

P

PBS Phosphate Buffered Saline

PEG Poly(ethyleneglycol)

PET Positron Emission Tomography

PFA paraformaldehyde

PFS progression-free survival

PGP P-glycoprotein

PI propidium iodide

PI3K phosphatidynositol-4,5-biphosphate-3-kinase

PI3K/AKT Phosphatidylinositol-4,5-bisphosphate 3-kinase/ Protein kinase B

PIP3 phosphatidynositol-3-phosphate

PKC protein kinase C

PLCg phospholipase Cg

PLGA biodegradable copolymer polylactic-coglycolic acid

Q

qPCR quantitative Polymerase Chain Reaction

R

RB Retinoblastoma

RB1 retinoblastoma protein 1

ROS reactive oxygen species

RT Radiation Therapy

RTKs receptor tyrosine kinases

RTemp Room Temperature

RTOG Radiation Therapy Oncology Group

S

SES socioeconomic status
SF serum-free
SHH Sonic hedgehog
SLpH sterically stabilized pH-sensitive liposome
SOX2 sex-determining regions Y-Box
SRT Stereotactic Radiation Therapy
SSCs somatic stem cells
STAT signal transduction and transcription activator
SUV small unilamellar vesicles

T

T targeted
TBST Tris-buffered salin with tween
TERT telomerase reverse transcriptase
TGF-α transforming growth factor-α
TJs tight junctions
TKIs tyrosine kinase inhibitors
TMX tamoxifen
TMZ temozolomide
TP53 Tumor protein p53
TRAIL TNF- related apoptosis-inducing ligand

U

UV ultraviolet

V

VEGF vascular endothelial growth factor
VEGFR vascular endothelial growth factor receptor

W

WB western blot
WHO World Health Organization

LIST OF FIGURES

LIST OF TABLES

Summary

Glioblastoma (GBM) is the most malignant primary tumor of the central nervous system. Despite all efforts, the median survival time for GBM patients remains approximately between 12 to 15 months under therapy. GBM is a diffuse astrocytoma, highly proliferative, angiogenic, and locally invasive, that develops resistance to the alkylating agents used in chemotherapy, such as temozolomide (TMZ), which is considered part of the *gold standard* treatment. This limited success appears to be related with several mechanisms, namely: 1) the occurrence of gene mutations, that cause permanent activation and/or inhibition of several molecular signalling pathways involved in tumor growth and proliferation, such as protein kinase C (PKC) activation, cell survival, tumor suppressor genes and apoptosis; 2) the presence of a population of cells known to be chemo and radioresistant, the glioma stem-like cells (GSCs), that are responsible for generating tumor heterogeneity and recurrence after therapy, and; 3) the inexistence of a recognized specific therapeutic target for non-GSCs and GSCs that would permit the development of more specific therapeutic approaches for this neoplasia.

Therefore, in this work we aimed to: 1) study the PKC activation contribution to the aggressiveness of GBM, emphasizing the importance of combined therapeutic protocols, including TMZ with PKC inhibitors, namely tamoxifen (TMX); 2) characterize the GSCs and study their plasticity to understand glioma stem-like cells state and its differentiation properties, in order to contribute to the prevention of tumor recurrence; and 3) evaluate the potential of specific cell surface markers as therapeutic targets to non-GSCs and GSCs, allowing the accessibility of therapeutic agents most exclusively to the tumor niche, by a liposome-mediated drug delivery approach.

First, using two GBM cell lines, the U87 and U118 cells, we observed that the combination of TMX and TMZ alters the phosphorylation status of PKC, by western blot. We found that TMX is an inhibitor of the p-PKC and that this combination is more effective in the reduction of proliferation and in the increase of apoptosis than each drug alone, by flow cytometry, which presents a new therapeutic strategy in GBM treatment. We then

concluded that the combination of TMX and TMZ seems to potentiate the effect of each other in GBM cell lines.

In order to study the heterogeneity between GBM cells and further understand the variability in the chemotherapeutic response, we next isolated and characterized a human GBM cell line, termed GBM11, obtained by surgical biopsy from a patient bearing a recurrent GBM, and compared the effect of TMX in monotherapy and in combination with TMZ on this GBM cell line with that observed in U87 and U118 cell lines. We observed that the effect of TMX plus TMZ or with TMX alone on GBM11 cells proliferation, death or migration capability, by flow cytometry and scratch assays, was similar, suggesting that, for recurrent tumors, the best choice of second-line treatment may be TMX alone, which may also reduce putative side effects of combined treatment with TMZ.

The chemo- and radioresistance of GBM are also due to GSCs which contribute to tumor growth and relapse, highlighting this cell population as a main focus for GBM therapeutic research. We considered that the understanding of GBM stem state plasticity is of utmost importance to identify the mechanisms involved in GSCs resistance to therapy, which may justify tumor recurrence and so, constitute a step forward to the identification of new approaches to treat GBM. Our results demonstrated that, in four GBM cell lines and in the respectively GSC lines, the plasticity of the GBM stem-like cell state is based on the modulation of specific markers expression associated with this state, such as SOX2 or as Connexin 46 and 43, through immunofluorescence, western blot and PCR real time assays. Moreover, by immunohistochemistry analyses, we observed that this dynamic expression is in accordance with the upregulation of these stem-like cell markers in human samples of higher glioma grades, namely GBM, compared to lower grades, suggesting a direct correlation with the poor prognosis of GBM patients.

As so, due to the plasticity of the stem-like cells status, the strategy of targeting both GSCs and non-GSCs may represent a promising approach in order to overcome tumor aggressiveness, and eventually to avoid the known chemotherapeutic side effects, which could improve the survival time and quality of life of GBM patients.

In this regard, we next evaluate the potential of the cell surface nucleolin (NCL), described as overexpressed in cancer cells, as a target to specifically recognize non-GSCs and GSCs, taunting a possible therapeutic target for drug delivery in two different GBM cell lines. For that, we used a previously designed F3-peptide-targeted sterically stabilized

pH-sensitive liposome (SLpH), which specifically recognizes nucleolin, as a tool to target overexpressed-nucleolin cells.

Overall, we showed that NCL overexpression ensures an efficient drug delivery in both cells with stem-like and non-stem-like phenotypic characteristics, by flow cytometry assays, which could validate NCL as a potential therapeutic target in GBM.

Altogether, our results showed: 1) a synergistic effect of TMX and TMZ in GBM cell lines and a more efficient effect of TMX alone in recurrent GBM compared to the combined therapy; 2) the plasticity of stem-like cell state through the reversibility of stem-like cell markers expression, and the identification of putative markers associated with this reversibility, the SOX2 and Cx46 and 43, which constitutes a step closer to the understanding of stem cell behaviour; and 3) that the success of targeting both non-GSCs and GSCs, through the nucleolin target, may be the basis for developing a specific treatment for GBM.

Keywords: Glioblastoma; PKC activation; Cell heterogeneity; Stem-like cells plasticity; Specific target drug delivery; Resistance; Targeted therapy.

Resumo

O Glioblastoma (GBM) é o tumor primário mais maligno do sistema nervoso central. Apesar de todos os esforços, o tempo médio de sobrevivência para doentes com GBM permanece aproximadamente entre os 12 a 15 meses sob terapia. O GBM é um astrocitoma difuso, altamente proliferativo, angiogénico e localmente invasivo, que desenvolve resistência aos agentes alquilantes utilizados na quimioterapia, como a temozolomida (TMZ), que é considerada parte do tratamento padrão. Este sucesso limitado parece estar relacionado com vários mecanismos, tais como: 1) a ocorrência de mutações genéticas que causam ativação permanente e / ou inibição de várias vias de sinalização molecular envolvidas no crescimento e proliferação de tumores, como a ativação da proteína cínase C (PKC), na sobrevivência celular, na inibição de genes supressores de tumores e apoptose; 2) a presença de uma população de células conhecidas como quimio- e radiorresistentes, as células de glioma do tipo estaminal (GSCs), que são responsáveis pela heterogeneidade tumoral e recorrência após a terapia e; 3) a inexistência de um alvo terapêutico reconhecido para não-GSCs e GSCs que permita o desenvolvimento de abordagens terapêuticas mais específicas para esta neoplasia.

Assim, neste trabalho, objetivámos: 1) estudar a contribuição da ativação da PKC para a agressividade do GBM, enfatizando a importância de protocolos terapêuticos combinados, incluindo a TMZ com inibidores de PKC, nomeadamente o tamoxifeno (TMX); 2) caraterizar as GSCs e estudar a plasticidade das propriedades destas células estaminais do GBM, no sentido de compreender o estado estaminal do glioma e, consequentemente, entender as propriedades de diferenciação, que contribuem para a recorrência do tumor; e 3) avaliar o potencial de marcadores de superfície celular específicos, como alvos terapêuticos para as não-GSCs e GSCs, a fim de permitir a acessibilidade de agentes terapêuticos mais exclusivamente ao nicho do tumor, por meio de uma abordagem de administração de fármacos mediada por lipossomas.

Inicialmente, usando duas linhas celulares de GBM, a U87 e a U118, observámos que a combinação de TMX e TMZ altera o estado de fosforilação da PKC, por western blot. Descobrimos que o TMX é um inibidor da p-PKC e que esta combinação é mais eficaz na redução da proliferação e no aumento da apoptose do que cada fármaco em monoterapia,

através de ensaios de citometria de fluxo, o que pode representar uma nova estratégia terapêutica no tratamento do GBM. Concluímos, então, que a combinação de TMX e TMZ potencializa o efeito entre si nas linhas celulares de GBM.

No sentido de estudar a heterogeneidade entre células de GBM e compreender melhor a variabilidade da resposta à quimioterapia, isolámos e caracterizámos uma linha celular de GBM humana, denominada GBM11, obtida através de uma biópsia cirúrgica de um doente com glioblastoma recorrente, e comparámos o efeito do TMX em monoterapia e em combinação com a TMZ, nesta linha celular, com o observado nas linhas celulares U87 e U118. Na verdade, observámos que o efeito do TMX e TMZ ou do TMX sozinho nas células de GBM11 sobre a proliferação celular, morte ou capacidade de migração, através de ensaios de citometria de fluxo e migração, era semelhante, o que pode sugerir que, para os tumores recorrentes, como o caso do GBM11 previamente tratado com TMZ, a melhor escolha do tratamento de segunda linha pode ser apenas TMX, a fim de reduzir os efeitos secundários putativos do tratamento combinado com TMZ.

A quimio- e a radiorresistência do GBM devem-se, também, à existência de GSCs, que contribuem para o crescimento tumoral e recorrência destacando-se, assim, esta população celular como o foco principal da investigação terapêutica no GBM. Consideramos que a compreensão da plasticidade do estado estaminal no GBM é de extrema importância para identificar os mecanismos e fatores envolvidos na resistência das GSCs à terapia, o que pode justificar a recorrência do tumor e, portanto, constituir um progresso na identificação de novas abordagens terapêuticas. Os nossos resultados demonstraram, em quatro linhas celulares de GBM e nas respetivas linhas de GSCs, a plasticidade do estado estaminal com base na modulação da expressão de marcadores específicos associados, tais como o SOX2 e outros marcadores como a Conexina 46 e 43, através de ensaios de imunofluorescência, western blot e PCR em tempo real. Além disso, através de ensaios de imunohistoquímica, verificámos que essa expressão dinâmica está de acordo com a regulação positiva destes marcadores celulares em graus superiores de amostras humanas de glioma, nomeadamente no GBM, comparativamente a graus inferiores, sugerindo uma correlação direta com o mau prognóstico de doentes com GBM.

Assim, devido à plasticidade do estado estaminal, a estratégia de atingir designadamente ambas as GSCs e não-GSCs pode representar uma abordagem importante no sentido de diminuir a agressividade do tumor e, eventualmente, evitar os efeitos

colaterais quimioterapêuticos conhecidos, o que pode melhorar o tempo e a qualidade de vida de doentes com GBM.

Neste sentido, avaliámos o potencial da nucleolina (NCL) de superfície celular, descrita como estando sobre-expressa nas células tumorais, como um alvo terapêutico para o reconhecimento específico de ambas as não-GSCs e GSCs, contribuindo para a entrega direcionada de fármacos encapsulados em nanopartículas, em duas linhas celulares de GBM. Para isso, utilizámos um lipossoma previamente desenhado, sensível ao pH e estericamente estabilizado, contendo na sua constituição um péptido F3, capaz de reconhecer especificamente a nucleolina constituindo, assim, uma ferramenta- alvo para as células com sobre-expressão de nucleolina. Em suma, demostrámos que a sobre-expressão de nucleolina *per se* pode identificar ambas as não-GSCs e GSCs, através de ensaios de citometria de fluxo, mediando a entrega direcionada intracellular de fármacos, o que pode validar a NCL como um potencial alvo terapêutico no GBM.

Em conclusão, o presente estudo demonstrou: 1) um efeito sinergístico do TMX e TMZ em linhas celulares de GBM e um efeito mais eficiente do TMX em monoterapia numa situação de GBM recorrente em comparação com a terapia combinada; 2) a plasticidade do estado estaminal através da reversibilidade da expressão dos marcadores de células do tipo estaminal e conduziu à identificação de três marcadores putativos associados a essa reversibilidade, o SOX2 e a Cx46 e 43, constituindo um passo mais próximo na compreensão do comportamento das células estaminais; e 3) que o sucesso em atingir especificamente células não-GSCs e GSCs, através da sobre-expressão de nucleolina, poderá ser a base de desenvolvimento de um tratamento específico para o GBM.

Palavras-chave: Glioblastoma; Ativação de PKC; Heterogeneidade celular; Plasticidade de células do tipo estaminal; Entrega específica do fármaco; Resistência; Terapia alvo.

CHAPTER 1

Introduction

"The beginning of all sciences is the astonishment of things being what they are."
Aristóteles

1.1.1 Glioblastoma Overview

Gliomas are known to be the most common primary malignant tumors of the central nervous system (CNS) in adults (Ostrom *et al.,* 2014).

Regarding the cell origin of gliomas, it is very important to understand the normal process of glial cell development. In the central nervous system, neural stem cells (NSCs) are localized in the ventricular zone of embryonic brains. In the case of adult brains, NSCs are localized in the subventricular zone and subgranular zone of the dentate gyrus, and give rise to both neurons and glial cells (Rycaj and Tang, 2015; Zong *et al.,* 2015). In the figure 1.1 is represented the cellular origin of gliomas.

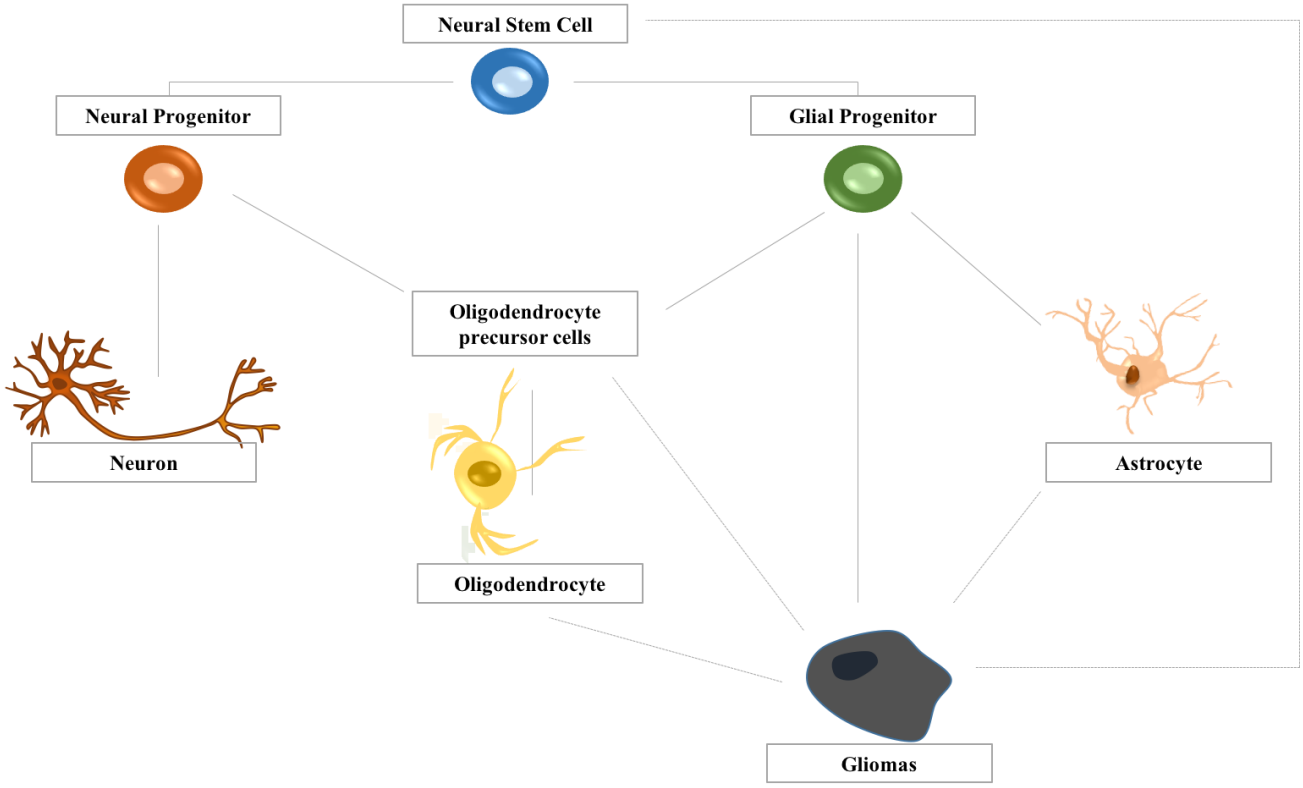

Figure 1.1 Glioma cells origin. Neural stem cells (NSCs) give rise to neurons, astrocytes, and oligodendrocyte precursor cells (OPCs), that can differentiate into oligodendrocytes.

[1] The present 1.1 section of the chapter 1 contains images and tables that are original or presented as originally published under the respective license of copyright permission. The original images were draw based on the literature mentioned in each one.

Oligodendrocyte, OPCs, glial progenitor and astrocytes constitute the cell origin types for malignant gliomas cells (Image originally draw based on Zong *et al.,* 2015 and Gruber *et al.,* 2017)

The glial cells can be astrocytes and oligodendrocyte precursor cells (OPCs) that, although it is a stable cell type in the adult brain, can in turn differentiate into oligodendrocytes. Ultimately, due to genetic and epigenetic mutations, a minor stem cell subpopulation within these cells, the Cancer Stem Cells (CSCs), can give rise to tumor cells and originate oligodendrogliomas, oligoastrocytomas, or the astrocytomas (Rycaj and Tang, 2015; Zong *et al.,* 2015). The CSCs theory will be discussed with more detailed in the section 1.2 of this chapter.

Similarly to the NSCs and OPCs, astrocytes may also retain some limited capacity to proliferate, especially regarding brain injuries. This regenerative potential makes the NSC, OPC, and astrocytes the prime suspects as the cells of origin of gliomas (Zong *et al.,* 2015).

Among all gliomas, the astrocytomas, oligoastrocytomas and oligodendrogliomas are the most known. Since this dissertation is focus on glioblastoma, from now on we are going to direct this overview specifically to this type of gliomas.

Glioblastoma (GBM) is a uniformly fatal primary brain tumor classified by the World Health Organization as the most malignant astrocytoma (WHO Grade IV) (Paff *et al.,* 2014; Ringertz, 1950; Urbańska *et al.,* 2014).

GBMs are high grade gliomas with predominantly astrocytic differentiation. They are characterized by nuclear atypia, cellular pleomorphism, mitotic activity, diffuse growth pattern, microvascular proliferation and/or necrosis.

The high cellular proliferation and the formation of thrombus lead to difficulties in cell nutrition and to the existence of necrotic foci in the central area of the tumor. These necrotic foci result from insufficient blood supply and are usually surrounded by pseudopalisading areas (Urbańska *et al.,* 2014; Wilhelmsson *et al.,* 2003).

These characteristics constitute the main features of GBM and are the result of genomic instability and deregulation of several molecular signalling pathways that determine a huge cellular and vascular proliferation and a high resistance to chemotherapy. Therefore, GBM is considered the most common and aggressive primary brain tumor in

adults, accounting for more than 50% of all gliomas. Despite aggressive therapies, just 5% of the patients survive more than 5 years (Ohgaki and Kleihues, 2007; Ostrom *et al.,* 2014).

1.1.2 Glioblastoma Classification

The classification of gliomas started to be based on histopathological features. Next, genetic and molecular features were also introduced to give rise to a more complex, but more precise classification of gliomas (Louis *et al.,* 2016; Stupp *et al.,* 2005). Actually, the current WHO classification is predicated on the concept of combined phenotypic and genotypic classification (Louis *et al.,* 2016).

Whereas all astrocytic tumors where previously grouped together, in the new classification, all diffuse gliomas (astrocytic or not) are grouped together, based not only on their growth pattern and behavior, but also on their *IDH1* and *IDH2* genetic *status*, which provides a dynamic classification based on the phenotype and genotype grouping tumors that share similar prognostic factors (Louis *et al.,* 2016). In this new classification, the diffuse glioma category includes the grade II and III astrocytic tumors, the grade II and III oligodendrogliomas, the more rare grade II and III oligoastrocytoma and the grade IV glioblastomas (Louis *et al.,* 2016) (Figure 1.2).

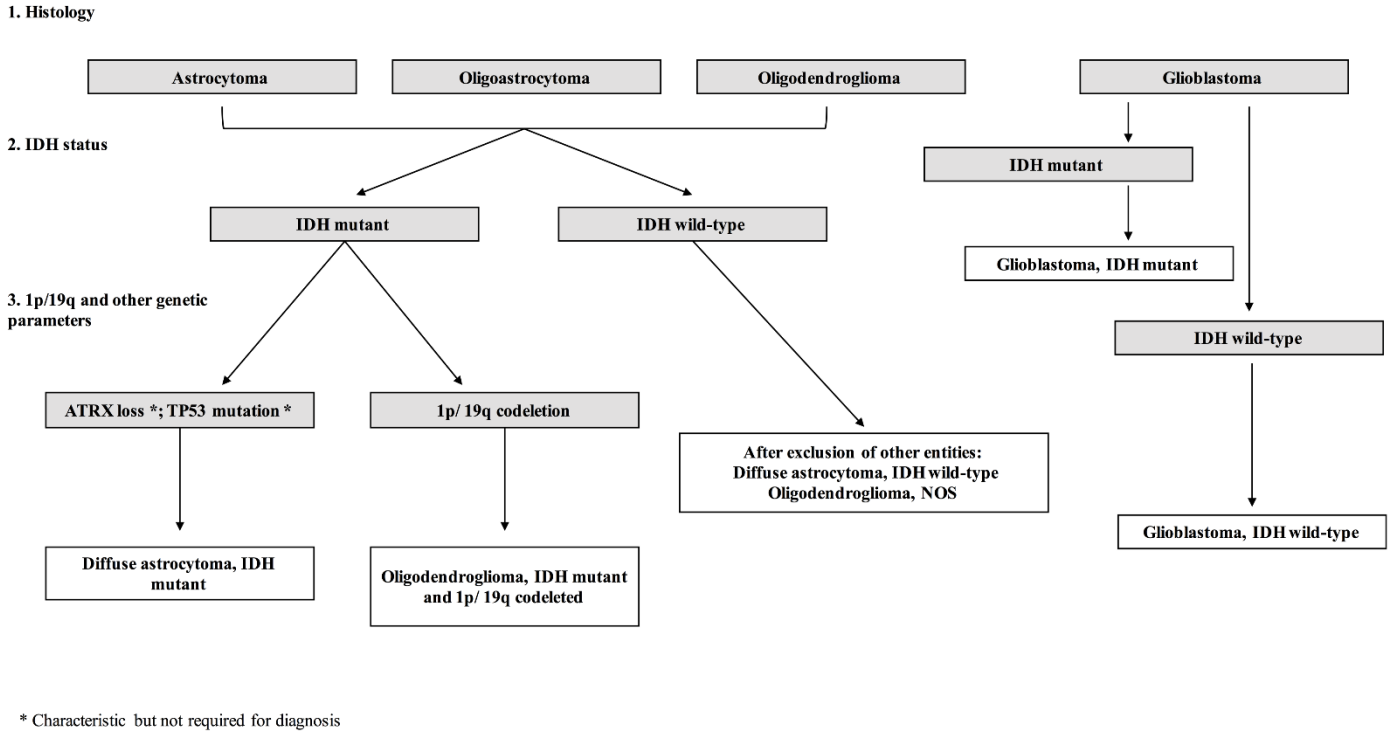

Figure 1.2 Classification of diffuse gliomas accordingly with WHO 2016. This scheme is a summary of the gliomas classification based on: 1) Histological based classification; 2) *IDH*

status; and 3) other genetic parameters of 2016 WHO classification. Regarding the histology, the gliomas can be classified as astrocytoma, oligoastrocytoma and oligodendroglioma. The IDH status divide the gliomas as *IDH* mutant and *IDH* wild-type, and the genetic parameters, like the 1p/19q, the *TP53* mutation, the *ATRX* loss, can also distinguish different gliomas (Image originally draw based on Louis *et al.,* 2016).

The 2016 update of WHO classification of tumors of the central nervous system is based on a grading scheme called a 'malignancy scale' ranging across a wide variety of neoplasms rather than a strict histological grading system. This grading scheme is similar to that of the Ringertz (Ringertz, 1950) and of St Anne-Mayo (Daumas-Duport and Varlet, 2003; Dunn *et al.,* 2012; Stupp *et al.,* 2005). However, the differences between WHO and St Anne-Mayo classification have important contradictions, if we look to the grading of astrocytomas, or to diffuse and aggressive tumors.

In table 1.1 is represented the histological classification of astrocytic tumors grading according to 2016 WHO's classification (Louis *et al.,* 2016).

Table 1.1 Histological grading of astrocytic tumors according to 2016 WHO classification.

Grade II	Cytological atypia	Low grade infiltrative astrocytomas
Grade III	Cytological atypia; anaplasia and mitotic activity	Anaplastic astrocytomas
Grade IV	Cytological atypia; anaplasia; mitotic activity; microvascular proliferation and/ or necrosis	Glioblastomas

Since the main focus of this thesis is the GBM we next described the classification of this particular tumor taking into account the histopathological, genetic and molecular features.

Histopathologically, GBM is considered an astrocytoma due to the resemblance of the tumor cells to astrocytes. In addition, it is also possible to identify small polymorphic cells, anaplasia and significant anisokaryosis, where the term "multiforme" was initially derived, but no longer used. In a Haematoxylin-Eosin staining (H&E), it is possible to detect polygonal or spindle-shaped cells with irregular borders and an acidophilic fibrillary cytoplasm, nuclei atypia, microvascular proliferation with the newly developed vessels, necrotic areas and brisk mitotic activity, which constitute the main histopathological

features for diagnosis (Figure 1.3) (Brat and Van Meir, 2004; Kleihues *et al.,* 2002; Linkous and Yazlovitskaya, 2011; Schultz *et al.,* 2005).

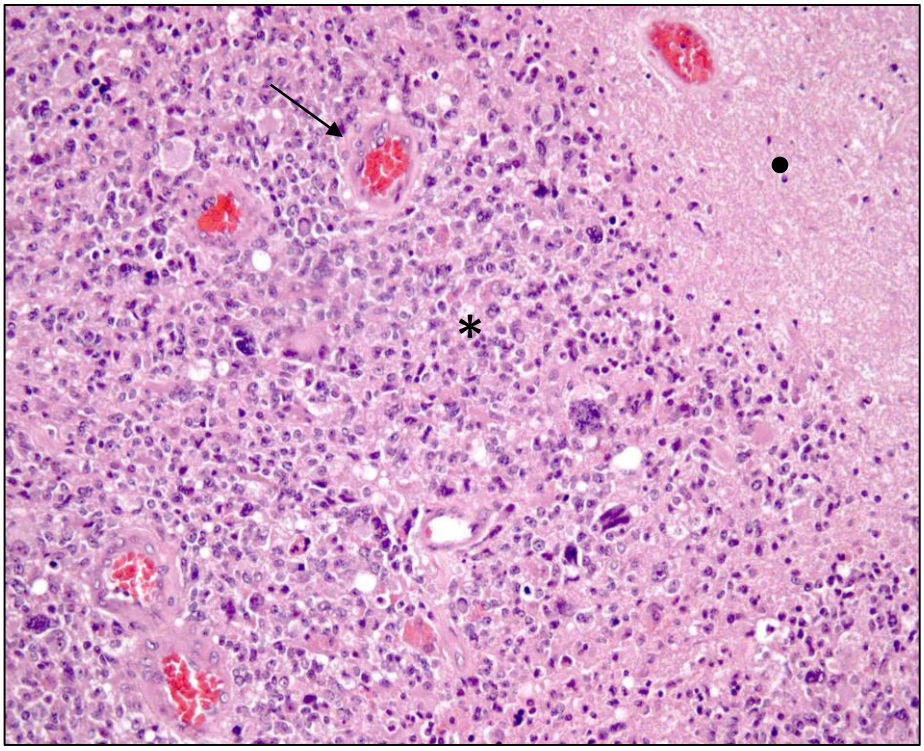

Figure 1.3 Haematoxylin and eosin stain of a human GBM sample. The characteristic of geographical necrosis (•), highly anaplastic glial cells (*), pleomorphic nuclear atypia, and microvascular proliferation with an arrow are observed. Amplification 200x.

Genetic alterations were suggested to be associated with the malignancy of gliomas. The Cancer Genome Atlas Research Network (Cancer Genome Atlas Research Network, 2008) started with a systematically study regarding the genetic alterations presented in GBM that were translated in some molecular cell signalling pathways deregulations:

(i) cyclin-dependent kinase inhibitor 2A/2C [*CDKN2A/ CDKN2C*] deletion that leads to retinoblastoma (RB) signalling deregulation;

(ii) *CDKN2A* deletion and *TP53* mutation that leads to alterations in tumor protein 53 (TP53) signalling;

(iii) phosphatase and tensin homolog/neurofibromin 1/phosphatidylinositol-4,5-bisphosphate 3-kinase, catalytic subunit alpha [*PTEN/NF1/PIK3CA*] mutation and epidermal growth factor receptor/platelet derived growth factor receptor

[EGFR/PDGFRA] amplification that leads to receptor tyrosine kinase signalling deregulation (Ostrom *et al.,* 2014).

These findings, as mentioned previously, incorporate well-stabilized molecular parameters into the classification of diffuse gliomas, which gives huge importance, not only to the microscopy parameters, but also incorporates molecular characteristics (Louis *et al.,* 2016).

As so, in the 2016 CNS WHO tumors classification, GBMs are divided into:

(i) **glioblastoma, *IDH*-wildtype** (about 90% of cases), which corresponds to the primary **or *de novo* GBM** and predominates in patients over 55 years of age. This type of GBM also includes mutations in *TERT* (72%), *EGFR* (35%), *TP53* (27%), and in *PTEN* (24%). Also includes *CDKN2A/p16* deletion in chromosome 9p and a loss of heterozygosity on chromosome 10 (Fujisawa *et al.,* 2000; Nonoguchi *et al.,* 2013).

(ii) **glioblastoma, *IDH*-mutant** (about 10% of cases), which corresponds to the **secondary GBM** with a history of prior lower grade diffuse glioma, that preferentially arises in younger patients. This type of GBM includes mutations in *TERT* (26%), *TP53* (81%), and *ATRX* (71%). Exceptionally, the *EGFR* and *PTEN* mutations can also occur as well as the loss of heterozigoty on chromosome 10 (Fujisawa *et al.,* 2000; Louis *et al.,* 2016; Ohgaki and Kleihues, 2005).

(iii) **glioblastoma, NOS** (not otherwise specified), a diagnosis that is reserved for those tumors for which full *IDH* evaluation cannot be performed (Fujisawa *et al.,* 2000; Louis *et al.,* 2016; Nonoguchi *et al.,* 2013).

The GBM referred in (i) and (ii) are the most common types and the specific characteristics, published in WHO 2016 classification, are summarized in the table 1.2. The high relevance of *IDH1* to the classification of GBMs is based on its relation with DNA damage. In fact, IDH1 catalyzes the oxidative decarboxylation of isocitrate to alfa-ketoglutarate, reducing NADP to NADPH and liberating CO_2. Deficiency in IDH1 leads to an increase of lipid peroxidation, DNA damage, and so a decrease in the survival after oxidant exposure (Louis *et al.,* 2016).

Table 1.2 Key characteristics of *IDH*-wildtype and *IDH*-mutant glioblastomas based on WHO 2016 classification (based on Louis *et al.,* 2016).

GBM	IDH1-wildtype	IDH1-mutant
Synonym	Primary GBM	Secondary GBM
Precursor Lesion	*de novo*	Diffuse astrocytoma (WHO II) Anaplastic astrocytoma (WHO III)
Proportion of GBM	~90%	~10%
Median age at diagnosis	~62 years	~44 years
Median overall survival	~9-15months	~24-31 months
TERT mutations	~72%	~26%
TP53 mutations	~27%	~81%
ATRX mutations	Exceptional	~71%
EGFR amplification	~35%	Exceptional
PTEN mutations	~24%	Exceptional

The incorporation of the molecular characteristics in the classification of GBM will contribute to a more precise categorization for epidemiological purposes, to the introduction for clinical trials and experimental studies, and overall, for a more rigorous description of these neoplasias (Louis *et al.,* 2016).

1.1.3 Epidemiology

The astrocytomas comprise 48% of all brain tumors (Figure 1.4) (Dolecek *et al.,* 2012; Ohgaki and Kleihues, 2005; Schwartzbaum *et al.,* 2006). GBM is primarily diagnosed at older ages with the median age of 62 years, which constitutes the most powerful prognostic factor of poor prognosis. Although GBMs could manifest at any age, they are rare at individuals younger than 40 years (Louis *et al.,* 2016). The epidemiological data show that incidence of GBM in Europe, North America and in Australia is 3–4 per 100 000 adults each year (Louis *et al.,* 2016). The incidence rate in men in comparison to

women is about 1.4:1 in the USA and Europe (Louis *et al.,* 2016). GBM is uncommon in children accounting only for approximately 3% of all brain tumors in age range from 0 to 19 years old, with a proportion rate in male in comparison to female children of 3.3:1 (Mahvash *et al.,* 2011). However, there are no morphological differences between GBM occurring in children and adults (Ostrom *et al.,* 2014; Thakkar *et al.,* 2014).

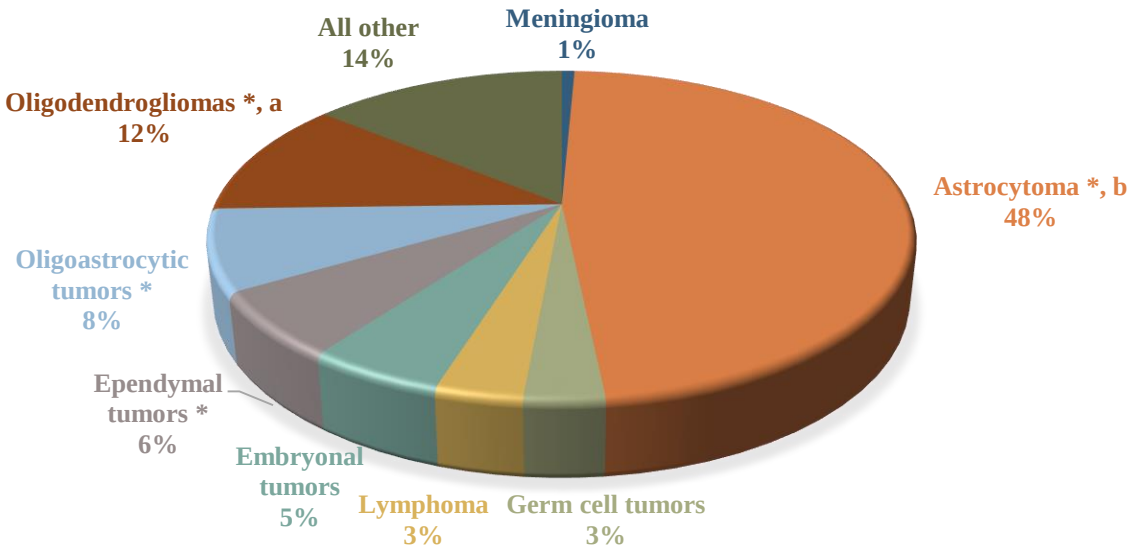

Figure 1.4 Histological distribution of brain tumors. * All or some of this histology is included in the Central Brain Tumor Registry of the United States (CBTRUS) definition of gliomas. Percentages may not add up to 100% due to rounding. a - includes oligodendroglioma and anaplastic oligodendroglioma; b - includes pylocitic astrocytoma, diffuse astrocytoma, anaplastic astrocytoma and unique astrocytoma variants (Data based on Dolecek *et al.,* 2012 and Ostrom *et al.,* 2014).

Regarding ethnicity, white people have the highest incidence rates of GBM, followed by blacks, Asian/Pacific Islanders and American Indian/Alaska Native (Ostrom *et al.,* 2014).

Factors associated with GBM risk are still not well identified. However, previous radiation therapy, decreased susceptibility to allergy, immune factors and related-immune genes, have been referred as important risk factors (Ohgaki and Kleihues, 2005).

The failure in the identification of the possible risk factors involved in the development of GBM are related to several reasons, namely: 1) the existence of small sizes of study groups; 2) the existence of false-positive results; 3) the identification of invalid or imprecise exposure measures; 4) the inherited or developmental variation in metabolic and repair pathways; 5) the multiple variables and conditions (such as allergies); 6) the

differential diffusion of chemicals across the blood–brain barrier; and 7) the metabolic and repair pathways differentially expressed in the brain (Schwartzbaum *et al.,* 2006).

Environmental exposure and risk of GBM development -

High socioeconomic status (SES) is associated with increased risk of GBM (Kitahara *et al.,* 2012; Ostrom *et al.,* 2014; Thakkar *et al.,* 2014).

There is no substantial evidence of GBM association with life-style characteristics, such as smoking, alcohol consumption, abuse drugs, or dietary exposure to N-nitric compounds. Inconsistent results have been also published regarding the risk of GBM and the use of mobile phones (Deltour *et al.,* 2012). The only consistently evidence that established an exogenous environmental cause with GBM development is the exposure to therapeutic or high-dose radiation to the head and neck. On the other hand, a decreased risk has been described among individuals with a history of allergies and/or atopic diseases (Louis *et al.,* 2016; Schwartzbaum *et al.,* 2006).

Besides the difficulties associated to the epidemiologic evaluation, the large range of studies that have examined environmental risk factors for GBM are considerably large, and so we cannot place in part the potential influence of environmental factors in GBM development.

Genetic background and risk of GBM development -

GBM is believed to be a sporadic tumor and not with a hereditary inheritance, despite the fact that there are a few descriptions of its occurrence in related persons.

As mentioned, a lower risk of GBM development has been associated with allergies or atopic diseases, mainly asthma, eczema, psoriasis (Brenner *et al.,* 2002; Lachance *et al.,* 2011; Schwartzbaum *et al.,* 2006). On the other hand, it is referred that short term (< 10 years) use of anti-inflammatory medications is associated with a protective effect against GBM, especially among individuals with no history of asthma or allergies (Scheurer *et al.,* 2011). In opposite, increased risk of GBM is associated with inherited genetic variation in a region containing cyclin-dependent kinase inhibitor 2B (*CDKN2B*) on chromosome 9p21 and in 2 SNPs in regulator of telomere elongation helicase 1 (one in the 9p21 region, the rs1412829, near *CDKN2B,* and the other one in the 20q13.3, the rs6010620, intronic to

RTEL1) (Ostrom *et al.,* 2014; Thakkar *et al.,* 2014; Wrensch *et al.,* 2009). In spite of many genes and related pathways are still unknown, a considerable number of potential candidate genes and their related syndromes have been identified as involved in gliomagenesis, namely: the *neurofibromatosis type 1* and *neurofibromatosis type 2* genes in neurofibromatosis; the *tuberous sclerosis I* and *tuberous sclerosis II* genes mutations in tuberous sclerosis; *P53* and *checkpoint kinase 2* (*CHECK2*) genes related to retinoblastoma and Li–Fraumeni syndrome; DNA repair gene mutations involved in Turcot's syndrome; and finally mutations in *PTEN* gene related to the multiple hamartoma syndrome (Ichimura *et al.,* 2004).

1.1.4 Localization, Morphology and Diagnosis

Localization and morphological features -

GBM develops in the brain, in cerebral hemispheres and in subcortical white matter and deeper grey matter. It's a tumor widely characterized by an infiltrating growth that makes able the invasion into the adjacent cortex, through the corpus callosum, into the contralateral hemisphere (Lakhan *et al.,* 2009; Louis *et al.,* 2016).

Whereas primary GBM gave a wide-spread anatomical distribution, the secondary GBM have a striking predilection for the frontal lobe, surrounding the rostral lateral ventricles (Louis *et al.,* 2016).

As previously described in 1.1.1 section, the most accepted hypothesis is that GBMs arise from the malignant transformation of either a bipotential precursor cell or a more primordial cell, the neuro stem cell, which has the capacity of self-renewal, express markers of development regulation and is tumorigenic in animal models (Louis *et al.,* 2016).

Morphologically, GBM cells are usually small polymorphic with anaplasia and significant anisokaryosis. Specifically, GBM cells are polygonal to spindle-shaped with acidophilic cytoplasm and indistinct cellular borders. Their nuclei are oval or elongated and have coarsely clumped hyperchromatic with multiply distinct nucleoli located centrally or pericentrally. Overall, GBM cells have increased nuclear to cytoplasmic ratio and show nuclear pleomorphism. Some cells contain intranuclear inclusions. Besides that, binuclear and multinucleated cells, lymphocytes, neutrophils, macrophages and necrotic cells can be also present, whereas better-differentiated neoplastic astrocytes are usually discernible, at

least locally (Louis *et al.,* 2016; Schultz *et al.,* 2005). Vascularization is another important feature of GBM (Linkous and Yazlovitskaya, 2011). The newly developed vessels are usually morphologically similar to renal glomeruli and their endothelial cells are phenotypically different from normal ones. The surface of these vessels is covered with a discontinuous layer of pericytes, without any contact with astrocyte processes. GBM shows vascular thrombi leading to endothelial cell damage and proliferation. Together with the prominent microvascular proliferation, necrotic foci are also an essential diagnostic feature for GBM. Necrosis can be seen as large areas within the central area of the tumor, resulting from insufficient blood supply in all primary glioblastomas. It can be also seen as small areas with irregularly shaped necrotic foci surrounded by pseudopalisading areas created by radially oriented glial cells, that can be observed in both, primary and secondary glioblastomas (Kleihues *et al.,* 2002). The major morphologic characteristics of glioblastoma cells are represented on figure 1.5.

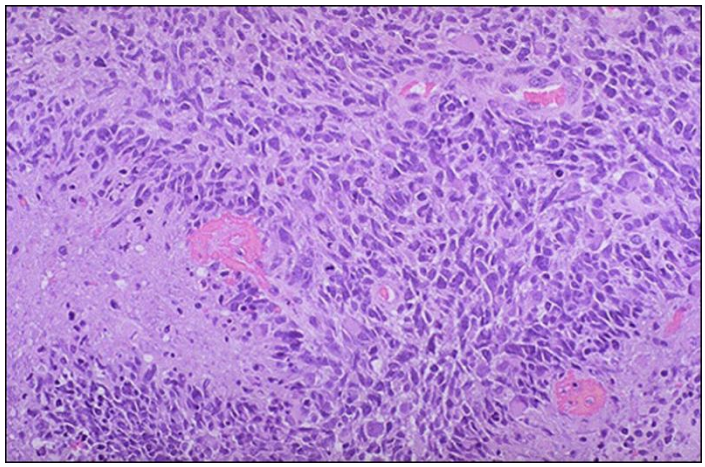

Figure 1.5 Morphological hallmarks of glioblastoma. In the image above is visible an ischemic necrosis area surrounded by palisading tumor cells in the left side, a vascular proliferation with glomeruloid appearance in red, an increase nuclear to cytoplasmatic ratio and nuclear pleomorphism (Image from *PathologyOutlines* with copyright permission of the author Edward C. Klatt, Professor of Pathology).

The increased aggressiveness of GBMs is accompanied by an increase degree of atypia, nuclear hyperchromatosis, increased mitotic index, presence of necrotic areas and atypical blood vessels. It has been hypothesized that the low metastatic potential of GBM results from several factors, mainly the barrier created by cerebral meninges, the rapid tumor growth and short course of this disease, and also the fact that the brain is devoid of lymphatic vessels, so metastases through this pathway are blocked (Robert and Wastie,

2008). However, glioblastoma present a higher invasive behavior, such that tumor cells can infiltrate from the primary mass into brain parenchyma. In fact, glioma stem-like cells are the primary source of invasion and could lead to tumor recurrence (Sayegh *et al.,* 2014).

Clinical Signs -

GBM has a rapidly development and primarily manifest as focal neurological deficits. Depending on the localization in the brain area and the increasing intracranial pressure, the most common signs of GBM include headaches, ataxia, dizziness, vision disturbances (blurred vision, diplopia), nausea and vomiting (Urbańska *et al.,* 2014).

Complementary diagnostic tests -

Advances in neuroimaging have improved the characterization of the tumors in a non-invasive manner, leading to a better diagnosis and improving therapy (Kao *et al.,* 2013).

Computed tomography (CT) may be the first modality employed in a patient presenting with a brain tumor. However, magnetic resonance imaging (MRI) is the most important imaging modality for brain tumor diagnosis. In fact, while CT is largely relegated to emergent imaging in the detection of haemorrhage, herniation and hydrocephalus, MRI can potentially detect the calcification within brain tumors (Mabray *et al.,* 2015).

Since MRI does not use ionizing radiation is thus preferred over CT in children and in patients requiring multiple imaging examinations. Also, MRI has a much greater range of available soft tissue contrast than CT, which makes possible to depict anatomy in greater detail, as well as is more sensitive and specific for abnormalities within the brain itself compared to CT, allowing the evaluation of structures that may be obscured by artefacts from bone in CT images (Zhou *et al.,* 2011).

Therefore, MRI is crucial for posterior GBM diagnosis by histopathological analysis and for more than 20 years it has been used in the clinic of gliomas to serve as a guide for clinical treatment (Li *et al.,* 2012). The determination of the location of the lesion within the brain, either for treatment or biopsy planning, the evaluation of mass effect, as well as the ventricular system and vasculature, constitute the primary factors evaluated in a MRI that would suggest a possible diagnosis. The most common MRI approaches used to evaluate brain tumors in the clinical setting are: the T2-weighted or fluid-attenuated

inversion recovery (FLAIR) images, which generally show increased water content in tumors, and gadolinium (Gd)-enhanced T1-weighted images that indicate blood-brain barrier disruption (Figure 1.6). These approaches used in combination can determine the extent of tumor involvement and assess the therapeutic response (Zhou *et al.,* 2011).

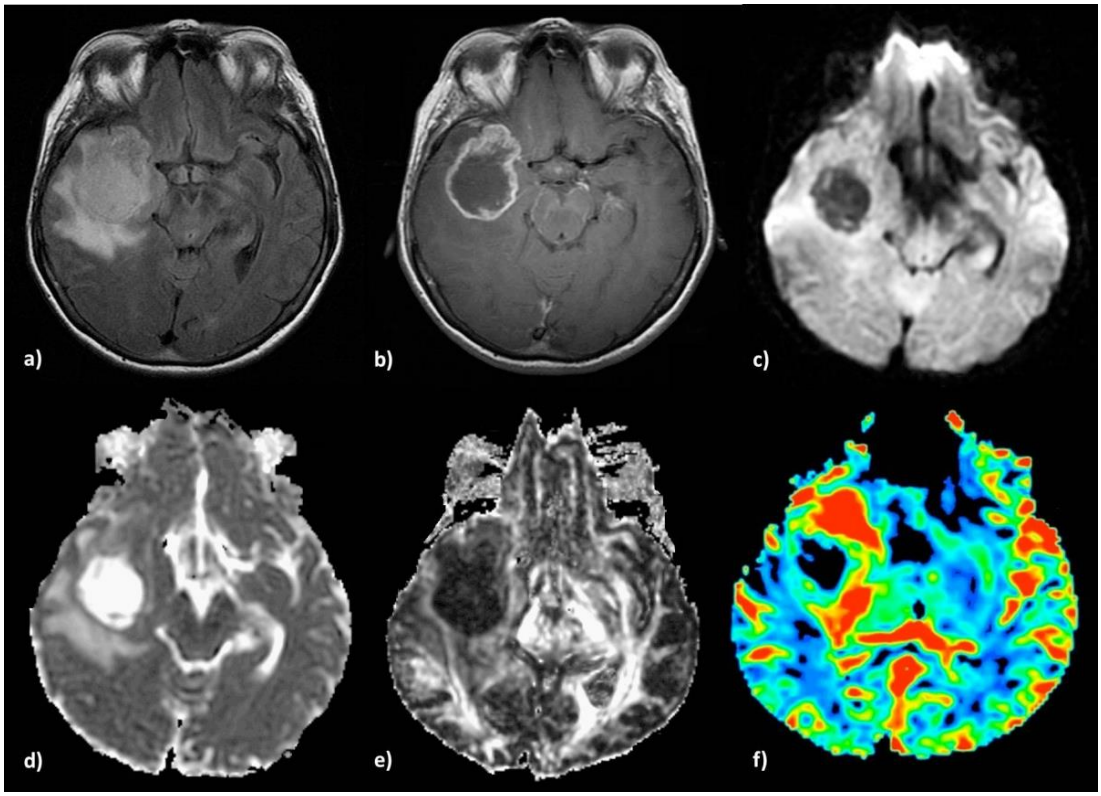

Figure 1.6 Glioblastoma imaging in a 65-years old women. Axial T2-weighted (a) and T1-weighted post-contrast (b), demonstrating a right temporal lesion with surrounding edema and ring-shaped enhancement. Diffusion weighted images with low signal intensity (c), higher intratumoral apparent diffusion coefficient (ADC) (d), lower-intratumoral fractional anisotropy (FA) (e) and high peritumoral residual cancer burden (RCB) (f), which shows tumor infiltration in the surrounding parenchyma (Image as originally published in Svolos *et al.,* 2014. License: BioMed Central Ltd. 2014).

Although it can rarely metastasis, the GBM can frequently disseminate along the white matter tracts involving the contralateral hemispheres, crossing corpus callosum into occipital and temporal lobes resulting in a butterfly pattern on MRI imaging ("butterfly glioma") (Figure 1.7) (Agrawal, 2009; Urbańska *et al.,* 2014).

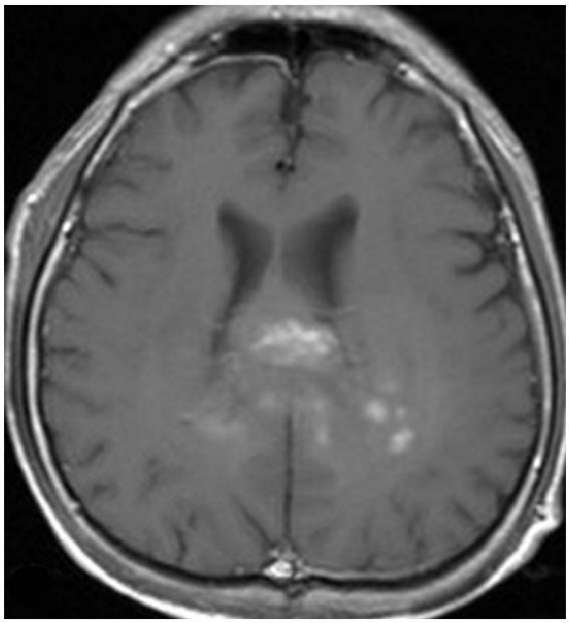

Figure 1.7 Contrast-enhanced T1-weighted image. The image above demonstrates a butterfly glioblastoma pattern in a MRI image (Image as originally published in Urbańska *et al.,* 2014. License: Termedia, 2014, Creative Commons Attribution-Noncommercial 3.0 Unported).

The differentiation between recurrent tumor, radionecrosis or scar tissue on the basis of MRI findings alone may be difficult. As so, Positron Emission Tomography (PET) scanning is useful in this regard bringing information about tumor hypoxia, necrosis, proliferative activity or vasculature (Lee *et al.,* 2013).

Despite the more usual imaging techniques used to identify GBM were the ones described before in more detail, an overview of other imaging techniques in brain tumor and the general major utility is presented in table 1.3.

Table 1.3. Imaging methods and the major utility in brain tumor diagnosis.

Imaging technique	Major utility in brain tumor imaging
CT	Mass effect, herniation, hydrocephalus, haemorrhage, calcifications
Pre and post-contrast T1	Necrosis, extent of the enhancing portion of the tumor
T2/T2 FLAIR	Peri-tumoral edema (vasogenic and in infiltrative)
T2* susceptibility sequence (SWI)	Blood products, calcifications, radiation induced chronic micro-haemorrhages
DWI/ADC	Reduced in highly cellular portions of tumor, post-operative injury

DTI	Tractography for surgical planning/navigation
Perfusion (generally DSC)	Tumor/tissue vascularity
MR spectroscopy	Metabolic profile
fMRI	Pre-operative functional mapping, research into treatment effects
PET/MR	Potential new radiotracers

ADC, apparent diffusion coefficient; CT, computed tomography; DSC, dynamic susceptibility contrast-enhanced; DTI, diffusion tensor imaging; DWI, diffusion weighted imaging; FLAIR, fluid attenuated inversion recovery; fMRI, functional magnetic resonance imaging; PET, positron emission tomography; SWI, susceptibility weighted imaging (Table based on Mabray *et al.,* 2015).

After the imaging identification of a solid mass, definitive diagnosis is based, primarily, on histopathological examination of the removed tumor by surgery, using traditional histologic methods. In cases that neurosurgical tumor resection is not possible due to the dangerous localization of the tumor mass, neuronavigation brain biopsy or stereotaxic biopsy are also performed (Orringer *et al.,* 2012).

Morphological diagnosis is based on criteria defined by the WHO classification, as previously described, which stage the tumors in the central nervous system according the grade of malignancy, proliferative index, response to treatment and survival time. Briefly, grade I includes low malignant tumors; grade II is used for relatively low malignant tumors; grade III includes tumors of minor grade of malignancy, while grade IV denotes the most malignant tumors, the glioblastomas (Urbańska *et al.,* 2014).

Finally, the confirmation of the primary diagnosis is performed on the basis of glioma cells immunohistochemistry. In this sense, glioma cells are positive to glial fibrillary acidic protein (GFAP), the major intermediate filament protein of mature astrocytes, both in normal and pathological conditions (Messing and Brenner, 2003), even if it is possible that some GBM cells are not stained by GFAP too. Also, the acid protein S100 present in glial cells is another specific marker for tumors of the central nervous system, but its expression cannot constitute a basic criterion in differential diagnosis (Dohan *et al.,* 1977; Urbańska *et al.,* 2014). The determination of the cytokeratins expression through the antibody cocktail AE1/AE2 constitutes another marker of GBM. Nestin is also frequently expressed in GBM and is diagnostically useful to distinguish glioblastoma from other high-grade gliomas (Louis *et al.,* 2016). GBMs with missense *TP53* mutations show strong and diffuse immunohistochemical expression of P53 in 21-

53% of the cases. EGFR expression also occurs in 40-98% of GBMs. Finally, the secondary GBMs also show present mutations in *IDH1* expression (R132H) (Liu *et al.,* 2016; Louis *et al.,* 2016).

1.1.5 Treatment of glioblastoma

The median survival of GBM patients is generally one-two years from the time of diagnosis. Standard therapy consists firstly of maximal surgical resection of the tumor to the extent that is safely feasible, and is followed by six weeks of radiotherapy with concomitant and adjuvant chemotherapy with the *gold standard*, temozolomide (TMZ), in a multimodality approach commonly referred as the "Stupp regimen" (Stupp *et al.,* 2005). Surgical treatment, chemotherapy and radiotherapy prolong the overall survival of GBM patients only to 12-15 months (Stupp *et al.,* 2009).

Surgery -

The GBM localization on brain affects treatment options and prognosis. Patients with GBM in frontal lobe are known to survive longer (~ 11.4 months) than those that have the tumor in the temporal lobe (~ 9.1 months) or in the parietal lobe (~ 9.6 months) after surgery (Chakroun *et al.,* 2017).

One of the factors actually used to determine if a patient is a good surgical candidate is the Karnofsky Performance Scale (KPS) index, a baseline parameter and a post-operative measure, traducing that a KPS index > 90 prolonged the functional outcome of patients. A KPS index greater than or equal to 70 is generally the minimum for offering surgical intervention (Young *et al.,* 2015).

The main surgical goals are to establish a pathological diagnosis, relieve mass effect, and achieve a gross total resection to facilitate adjuvant therapy (Moiyadi and Shetty, 2012). In fact, it is known that the removal of 98%, or more, of the tumor mass identified in MRI conduct to a statistically significant increase in patient survival (Miller *et al.,* 1988).

To conduct a maximal overall survival, minimize morbidity and maximizing quality of life, the surgical approach must be individualized for each patient, in a way to maintain the patient's pre-operative KPS. As so, a variety of surgical techniques are resumed in table 1.4 (Young *et al.,* 2015).

Table 1.4. Neurosurgical technique for glioblastoma treatment.

Neurosurgical technique	Major utility in brain tumor resection
Awake craniotomy	Performed when a glioma is located near eloquent cortex in areas that include: the pericentrally gyrus (motor strip), corticospinal tracts, Broca's speech area, Wernicke's speech area, and the brainstem.
Standard craniotomy approach	Standard craniotomy approach with the patient under general anaesthesia.
Extent of resection (EOR)	EOR is associated with longer survival time in GBM patients.
Surgical adjuncts	Includes neuronavigation, functional mapping, intraoperative fluorescent dyes, and intraoperative MRI (iMRI).

Since it is unlikely that all tumor cells can be removed via surgery, leaving potential for recurrence, the modalities described before are thus far the most efficacious methods available for accurate and precise tumor resection until nowadays.

Radiotherapy -

Although GBM rarely metastasizes outside the central nervous system, it can infiltrate throughout the brain making a tumor difficult to treat with radiation. Radiation Therapy (RT) has been shown to prolong survival in patients with GBM compared to surgery alone from 3-4 months to 7-12 months (Stupp *et al.,* 2005). The best results are obtained when radiotherapy is performed after the surgery (Chang *et al.,* 2007; Combs *et al.,* 2007). Radiation is responsible for single and double-strand DNA breaks inducing cell death and reducing proliferation. Although radiation has demonstrated efficacy, the dose, fractionation and target delineation have been part of an ongoing research for improvement (Pelloski and Gilbert, 2007). In fact, the full brain radiotherapy maximizes the extent of cancer cells that can be eradicated but it has the risk of memory loss. On the other hand, localized radiotherapy is more specific, which justifies the less side effects, but it is not so efficient in eradicating cancer cells that invade the surrounding areas (Chakroun *et al.,* 2017).

There are three primary ways to administer radiation for the treatment of brain tumors, namely the External Beam Radiation Therapy (EBRT), the Stereotactic Radiation Therapy (SRT) and the Brachytherapy (Pelloski and Gilbert, 2007):

The EBRT is the conventional technique for administering radiation to the brain. Nonetheless, SRT and brachytherapy did not show an improvement over conventional treatment (Pelloski and Gilbert, 2007).

Notwithstanding the slight advantage of the use of radiotherapy, multiple factors limit the efficacy of radiation. Among them are changes in cell cycle progress, activation of oncogenes, inactivation of tumor suppressor genes, alteration of molecular signalling pathways, the existence of a population of glioma stem-like cells (GSCs), and the DNA repair proficiency (Naidu *et al.,* 2010).

Chemotherapy and limitations -

Chemotherapy is the use of chemical compounds to induce death in malignant cells. These compounds interact with cellular components, such as the cytoskeleton, cytoplasmic membrane, molecular signalling pathways and nucleic acids (Sathornsumetee *et al.,* 2007). However, as they interact with dividing cells they could interact with normal cells leading to secondary toxicity and side effects.

Temozolomide (TMZ, Temodal™ or Temodar™) is an oral alkylating agent with good blood-brain barrier (BBB) penetration developed in the 1990s. This drug showed benefit in GBMs and gaining approval for this kind of tumors by the United States Food and Drug Administration (FDA) in March 2005 (Theeler *et al.,* 2015; Yung *et al.,* 2000), after the randomized study performed by Stupp *et al.,* (Stupp *et al.,* 2005). Nowadays, TMZ is considered the drug *gold standard* of GBM treatment (Stupp *et al.,* 2005).

TMZ belongs to the novel family of alkylating agents, the imidazotetrazines. Besides its excellent bioavailability, TMZ has a small size (194,15 Da) that allows it to be rapidly absorbed in the digestive tract. Also, its lipophilic properties allow it to cross the BBB. TMZ does not present significant drug–drug interactions and cumulative myelotoxicity and remains stable in an acidic environment (Pelloski and Gilbert, 2007). However, when it interacts with neutral or alkaline conditions, like the environment of blood, TMZ undergoes hydrolysis, converting itself into the active compound MTIC (5-(3-dimethyl-1-triazenyl) imidazole-4-carboxamide), which is rapidly broken down to form the reactive compound, the methyldiazonium ion. In turn, the methyldiazonium ion, obtained from the degradation of MTIC, methylates guanine residues in DNA molecules, resulting in the formation of O^6- and N^7-methylguanine (Agarwala and Kirkwood, 2000; Newlands *et al.,* 1997). In the figure 1.8 is represented the mechanism of O6-methylguanine formation.

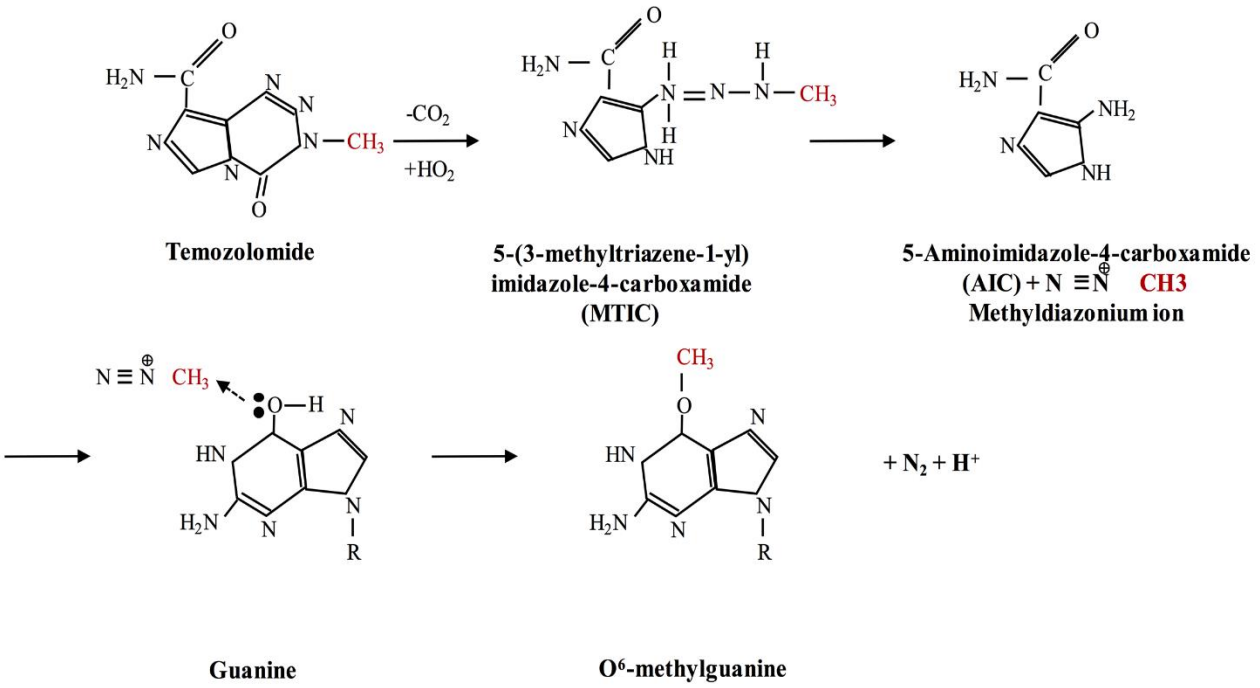

Figure 1.8 Mechanism of O^6-methylguanine formation. Temozolomide (TMZ) when undergoes hydrolysis converts itself into the active compound 5-(3-methyltriazene-1-yl) imidazole-4-carboxamide (MTIC), which is rapidly broken down to form the reactive compound, the methyldiazonium ion (AIC). Next, the AIC methylates guanine residues in DNA molecules, resulting in the formation of O^6- and N^7-methylguanine (Image originally draw based on Kaina *et al.,* 2007).

The cytotoxicity of TMZ, like many other alkylating agents, is primarily due to the methylation of the O^6 position of guanine. Although these DNA adducts represent 9% of the total DNA methylation events caused by TMZ, O^6-methylguanine induces DNA mismatch repair, which is unable to successfully repair the lesion, resulting in double-strand breaks that lead the cell to undergo apoptosis. In contrast, N^7-methylguanine and N^3-methyladenine, which constitute approximately 80% of the total methylation events, can be repaired by the base excision repair pathway and are generally not cytotoxic. As so, the only cellular mechanism capable of repairing these adducts is the enzyme O^6-methylguanine DNA methyltransferase (MGMT). Because the MGMT can reverse methylation at the O^6 position of guanine and neutralize the cytotoxic effects of alkylating agents, *MGMT* expression in brain tumors represents a key mechanism of resistance toward alkylating agents (Kaina *et al.,* 2007).

The *MGMT* expression in tumor cells is often regulated by epigenetic silencing of the gene via hypermethylation of CpG islands within the *MGMT* gene promoter. Tumor cells with a methylated *MGMT* promoter produce, consequently, less MGMT protein (Wick *et al.,* 2013).

Prior studies had made a correlation between the expression of the methylguanine-DNA methyltransferase (MGMT) protein and the outcome with nitrosourea- based treatment of malignant gliomas. A correlation was also made between methylation of the promoter region of the *MGMT* gene and the improved outcome with the TMZ-based chemoradiation regimen. Determination of the methylation status of the promoter region of the *MGMT* gene was successful obtained in 206 tumor samples (EORTC trial). Overall, there was a statistically significant improvement in both median survival and two-year survival rate for patients with methylated *MGMT*, which suggests that *MGMT* methylation is a positive prognostic factor (Jaeckle *et al.,* 1998; Stupp *et al.,* 2005).

TMZ effect has been investigated in combination with multiple cytotoxic agents or alternatively in monotherapy. Despite its relative advantages, the efficacy of TMZ is constrained by extra-CNS toxicities and biological limits to achieve sustained tumoricidal tissue concentrations, like most other systemic therapies (Wait *et al.,* 2015).

The size of the molecules, the lipophilicity, the short half-lives, the significant

hematologic toxicity, and, principally, the existence of a blood brain barrier and efflux pumps constitute the main limitations of chemotherapeutics. For this reason, novel methods of intracranial drug delivery after surgery are being developed in a way to avoid the adverse systemic effects of these medications. These methods will be discussed in more detail on the section 1.3 of this chapter.

1.1.6 Prognostic factors and clinical decisions

Beyond a vast analysis, age at initial diagnosis, and the time period when the medical treatment is performed, influenced the overall survival of GBM patients, being the older age (≥ 50 years) related to a worse prognosis (Schwartzbaum *et al.,* 2006).

Although age has important implications regarding patient management (comorbidities), patient age also seems to correlate with differences in tumor biology and pathogenesis being the first independent prognostic factor. As described above, primary (*de novo*) and secondary GBMs have strong associations with age. Typically, older patients are more likely to have primary GBMs, whereas secondary GBMs are more often associated with younger patients, who frequently have an established history of lower-grade gliomas (grade II–III). In this way, secondary GBM is associated with a better prognosis and increased overall survival when compared with primary GBM (Beyer *et al.,* 2016; Pelloski and Gilbert, 2007).

The second independent prognostic factor for survival is the time period in which the patients underwent treatment. Specifically, after the diagnose, which is usually tricky due to the common clinical signs, this time period under treatment not only depends on the patient's ability to tolerate treatment, but also on the extent of tumor burden in the brain (Beyer *et al.,* 2016).

Thirdly, the molecular alterations, as consequence of genetic abnormalities, constitute other important prognostic factor in GBM. Mutations in *TP53* gene, a tumor suppressor gene whose damage can cause genetic instability and compromise apoptosis, is frequently observed in low-grade astrocytomas and secondary glioblastomas (Louis, 1994). The *EGFR*, a member of the ErbB receptor tyrosine kinase family, that has a huge role in the proliferation, migration, and differentiation of neural progenitors and glial cells, present an increased amplification in primary glioblastomas (Doetsch *et al.,* 2002). Also the *MGMT* methylation is now well known as the main determinant of resistance to alkylating

agents, as described above (Kaina *et al.,* 2007). The isocitrate dehydrogenase (*IDH*) mutations, *IDH1* and *IDH2*, are mutually exclusive and are seen in lower grade gliomas. *IDH1* mutation is present in diffuse gliomas grade and diffuse anaplastic (II/III, respectively) and in secondary glioblastoma, and so generally associated with a better prognosis (Yan *et al.,* 2009). The *IDH1* mutation is mostly seen in younger patients in the R132 residue and *IDH2* mutation is seen in diffuse gliomas, specifically in the R172 residue (Parsons *et al.,* 2008). The mutations in alpha-thalassemia/mental retardation syndrome X-linked (*ATRX*) gene, situated on chromosome Xq21.1, leads to the loss of expression of nuclear protein, exclusively in tumor cells, and causes alternative lengthening of telomeres, resulting in loss of stability of the genome, frequently in secondary GBM (Abedalthagafi *et al.,* 2013). The telomerase reverse transcriptase (*TERT*) gene causes increased telomerase activity by adding hexamer repeats to the chromosomes, which results in the preservation of telomeres, and inhibits induction of senescence. *TERT* promoter mutations, C228T and C250T, in which transcriptional activity is increased by up to 4 times, results in tumorigenesis principally in primary GBM (Ranjit *et al.,* 2015; Reitman *et al.,* 2013).

The gain of chromosome 7p in combination with 10q loss is the most frequent genetic alteration in GBM, together with the *EGFR* amplification. Also, the allelic loss of the chromosomal region containing the *PTEN* gene occurs in 75- 95% of GBMs and mutations in *PTEN* gene are present in 30-44%, although *PTEN* mutations were not clearly associated with prognosis (Louis *et al.,* 2016).

Among all, on a molecular level, tumors associated with longer survival often exhibit two favourable molecular aberrations: *MGMT* promoter methylation and/ or *IDH* mutation (Louis *et al.,* 2016).

Therefore, surveillance and careful follow-up are extremely necessary due to the fact that high-grade gliomas have a well-known tendency to regrow, which occurs at the same site where the tumor arose. The indications for recurrent GBM are the surgery, radiation therapy, and chemotherapy. Second surgery is generally considered in the face of a life-threatening recurrent mass. Re-irradiation is performed to improve local tumor control and can take the form of conventional fractionation radiotherapy, fractionated radiosurgery, or single fraction radiosurgery (Ranjit *et al.,* 2015; Ryu *et al.,* 2014). Conventional chemotherapy for recurrent disease typically demonstrates a 5–15% response rate and a 15–25% six-month progression-free survival (PFS), which means that the responses to treatment are often not durable. However, unlike patients with newly

diagnosed disease, in the recurrent GBM there is no guide therapy, being the treatment options and decisions often determined by the specific clinical situation and treatment availability. Nonetheless, several clinical trials using alternative chemotherapeutics have been described in recurrent glioblastoma alone and/or in combination with TMZ. The molecular targets/ pathways more altered in GBM and the respective therapeutic strategies are presented in the sections 1.2 and 1.3 of this chapter, respectively.

1.2 CELLULAR AND MOLECULAR MECHANISMS OF GBM – IMPLICATIONS IN RESISTENCE[2]

1.2.1 General Introduction

Several studies have revealed that GBM comprises up to 52% of all gliomas and also constitutes up to 20% of all intracranial tumors (Stavrovskaya *et al.,* 2016). In spite of all efforts, the median overall survival of GBM patients remains only about 12 - 15 months under part of the *gold standard*, temozolomide (TMZ).

The molecular biology underlying GBM is complex, which highlight the need of specific treatment strategies. Among all these mechanisms, the deregulation of several molecular signalling pathways is the more important in GBM development. Also the existence of the blood-brain barrier (BBB), that makes almost all the chemotherapeutic agents inaccessible to the tumor site and, the existence of a population of stem-like cells known to be responsible for tumor recurrence after therapy, can contribute to GBM chemoresistance (Ohgaki and Kleihues, 2007; Ramirez *et al.,* 2013; Zong *et al.,* 2015).

The population of stem-like cells, described as chemo- and radioresistant as well as having a self-renewing stem cell-like phenotype, may contribute to tumor recurrence after conventional treatment, which may represent one of the most important targets in GBM therapy. The multiple intracellular and intercellular signalling pathways that are deregulated in GBM tumor cells are behind the uncontrolled cellular proliferation, propensity for necrosis, angiogenesis, and resistance to apoptosis that characterize the GBM (Castro *et al.,* 2011; Khosla, 2016; Piccirillo *et al.,* 2009; Sanchez-Martin, 2008; Sarkaria *et al.,* 2008; Stupp *et al.,* 2005).

In view of this wide range of possible therapeutic targets, several agents have been developed and evaluated in clinical trials. However, the results have been modest and still far from achieving successful in GBM treatment (Haar *et al.,* 2012).

In this regard, it seems critical to understand the reliable factors responsible for the failure of the most important chemotherapeutic agents, namely regarding the existence of

[2] The present 1.2 section of the chapter 1 is based on the review articles and book chapters published under the scope of this disertation. All images and tables are originally draw based on the literature mentioned in each one, or presented as originally published under the respective license of copyright permission.

a BBB; altered molecular and signalling mechanisms underlying GBM malignancy; the influence of the microenvironment on the maintenance of tumor aggressiveness; and the mechanisms behind glioma-stem-like cell (GSC) plasticity and modulation. Altogether, these factors may be critically important to understand tumor relapse and/ or chemoresistance (Meir *et al.,* 2010).

1.2.2 Blood-Brain Barrier and Glioblastoma

The blood-brain barrier was discovered by Edwin E. Goldmann using intravenous injections of trypan-blue dye in animals. He observed that trypan blue spread throughout the body, but did not stain the brain and spinal cord. However, when trypan blue was injected into the subarachnoid space, the central nervous system was stained, which confirmed the existence of an unknown barrier between the blood and the CNS structures (Dubois *et al.,* 2014; Goldmann, 1909).

In fact, the BBB prevents the penetration into the brain of almost all macromolecules and more than 95% of the small molecules, including anticancer drugs, which makes it one of the most important factors responsible for chemotherapy failure (Chakroun *et al.,* 2017). The presence of the BBB in the tumor area, the blood-brain tumor barrier (BBTB), and the invasiveness of these tumors, are the leading causes responsible for the low 5-year survival rate in patients with GBM (Chakroun *et al.,* 2017).

Anatomically, the BBB is formed by a neurovascular unit that comprises endothelial cells reinforced by astrocytes, pericytes and perivascular macrophages, forming the so-called neurovascular unit. Together with an extensive network of capillaries, the BBB prevents various substances in the bloodstream from entering the brain. BBB can be also formed by the choroid plexus (CP), which is a group of thin membranes located inside the lateral, third and fourth ventricles that produces the cerebrospinal fluid (CSF) in the ventricles of the brain. The CP is composed of a monolayer of specialized epithelial cells that are derived from the ependyma that covers the ventricle walls. This group of membranes is tenfold more extensively vascularized than the brain parenchyma itself, which makes BBB dysfunction a significant contributor to the pathogenesis of a variety of brain disorders (Almutairi *et al.,* 2016; Dubois *et al.,* 2014; Redzic *et al.,* 2005).

GBMs growth are closely associated with the formation of new vessels, since they are the most vascularized tumors in humans. Studies have revealed that the vast majority of gliomas are associated with existing vessels that can displace the astrocytic endfeet from

the vascular surface. This can cause a loss of endothelial cell tight junctions (TJs), resulting in the extravasation of blood-borne molecules such as albumin, cadaverine, or Cascade Blue® tracers into the brain's parenchyma. Furthermore, the vessels that were occupied by gliomas, no longer respond to astrocyte-released vasoregulators (Watkins *et al.,* 2014). As such, astrocyte proliferation, as well as alterations in the microenvironment, interfere with the interactions of astrocytes and endothelial cells and, consequently, cause a loss of the TJs and BBB integrity (Bertossi *et al.,* 1997).

Specifically, in GBM the development of vasogenic brain edema increases dramatically the intracranial pressure (ICP) and induces BBB leakage. The disruption of the BBB can be detected through magnetic resonance imaging, using a contrast medium (Sage and Wilson, 1994). The difficulty of some substances in crossing the BBB is due to the molecular weight, lipid solubility, and polarity (Jue and McDonald, 2016). Additionally, the presence of multiple transport proteins in the endothelial lining of the BBB vascular component also inhibits drugs from reaching the tumor tissue (Van Tellingen *et al.,* 2015). The microvessel density is an important indicator of the prognosis in patients with GBM (Noell *et al.,* 2012).

Pazopanib, paclitaxel, and doxorubicin are some of the substances that have enormous difficulty in crossing the BBB. In fact, pazopanib, an oral VEGF inhibitor with positive results in renal-cell carcinoma, breast and lung cancer, cannot be used in GBM patients due to the BBB and efflux mechanism, described in more detailed in the next sections (Mao *et al.,* 2012). The figure 1.9 is a schematic representation of the blood-brain barrier constitution.

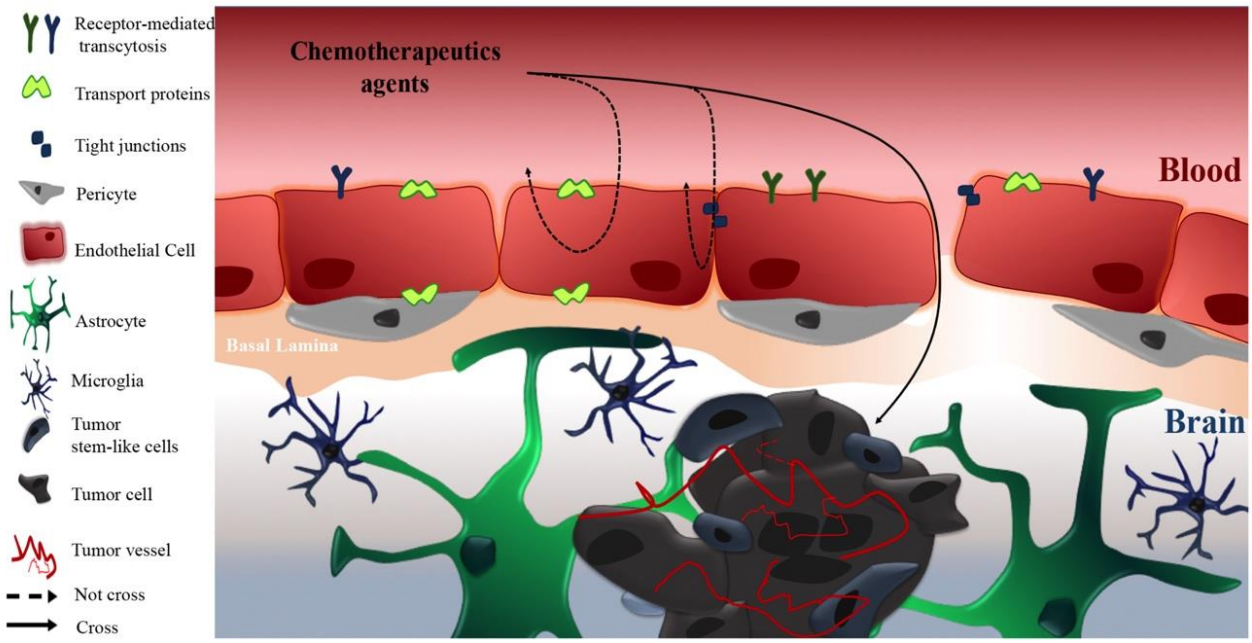

Figure 1.9 Schematic representation of the Blood-Brain Barrier. The BBB is composed of several cell types in combination, including highly specialized and polarized endothelial cells, a basal lamina, pericytes and astrocyte endfeet, which are responsible for establishing communication with neurons in the so-called neurovascular unit. The neurovascular unit is important to maintain optimal brain function. In this image are represented the respective cells or structures: receptor-mediated transcytosis, protein's transporter, tight junctions, pericytes, endothelial cells, astrocytes, microglial cells, tumor stem-like cells, tumor cells and tumor vessels (Image originally draw based on Dubois *et al.,* 2014).

1.2.3 Genetic and Molecular alterations in Glioblastoma

There are indubitably several genetic and other molecular alterations present in GBM that lead to the deregulation of major signalling pathways, resulting in brain tumor growth and progression (Crespo *et al.,* 2015).

Glioblastoma *IDH*-wild-type (about 90% of cases) corresponds, most frequently, to the clinically defined primary or *de novo* GBM, and the glioblastoma IDH-mutant (about 10% of cases) corresponds to the secondary GBM, with a history of prior lower grade diffuse glioma that preferentially arises in younger patients (Fujisawa *et al.,* 2000; Louis *et al.,* 2016; Nonoguchi *et al.,* 2013). The gene mutations/ alterations that characterize each GBM type were described in more detailed in the previous section 1.1.

In general, primary GBMs are characterized by several genetic and epigenetic mutations. The main alterations previously reported are the presence of a mutation of the epidermal growth factor receptor (*EGFR*), and/or a mutation on chromosome 7p; the

homozygous deletion of the cyclin-dependent kinase inhibitor 2A gene (*CDKN2A/p16*) in chromosome 9p (with absence of the CDKN2A-p16INK4a and/or the CDKN2A-p14ARF b transcripts); deletion of the phosphatase and tensin homolog (*PTEN*) in chromosome 10; *IDH1/2* mutations; and hypermethylation of the *MGMT* promoter (Carmo *et al.,* 2011b; Crespo *et al.,* 2015), as mentioned. These genetic alterations seem to be critical to the development of GBM, and may contribute to the heterogeneity that characterizes these tumors (Popescu *et al.,* 2016). The affected genes are critical to the signalling pathways that are involved in the control of proliferation and survival of astrocytes, which may explain the aggressiveness of GBM. An illustration of the genetic and molecular alterations is shown in figure 1.10 and described in more detail next.

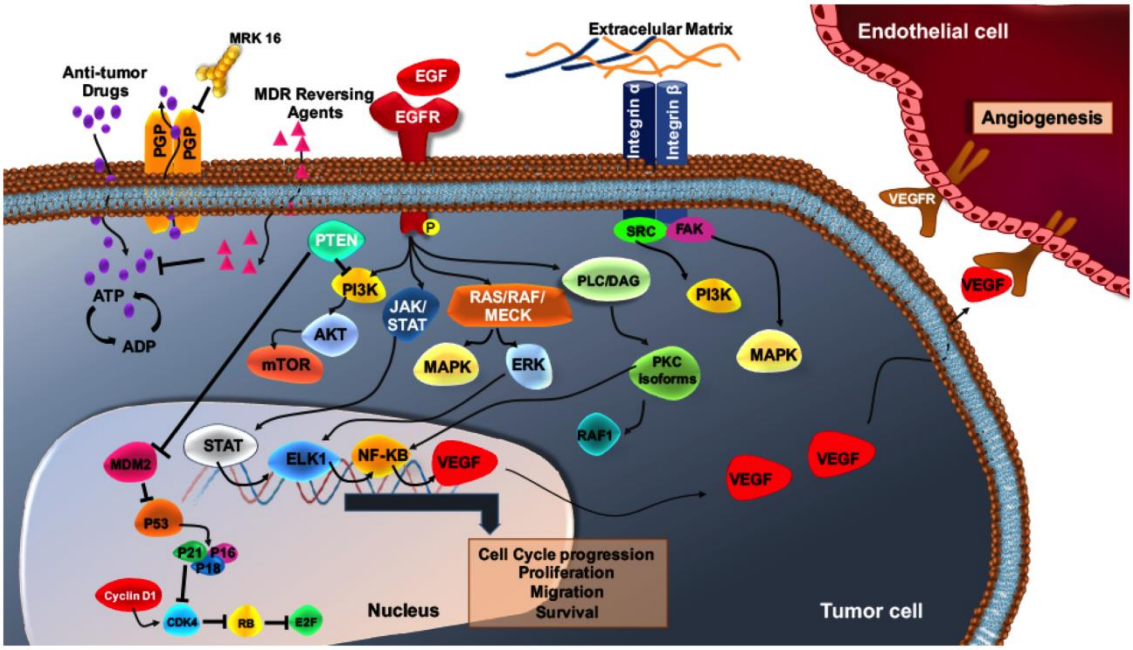

Figure 1.10 Molecular Signalling Pathways altered in Glioblastoma. A few molecular alterations have been identified in GBM as the deregulation of protein transporters and channels, namely Glycoprotein P (PGP), involved in drug efflux; deregulation of signal-transduction pathways, mainly those downstream of epidermal growth factor receptor (EGFR), such as the RAS/ RAF mitogen-activated protein kinase (MAPK), the Phosphatidylinositol-4,5-bisphosphate 3-kinase/ Protein kinase B (PI3K/AKT), and the signal transduction and transcription activator (STAT). Others are the protein kinase C (PKC) pathway, tumor suppressor P53 deregulation, the retinoblastoma protein (RB) pathway, the vascular endothelial growth factor (VEGF) signalling and integrin function deregulation. Together, these molecular alterations culminate in the cell-cycle progression, cell survival and proliferation, and in an increase of cell-migration capability in tumor cells, particularly in GBM cells (Image originally draw based on Haque *et al.,* 2011 and Li *et al.,* 2016).

Genetic alterations with clinical impact -

Amplification and/or mutation of the *EGFR* gene (7p11.2) occur in 36% to 60% of primary GBMs. The most common *EGFR* mutant type is variant 3 (*EGFRvIII*), a 801-bp in-frame deletion of exons 2 to 7. This mutation leads to a constitutively active protein expression, which, in turn, leads to the increase in cellular proliferation and survival of mutated cells, since it activates the EGFR – phosphatidylinositol3-kinase (PI3K) pathway (Popescu *et al.,* 2016). All primary GBMs with *EGFR* amplification show EGFR overexpression (Crespo *et al.,* 2015; Hatanpaa *et al.,* 2010).

The homozygous deletion of the cyclin-dependent kinase inhibitor 2A (*CDKN2A)* gene, which encodes the p16INK4a and p14ARF tumor suppressors, is more frequently observed in primary than in secondary GBMs (Ohgaki and Kleihues, 2007). CDK4 and CDK6 phosphorylate the retinoblastoma protein 1(RB1), which induces the release of the transcription factor E2F, facilitate the cell cycle progression from the G1 to S phase. About 80% of primary GBMs show alterations in the CDKN2A/p16-CDK4/6-RB pathway, for which *CDKN2A* gene deletion or mutation, *CDK4* amplification, and *RB1* mutation or deletion are the main reasons (Goldhoff *et al.,* 2012).

Loss of heterozygosity (LOH) of chromosome 10 is present in up to 70% of primary GBMs. One of the most commonly deleted chromosomal regions is 10q23-24 (25%), where the *PTEN* is localized. Primary GBMs frequently show the loss of chromosome 10 in association with EGFR signalling, which suggests an important interaction between EGFR signalling and the suppressor genes localized in chromosome 10 in the aggressive features of GBM (Carico *et al.,* 2012; Crespo *et al.,* 2015).

Another important genetic alteration in GBM is isocitrate dehydrogenase (*IDH*) gene mutations (Yan *et al.,* 2009), as referred. In gliomas, *IDH1/2* mutations are associated with an increased DNA hypermethylation profile. Isocitrate dehydrogenase catalyses the oxidative decarboxylation of isocitrate to α-ketoglutarate, leading to the production of NADPH. The IDH1 protein is believed to play a substantial role in cellular control of oxidative damage, through generation of NADPH; and the IDH2 plays an important role in intermediary metabolism and energy production. The *IDH1/2* mutations are involved in inactivation of tumor-suppressor genes via hypermethylation of their promoters. Gliomas with mutated *IDH1* and *IDH2* have a better prognosis than gliomas with wild-type *IDH*

(Cohen *et al.,* 2013). Parsons et al. (2008) revealed the presence of recurrent (12%) point mutations in the active site of *IDH1* (Parsons *et al.,* 2008). The *IDH1* mutations in diffuse gliomas seem to be strongly associated with *TP53* mutation and also with del(1p)/del(19q), indicating that they may represent an early event (Parsons *et al.,* 2008). *IDH* mutations are more common in secondary GBM (~ 80%) compared to primary GBM (5%) (Jue and McDonald, 2016; Lin and Scott, 2012).

Also as previously described, the *MGMT* gene (coded at chromosome 10q26) is also an important alteration in GBM, since it is frequently silenced by promoter hypermethylation, in association, or not, with monosomy of 10/del(10q). Currently, *MGMT* methylation promoter *status* has been established as a strong clinically relevant factor in GBM patients, although the mandatory testing for this biomarker in routine practice is highly controversial. Studies have encouraged mandatory testing for *MGMT* promoter *status* in routine practice in elderly GBM patients, due to the observation of a strongly predictive value of this biomarker and a potent predictor of response to treatment with alkylating agents, namely temozolomide (TMZ) (Zawlik *et al.,* 2009). In the presence of TMZ, an alkyl group is added to the O^6-position of guanine, inducing a DNA mismatch, and consequently a DNA double-strand breakage, which culminates in apoptosis of proliferating cells. The MGMT protein has the opposite effect than the TMZ, by repairing DNA damage before the next cell cycle. However, when the *MGMT* promoter is hypermethylated, transcription is blocked, leading to lack of the MGMT protein, while enhancing the cytotoxic effects of the alkylating drug(s) (Crespo *et al.,* 2015). The *MGMT* promoter is methylated in approximately 50% of newly diagnosed GBMs, and in a higher percentage (73%) in secondary glioblastomas (Kaina *et al.,* 2007; Lin and Scott, 2012; Ohgaki and Kleihues, 2007).

Summarizing, in GBM several tumor suppressor genes and oncogenes are inactivated or activated, respectively. Primary GBMs are characterized by *EGFR* amplification, *PTEN* mutation, and absence of *IDH* mutations, while secondary GBMs are characterized by *TP53* mutations, *IDH* mutations, and lack of *EGFR* amplification (Lin and Scott, 2012). Recently, Jiao *et al.,* (2012) also described *ATRX* mutations in diffuse glioma, associated with an alternative lengthening of telomeres in secondary GBM (Jiao *et al.,* 2012), as previously described in section 1.1. These main genetic alterations culminate in several molecular alterations, mainly: 1) deregulation of protein transporters and channels involved in control of cancer progression, owing to their protection by the BBB (Abbott, 2013; Cong *et al.,* 2015); 2) deregulation of signal-transduction pathways, mainly those

downstream of EGFR, which become activated in GBM due to autophosphorylation, such as the RAS/ RAF/ MAPK, the Phosphatidylinositol-4,5-bisphosphate 3-kinase/ Protein kinase B (PI3K/AKT/mTOR), and the signal transduction and transcription activator (STAT) and finally, 3) the deregulation of the protein kinase C (PKC) pathway, the P53 and RB pathway, and the integrin function (Arora and Scholar, 2005; Baselga, 2006; Carmo *et al.,* 2013).

Cell signalling pathways altered in GBM -

EGFR/ AKT/ PTEN pathway

The endothelial growth factor receptor (EGFR) is a member of the ERBB family of receptor tyrosine kinase proteins, which comprises not only the EGFR (termed ERBB1) (EGFR/HER1), but also the ERBB2 (HER2/neu), ERBB3 (HER3), and ERBB4 (HER4) (Mellinghoff *et al.,* 2005). In terms of structural composition, these receptors are composed of an extracellular ligand-binding domain, a transmembrane lipophilic domain, and an intracellular tyrosine kinase domain. Binding of a specific set of ligands to these receptors, namely the endothelial growth factor (EGF) and the transforming growth factor-α (TGF-α), promotes EGFR dimerization and the consequent autophosphorylation of tyrosine residues (Baselga, 2006). Upon autophosphorylation, several signal-transduction pathways, downstream of EGFR, become activated: 1) the rat sarcoma (RAS)/rapidly accelerated fibrosarcoma (RAF)/mitogen-activated protein kinase (MAPK) pathway; 2) the phosphatidylinositol-3-kinase (PI3K)/protein kinase B (AKT) pathway; 3) the janus kinase (JAK)/signal transducers and activators of the transcription (STAT) pathway; and 4) the protein kinase C (PKC) pathway (Arora and Scholar, 2005; Balça-Silva *et al.,* 2015; Baselga, 2006; Carmo *et al.,* 2013; Huang and Fu, 2015). Taking into consideration that these signalling pathways control cell growth, regulate cell survival and proliferation, and also that the overexpression of EGFR has been reported in several epithelial tumors, the EGFR/AKT/PTEN pathway is considered a potential target for cancer therapy (Baselga, 2006).

As previously mentioned, in GBM, the most common mutation is the *EGFRvIII*, which leads to the synthesis of a constitutively active protein that activates PI3K by its recruitment to the cell membrane (Feldkamp *et al.,* 1999; Gan *et al.,* 2013; Shinojima *et al.,* 2003). The phosphorylation of phosphatidynositol-4,5-bisphosphate (PIP2) to the

respective 3-phosphate originate phosphatidynositol-3,4,5-triphosphate (PIP3) that activates a range of downstream effector molecules such as AKT (Furnari *et al.,* 2007; Hirose *et al.,* 2005). In turn, the activated AKT regulates the functioning of downstream signalling proteins involved in cell cycle, proliferation, apoptosis and invasion, contributing to tumorigenesis. On the other hand, the action of PI3K can be antagonized by the action of the *PTEN* gene. PTEN protein removes the third phosphate from the inositol ring of PIP3, inhibiting the PI3K pathway, which makes *PTEN* a tumor suppressor gene (Mellinghoff *et al.,* 2005). In this way, *PTEN* is also associated with the G1 cell cycle arrest and apoptosis, along with regulating cell differentiation (Di Cristofano and Pandolfi, 2000).

AKT is essential for gliomagenesis, although its downstream effectors are still incompletely identified. However, the serine/threonine kinase mTOR, which forms the catalytic core of at least two functionally distinct complexes, mTORC1 and mTORC2, is associated with increased cell proliferation, mainly in GBM, enhancing motility and promoting glioma cell proliferation *in vitro* (Akhavan *et al.,* 2010). mTOR is responsive to growth-inhibitory signals, mainly the depletion of glucose, amino acids and ATP, hypoxia, and lack of growth factors (Wullschleger *et al.,* 2006).

Protein Kinase C pathway

We previously described the importance of Protein Kinase C (PKC) in glioma proliferation (Balça-Silva *et al.,* 2015). The activation of PKC modulates a wide range of cellular responses, mainly in gene expression, cell proliferation, survival and migration (Carmo *et al.,* 2013). PKC is a serine/threonine kinase that belongs to the PKC family, and was identified as a receptor for diacylglycerol (DAG) (da Rocha *et al.,* 2002; Basu and Sivaprasad, 2007; Martiny-Baron and Fabbro, 2007; Steinberg, 2008). PKC isoforms are classified into three groups, according to their activation mechanisms: the classical isoforms α, βI, βII, γ; the novel PKC isoforms δ, ε, θ, η, μ; and the atypical PKC isoforms ι/λ and ζ (Carmo *et al.,* 2013). In general, the PKC isoforms are inactive and located in the cytoplasm. After activation they translocate to the plasma membrane, or the cytoplasmic organelles and nucleus, which makes possible the modulation of several cellular mechanisms, mainly cell proliferation, differentiation, cell death, and neuronal activity (Figure 1.11) (Carmo *et al.,* 2013). PKC is directly involved in tumorigenesis due to its capability to regulate molecular signalling pathways involved in tumor-development

processes, mainly cellular proliferation, survival, migration, or chemoresistance (Griner and Kazanietz, 2007; Totoń *et al.,* 2011). However, the contribution of the PKC family to the development of GBM is poorly understood. The PKCα is important as a pro-mitotic, pro-survival, and pro-proliferative effect in glioma cell lines (Brennan *et al.,* 2009). PKCβ is involved in vascular endothelial growth factor receptor 2 (VEGFR2) signalling, and also interacts with the phosphatase and tensin homolog (PTEN)/PI3K/AKT pathway, which makes it important for glioma angiogenesis in a way that contributes to the increase of cell proliferation and resistance to apoptosis (Graff *et al.,* 2005). PKCδ acts as a pro- or anti-apoptotic kinase, depending on the cell type. In glioma cells, PKCδ acts as an anti-apoptotic, protecting cells from cell death induced by TNF- related apoptosis-inducing ligand (TRAIL) (Okhrimenko *et al.,* 2005). PKCε is considered an important marker of negative outcome, mainly in anaplastic astrocytoma, GBM, and gliosarcoma. The PKCε knockdown sensitized glioma cells to apoptosis (Sharif and Sharif, 1999). PKCη is also related to increased GBM cell proliferation through the activation of the ERK pathway (Uht *et al.,* 2007).

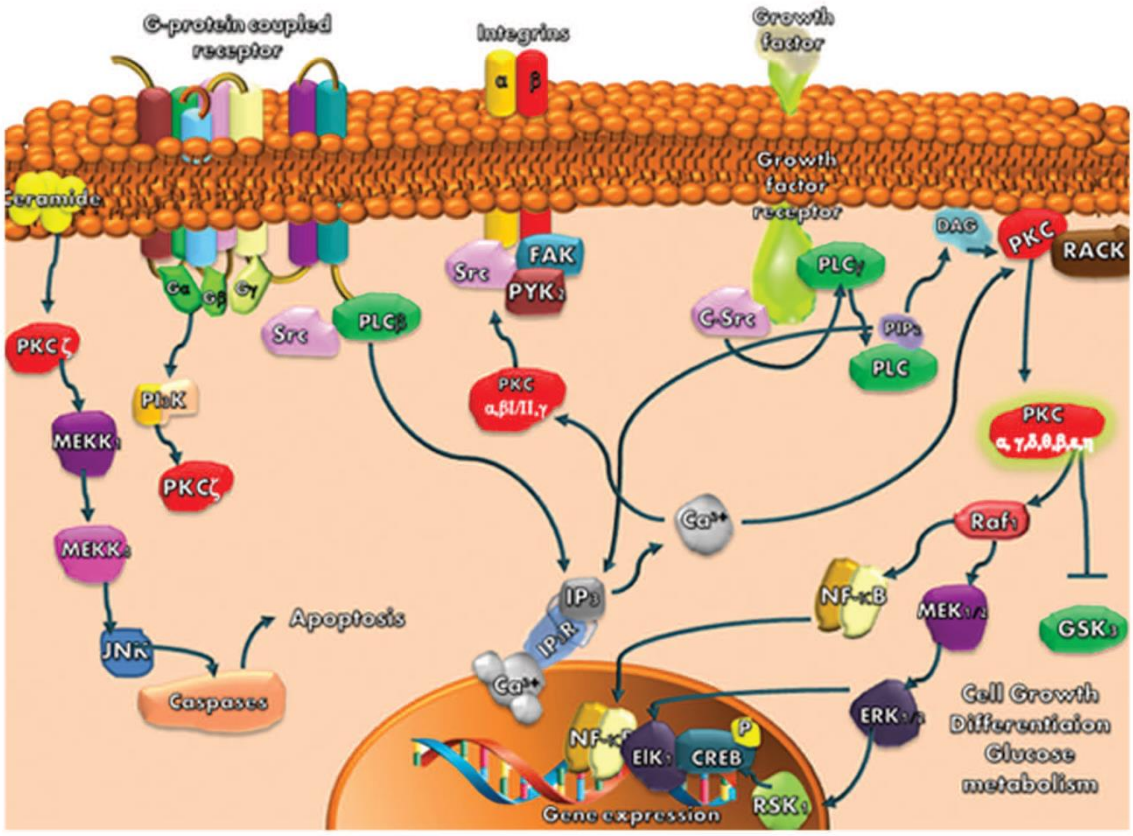

Figure 1.11 PKC isoforms signalling pathways. The different PKC isoforms modulate several cellular mechanisms, mainly cell proliferation, differentiation, cell death, and neuronal activity

(Image as originally published in Carmo *et al.,* 2013 under the copyright permission of Taylor & Francis journal).

The PKCι isoform contributes to a deregulation of upstream PI3K signalling, contributing to invasion of GBM cells, cell-cycle progression, and increased proliferation (Baldwin *et al.,* 2010). Finally, the PKCζ isoform is responsible for a mitogenic phenotype in GBMs, through activation of the PI3K/AKT pathway (Aeder *et al.,* 2004). The PKC family is upregulated in high-grade gliomas compared with normal astrocytes, and this upregulation correlates with greater tumor proliferation, which makes PKC a candidate for the development of molecularly targeted therapies (Carmo *et al.,* 2013; Lau *et al.,* 2014).

P53 signalling pathway

P53 is known as the "guardian of the genome". The main function of *P53* is to ensure that DNA is copied correctly, which means that it induces apoptosis during DNA and cell duplication if there are mutations. This signalling pathway is activated in response to several stress signals, which culminate in the activation of several mechanisms that contribute to tumor suppression. The P53 function is intrinsically related to phosphorylation of Ser15 and Ser20 of the P53 N-terminal. The E3-ligase MDM2 usually targets P53 for degradation in the proteasome, but after phosphorylation it does not occur, which results in protein stabilization and accumulation in the nucleus, where it regulates the potential of several genes that control the cell cycle, apoptosis and DNA repair (do Carmo *et al.,* 2010). This function makes *P53* an extremely important tumor-suppressor gene, and its loss of function is a feature common to several cancers (Milinkovic *et al.,* 2012). *P53* gene mutations are present in about 30% of primary GBM and occur more frequently in secondary GBM (about 65%) (McLendon *et al.,* 2008). PTEN, a tumor suppressor enzyme that is frequently mutated in GBM, protects wild-type *P53* from inactivation and degradation through the inhibition of PI3K and inhibition of *MDM2* transcription (Mayo *et al.,* 2002). Since MDM2 regulates the P53 activity, the inhibition of P53-MDM2 is considered a potential therapeutic approach (Shangary and Wang, 2009).

Retinoblastoma signalling pathway

Retinoblastoma (RB) is a tumor suppressor gene located at the chromosome 13q14 that inhibits gene transcription by arresting the cell cycle in the G1-S phase, preventing cell proliferation. The RB pathway includes several proteins, mainly the cyclin-dependent

kinase inhibitor (CDKN), the cyclin D-dependent protein kinases (CDK4, CDK6), the E2F-family, and the RB-family (RB, p107, p130) of transcription factors (Knudsen and Wang, 2010; Meir *et al.,* 2010; Scambia *et al.,* 2006). RB activation depends on the phosphorylation status, which is high in quiescent or differentiated cells (Harbour and Dean, 2000). Hypophosphorylated (active) RB binds to the E2F family of transcription factors, blocking cell cycle and proliferation. By acting through E2F, RB alters the proteins needed for the S-phase (Zeng *et al.,* 2015). The inactivation of RB inhibits the capability of cells to suppress cell proliferation, which leads to uncontrolled cell division. In GBM, the *RB1* gene is mutated in 25% of high-grade gliomas, while the loss of 13q is characteristic of the transition from low-grade to intermediate-grade gliomas (Zeng *et al.,* 2015).

Vascular endothelial growth factors

Vascular endothelial growth factors (VEGFs) are produced mainly by endothelial, hematopoietic and stromal cells, in response to hypoxia or after stimulation with growth factors, mainly the transforming growth factors (TGFs) or interleukins. VEGFs can bind to their respective receptors (VEGFRs), which induces its dimerization and subsequent phosphorylation, leading to the activation of several intracellular signalling molecules: PI3K, phospholipase Cg (PLCg), PKC, nitric-oxide synthase (NOS), MAPKs, and focal adhesion kinases (FAKs) (Karkkainen and Petrova, 2000).

The VEGF family and the respective receptors is used in cancer therapy as regulators of angiogenesis and vascular permeability, thus reducing tumor growth. The overexpression of *VEGFR1* in tumor cells leads to cell survival and invasion (Carmo *et al.,* 2011a; Huang and Fu, 2015). The activation of VEGF/VEGFR is associated with anti-EGFR drug resistance, through activation of downstream signal pathways via EGFR-independent mechanisms (Bianco *et al.,* 2008). The most important therapeutic applications of VEGF in GBM are described in more detail in the next section of this chapter.

Integrin signalling pathway

The invasiveness capacity of glioma cells is intended as an active translocation of glioma cells through host cellular and extracellular matrix barriers. Glioma cells invasion

is based on: 1) loss of adhesion of cells to proteins of the external cellular matrix (ECM); 2) degradation of the ECM components by proteases secreted by glioma cells and 3) migration of cells into the new space through the ECM (Uhm *et al.,* 1997).

Basically, ECM is composed by proteoglycans, glycoproteins, collagens and contains fibronectin, laminin, tenascin, hyaluronic acid and vitronectin. ECM modification mostly originates the loss of contact, which in the case of tumor, allow tumor cells to freely migrate and invade the surrounding tissues. Therefore, changes in these ECM components are known to modulate brain tumor growth, proliferation and invasion. In fact, during the tumor invasion, independent, but coordinated, processes are presented: 1) the tumor mass detaches from the original location, which implicates downregulation of neural cell adhesion molecules (NCAMs) and E-cadherin, as well as upregulation of cell surface glycoprotein (CD44), as an adhesion molecule; 2) the interaction with the extracellular matrix (ECM), mediated by integrins and tenascin-C, which leads to the degradation and remodeling of the ECM, including the modulation of the metalloproteinase (MMP) activity. These proteases are responsible for the breakdown of the basal membrane, creating and maintaining a microenvironment that facilitates tumor cell survival (Moura-Neto *et al.,* 2014).

The most common molecules that allow glioma cells to adhere to the ECM are the integrins, playing a major role in glioma cell-matrix adhesion (Onishi *et al.,* 2013). Integrins form dimers between 18 different α and 8 β subunits, which form 24 known α/β integrin pairs with specificity for different ECM proteins, namely fibronectin, laminin, vitronectin, thrombospondin, fibrinogen/fibrin, matrix metalloproteinase-2, and fibroblast growth factor 2, via an arginine- glycine-aspartic acid peptide (Figure 1.12) (Humphries, 2006; Hynes, 2002; Lau *et al.,* 2014; Moura-Neto *et al.,* 2014). Elevated expression of integrin receptors has been detected in GBM tumor samples, mainly the integrins α2β1, α5β1, α6β1 α9β1, and αvβ3, in contrast to their expression in normal brain tissue, which suggests that integrins have important functions during GBM progression, namely in the activation of several signalling cascades that mediate cellular adhesion, proliferation, survival and migration, namely PI3K and MAPK. Particularly, the integrin αvβ3 is thought to play a central role in glioma invasion, binding to bronectin, vitronectin, and tenascin-c, and therefore, the overexpression of αvβ3 integrin signifies a poor prognosis in glioma (Nakada *et al.,* 2013; Riemenschneider *et al.,* 2005; Zeng *et al.,* 2015).

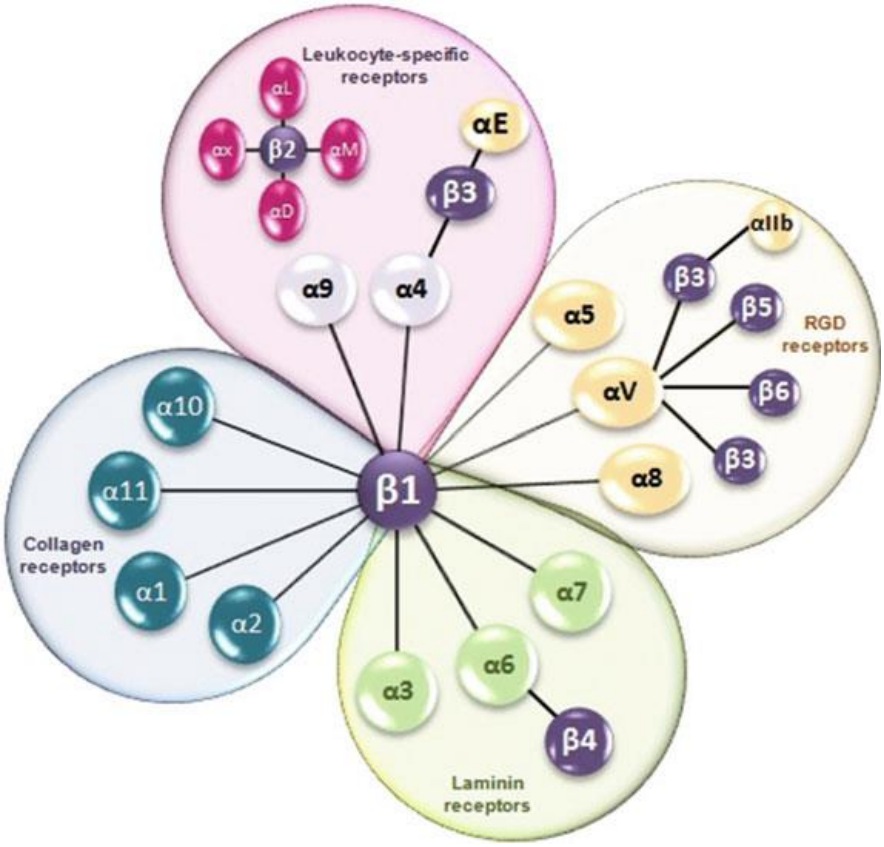

Figure 1.12 The integrin subfamilies. Integrins are the main receptors for ECM proteins, counter receptors (intercellular adhesion molecules (ICAMs), and vascular cell adhesion molecule (VCAM)), and soluble molecules (fibrinogen). There are four different subfamilies: the RGD-binding integrins (yellow), laminin-binding integrins (green), leukocyte integrins (pink), and collagen integrins (blue) (Image as originally published in Moura-Neto *et al.,* 2014. License number: 4012940949469).

Protein Transporters

GBM show alterations in the protein-transport pathways involved in regulating cell-signalling pathways and in the control of tumor-cell homeostasis and development. Several studies have revealed that targeting ion transporters and channels, in cancer cells, may open new prospects for cancer therapy (Cong *et al.,* 2015). Changes in transporters are critical not only when they occur in astrocytes, but also when they occur in endothelial cells. Among the several components of the BBB previously mentioned, drug transporters are located in BBB endothelial capillaries, taking part in their defense functions. Drug transporters are critically involved in the passage of chemotherapeutic agents, exporting foreign substances from cells (Deeken and Loscher, 2007; Hartz and Bauer, 2011; Miller, 2015; Pardridge, 2003). Among the ion-transporter proteins, the most important are the

sodium-potassium-chloride co-transporter isoform 1 (NKCC-1) and sodium-hydrogen exchanger isoform 1 (NHE-1). NKCC-1 belongs to the *SLC12 cation-chloride co-transporter* (*CCC*) gene family, and transports $1Na^+$, $1K^+$ and $2Cl^-$, through the cell membrane, maintaining homeostasis of intracellular water and salt, in both astrocytes and endothelial cells. NHE is a group of membrane proteins that transport one H^+ from cells in exchange for one Na^+ into cells, maintaining the optimal pH of tumor cells. NHEs are critically important in glioma cell proliferation, migration, invasion, metabolism, and apoptosis (Cong *et al.,* 2015; Glunde *et al.,* 2002; Reshkin *et al.,* 2000; Russell, 2000; Su *et al.,* 2002).

Specifically, NKCC-1 plays a key role in regulating the cell-cycle progression and proliferation, through modulating the cell volume. In human glioma, NKCC-1 protein is overexpressed and is positively correlated with the tumor grade. Also, NKCC-1 is an essential ion cotransporter in glioma progression, by counteracting TMZ-induced apoptosis, and facilitating migration and invasion. Therefore, inhibition of NKCC-1 with bumetanide may be a feasible therapeutic strategy for glioma treatment, through augmenting the toxicity of chemo-radiotherapy. Several kinases have been proposed to regulate NKCC-1 activity through phosphorylation. Among them are the WNKs/SPAK/OSR1 cascade, as well as protein kinase A, protein kinase C, Rho, Janus kinase 2, and CamKinase II (Cong *et al.,* 2015). NHE regulates the pH, causing acidification of the extracellular microenvironment. The increase of NHE-1 activity is associated with multiple Ser/Thr residue phosphorylation in the C-terminal tail region, and is overexpressed in brain tumors (Attaphitaya *et al.,* 1999).

Also, the ATP-binding cassette (ABC) transporters move biologically important substrates across the cell membranes, including amino acids, cholesterol, and hydrophobic drugs and antibiotics (Glunde *et al.,* 2002; Huang and Fu, 2015; Hubensack *et al.,* 2008; Reshkin *et al.,* 2000; Russell, 2000). The group of ATP-dependent protein transporters, which transport ATP-dependent proteins through concentration gradients, consists of the ABC transporter family, which includes P-glycoprotein (PGP), multi-drug-resistance protein (MRP), and breast cancer-resistance protein (BCRP) (Molnár *et al.,* 2010). These proteins are involved in diverse regulation processes that are responsible for efflux of substances from tumor cells (Haar *et al.,* 2015). Specifically, overexpression of PGP, encoded by the *MDR1* gene, confers resistance to a wide variety of antitumor drugs such as vinblastine, vincristine, and doxorubicin, among others. PGP is located on the plasma membrane of the more resistant cancer cells, and transports the antitumor drugs in an ATP-

dependent manner (de Vries *et al.,* 2012; Hamada and Tsuruo, 1988; Molnár *et al.,* 2010; Tsuruo *et al.,* 2003). PGP has also been detected in blood vessels that supply human gliomas and metastatic brain tumors (Haar *et al.,* 2015).

Since MDR1 mRNA expression in gliomas has proved to be correlated with certain clinical drug-resistance mechanisms, the *MDR1* promoter activity in cancers is up-regulated. This is consistent with the presence of some anticancer drugs, DNA-damaging agents, heat-shock stimuli, ultraviolet irradiation, or even as a consequence of tumor progression, through mutation of the tumor suppressor gene *P53* and/ or activation of the *RAS* oncogene (Tsuruo *et al.,* 2003).

1.2.4 Cancer stem-like cells in brain tumors

Cancer stem-like cells (CSCs) were first identified in GBM in 2004, as glioma stem-like cells (GSCs), according to the cell-surface expression of the CD133 protein (Singh *et al.,* 2004). The CSC model posits that, among all cancerous cells, a few can act as stem cells that reproduce themselves and sustain the cancer, similarly to normal stem cells that have the ability to renew and sustain the organs and tissues. However, because not all cells of the putative CSC population are able to seed tumors, the concept of tumor initiating cells (TIC) was introduced. These cells can either be a normal adult stem cell, in the case of the neuronal lineage, the neuronal stem cell (NSC), or a differentiated cell that has gone to oncogenic processes, thus acquiring a stem-like character. The expansion of these cells by acquiring mutations during progression may result in the development of the CSC (Fonseca *et al.,* 2017).

A CSC is responsible for tumorigenesis, as it is capable of self-renewal and differentiation into the various cellular types that comprise the tumor, contributing to the heterogeneity and complexity of tumors. Despite being abnormal, these CSC share features of normal stem cells, namely the self-renewal and differentiation capacity, as mentioned (Fonseca *et al.,* 2017). As such, GSCs represent a subpopulation of cells within GBM that is characterized by increased resistance to chemo- and radiotherapy. Residual tumor cells, mainly GSCs in GBM niches around the tumor niche, lead to recurrence even after intensive primary treatment, which suggests that GSCs are crucial to GBM resistance (Bao *et al.,* 2006; Hide *et al.,* 2013; Liebelt *et al.,* 2016). Thus, GSCs are considered an important target for GBM therapy since they are at the basis of the poor prognosis, treatment failure, and disease relapse (Seymour *et al.,* 2015).

Glioma stem-like cell molecular and transcription factors -

Normal stem cells (NSCs) have the ability to self-renew and differentiate. GSCs and NSCs share several intracellular and extracellular signalling pathways, crucial in GSC malignancies understanding, and therefore potential targets for anti-GSC therapy (Jhanwar-Uniyal *et al.,* 2015; Liebelt *et al.,* 2016; Seymour *et al.,* 2015). Regarding membrane-bound receptor-mediated signalling, the CD133 is one of two members of the pentaspan transmembrane glycoprotein prominin family and a human homolog of the originally isolated mouse PROM1 located in stem cells (Weigmann *et al.,* 1997). However, due to unresolved problems, there is much contradictory information regarding the potential of CD133 to be classified as a marker for GSC isolation (Beier *et al.,* 2007; Ogden *et al.,* 2008). Also, the L1 cell-adhesion molecule (L1CAM/ CD171) is a membrane-bound receptor and a regulator of cell survival, preferentially expressed in CD133+ GSCs, overexpressed in human gliomas, and related to the invasive phenotype (Bao *et al.,* 2006; Izumoto *et al.,* 1996). As described above, receptor tyrosine kinases (RTKs) are also cell-surface receptors for many growth factors, cytokines, and hormones, and are critical in the development of many cancers, mainly the amplification of the EGF receptor (*EGFR*) gene; targeting EGFR leads to the eradication of GSCs (Inda *et al.,* 2010). The TGF-ß superfamily of proteins are membrane-bound receptors that play a critical role in maintaining the self-renewal and multi-lineage differentiation potential of glioma cell lines, mainly through the SOX4-mediated SOX2 induction (Ikushima *et al.,* 2009). Another membrane-bound receptor is NOTCH, which when activated is involved in regulating self-renewal, cell growth, and clonogenic survival capability of GSCs (Gaiano and Fishell, 2002; Wang and Dai, 2010). Regarding the intercellular signalling pathways that are responsible for stemness, the IL-6 protein, from the IL-6 family of cytokines, is a ligand correlated with poor survival of GBM patients, since phosphorylation and nuclear translocation of STAT3 are associated with histopathologically higher grades of human gliomas (Weissenberger *et al.,* 2004). The Sonic hedgehog (SHH) and WNT pathways play an important role in normal stem-cell regulation and in tumorigenesis. The SHH ligand is expressed in glioblastoma-derived neurospheres and binds to the Patched-1 (Ptc1) receptor, resulting on the loss of Ptc1 activity and in the consequent activation of Smoothened (SMO), which leads to the activation of the transcription factors of the GLI family. In fact, some studies correlate SHH signalling in PTEN-positive GBMs with

reduced patient survival (Bar *et al.,* 2007). The WNT signalling pathway also controls the size of the NSC population through ß-catenin activation. ß-catenin translocates into the nucleus and binds to the TCF/LEF. Finally, as described above, integrins also interfere with the activation of several signalling cascades that culminate in CSC proliferation (Riemenschneider *et al.,* 2005).

Regarding stem-cell transcription factors that are involved in cell maintenance, the sex-determining regions Y-Box (SOX2), octamer-binding transcription factor 4 (OCT4), and Nanog homeobox (NANOG) are critical components in maintaining pluripotency in embryonic stem cells (ESCs) and somatic stem cells (SSCs) (Seymour *et al.,* 2015). SOX2, OCT4, and NANOG are highly expressed in subpopulations of GSCs, maintaining self-renewal and cellular proliferation, which contribute to the multilineage potential and heterogeneity of GSCs (Gaiano and Fishell, 2002). *SOX2* encodes a transcription factor consisting of 317 amino acids, and contains a high-mobility group DNA-binding domain (Boyer *et al.,* 2005). OCT4 is a member of the Pit–Oct–Unc transcription family that activates and represses genes (Karoubi *et al.,* 2010). Finally, NANOG is a homeobox protein that cooperates with SOX2 and OCT4 in regulating genes that are vital to the early development of ESCs (Loh *et al.,* 2006). Growing evidence correlates the expression of SOX2, OCT4, and NANOG with pathological grades of gliomas, by promoting self-renewal as well as the multilineage potential within GSCs (Du *et al.,* 2009; Favaro *et al.,* 2014; Niu *et al.,* 2011) (Figure 1.13).

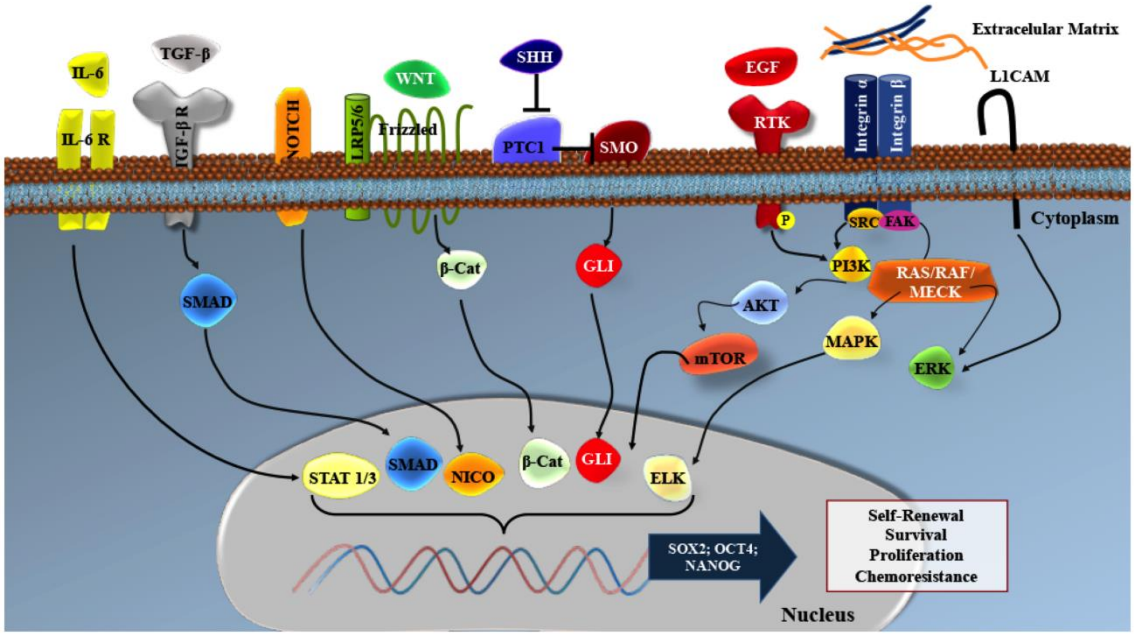

Figure 1.13 Glioma stem-like cell signalling pathways. Some alterations in molecular signalling culminate in deregulation of transcription-factor expression, which characterizes GBM cells, mainly: the receptor tyrosine kinases (RTKs), through amplification of the EGF receptor (*EGFR*) gene that targets EGFR; the transforming growth factor beta (TGF-ß) superfamily protein receptor, through the transcription factor SOX4-mediated SOX2 induction; the L1 cell adhesion molecule (L1CAM, CD171); the NOTCH receptor; the interleukin IL-6 protein, through phosphorylation and nuclear translocation of signal transducer and activator of transcription 3 (STAT3); the Sonic hedgehog (SHH) through the Ptc1 receptor; and WNT through the frizzled receptor pathways. Together they culminate in the deregulation of the expression of SOX2, OCT4, and NANOG transcription factors, leading to cell renewal, survival, proliferation, and chemoresistance modulation (Image originally draw based on Matsui, 2016).

Glioma stem-like cell targets linked to therapy resistance -

Glioblastoma stem cells exhibit proliferative and self-renewal properties, and also show multi-lineage differentiation into astrocytes, neurons, and oligodendrocytes. GSCs are known to be chemo- and radioresistant. Bao and coworkers demonstrated that GSCs show greater resistance to radiation than traditional glioblastoma cells, *in vivo* and *in vitro* (Bao *et al.,* 2006). GSCs express a high level of multidrug-resistant proteins and transporters associated with detoxification, which consequently confers multidrug resistance; and also show elevated expression of reactive oxygen species (ROS) and DNA damage response (Bao *et al.,* 2006; Haar *et al.,* 2012).

The elimination of GSCs is mainly focused on the 1) direct ablation of GSCs by targeting cell surface markers and specific molecular signalling pathways that are required for maintaining GSC stemness, such as those described above; and 2) modulation of GSCs interaction with their microenvironment, mainly the angiogenesis process, and their immune evasive properties (Karoubi *et al.,* 2010; Liebelt *et al.,* 2016; Sul and Fine, 2010)

Among the therapeutic targeting of GSCs by surface receptors, the relationship between the L1 cell adhesion molecule (L1CAM/ CD171), a regulator of cell survival preferentially expressed on CD133+ GSCs, and the maintenance of the stem-cell state, is well described (Bao *et al.,* 2006).

On the other hand, therapeutic targeting of GSCs by signalling pathways, such as NOTCH, SHH, WNT, VEGF, and STAT3, are also important for regulating GSC self-renewal and differentiation. Specifically, inhibition of NOTCH activation by γ-secretase inhibitors (GSIs) resulted in diminished proliferative capability and increased neuronal differentiation. Also, treating glioblastoma-derived spheres with an SHH inhibitor, cyclopamine, may reduced the formation of new neurospheres. The STAT3 pathway is also

required for GSC maintenance through TLR9 upregulation, and silencing TLR9 expression abrogated GSC development (Herrmann *et al.,* 2014; Liebelt *et al.,* 2016; Pistollato *et al.,* 2009).

Clinical impact of glioma stem-cell plasticity -

Until recently, the cellular differentiation process has been considered to be unidirectional, which means that a CSC can differentiate into a non-CSC, a process that would be accompanied by the variation in the expression of stem-like cell markers. This mature state was considered to be permanent, and the phenotypes of these cells were considered to be inelastic (Deheeger *et al.,* 2014). However, growing evidence from recent studies contradicts the concept of a unidirectional flow of cellular hierarchy, and instead suggests a bidirectional process that can be dynamic (Hitomi *et al.,* 2015). In this case, differentiated cells, under appropriate conditions, can reverse their mature fate and reacquire the stem-like state by an Epithelial-to-Mesenchymal Transition (EMT) process, which suggests that the phenotypic plasticity of cancer cells is less random than was first thought (Chaffer *et al.,* 2013; Tam and Weinberg, 2013).

In fact, CSC interactions with the surrounding microenvironment dictate the balance between self-renewal and differentiation states via growth factors, extracellular matrix, and communication with adjacent cells, trough cell-to-cell communication proteins, as connexins (Hitomi *et al.,* 2015).

Gap junctions (GJ) are formed by six connexin subunits that assemble at the interface between adjacent cells, allowing direct cell-cell communication for molecules less than 1 kDa in size. Specifically, the connexin family contains over 20 proteins with tissue-specific expression and function that are named according to predicted molecular weight, and play a key role in several processes inherent to cell migration and invasion, namely in tumor cells (Naus and Giaume, 2016). Connexins may exert both tumor-suppressor and oncogenic functions, namely connexin 43 (Cx43) and connexin 46 (Cx46) (Orellana *et al.,* 2012; Soares *et al.,* 2015). In fact, the expression of Cx43 has been correlated with the distinction between tumor subpopulations, since it is highly expressed in tumor cells that lack stem-like phenotypic characteristics. Accordingly, Cx43 has been described to be decreased in GBM compared with lower grade tumors (Soroceanu *et al.,* 2001). On the other hand, stem-like cells have been described to present high expression of Cx46,

suggesting that, during cell differentiation, there is a reduction of Cx46 and consequently an increase of Cx43 (Hitomi *et al.,* 2015).

The elevated cellular density in GBM increases the opportunity for direct cell communication, and the accumulating evidences suggest that CSCs maintenance also depends on cell-cell interactions, making the understanding of the connexins function and expression in GBM of utmost importance (Hitomi *et al.,* 2015).

Overall, since the CSCs are the cell population responsible for tumor recurrence, understanding the mechanisms underlying the molecular tumor cellular plasticity process, specifically the molecular signals of de-differentiation into CSC, and their role in promoting therapeutic resistance, would be of utmost importance for developing effective therapeutic strategies to improve the prognosis of patients diagnosed with GBM (Friedmann-Morvinski and Verma, 2014; Jackson *et al.,* 2015; Safa *et al.,* 2015).

1.3 THERAPEUTIC STRATEGIES IN GLIOBLASTOMA[3]

Despite all the evidence gathered to date, the mechanisms underlying gliomagenesis and those involved in GSCs and in GBM chemoresistance remain unclear. Due to its heterogeneity, GBM includes different cells of origin and different molecular steps of differentiation. From the therapeutic point of view, this heterogeneity presents a unique challenge for GBM treatment. In recent years, the molecular signature of GBMs and the mechanisms underlying the aggressiveness of these tumors have been studied and identified, mainly the above-mentioned alterations in several signalling pathways that control cellular proliferation, as well as the maintenance and plasticity of the stem-like cell state. Since the tumor microenvironment is essential to maintain GSC stemness, targeting the microenvironment is also a promising approach for treating glioblastoma.

There is an increasing need to perform combined therapy, adjusted to the genetic and molecular alterations of each patient and consequently, mitigating the side effects of treatment. Nanocarriers, which are small lipophilic molecules, have attracted increasing attention in brain- and tumor-targeted drug-delivery systems, owing to their potential ability to target cell surface specific molecules and to cross the blood-brain barrier and deliver the drug specifically to the tumor cells, improving efficacy and thus reducing non-specific toxicity. Combined therapeutic strategies, targeting both the stem cells and non-stem cells in the brain tumor, could become the most effective approach to increase the survival of GBM patients.

1.3.1 Targeted therapy in Glioblastoma

Although current therapy regimens have improved over the past 20 years, overall patient survival has not yet risen to the levels obtained for other solid tumors. In this sense, new therapies are currently in clinical trials for use in combination with the current standard of care in a way to improve treatment efficacy. The identification and characterization of molecular markers in brain tumors is truly important in a way to identify specific targets

[3] The images and tables from the present 1.3 section of the chapter 1 are original draw based on the literature mentioned in each one.

for treat patients with GBM (Haque *et al.,* 2011). These therapies are also designed for use in combination with the current standard of care in way to improve treatment efficacy and circumvent chemoresistance.

Regarding the **mechanisms of GBM resistance**, *MGMT* expression represents one of the most important marker of TMZ resistance in GBM patients. Studies showed that *MGMT* methylation is a predictive biomarker for better response to therapy (Spiegl-Kreinecker *et al.,* 2010). Investigational approaches to suppress MGMT activity include, for one hand the dose-intense temozolomide regimens, which may deplete the enzyme, and for the other hand the combination therapy with O^6-benzylguanine or other MGMT inhibitors (Jung *et al.,* 2010; Morandi *et al.,* 2010). However, MGMT inhibitors, namely the pseudosubstrate *O6*-BG, are in phase I clinical trials, have had limited efficacy, which is due, even not exclusively, to the dose-limiting myelosuppression when combined with cytotoxic chemotherapy. Recently, other approaches utilize RNAi to directly interfere with MGMT protein expression, the MGMT-siRNAs and a novel liposome, LipoTrust™ EX Oligo for the siRNA delivery. In these studies the MGMT was efficiently knocked down in glioma cells lines, GBM-stem like cells, and *in vivo* glioma tumors (Kato *et al.,* 2010). Also Bortezomib (BTZ, PS-341), a boronic acid dipeptide, showed to inhibit the proteasome and markedly reduces the levels of MGMT mRNA and protein (Vlachostergios *et al.,* 2013). On the other side, overexpression of WTP53 can suppress MGMT activity and make glioma cells more sensitive to TMZ (Ramirez *et al.,* 2013; Srivenugopal *et al.,* 2001).

Together with the MGMT, the Mismatch Repair (MMR) loss is also thought to be linked with TMZ resistance (Ghosal and Chen, 2013). In fact, the DNA repair enzyme poly(ADP-ribose) polymerase (PARP) may promote chemotherapy resistance in patients with glioblastoma. In this context, the PARP inhibitors, such as BSI-201 and ABT-888, may be effective when combined with radiotherapy and chemotherapy (Johannessen *et al.,* 2008).

Clinical data, together with *in vitro* studies, suggest that PGP has also an important role in the acquisition of TMZ resistance, in GBM cells. The efflux transporter MDR1/PGP is expressed in both low- and high-grade gliomas, suggesting an intrinsic resistance of these tumors to anticancer drugs. Chemoresistance is caused by the expression of efflux transporters in brain tumor cells, endothelial cells of both brain tumors and normal brain capillaries as well. Co-administration of chemotherapy or targeted therapy with inhibitors

of the active efflux transporters may thus increase drug concentration in the intracellular space. Tissue samples from patients who exhibited TMZ resistance and tumor recurrence showed increased levels of PGP (Munoz *et al.,* 2015; Schaich *et al.,* 2009). To avoid drug efflux transport, some MDR-reversing agents that can inhibit PGP-mediated drug transport have been used in studies of GBM, namely verapamil, PSC-833, MS-209 or MRK16, and a monoclonal antibody against PGP (Naito and Tsuruo, 1989; Sato *et al.,* 1995; Sheehy *et al.,* 2015; Thiebaut *et al.,* 1987).

Finally, a well known described cause of GBM chemoresistance is also the presence of CSCs. The GSCs potential, as a truly important target for the therapeutic management of GBM, was already described in the previous section (1.2) of this chapter.

Regarding the **molecular signalling pathways** involved in the GBM malignancy, EGFR is one of the most attractive therapeutic target. In fact, increased EGFR signalling drives tumor cell proliferation, invasiveness, motility, angiogenesis, and inhibition of apoptosis. Moreover, blocking EGFR signalling with small molecule inhibitors, or the expression of dominant-negative EGFR (EGFR-CD533), have been proved to significantly attenuate the DNA damage response (DDR). In this way, small-molecules that are EGFR inhibitors, such as Gefitinib and Erlotinib are reported to be well tolerated in patients with GBM (Hsu and Wakelee, 2009).

In the same signalling pathway, as previously mentioned, also the PI3K/AKT/mTOR is frequently increased due to the receptor tyrosine kinase overactivity, mutated oncogenic PI3K subunits, and/or loss of PTEN tumor suppressor activity. Either way, several mTOR inhibitors such as Sirolimus (rapamycin), Temsirolimus (CCI-779), Everolimus (RAD001), and Ridaforolimus (AP23573) have been tested with minimal activity against glioblastoma (Dasari *et al.,* 2010; Lee *et al.,* 2012; Li *et al.,* 2016; Reardon *et al.,* 2010).

Regarding the importance of PKC in GBM proliferation, some PKC inhibitors have also been described for the treatment of recurrent glioblastoma, namely: Tamoxifen (TMX), a non-steroidal agent well known in the treatment of estrogen receptor–positive breast cancer, which inhibits PKC, increasing cellular apoptosis (Balça-Silva *et al.,* 2015; Millward *et al.,* 1992) and also initially tested in a II phase clinical trial by Couldwell and coworkers (Couldwell *et al.,* 1994); and Enzastaurin (EZT), a small molecular inhibitor of PKCβ, used to treat a variety of tumors, that are in a Phase III clinical trial in GBM (Wick *et al.,* 2009).

Given the utmost importance of the inhibition of angiogenesis in GBM, the new generation of antiangiogenic drugs, evaluated in clinical trials, uses the anti-VEGF antibody bevacizumab, which neutralizes VEGF and was approved for used in recurrent GBM in 2009. Bevacizumab has also been evaluated in phase III clinical trials for newly diagnosed glioblastoma, with, unfortunately, no improvement in overall survival (Cohen *et al.,* 2013; Huang and Fu, 2015). Two large, randomized phase III trials, AVAglio and Radiation Therapy Oncology Group (RTOG) 0825 demonstrated that the combination of bevacizumab with radiation and temozolomide conferred no benefit in terms of overall survival in newly diagnosed glioblastoma patients. Still, both studies found that the progression-free survival (PFS) was prolonged by approximately 3 to 4 months, reaching statistical significance in the AVAglio study, although not in the RTOG 0825 study. In clinical trials, the use of bevacizumab has been shown to decrease peritumoral edema, reducing the need for chronic corticosteroid use in up to 70% of patients and allowing a reduction of side effects (Soffietti *et al.,* 2014; Weathers and de Groot, 2015).

Also, cediranib, sunitinib, pazopanib, vandetanib, and sorafinib, VEGFR tyrosine kinase inhibitors (TKIs) that block the tyrosine kinase activation site of VEGFR, have undergone evaluation in phase I/II clinical trials. Of these agents, only cediranib has advanced to a phase III clinical trial, the REGAL trial. Still, the response rate was of 28% to 38% in the cediranib-containing arms, which is similar to the response rates observed with bevacizumab in the BRAIN study (28.2% to 37.8%) (Seystahl *et al.,* 2013; Weathers and de Groot, 2015).

The poor prognosis of GBM patients is also related to diffuse brain invasion and interaction of tumor cells with ECM. Among others, cilengitide, an inhibitor of αVβ3 and αVβ5 integrins, has been used in phase I/II clinical trials (Chamberlain *et al.,* 2012; Schittenhelm *et al.,* 2013; Zeng *et al.,* 2015). Recent studies also suggested other integrin inhibitors, namely shikonin, a naphthoquinone with anti-tumor properties, when combined with TMZ (Matias *et al.,* 2017).

The most frequent chemotherapeutic agents used to circumvent GBM treatment are summarized in table 1.5.

Table 1.5. Alternative chemotherapeutic approaches in GBM.

Molecular Targets	Chemotherapeutic Agents	References
EGFR	Gefitinib Erlotinib Cetuximab	Uhm *et al.,* 2011 Raizer *et al.,* 2010 Combs *et al.,* 2006
PI3K/AKT/mTOR	Everolimus	Li *et al.,* 2016
VEGF/ VEGFR	Vatalanib Bevacizumab	Gerstner *et al.,* 2011 Gilbert *et al.,* 2014
PKC	Tamoxifen Enzastaurin	Robins *et al.,* 2006 Wick *et al.,* 2010
Integrin Antagonists	Cilengitide	Gilbert *et al.,* 2012
Proteasome inhibitors	Bortezomib	Phuphanich *et al.,* 2010

EGFR: epidermal growth factor receptor; PKC: protein kinase c; VEGFR: vascular endothelial growth factor receptor; Ras/ MAPK: mitogen-activated protein kinases.

1.3.2 Novel drug delivery approaches in Glioblastoma

Given the high frequency of brain cancer (primary and secondary) and its devastating effects, the efforts to identify techniques that would be able to improve the efficacy of the delivery of drugs to the central nervous system (CNS) remain in the spotlight (Blakeley, 2008; Karim *et al.,* 2016).

Since brain tumors possess many distinctive characteristics from peripheral tumors due to their molecular oncogenic pathways and several resistance mechanisms, many factors must be taken into consideration to overcome effective brain tumor-targeted drug delivery, such as the barriers included in the whole process, the tumor microenvironment, and tumor cells (Wei *et al.,* 2014).

In principle, the administration of chemotherapy to brain tumors is **local delivery** or **systemic delivery**. The local administration circumvents the difficulties imposed by the barriers mentioned before, but it has also limited ability to reach distant infiltrating tumor cells. On the other hand, systemic delivery should overcome the impediment posed by the blood-brain barrier (BBB) or the ABC efflux transporters. Overall, systemic delivery relies on the fact that exists a vascular bed as a delivery vehicle, which provides the deliver of

the drug to the tumor. In this regard, a compound must start to possess some properties that aimed to facilitate the delivery, namely the low molecular weight, the lack of ionization at physiological pH, and lipophilicity (Susan Chang, 2011). Thus, only a small proportion of systemically administered agents will reach the CNS either oral or intravenously. Regarding GBM, temozolomide is well known to be able to cross the BBB, as well as lomustine, procarbazine and tamoxifen. However, there are also a few limitations associated with the oral administration as the stability in gastric acid, absorption through the gastric mucosa, inactivation by intestinal enzymes, hepatic metabolism, biliary excretion and treatment-induced emesis (Susan Chang, 2011).

Almost all recent drug developments in neuro-oncology either try to improve the technique of drug delivery or fail on this account (Siegal, 2013). In fact, GBM has a relatively rapid and quiet evolution, at the time of diagnosis, which explains that some studies indicate that BBB has already some degree of permeability due to the abnormal structural features in endothelial cells, resulting in enhanced permeability of the BBB when compared with normal brain tissue (Zhang *et al.,* 2015).

Strategies that rely on local delivery -

There are a few strategies that incorporate the local delivery of drugs to brain tumors:

1) implantable **controlled-release polymer** systems (failed phase II clinical trial). These biodegradable polymers release the drug by a combination of diffusion and hydrolytic polymer degradation. Actually, the only local chemotherapy approved by Food and Drug Administration (FDA) is carmustine (BCNU) wafers. Carmustine, an alkylant agent, has the capacity to induce cancer cells death via binding to the O^6 position of guanine in DNA, cross-linking the two strands, and so preventing DNA replication (Chakroun *et al.,* 2017). The carmustine wafers are implanted into the resection cavity of the tumor. However, the therapy is limited to the subclass of tumors that are resectable with a small volume of residual neoplasm, since it presents several limitations, namely: it has a half-life of 15 minutes, which is too short for the active drug to diffuse across large distances before degradation occurs; can potentially enter in the circulatory system by capillary loss; and the structure of the wafers does not permit the intimate contact with the tissue (Brem *et al.,* 1991; Chakroun *et al.,* 2017; Siegal, 2013; Westphal *et al.,* 2006).

2) various catheter devices for **intracavitary drug delivery** (few phase II studies). Craniotomy-based drug delivery approach allows the pharmaceutical molecule to be delivered directly in the brain tissue via intracerebral implantation or intracerebral-ventricular injection. However, the release is limited by the diffusion capacity of the drug. An example is the radioactive ligand attached to antitenascin antibodies (Buonerba *et al.,* 2011; Pardridge, 2002).
3) **convection-enhanced delivery** (CED) (failed phase II/ III clinical trails). The CED is a catheter connected to a syringe pump placed in the tumor tissue, which makes possible drug administration continuously under positive pressure. This procedure will allow the local distribution of a significant amount of highly concentrated therapeutic molecules, reaching very low systemic secondary effects. However, this strategy is not widely used due to the risk of backflow and possible reduction of the therapy efficacy (Allard *et al.,* 2009; Lidar *et al.,* 2004).

Altogether, the major limitation of local delivery techniques is their failure to reach distant infiltrating tumor cells, which in turns constitute a major requirement for the therapy to achieve a durable effect. Due to the invasive nature of these techniques and the restricted boundaries of drug distribution, it is not surprising that these procedures largely remain experimental or have already failed in clinical trials (Siegal, 2013).

Strategies that rely on systemic delivery -

There are a few strategies that incorporate the systemic delivery of drugs to brain tumors and associated methods that improve this drug transport:

1) the improvement in passive drug transport by **manipulation of the drug**, thus increasing the plasma concentration, or by transient opening of the BBB. Drug manipulation may include chemical modification to improve the drug's capability to passively cross the barrier, namely through its lipidization, avoiding protein binding and inducing a prolonged plasma half-life. The lipidization strategy, based on the chemical modification of the drug to produce a more lipophilic prodrug, can be used in a way to increase systemic drug delivery. This is possible by modifying the hydrophilic groups to lipophilic groups, which must be reversible, and after in the brain, the prodrug should be converted back to the parent compound by a

chemical or enzymatic process. This is the case of temozolomide (TMZ) (Gabathuler, 2010). Other alternative strategy for drug manipulation is the design of prodrugs that are recognized and transport by the influx transporter systems (Pardridge, 2012).

2) The increase of **drug concentration in the plasma** by high-dose chemotherapy (HD- CTx), intravenous bolus drug injection, and intra-arterial drug injection, although not yet establish for CNS (Siegal, 2013).
3) The induction of **transient disruption of the BBB** to enhance passive drug transport across the barrier by osmotic BBB disruption (BBBD), biochemical disruption, and ultrasound-mediated BBBD, next to the natural permeability associated to tumor inflammation. Among them, the osmotic BBB disruption is the only one under experimental treatment in brain tumors (Siegal, 2013). Specifically, the intra-arterially infuse of hyperosmotic agents, such as mannitol, opens the tight junctions (TJs) of the cerebral endothelial cells enhancing the passage of drugs across the BBB. Briefly, the resulting high sugar concentration in brain capillaries takes up water out of the endothelial cells, shrinking them, thus opening TJs. This effect usually lasts for 20-30 minute, during which time drugs diffuse freely, that would not normally cross the BBB. However, a considerable number of disadvantages, namely the physiological stress, transient increase in intracranial pressure, and unwanted delivery of anticancer agents to normal brain tissues, distances this approach from the use on humans (Mukhopadhyay *et al.,* 1995). Conventional radiation therapy used to treat primary and metastatic brain cancer also increases BBB permeability in both preclinical models and in patients. Anyway, the biochemical BBBD, using mediators of the inflammatory response, namely the bradykinin agonist RMP-7, which can cause transient vascular leakage and increased blood vessels (Borlongan and Emerich, 2003; Ford *et al.,* 1998), as well as the ultrasound-mediated BBBD, by the intravenous injection of performed gas bubbles before pulsed ultrasound treatment generating mechanical stresses to blood vessels, have not gained wide clinical acceptance (Liu *et al.,* 2010).
4) Blocking **active efflux transporter mechanisms**, known to contribute to brain tumor drug resistance, as previously described in more detailed in the section 1.2. Besides a variety of PGP inhibitors have been experimented, the results have been still disappointing due to the toxicity (Kemper *et al.,* 2003; Siegal, 2013; Sikic *et al.,* 1997).

5) The use of **drug carriers for drug delivery** to brain tumors. Recent advances in nanotechnology have created exciting opportunities to improve the efficiency of drug delivery to the CNS. Actually, a drug that is poorly distributed to the brain, can be loaded onto a nanocarrier system that would interact with the microvascular endothelium at the BBB, eventually leading to higher drug concentrations in brain parenchyma. These nanocarriers can be further modified for enhanced CNS selectivity and permeability with targeting moieties that will preferentially bind to putative receptors or transporters expressed either in BBB or tumor cells. Among these nanocarriers are the nanoparticles (including polymeric or solid lipid nanoparticles, lipid or albumin nanocapsules, micelles and liposomes) and the nanovesicles (exosomes) (Lakhal and Wood, 2011; Sarin *et al.,* 2008). There are several studies regarding drug carriers for drug delivery in the literature. Anyway, regarding the main focus of this thesis, we are going to center our attention to liposomes in the further sections. A summary of the local delivery and systemic delivery techniques and each limitations is presented on figure 1.14.

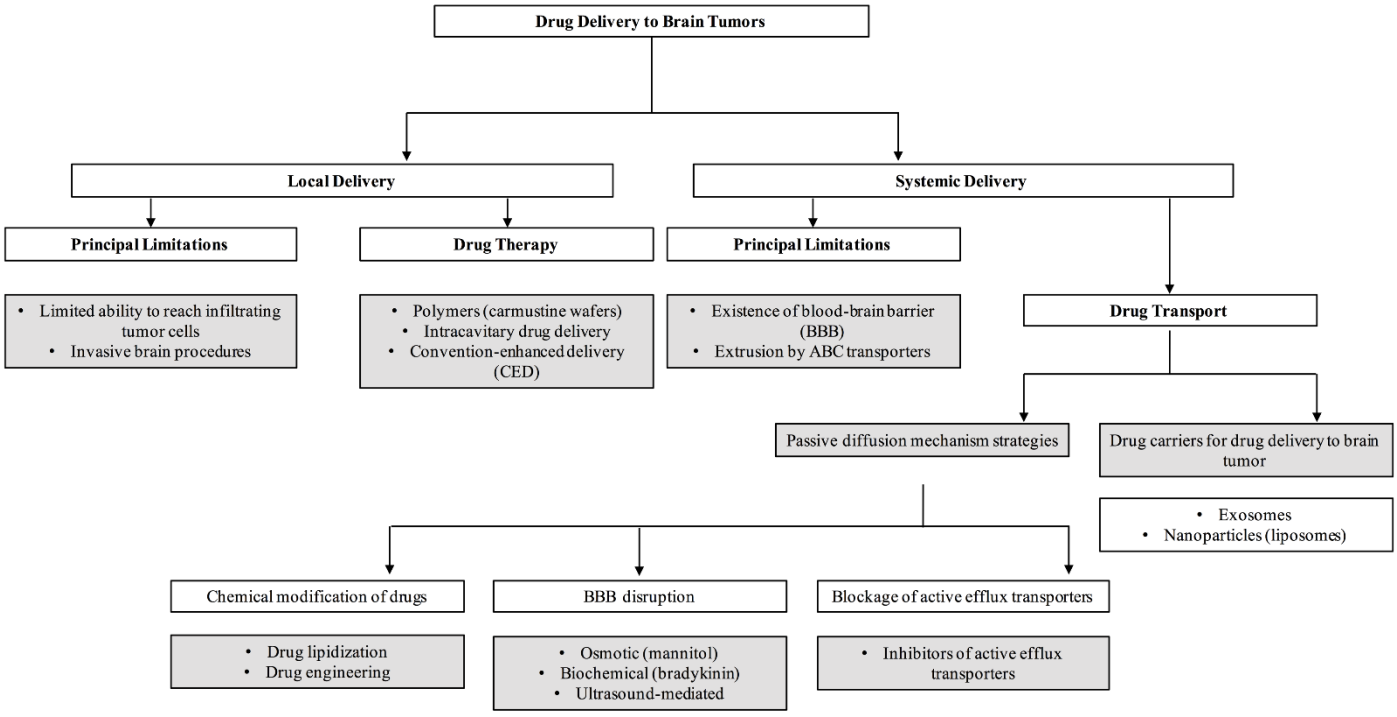

Figure 1.14 Drug delivery strategies to brain tumors and principal limitations. Local and systemic delivery are the two main strategies to drug delivery to brain tumors. The use of carmustine wafers are an example of drug therapy based on local delivery. In turn, drug carriers for drug delivery, for instance the liposomes, constitute a main strategy for systemic delivery (Image originally draw based on Siegal, 2013).

Altogether, all these methods have the same barriers to achieve the tumor sites. Specifically, the blood-brain barrier (BBB), described in more detailed in the previous 1.2 section, which includes the blood-brain tumor barrier (BBTB); the weak enhanced permeability and retention effect (EPR); the irregular vasculature of the tumor; increased interstitial pressure; intratumoral hypoxia; and active efflux transport mechanisms at the BBB constitute the main limiting factors for penetration of drugs (Siegal, 2013; Wei *et al.,* 2014). In fact, the BBB, besides the highly selective active interface that regulates the traffic of various molecules between the systemic circulation and the brain interstitial fluid to maintain homeostasis in the CNS, presents a variety of efflux transporters, which can actively pump-out a wide range of drugs including various anti-cancer agents, namely doxorubicin (DXR), through the cell membrane (Karim *et al.,* 2016; Sharom, 2011). The blood–brain tumor barrier (BBTB), similar to blood–brain barrier (BBB), is located between brain tumor tissues and microvessels formed by highly specialized endothelial cells (ECs), limiting the paracellular delivery of most hydrophilic molecules to tumor tissue (Figure 1.15).

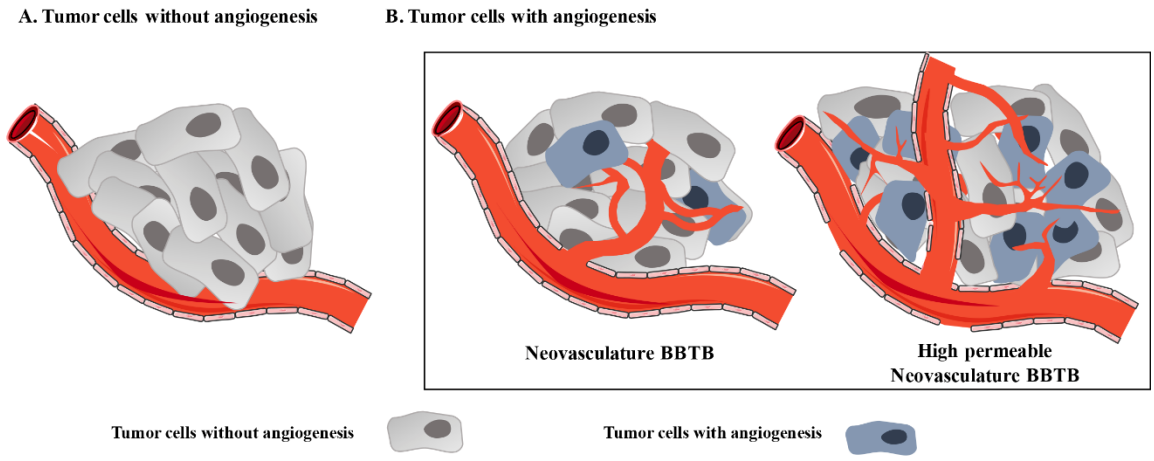

Figure 1.15 Stages of the blood-brain tumor barrier formation. A) Tumor cells without angiogenesis and B) tumor cells with angiogenesis (Image originally draw based on Wei *et al.*, 2014).

When the tumor cell clusters grow to a certain volume the BBB will be damaged and the BBTB be formed. Hence, the receptors presented on the BBB/BBTB provide a chance for gliomas-targeted drug delivery (Wei *et al.,* 2014).

Among the expectations from drug therapy, the issues related to the strategy used for delivery to the brain cannot be separated: (1) effectiveness; (2) favorable adverse effects profile, including systemic and neurotoxicity; (3) easy introduction (assimilation) into clinical practice; (4) feasible repeated or continuous administration, and (5) the agent and delivery strategy should be useful for any tumor size and CNS location (Siegal, 2013; Wei *et al.,* 2014).

In fact, besides the lack of clinical success, temozolomide (TMZ) changed clinical practice for glioblastoma. Regarding the 5 expectations mentioned above, it becomes clear that TMZ fulfills all of them (Siegal, 2013).

Anyway, nanocarriers, namely liposomes, are one of the highly potential drug transport systems that have gained huge attention over the last few decades for provide specific drug delivery, including to the brain, avoiding a wide range of side effects (Gabathuler, 2010; Koo *et al.,* 2006).

Liposomes as a drug delivery system

Liposomes are considered to be one of the most biocompatible vesicular drug carriers with a capacity for accommodating both hydrophilic and hydrophobic compounds. Since their discovery in the 1960s by Bangham, *in vitro* studies have indicated that liposomes are taken into cells via endocytosis, which may increase the efficiency of intracellular drug delivery. However, after endocytosis by cells, the conventional liposomes, entrapped in the endosome organelle, are destined to the lysosome, where the contents may be degraded by enzymes. This pathway may limit the intracellular concentration of the drug (Bangham and Horne, 1964).

There are a range of different liposomes such as positively-charged liposomes, pH-sensitive liposomes, ligand or peptide grafted liposomes, virosomes, magnetic liposomes and gold or silver particle-containing liposomes (Karim *et al.,* 2016). The current understanding for targeted delivery of nanoparticles in tumors is based on a combination of several independent concepts, involving events associated with the 1) enhanced permeability and retention (EPR) effect, 2) nanoparticle properties and design, 3) increased retention in the circulation due to PEGylation, and 4) ligand- receptor type interactions (Han Bae and Park, 2011).

It is known that the EPR effect is due to the unique vascular characteristics of the tumor tissue and the lack of a lymphatic recovery system in the solid tumor. In this sense,

besides nanoparticles show higher tumor accumulation relative to controls, only a very small fraction (5%) of the total administered formulation is actually delivered to the intended target site (Han Bae and Park, 2011; Maeda *et al.,* 1985).

Based on its size and number of bilayers, liposomes can be classified into: small unilamellar vesicles (SUV); large unilamellar vesicles (LUV) and multilamellar vesicles (MLV) (Figure 1.16).

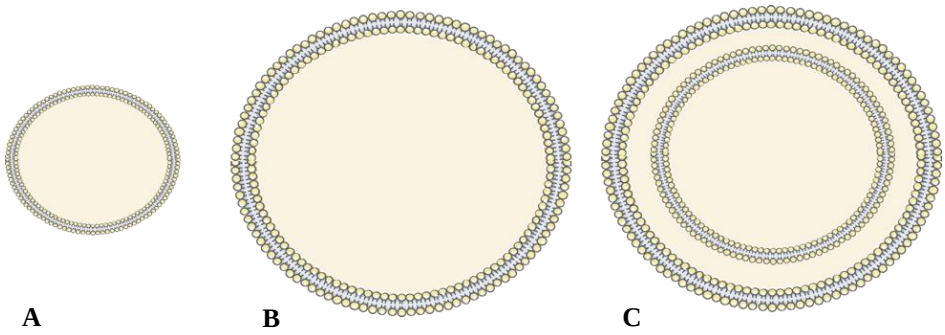

Figure 1.16 Classification of liposomes on the basis of size and number of bilayers. A) Small unilamellar vesicles, B) large unilamellar vesicles and C) multilamellar vesicles (Image originally draw based on Calixto *et al.,* 2014).

In fact, size is an important factor for controlling tumor accumulation kinetics and for preventing diffusion back into the systemic vascular bed. Some studies have shown that liposomes (with 90 nm of diameter) extravasate from leaky tumor vessels but do not diffuse away effectively from the tumor even after a week. As so, smaller particles (in the range of 50–300 nm) have slower removal from the circulation compared with those having larger sizes (Yuan *et al.,* 1994).

On the other hand, accumulation of nanoparticles in tumors is based on blood circulation and extravasation, which means that extending time in the systemic circulation is an important strategy taken to increase the fraction of nanoparticles reaching a target tumor. In this sense, cationic liposomes, positively charged nanocarriers, interact with the negatively charged serum proteins forming aggregates that usually accumulate in the lungs, liver and spleen (Gomes-da-Silva *et al.,* 2012a). Poly(ethyleneglycol) (PEG)-grafted nanocarriers have been used extensively to modify the pharmacokinetics of the drug itself and/or the nanoparticles. In fact, PEGylated nanoparticles have increased systemic circulation times, due to its hydrophilic nature that provides an aqueous shield around the nanoparticle surface, which leads to a decrease of the extent opsonisation, and the subsequent recognition by the macrophages of the mononuclear phagocytic system, leading to an increase of a nanoparticle blood residence time (Gomes-da-Silva *et al.,* 2012a).

Studies revealed a 100% increase in tumor accumulation of nanoparticles following PEGylation (Litzinger *et al.,* 1994).

Nonetheless, some limitations have been associated with PEG-derivate lipids, namely the occurrence of an immune response, which may lead to their rapid blood clearance. In fact, studies revealed that only about 5% of the administered particles remains in the systemic circulation after 12 h with about 80% of the initial dose being eliminated in less than a few hours ending up in the liver and spleen, with a lesser extent being in the lungs and kidneys (Hong *et al.,* 2009).

To overcome these issues several PEG-derivated lipids with different lengths of the acyl chain anchor presenting were synthesized, such as ceramides (PEG-Cer)[18] or diacylglycerols (PEG-S-DAGs). As so, as the length of the acyl chain increases the PEG time on the nanoparticle surface also increases (Ambegia *et al.,* 2005).

More recently, pH-sensitive liposomes (PSL) were established to enhance the intracellular delivery of drug content to cytosol via a process known as 'endosome escape' (Leite *et al.,* 2012; Momekova *et al.,* 2010; Simões *et al.,* 2004). The pH-sensitive liposomes rapidly become destabilized in the acidic pH environment of the tumor tissues, being capable of delivering anti-cancer drugs to specific cancer cells, enhancing cellular internalization and rapid intracellular drug release (Zhao *et al.,* 2016).

Liposomes in GBM treatment

One of the most attracting characteristics that make liposomes an interesting drug delivery strategy for GBM is their capability to cross the BBB (Alyautdin *et al.,* 2014; Karim *et al.,* 2016). In this way, the non-specific side effects of the anti-tumor agents would expected to be reduced (Liu and Lu, 2012).

In fact, nanoparticle delivery systems present some advantages over conventional anticancer chemotherapy, namely: protection of drugs from degradation in the body; enhanced absorption into tumor cells; and decreased interaction of drugs with normal cells. However, some difficulties related to drug delivery may also occur, such as troublesome solubility and biological availability, short time in circulation, and inconvenient biodistribution to the target organ (Bhowmik *et al.,* 2015; Cerna *et al.,* 2016).

Specifically, sterically stabilized F3-targeted pH-sensitive liposomes have been recently designed (Gomes-da-Silva *et al.,* 2013a). These liposomes were designed to target a receptor overexpressed in the surface of cancer cells and cells that constitute the tumor

microenvironment, like endothelial cells from angiogenic blood vessels, specifically, nucleolin (NCL). In this way, it became possible to develop multi-targeting strategies toward the tumor microenvironment (Moura *et al.,* 2012).

These F3-targeted pH-sensitive liposomes incorporate in their composition the fusogenic lipid 1,2-dioleoyl-sn-glycero-3-phosphoethanol-amine (DOPE), which has an inverted cone-shape, and a stabilizer cholesteryl hemisuccinate (CHEMS). A stable lipid bilayer is formed at physiological pH. However, under acidic conditions, namely in the endocytic pathway, CHEMS is protonated, loosing its ability to stabilize the inverted cone-shape of DOPE, leading to the destabilization of the liposomal membrane. With the destabilization, it is possible to the liposomes to release the encapsulated siRNA or the drug into the cell cytoplasm. Also, these F3-targeted pH-sensitive liposomes were stable and biocompatible with blood and no signs of toxicity were observed upon multiple systemic administrations (Moura *et al.,* 2012). These liposomes have been demonstrated a relevant increased efficacy against chemo-resistant cells (Fonseca *et al.,* 2015). In fact, authors observed a significantly increase in cytotoxicity against breast cancer and endothelial cells from tumor blood vessels relative to the non-targeted sample (Fonseca *et al.,* 2017; Moura *et al.,* 2012).

Regarding GBM, several preclinical studies have shown an active targeting by grafting certain endogenous ligands or monoclonal antibodies on liposome surface, improving GBM targeted drug delivery relatively to passively-targeted nanocarrier, although no nanodrug is yet approved for brain tumor therapy (Cerna *et al.,* 2016).

Anyway, regarding the **preclinical studies**, there are a few interesting studies in GBM, which will be briefly summarized next.

An *in vivo* study of DXR on subcutaneous mouse glioma model, an interleukin-13 (IL13) grafted liposomal formulation of the drug, significantly improved the cytotoxicity and tumor accumulation compared to the free DXR. Intraperitoneal injection of the targeted liposome significantly decreased the tumor size compared to the untargeted liposomes (Karim *et al.,* 2016).

Liposomes have been also used for human *EGFR* antisense gene therapy for GBM. The gene was in a nonviral plasmid, which was encapsulated in PEGylated 1-palmitoyl-2-oleoyl-sn- glycerol-3-phosphocholine (POPC) liposomes conjugated to 83-14 murine mAb to the human insulin receptor (HIR). The liposome formulation was tested against U87 glioma cell line and about 70-80% cell growth was inhibited (Zhang *et al.,* 2002).

Liposomal formulation of oxaliplatin (Lipoxal®), a platinum analogue, which acts as radiosensitizer and improves the efficacy of radiotherapy, was tested on F98 glioma model (cells implanted in the right hemisphere) on Fischer rats. The authors observed that the concentration of oxaliplatin in the tumor was 2.4 times higher for Lipoxal® after 24 hours compared to the free oxaliplatin and the median survival time of the rats was improved to 29.6 ± 1.3 days, compared to 21.0 ± 2.6 days. Additionally, the liposomal formulation markedly reduced the toxic effects observed with free oxaliplatin (Karim *et al.,* 2016).

Gromnicova *et al.,* found that gold nanoparticles glucose-coated cross brain endothelium three times faster than the non-brain endothelium (Gromnicova *et al.,* 2013). These nanoparticles were selected because the glucose transporter Glut-1 is expressed on brain endothelium and astrocytes, which make it preferentially taken by brain-endothelium, selectively cross it, compared to non-brain endothelia, and localize in astrocytes (Gromnicova *et al.,* 2013).

Also Huwyler *et al.,* investigated daunorubicin-loaded liposomes with anti-transferrin receptor antibody, using an animal model, and found increased brain daunorubicin concentration compared with free drug. (Huwyler *et al.,* 1996).

A two-dose regimen of topotecan non- PEGylated liposomes, locally administered with paramagnetic gadodiamide nanoparticles, increased survival rates in a U87MG glioblastoma intracranial xenograft model, compared with controls, and the authors verified that the effect was topotecan dose-dependent (Grahn *et al.,* 2009).

Finally, our group have been verifying that the F3-targeted pH-sensitive liposomes fulfill the physico-chemical requisites demanded to a nanocarrier for systemic delivery of siRNA and drugs, like doxorrubicin (DXR), by the specific internalization of F3 peptide by nucleolin, a cell surface receptor overexpressed in tumor cells, as in breast cancer and HMEC-1 endothelial cells (Moura *et al.,* 2012).

Regarding the **clinical trials** in brain tumors, although none was sufficiently successful to achieve clinical practice, some of them have been considered important steps in the understanding of the targeted-therapy approach.

A phase I clinical study of paclitaxel-Angiopep-2 peptide-drug conjugate was shown to bind to the low-density lipoprotein receptor-related protein-1 receptor (GRN1005) and was carried out in patients with recurrent glioma grade II-IV. Although

the clinical data show that GRN1005 facilitated the penetration of paclitaxel into tumor tissue, the interim analysis of the phase II trial did not show therapeutic response (Cerna *et al.,* 2016; Drappatz *et al.,* 2013; Owonikoko *et al.,* 2014).

Transferrin conjugated with diphteric toxin (Tf-CRM107) showed low toxicity and tumor response in patients with recurrent high grade brain tumors in phase I and II clinical trials. Unfortunately, an early phase III clinical trial using this therapy had terminated due to disappointing preliminary results (Arko *et al.,* 2010; Weaver and Laske, 2003).

In a clinical study, Koukourakis *et al.,* treated several GBM patients, undergoing radiotherapy, with stealth® liposomal DOX (Caelyx®). Caelyx® is a PEGylated liposome formulation of DXR hydrochloride. The intratumoral tissue concentration of DXR was 13–19 folds higher than in normal brain tissue (Koukourakis *et al.,* 2000). However, a phase II-trial to evaluate the activity of PEG-DXR and prolonged administration of TMZ, in addition to standard radio-chemotherapy in the first-line treatment of patients with GBM, did not show meaningful improvement of the patient's outcome compared to the standard-of-care established (Koukourakis *et al.,* 2000; Stupp *et al.,* 2009). Although this combined therapy slightly increased the median overall survival of the total study population to 17.6 months as compared to 14.6 of the standards therapy, this difference did not reach statistical significance (Koukourakis *et al.,* 2000; Stupp *et al.,* 2005). Later, Hau *et al*. demonstrated that pegylated liposomal doxorubicin (Caelyx®) in patients with recurrent high-grade glioma was efficacious and well tolerated (Hau *et al.,* 2004), bringing us back to more promising clinical trials. Similarly, in a clinical study of liposomal doxorubicin (Caelyx®) in patients with high-grade gliomas, Fabel *et al*. also found improved overall survival than in past trials using conventional therapies (Fabel *et al.,* 2001).

In our point of view, although there is still long way to go with regard to the success of nanocarrier therapy, some of the results described in the literature suggest that this drug delivery strategy has an interesting potential for the future of oncobiology of the tumor, namely in therapy of high grade brain tumors, a topic of great potential interest for scientists and clinicians.

CHAPTER 2

Hypothesis and Objectives

'The task is not so much to see what no one has seen but think what nobody has yet thought about what everyone sees.'
Arthur Schopenhauer

2.1 HYPOTHESIS

Since Glioblastoma (GBM) is the most aggressive type of brain tumor with rapid development, poor prognosis and lower survival, the identification of the mechanisms underlying the resistance to current therapy remain still a challenge.

Literature has been pointed several factors that are related to the resistance of GBM to conventional treatment. Among all, the deregulation of important molecular signalling pathways related with tumor proliferation and migration capability; the existence of a population of stem-like cells, the glioma stem-like cells (GSCs), known to be chemo and radioresistant, and so responsible for tumor recurrence after surgery; and the inexistence of recognized specific molecular markers capable of distinguish tumor cells from healthy ones, allowing a variety of undesirable side effects, are the most relevant ones (Figure 2.1) (Allen *et al.,* 2002; Borovski *et al.,* 2011; Mao *et al.,* 2012; Martuscello *et al.,* 2016; Sarkaria *et al.,* 2008; Seymour *et al.,* 2015).

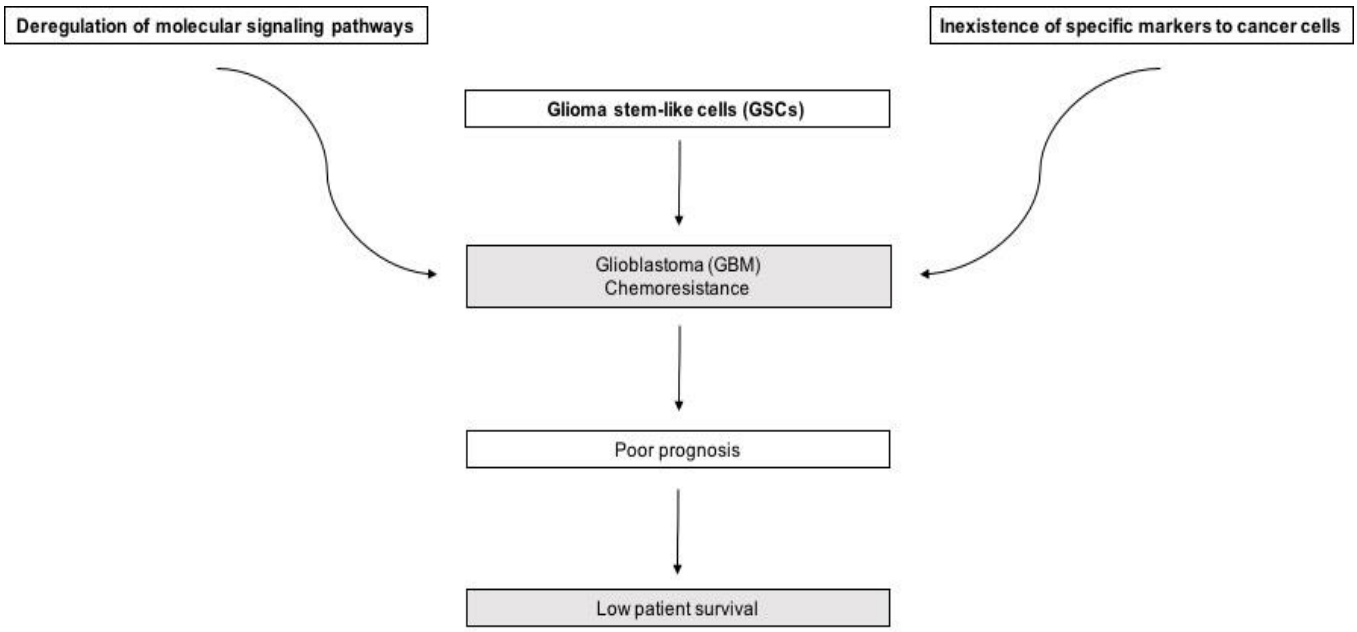

Figure 2.1 Principal factors of glioblastoma chemoresistance. Deregulation of molecular signalling pathways, the existence of GSCs and the inexistence of recognized specific markers to target cancer cells lead to GBM chemoresistance, poor prognosis, and ultimately lead to low patient survival.

Taking these observations into account, it is of utmost interest to study the principal molecular mechanisms deregulated in GBM, as well as, understand the stem cell state in order to provide new insights in the biology of tumor recurrence, and finally identify the most relevant biomarkers that could be potentially used as a specific target in this tumor. Altogether, these different approaches, that contribute to the resistance of GBM, could provide new insights in preventive and personalized strategies that, consequently, could improve quality of life and clinical care of GBM patients.

In this regard, herein we **hypothesized** that a specific and personalized approach to cancer cells, most importantly to glioma stem-like cells, could not only contribute to the understanding of stem-like cell state plasticity but also to the identification of overexpressed surface molecular markers, contributing to a better outcome and less side effects than the conventional therapy (Figure 2.2).

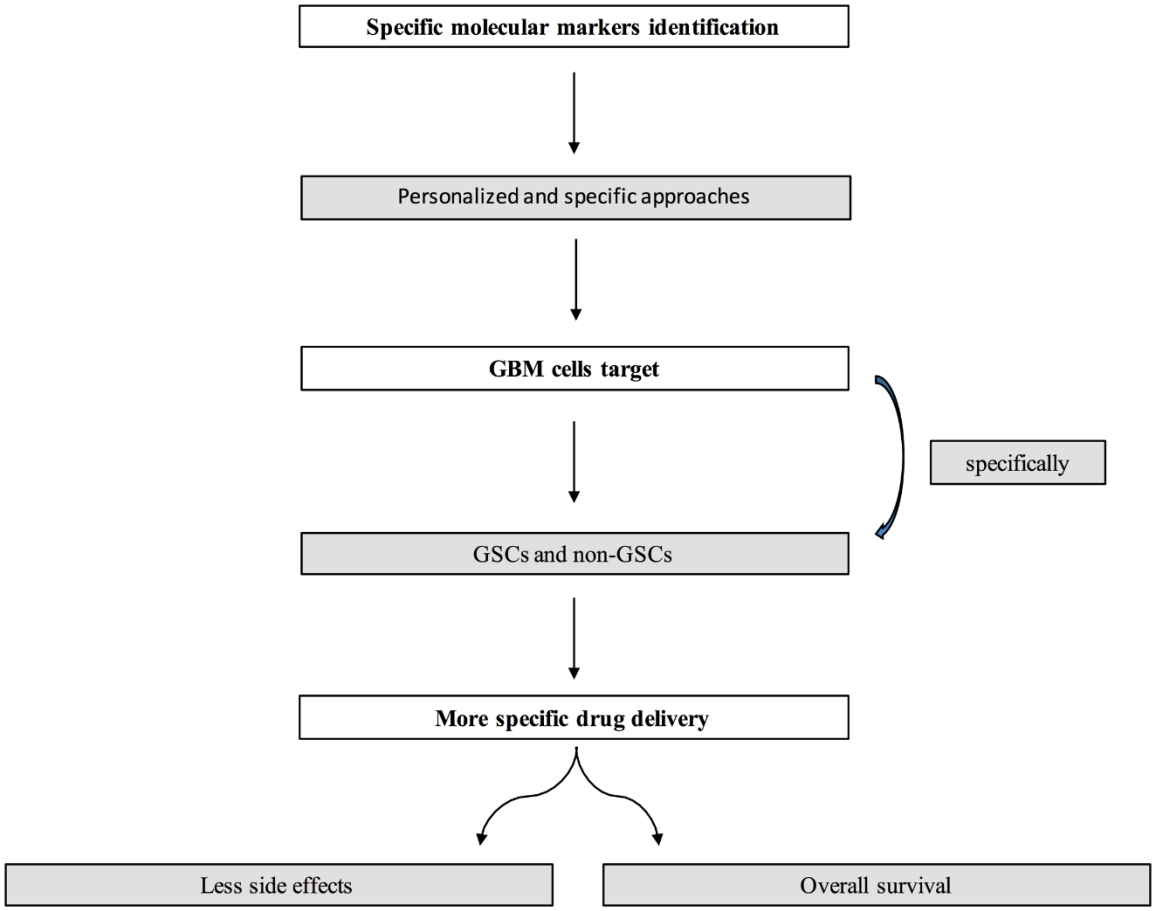

Figure 2.2 Hypothesis. Specific molecular markers identification could lead to identify personalized and specific approaches to GBM cells, GSCs and non-GSCs, and probably induce more specific drug delivery, consequently less side effects, and an overall patient survival.

2.2 OBJECTIVES

The present study **aimed** to: investigate the effects of the combined therapy in the regulation of constitutive signalling pathways of utmost importance in the GBM proliferation, namely p-PKC; study the stem-like cell plasticity in a way to understand the resistance of glioma stem-like cells that contributes to GBM recurrence and chemoresistance and, finally, study the potential of a specific marker for tumor cells, specially to GSCs and non-GSCs, as a target in glioblastoma.

In this regard, we addressed the following **four specific objectives**:

1) Study the modulation of important molecular signalling pathways known to be deregulated in GBM malignancy, specifically PKC, through the combination of Tamoxifen (TMX), a known PKC inhibitor, with TMZ, the *gold standard* for GBM treatment – ***Chapter 3****;*

The PKC molecular pathway will be evaluated as a possible target to achieve an antitumor effect. For that, a well described PKC inhibitor, tamoxifen (TMX), will be used to modulate PKC expression. We will also evaluate the response to treatment with the combination of tamoxifen (TMX) with temozolomide (TMZ), in different GBM cell lines, the U87 and the U118 cells.

2) Understand the potential success of this combined therapy in an isolated GBM cell line obtained from a human patient bearing a recurrent GBM – ***Chapter 4****;*

A detailed characterization of a GBM cell line, isolated and established in our laboratory from a human GBM and submitted to TMX and TMZ in combination, in a way to clarify the potential of the proposed therapeutic approach in a heterogeneous range of GBM cell lines.

3) Characterize the stem-like properties of isolated stem-like cells in GBM (GSCs), and study the mechanisms underlying stem-like cell state plasticity, to clarify the chemotherapeutic resistance of GBM– ***Chapter 5****;*

Due to their chemo and radioresistance capability, the GSCs are at the source of tumor recurrence and treatment failure. The understanding of the molecular mechanisms underlying stem-like cell state plasticity could improve the knowledge about their resistance and push forward the design of new approaches that could target these more resistant cells. Moreover, the association of specific markers expression to a more resistant cell state could lead to better specific strategies and predict tumor response to therapy.

4) Study the potential of Nucleolin as a target in glioblastoma cells – ***Chapter 6****;*

The lack of existence of a recognized specific marker for cancer cells, avoiding healthy ones, is a huge limitation to the conventional chemotherapy. Since Nucleolin (NCL) is overexpressed in a variety of cancer cells, we aimed to test the potential of this protein as a target to identify GBM cells, specifically GSCs and non-GSCs. We used a developed F3-targeted poly (ethylene glycol) (PEG) sterically stabilized pH-sensitive liposome, previously developed by our group, that specifically targets NCL. We investigated whether NCL could serve as a surface bound targeting moiety for GBM therapy, and constitute a step forward in the development of more specific therapies to overcome GBM malignancy and the poor response to treatment.

CHAPTER 3

Tamoxifen in combination with Temozolomide induce a synergistic inhibition of PKC-pan in GBM cell lines

Joana Balça-Silva, Diana Matias, Anália do Carmo, Henrique Girão, Vivaldo Moura-Neto, Ana Bela Sarmento-Ribeiro, Maria Celeste Lopes. 2015

Biochim Biophys Acta. 1850 (4), 722-32.

3.1 ABSTRACT[4]

BACKGROUND: Glioblastoma (GBM) is a highly proliferative, angiogenic grade IV astrocytoma that develops resistance to the alkylating agents used in chemotherapy, such as temozolomide (TMZ), which is considered part of the *gold standard*. The mean survival time for GBM patients is approximately 12 months, increasing to 15 months after TMZ treatment. The resistance of GBM to chemotherapy seems to be associated to genetic alterations and to the constitutive activation of several signalling pathways. Therefore, the combination of different drugs with different mechanisms of action may contribute to circumvent the chemoresistance of glioma cells. Here we describe the potential synergistic behavior of the therapeutic combination of tamoxifen (TMX), a known inhibitor of PKC, and TMZ in GBM. METHODS: We used two GBM cell lines incubated in absence and presence of TMX and/ or TMZ, and measured cell viability, proliferation, apoptosis, cell cycle, migration ability, cytoskeletal organization and the phosphorylated amount of the p-PKC-pan. RESULTS: The combination of low doses of TMX with increasing doses of TMZ shows an increased antiproliferative and apoptotic effect compared to the effect of TMX alone. CONCLUSIONS: The combination of TMX and TMZ seems to potentiate the effect of each other. These alterations seem to be associated to a decrease in the phosphorylation status of PKC. GENERAL SIGNIFICANCE: We emphasize that TMX is an inhibitor of the p-PKC-pan and that these combination is more effective in the reduction of proliferation and in the increase of apoptosis than each drug alone, which presents a new therapeutic strategy in GBM treatment.

Keywords: Glioblastoma; Temozolomide; Tamoxifen; Chemotherapy; p-PKC; Synergism.

[4] This chapter contains the text and the figures originally published in *Joana Balça-Silva, Diana Matias, Anália do Carmo, Henrique Girão, Vivaldo Moura-Neto, Ana Bela Sarmento-Ribeiro, Maria Celeste Lopes. 2015. Biochim Biophys Acta. 1850 (4), 722-32.* Copyright permission with the license number: 4007531147202.

3.2 INTRODUCTION

Glioblastoma (GBM) is the most common and the most aggressive type of primary brain tumor, comprising almost 50% of all diagnosed glioma (Hadjipanayis and Van Meir, 2009; Ohgaki and Kleihues, 2005; Schwartzbaum *et al.,* 2006). Glioma cells show a very high rate of proliferation, are highly resistant to apoptosis and have an increased ability to migrate, characteristics sustained by the constitutive activation of several signalling pathways, cytokines and chemokines production (Hattermann and Mentlein, 2013), catepsin activity (Primon *et al.,* 2013) among others. Local migration of glioma cells turns impossible the complete resection of the tumor and consequently also contributes to the reduced mean survival time of GBM patients. Without treatment the mean survival time of GBM patients is 12 months, which improved when patients began to receive chemotherapy with temozolomide (TMZ). Since then, the mean survival rate has increased to 15 months, and the percentage of patients that survive for 2 years has increased by 17% compared to patients not treated with TMZ (Stupp *et al.,* 2005). TMZ is the leading compound in a new class of chemotherapeutic alkylating agents that enter the cerebrospinal fluid and do not require hepatic metabolism for activation (Friedman *et al.,* 2000). This alkylating agent induces the formation of O^6-methylguanine in DNA, which mispairs with thymine during the DNA replication, leading to activation of the apoptotic pathways. Taking these characteristics into consideration, it was expected that TMZ would increase very significantly the survival of GBM patients (do Carmo *et al.,* 2010; Kanzawa *et al.,* 2004; Patel *et al.,* 2012; Pollack *et al.,* 1990; Zhang *et al.,* 2012). According to previous studies, the limited success of TMZ in GBM treatment appears to be related to the activity of O^6-methylguanine-DNA methyltransferase (MGMT), and to the occurrence of gene mutations that cause permanent activation of several survival signalling pathways such as the AKT, ERK1/2 MAP kinase and also protein kinase C (PKC) (Carmo *et al.,* 2011a; do Carmo *et al.,* 2010; Pollack *et al.,* 1990).

PKC is a family of serine/threonine-specific protein kinases that are involved in the development of many tumors, due to their ability to regulate signalling pathways involved in cellular transformation, proliferation, survival and migration. Nevertheless, some studies have reported that several PKC isoforms may also act as tumor suppressors since they can activate pro-apoptotic pathways (Carmo *et al.,* 2013). Because of the variability of cell functions controlled by PKC isoforms, the contribution of this kinase family to the development of GBM is poorly understood, and its contribution to glioma cell proliferation,

apoptosis and migration is not fully elucidated (Carmo *et al.,* 2013; Puchner and Giese, 2000; Robins *et al.,* 2006). One of the PKC inhibitors is tamoxifen (TMX), which has an anti-angiogenic effect, low toxicity, minimal side effects, low cost, and the capability to cross the blood-brain barrier (Brandes *et al.,* 1999; da Rocha *et al.,* 1999; Massarweh *et al.,* 2008; Patel *et al.,* 2012; Scaltriti and Baselga, 2006) . Previous studies reported in several types of tumor cells that TMX induces apoptosis and reduces tumor cell migration in a PKC-dependent manner (Alves *et al.,* 2011; Kim *et al.,* 2007; O'Brian *et al.,* 1985). In glioma cell lines the results with TMX were controversial and the clinical trials reported that TMX increased the survival of GBM but in a reduced percentage of patients (Cho *et al.,* 1999; DI Cristofori *et al.,* 2013; Patel *et al.,* 2012; Yung *et al.,* 2000).

Taking into account that the activity of PKC in glioma cells is increased, the effect of TMX in glioma cells was not fully understood, the effect of TMZ in GBM patients is reduced, and combination therapies directed to different targets have now become common (Kahn *et al.,* 2012), we hypothesized that the combination of TMX and TMZ could be a promising therapeutic approach in the GBM treatment.

Thereby, in this study the main aim was to investigate the therapeutic effect of the combination of TMX and TMZ in the human GBM cell lines, U87 and U118, through the evaluation of the effect on the survival, proliferation, apoptosis and migration ability.

3.3. MATERIALS AND METHODS

3.3.1 Reagents

DMEM, fetal bovine serum (FBS) and propidium iodide (PI) (Borowski *et al.,* 2005) were supplied by Invitrogen (Paisley, UK). The Hoechst 33258 was purchased from Invitrogen (Paisley, UK). Protease and phosphatase inhibitors were supplied by Roche (Indianapolis, IN, USA). Antibodies for Phospho-AKT (p-AKT) and total AKT (t-AKT), Phospho-ERK1/2 (p-ERK 1/2) and total ERK1/2 (t-ERK 1/2) and p-PKC pan (the antibody detects endogenous levels of PKC α, β I, β II, δ, ε, η and θ isoforms only when phosphorylated at a carboxy-terminal residue homologous to serine 660 of PKC β II) were purchased from Cell Signalling Technology (Beverly, MA, USA). Mouse anti-actin antibody was purchased from Boehringer Mannheim (Germany). The phosphatase linked anti-mouse and anti-rabbit antibodies and the substrate for the phosphatase were obtained

from GE Healthcare (UK). PVDF membranes were purchased from Millipore (Billerica, MA, USA). TMZ and TMX and the other chemicals were purchased from Sigma Chemicals (St. Louis, MO, USA). TMZ and TMX were dissolved in dimethylsulfoxide (DMSO) at a stock concentration of 0.133M and 3mM, respectively. These stocks were aliquoted and diluted with culture medium according to the concentration used. The 5-ethynyl-2'-deoxyuridine (EdU) kit to detect cell proliferation was purchased from Invitrogen. The Annexin V (AV) was purchased from BD-Pharmingen (BioLegends, San Diego, California) and the PI/RNAse for cell cycle analysis was purchased from Immunostep (Salamanca, Spain).

3.3.2 Cell line culture conditions

The U87 and U118 GBM cell lines were purchased from the American Tissue Culture Collection (ATCC) and maintained in Dulbecco's modified Eagle's medium (DMEM) supplemented with 3.5 mg/ml glucose, 0.1 mg/ml penicillin, 0.14 mg/ml streptomycin and 10% inactivated FBS. The cultured cells were maintained at 37˚C in an atmosphere containing 95% air and 5% CO_2. Cells were subcultured every 48 h by lifting them with a cell scraper. The cells were then centrifuged and ressuspended in fresh DMEM. For the experiments, unsynchronized cells were treated with different concentrations of TMZ (200, 250 and 350 μM), taking into account the doses of TMZ used in clinical practice (150 mg/m^2 once per day for 5 days), and/or with two concentrations below the IC50 of TMX (5 and 7 μM) for 48 h (Ostermann *et al.,* 2004; Portnow *et al.,* 2009). The curve for the calculation of the drug concentration necessary to inhibit cell proliferation by 50% was fitted using *GraphPad Prism 5* for Windows (version 5.00; GraphPad Software, Inc., San Diego, CA, USA).

3.3.3 Cell viability using MTT assay

Metabolically active cells were assessed using the 3-(4,5-dimethylthiazol-2-yl)-2,5-diphenyl tetrazolium bromide (MTT) reduction colorimetric assay, as previously reported (Francisco *et al.,* 2011). Briefly, cells were plated in 6 multi-well plates and were incubated for 48 h with TMZ and TMX at different concentrations, alone or in combination. After 48 h of incubation, MTT (5 mg/ml) was added to each well at a final concentration of 0.5 mg/ml and left for 45 min. The blue formazan crystals were dissolved by adding 200

μL of acidified isopropanol (0.04 N HCl). The solubilized products were transferred to 96 well plates and the absorbance was read in a microplate reader at 570 nm, using 620 nm as the reference wavelength. Cytotoxicity was expressed as the percentage of cells surviving in relation to untreated cells. The drug concentration required to inhibit growth by 50 % (IC50) was estimated with *GraphPad Prism 5* for Windows (version 5.00; GraphPad Software, Inc., San Diego, CA, USA).

3.3.4 Study of protein expression by western blot

Cells were incubated with TMZ and/or TMX for 48 h and centrifuged at 1,500 rpm for 10 min at 4˚C. The supernatant was discarded; the cells were ressuspended in RIPA buffer (50 mM Tris HCl at pH 8.0, 150 mM NaCl, 1.0% NP-40, 0.5% sodium deoxycholate, 0.1% SDS and 2 mM EDTA, supplemented with protease and phosphatase inhibitors and DTT), and sonicated. The protein content of each sample was assessed and then the proteins were denatured. For that, buffer (Tris 0.5 mM, pH 6.8; 50% glycerol, 10% SDS, 10% 2β-mercaptoethanol and blue bromophenol) was added to each sample at a 1:1 ratio (Redjal *et al.,* 2006). The protein extracts were then boiled at 95˚C for 5 min before use. For the western blotting assay, 30 μg of protein was separated on a 12% SDS-PAGE and then transferred to a PVDF membrane. The PVDF membrane was incubated with a solution of 5% nonfat milk in TBST for 1 h at room temperature (RTemp) and incubated overnight at 4˚C with the primary antibody against p-AKT (1:1000), p-ERK1/2 (1:1000), or p-PKC (1:1000), diluted in TBST with 1% milk supplemented with azide. Immunocomplexes were detected with anti-rabbit antibody (1:1000), conjugated with alkaline phosphatase, and an enhanced chemifluorescence detection reagent was then used. Finally, the protein expression was quantified using the software *Image Quant TL for Windows* (version 2005; Amersham Biosciences, Piscataway, NJ, USA) with the expression of β-actin as a loading control for p-PKC, as well as total AKT and total ERK1/2 as a loading control for p-AKT, p-ERK1/2, respectively.

3.3.5 Cell cycle analysis by flow cytometry

The cell cycle analysis was performed by flow cytometry, using the detection kit PI/RNAse (Immunostep). For that, cells were incubated for 48 h with TMZ and/or TMX collected and washed with PBS and the pellet was ressuspended in cold 70% ethanol,

during vortex agitation, being incubated during 30 min on ice. After incubation period, cells were washed again and ressuspended in PI/RNAse solution. Then, 20.000 events were acquired and cells were evaluated through *CellQuestTM* and data analyzed by *modfif LTMM software*. The results are expressed by the percentage of cells in each phase of cell cycle with a mean ± SEM of at least three independent experiments.

3.3.6 Cell proliferation using EdU assay

Cells were plated in 6 multi-well plates with different TMZ and/or TMX concentrations, for 48 h. The effect of TMZ and TMX on the proliferation rate was assayed using the EdU kit. Briefly, at the end of the incubation period, EdU labeling solution was added to each well at a final concentration of 100 μM. The cells were incubated for 60 min at 37°C in a humidified atmosphere (5% CO_2). The cells were washed with PBS and incubated for 30 min at 4°C with a fixative solution of ethanol 70% on ice. Finally, the cells were incubated with Click-it reaction cocktail (PBS, CuSO4, fluorescent dye azide and reaction buffer additive) working solution for 30 min at 37°C in a humidified atmosphere (5% CO_2). The incorporation of EdU was analyzed by flow cytometry and data were analyzed with *modfif LTMM software*.

3.3.7 Cell apoptosis by flow cytometry

Cells were collected after 48 h of incubation with TMZ and/or TMX, washed with PBS, ressuspended in binding buffer and incubated with AV (BD Pharmingen) and PI (BioLegends) for 15 min in the dark. After incubation time, cells were diluted in binding buffer (0.1M HEPES, pH 7.4; 1.4 M NaCl; 25 mM $CaCl_2$) and analyzed using a FACSCalibur flow cytometer. The experiments were performed in triplicated and the analysis of the results was performed using the *Paint-a-Gate* TM program.

3.3.8 Staining with Hoechst 33258 for nuclei morphology evaluation

The Hoechst assay was performed as previously described (Carmo *et al.*, 2011a). Briefly, the cells were plated in 6 multi-well plates and incubated with TMZ and/ or TMX for 48 h. Next, the cells were washed in a PBS solution, detached and centrifuged at 1,500 rpm for 10 min. Cells were then incubated for 15 min with a 4% solution of

paraformaldehyde in 1% PBS, centrifuged at 1,500 rpm for 10 min, washed with PBS, and incubated with 5 μg/ml Hoechst 33258 solution for 5 min at RTemp. Then, the cells were washed and ressuspended in PBS and mounted on glass slides using anti-fade mounting medium. The images were captured under a Zeiss LSM 510 Meta confocal microscope at a magnification of 40 x, and viewed on a *Zeiss LSM image browser* (Version 4.2.0.121; Carl Zeiss Inc., Germany).

3.3.9 Evaluation of cell migration ability

Cell migration was studied according to the method described by Liang *et al.*, (Liang *et al.*, 2007). Briefly, cells were plated on 12 multi-well plates and when the cultures were confluent, TMZ and/or TMX were added at different concentrations, for 48 h. Next, the cell monolayer was scraped in a straight line with a p200 pipette tip, debris were removed by washing the cells with culture medium, and then new culture medium was added. The plate was then placed under the phase-contrast microscope and an image from each well was acquired. Cells were then photographed at 0, 2, 4 and 6 hours after the addition of drugs. The images in figure 3.7 were obtained before the addition of drugs and 6 h after the scratch. *ImageJ software* (National Institute of Health, Bethesda, MD, USA) was used to record the coordinates for each scratch location using a computer-controlled stage and the mean scratch width at 6 h was calculated to the original scratch width (0 h). Each experiment was repeated three times.

3.3.10 Analysis of F-actin filament organization

F-actin filament organization was studied according to protocols described by Romão LF *et al.*, (Romão *et al.*, 2008). Briefly, U87 and U118 cells were plated on round coverslips and then incubated with TMZ and/or TMX for 48 h. For detection of actin filaments, cells were fixed with 2.5% paraformaldehyde/ PBS for 20 min, permeabilized with 0.1% Triton X-100/ PBS for 3 min, and then incubated for 30 min with the Alexa Fluor 568 phalloidin staining solution (5 U/ml) in PBS containing 1% BSA. Nuclei were stained with DAPI for 2 min. The coverslips were mounted on glass slides and inspected under a *Zeiss LSM 510 Meta* confocal microscope at a magnification of 40 x, using a filter set with an excitation filter of 568 nm and a barrier filter of 585 nm, and viewed on a *Zeiss LSM image browser* (Version 4.2.0.121; Carl Zeiss Inc., Germany). The circularity

parameter was analyzed using *ImageJ software* (National Institute of Health, Bethesda, MD, USA).

3.3.11 Statistical analysis.

Statistical analysis was performed on *GraphPad Prism 5* for Windows (version 5.00; GraphPad Software, Inc., San Diego, CA, USA). All values are expressed as mean ± SEM. After confirmation of the assumption of normality and homogeneity of variance across groups, the groups were compared by nested design, including analysis of variance and post-hoc comparison with correction of α error according to *Bonferroni* probabilities to compensate for multiple comparisons. Statistical significance within groups was assessed by a one-way ANOVA and a *Dunnet's* test, with a significance threshold of $p \leq 0.05$.

3.4. RESULTS

3.4.1 Evaluation of glioma cell viability in the presence of TMX and TMZ

Cell viability was assessed using the MTT assay according to the method described by Francisco V *et al.,* (Francisco *et al.,* 2011). U87 and U118 cells were incubated for 48 h with increasing TMX (1, 2, 5, 7, 7.5 and 10 μM) and/or TMZ (50, 100, 150, 200, 250, 350, and 500 μM) concentrations. In the U87 cell line, TMZ did not induce a significant reduction in cells viability. In fact, the highest reduction in cell survival was 29.5% ± 6.7 achieved with the concentration of 500 μM, Figure 3.1A. Regarding the effect of TMX in the U87 cell line, the analysis of the dose-response curve revealed that the IC50 value was 9.1 μM, Figure 3.1A.

In the U118 cell line, TMZ had similar effects to those observed in the U87 cell line. The highest reduction in survival was 11.6% ± 32.2 detected when cells were incubated with the concentration of 150 μM, Figure 3.1B. The analysis of the dose-response curve revealed that the IC50 value of TMX was 7.3 μM.

When U87 (Figure 3.1A) and U118 cells (Figure 3.1B) were treated with the combination of TMX plus TMZ the maximum survival reduction was 50% ± 2.9 and 90% ± 2.0, respectively. These reductions were obtained when U87 and U118 cells were treated with TMX 5 μM plus TMZ 350 μM and TMX 7 μM plus TMZ 250 μM, respectively. Compared with TMX alone, in U87 cell line treated with TMX 7 μM the maximum survival reduction was 29.6% ± 18.7, when in U118 was 48.37% ± 12.6. Considering that NCCN guidelines version 2.2014 recommended for the treatment of central nervous system tumors the TMZ concentration of 350 μM and that the effect of different TMZ concentrations, on the reduction of cell survival, is not significantly different, the TMZ concentrations used in this study were 250 and 350 μM. Since the IC50 for the U118 cell line was 7.3 μM, for the next studies we used TMX concentrations bellow this value for the two cell lines.

A.

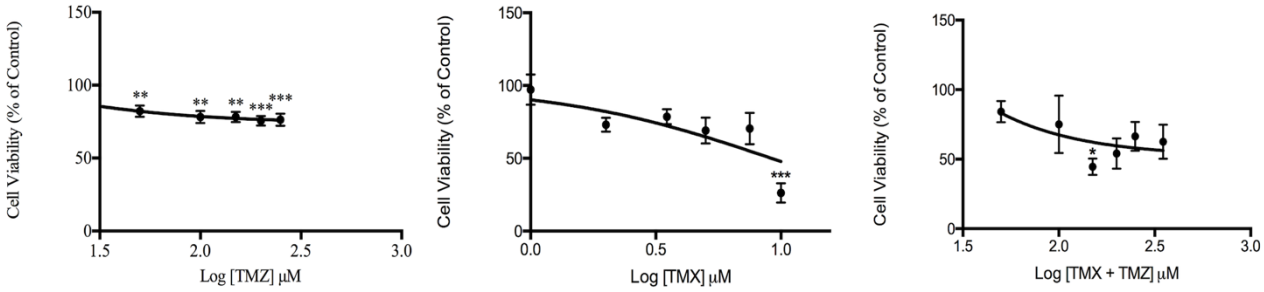

B.

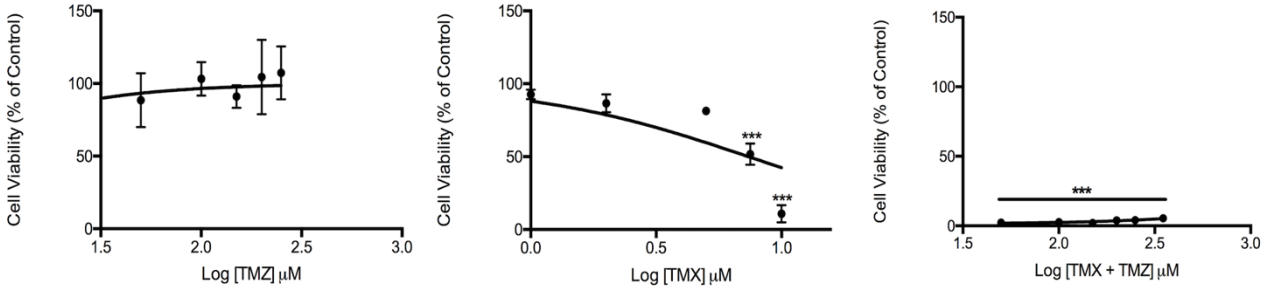

Figure 3.1 Evaluation of TMX and TMZ effect on cell viability, evaluated through MTT assay. U87 (A) and U118 (B) cells were exposed to TMX at 1, 2, 5, 7, 7.5 and 10 μM, respectively and were exposed to TMZ at 150, 200, 250, 350 and 500 μM, respectively. After 48 h of incubation, MTT assays were performed and cell growth and survival were determined by ELISA plate reading at 570 nm and reference 620 nm. The drug concentration required to inhibit growth by 50% (IC50) and the statistical analysis were estimated by *GraphPad Prism 5* for Windows (version 5.00; GraphPad Software, Inc., San Diego, CA, USA). Each value represents the mean ± SEM from three independent experiments, *p < 0.05, **p < 0.01, ***p < 0.001.

3.4.2 Phosphorylation status of p-PKC-pan in glioma cells

The analysis of the p-PKC-pan expression, by western blot, showed that it was constitutively expressed in both cell lines. In order to determine the effect of TMX on the amount of p-PKC-pan, the protein expression in the presence of TMX or in association with TMZ was evaluated by western blot (Figure 3.2). In U87 cells, the results showed that at 5 and 7 μM concentrations of TMX, the amount of p-PKC-pan was significantly reduced by 39.7% ± 4.3 and 39.1% ± 4.2, respectively ($p<0.05$ for both values), when compared to control cells (Figure 3.2A). This reduction was increased when cells were incubated with TMX plus TMZ. With the combination of TMX (7 μM) plus TMZ (350 μM) the amount of p-PKC-pan decreased 56.9% ± 6.1 as compared to control ($p <0.05$), which represents an additional decrease of 17.8% compared to TMX alone (Figure 3.2A).

In U118 cells, TMX also induced a significant reduction on the amount of p-PKC-pan but the decrease was less than that observed in the U87 cell line (Figure 3.2B). In fact, in cells incubated with 5 and 7 μM concentrations of TMX, there was a reduction of 27.6% ± 3.4 and of 28.9% ± 3.6, respectively, in the amount of p-PKC-pan ($p <0.05$ for both values) compared to control cells. However, when U118 cells were incubated with TMX (7 μM) plus TMZ (350 μM) the amount p-PKC-pan was reduced to 55.2% ± 6.9 as compared to that of the control cells, ($p <0.05$), which represents a decrease of 26.4% as compared to TMX alone.

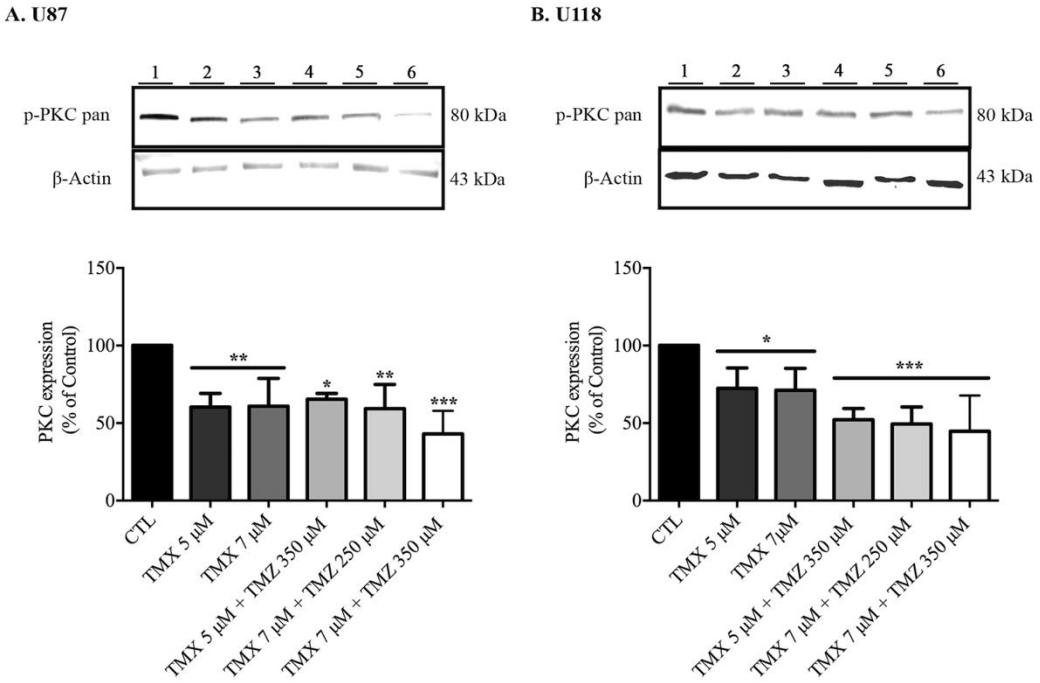

Figure 3.2 Effects of TMX and/or TMZ on p-PKC pan expression. Following the incubation of U87 and U118 cells with TMX and/ or TMZ for 48 h the protein extracts were prepared and used for western blot analysis with anti-p-PKC pan antibody. Loading control was performed with an antibody for β-ACTIN. In U87 (A) cells the p-PKC expression decreased when cells were treated with TMX at 5 μM and 7 μM about 39.7% ± 4.3 and 39.1% ± 4.2, respectively. Also, p-PKC pan expression decreased when cells were treated with combination of TMZ at different concentrations until 56.9% ± 6.1 at TMX 7 μM combined with TMZ 350 μM. In U118 (B) cells the p-PKC pan also decreased when cells were treated with TMX at 5 μM and 7 μM about 27.6% ± 3.4 and 28.9% ± 3.6, respectively. Also, p-PKC pan expression decreased when cells were treated with combination of TMZ at different concentrations until 55.2% ± 6.9 at TMX 7μM combined with TMZ 350 μM. Statistical analysis was performed in *GraphPad Prism 5* for Windows (version 5.00; GraphPad Software, Inc., San Diego, CA, USA). Each value represents the mean ± SEM from three independent experiments, * $p < 0.05$, ** $p < 0.01$, *** $p < 0.001$.

To determine if TMX affects the amount of the p-AKT and p-ERK ½, which are also involved in the proliferation and survival of glioma cells, the amount of the phosphorylated kinases was also evaluated by western blot in the presence of TMX and/or TMZ, (Figure 3.3). The analysis of the blots showed that in both cell lines the amount of p-AKT and p-ERK ½ was not altered by these chemotherapeutic drugs (Figure 3.3).

A. U87

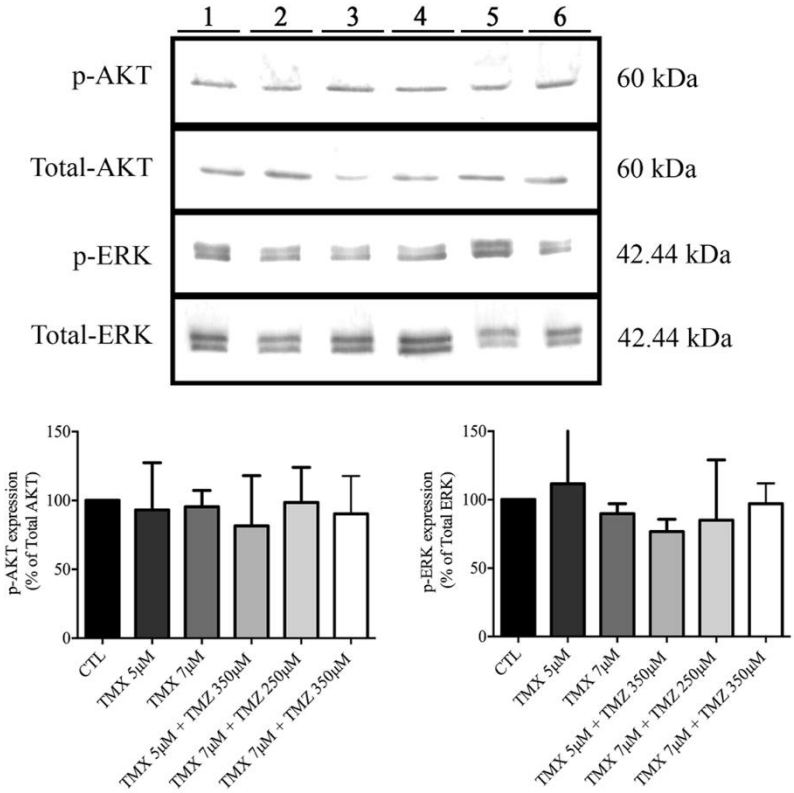
1
2
3
4
5
6
p-AKT
60 kDa
Total-AKT
60 kDa
p-ERK
42.44 kDa
Total-ERK
42.44 kDa
p-AKT expression (% of Total AKT)
p-ERK expression (% of Total ERK)
150
100
50
0
CTL
TMX 5μM
TMX 7μM
TMX 5μM + TMZ 350μM
TMX 7μM + TMZ 250μM
TMX 7μM + TMZ 350μM

B. U118

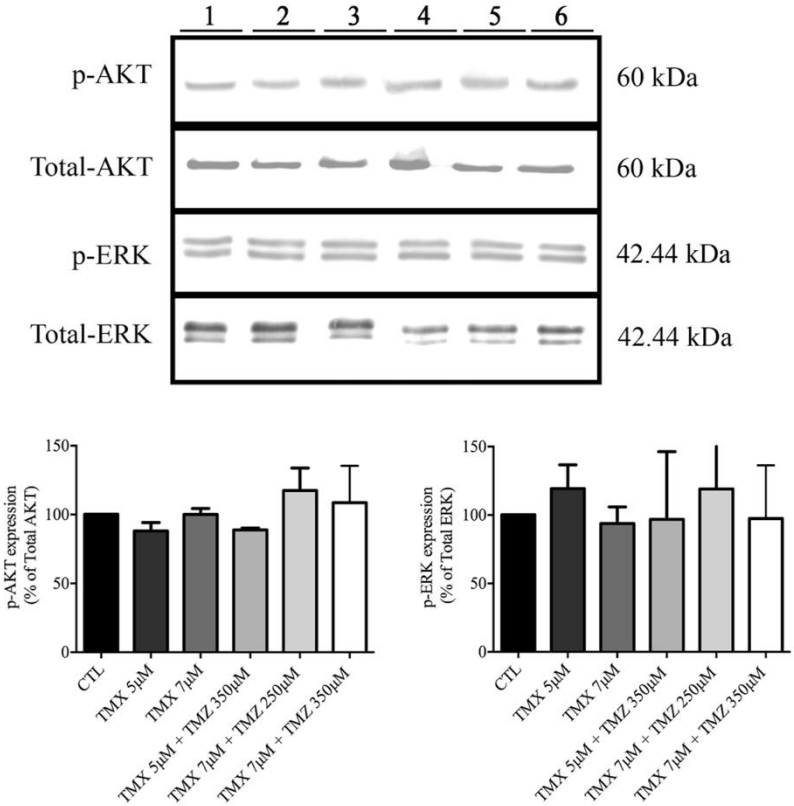
1
2
3
4
5
6
p-AKT
60 kDa
Total-AKT
60 kDa
p-ERK
42.44 kDa
Total-ERK
42.44 kDa
p-AKT expression (% of Total AKT)
p-ERK expression (% of Total ERK)
150
100
50
0
CTL
TMX 5μM
TMX 7μM
TMX 5μM + TMZ 350μM
TMX 7μM + TMZ 250μM
TMX 7μM + TMZ 350μM

Figure 3.3 Effects of TMX and TMZ on p-AKT and p-ERK 1/2 expression. Following the incubation of U87 (A) and U118 (B) cells with TMX and/ or TMZ for 48 h, the protein extracts were prepared and used for western blot analysis with anti-p-AKT and p-ERK ½ antibody. Loading control was performed with an antibody for total AKT and total ERK ½, respectively. Statistical analysis was performed in *GraphPad Prism 5* for Windows (version 5.00; GraphPad Software, Inc., San Diego, CA, USA). Each value represents the mean ± SEM from three independent experiments, $p < 0.05$.

3.4.3 Evaluation of glioma cell cycle in the presence of TMX and TMZ

U87 cells treated with the combination of TMX (7 μM) plus TMZ (350 μM), showed a decrease of 35.7% ± 12.2 of cells in the G0/G1 phase compared to control (untreated cells) and to TMX alone ($p < 0.001$). This decreased was accompanied by a statistically significant increase of the percentage of cells in S and G2/M phases comparing to control and to TMX alone, $p < 0.001$ (Figure 3.4A).

In the U118 cell line, the percentage of cells in each cycle phase was not affect by the TMX, or TMZ or by the combination of TMX plus TMZ neither as compared to control cells or to TMX alone (Figure 3.4B).

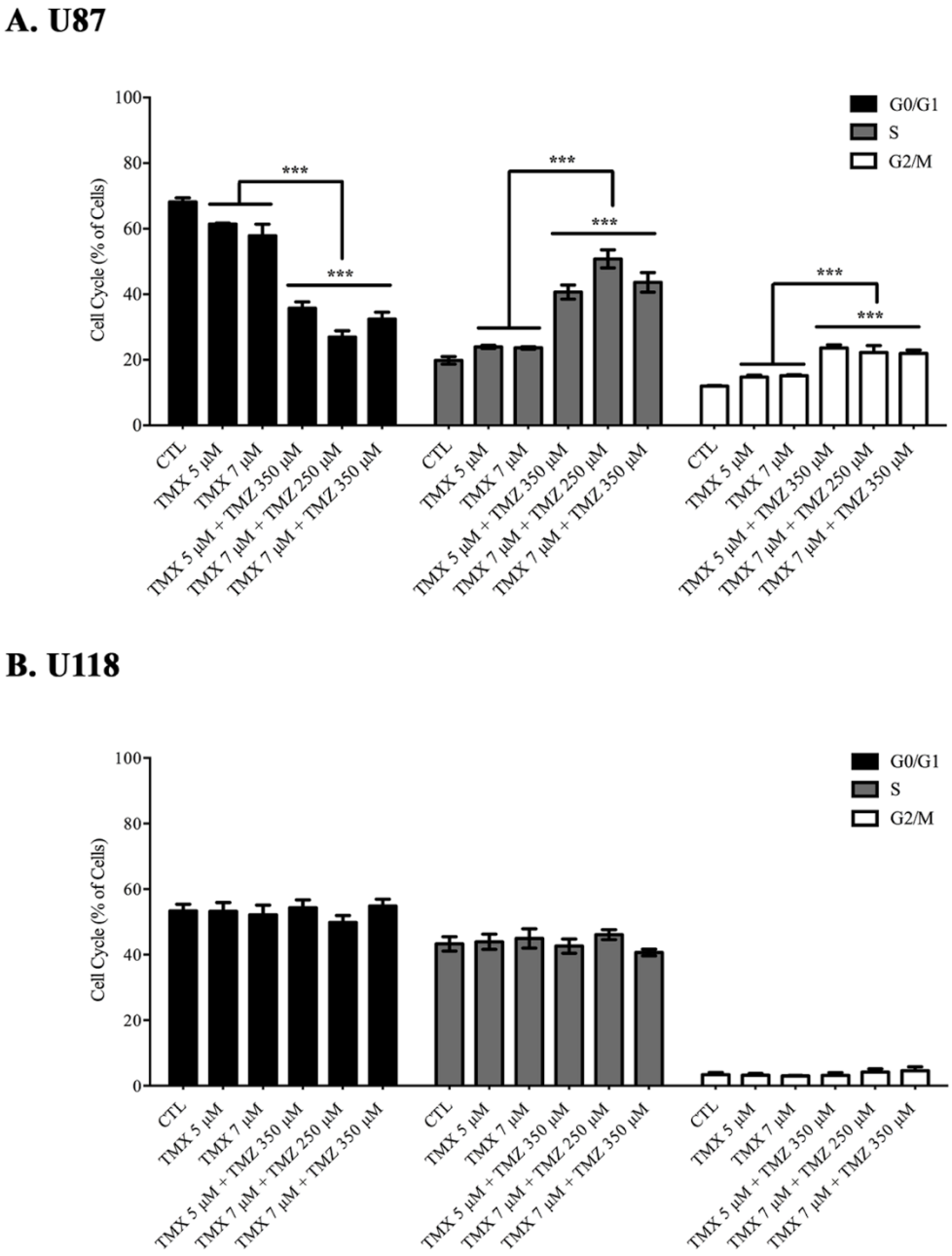

Figure 3.4 Effects of TMX and TMZ on cell cycle analysis by flow cytometry. U87 (A) and U118 (B) cells were treated with TMZ (200, 250 and 350 µM) and /or TMX (5 and 7 µM) for 48 h. Cell cycle analysis was determined by gating Sub-G0/G1, S, and G2/ M on the PI-area signal. A total of 10,000 events were analyzed for each experiment in a BD FACS Canto II (BD Biosciences). Statistical analysis was performed in *GraphPad Prism 5* for Windows (version 5.00; GraphPad Software, Inc., San Diego, CA, USA). Each value represents the mean ± SEM from three independent experiments, *p <0.05, **p <0.01, ***p <0.001.

3.4.4 Evaluation of glioma cells proliferation in the presence of TMX and TMZ

The effect of TMX and/or TMZ on glioma cell proliferation was evaluated by flow cytometry quantification of the incorporated EdU. In U87 cells, the proliferation rate was not significantly altered by TMX alone or by the combination with TMZ as compared to the proliferation rate in control cells (Figure 3.5A).

However, in U118 cells (Figure 3.5B) the proliferation rate decreased 2.8% ± 0.3 and 7.9% ± 1.1 in cells incubated with 5 and 7 μM of TMX, respectively, ($p > 0.05$). This decrease was greatly pronounced in cells treated with TMX plus TMZ. In fact, in cells incubated with TMX (5 μM) plus TMZ (350 μM), or incubated with TMX (7 μM) plus TMZ (250 μM) or even in cells incubated with TMX (7 μM) plus TMZ (350 μM) the proliferation rate decreased 52.5% ± 2.9, 59.2% ± 21.0 and 68.3% ± 2.3, respectively, when compared to control ($p < 0.001$ for the three conditions), which also represents a maximum decrease of 65.4% and 60.3% compared to TMX alone (5 μM and 7 μM, respectively), $p < 0.001$.

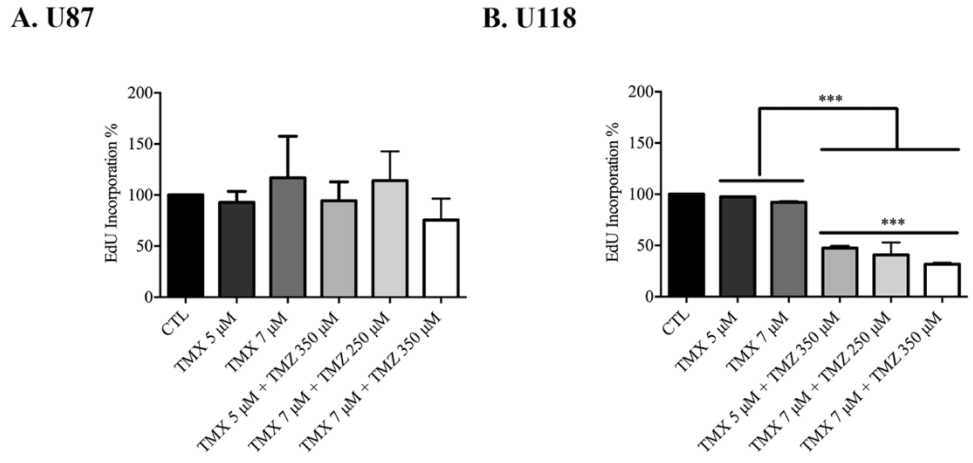

Figure 3.5 Effects of TMZ and TMX on glioma cell proliferation. U87 (A) and U118 (B) cells were incubated for 48 h in the presence of different concentrations of TMZ and/ or TMX. The proliferation rate was evaluated by measuring the incorporation of EdU. Statistical analysis was performed in *GraphPad Prism 5* for Windows (version 5.00; GraphPad Software, Inc., San Diego, CA, USA). Each value represents the mean ± SEM from three independent experiments, ***$p < 0.001$.

3.4.5 Evaluation of apoptosis in glioma cells in the presence of TMX and TMZ

The ability of TMX and TMZ to induce apoptosis was analyzed by flow cytometry using Annexin V/ propidium iodide incorporation, as shown in Table 3.1. In U87 cells incubated with TMX alone there was not a significant increase in the percentage of apoptotic cells. However, when cells were incubated with TMX plus TMZ the percentage of apoptotic cells significantly increased. This increase reached a maximum of 2.6% ± 4.0 in cells incubated with TMX (7 μM) plus TMZ (350 μM) as compared to control cells ($p < 0.05$) (Table 3.1). The percentage of necrotic cells was not affected by TMX alone, nor by the combination TMX plus TMZ.

In U118 cells, TMX alone or in combination with TMZ did not significantly alter the percentage of apoptotic cells. Nevertheless, in U118 cells incubated with TMX plus TMZ there was a significant reduction of viable cells, which was accompanied by an increase in the percentage of late apoptotic cells and by a statistically significant increase in the percentage of the necrotic cells which reached a maximum of 26.7% in cells incubated with 7 μM TMX and 350 μM TMZ, as compared to control ($p < 0.001$) and 21.9% compared to TMX 7 μM alone, $p < 0.05$ (Table 3.1).

Table 3.1 Effects of TMX and TMZ on cell apoptosis by Annexin-V/PI double-staining assay.

	Live Cells (%)	Apoptosis (%)	Necrosis (%)	Late Apoptosis (%)
U87				
Control	92.8 ± 0.6	1.4 ± 0.2	1.8 ± 0.4	4.0 ± 0.5
TMX 5 µM	90.1 ± 1.8	2.8 ± 0.8	2.5 ± 0.8	4.6 ± 0.9
TMX 7 µM	90.8 ± 1.1	2.6 ± 0.5	2.1 ± 0.1	4.4 ± 0.6
TMX 5 µM + TMZ 350 µM	90.5 ± 0.8	3.4 ± 0.6 *1	1.5 ± 0.2	4.6 ± 0.7
TMX 7 µM + TMZ 250 µM	88.1 ± 0.9 *	3.8 ± 0.6 **1	2.1 ± 0.4	6.0 ± 0.6*1
TMX 7 µM + TMZ 350 µM	88.2 ± 1.9 *	3.9 ± 0.8 **1	2.3 ± 0.3	5.5 ± 1.0
U118				
Control	85.8 ± 5.7	0.3 ± 0.2	11.1 ± 4.1	2.8 ± 1.7
TMX 5 µM	81.9 ± 7.8	1.7 ± 1.3	11.2 ± 2.2	5.2 ± 4.4
TMX 7 µM	77.3 ± 11.6	1.4 ± 0.5	15.9 ± 7.2	5.4 ± 3.9
TMX 5 µM + TMZ 350 µM	57.9 ± 6.4 *	1.3 ± 0.1	31.8 ± 3.2 **1	9.1 ± 3.0
TMX 7 µM + TMZ 250 µM	60.3 ± 9.2 *	1.1 ± 0.0	28.7 ± 4.0 *1	10.5 ± 6.5*1
TMX 7 µM + TMZ 350 µM	49.8 ± 6.6 **	1.2 ± 0.6	37.8 ± 5.9 ***1; *2	11.5 ± 3.4**1

*** p<0.05, ** p<0.01, ***p<0.001.**
[1] compared to control
[2] compared to TMX alone

3.4.6 Evaluation of nuclei morphology in glioma cells in the presence of TMX and TMZ

In order to study the nuclei morphology of glioma cells incubated with TMX alone or in combination with TMZ, nuclei from both cells lines was stained with Hoechst 33258. The results indicated that in both cells lines, after the incubation with the chemotherapy drugs alone or in combination, there was an increased number of cells with chromatin condensation, and of pycnotic nuclei with irregular contours (Figure 3.6).

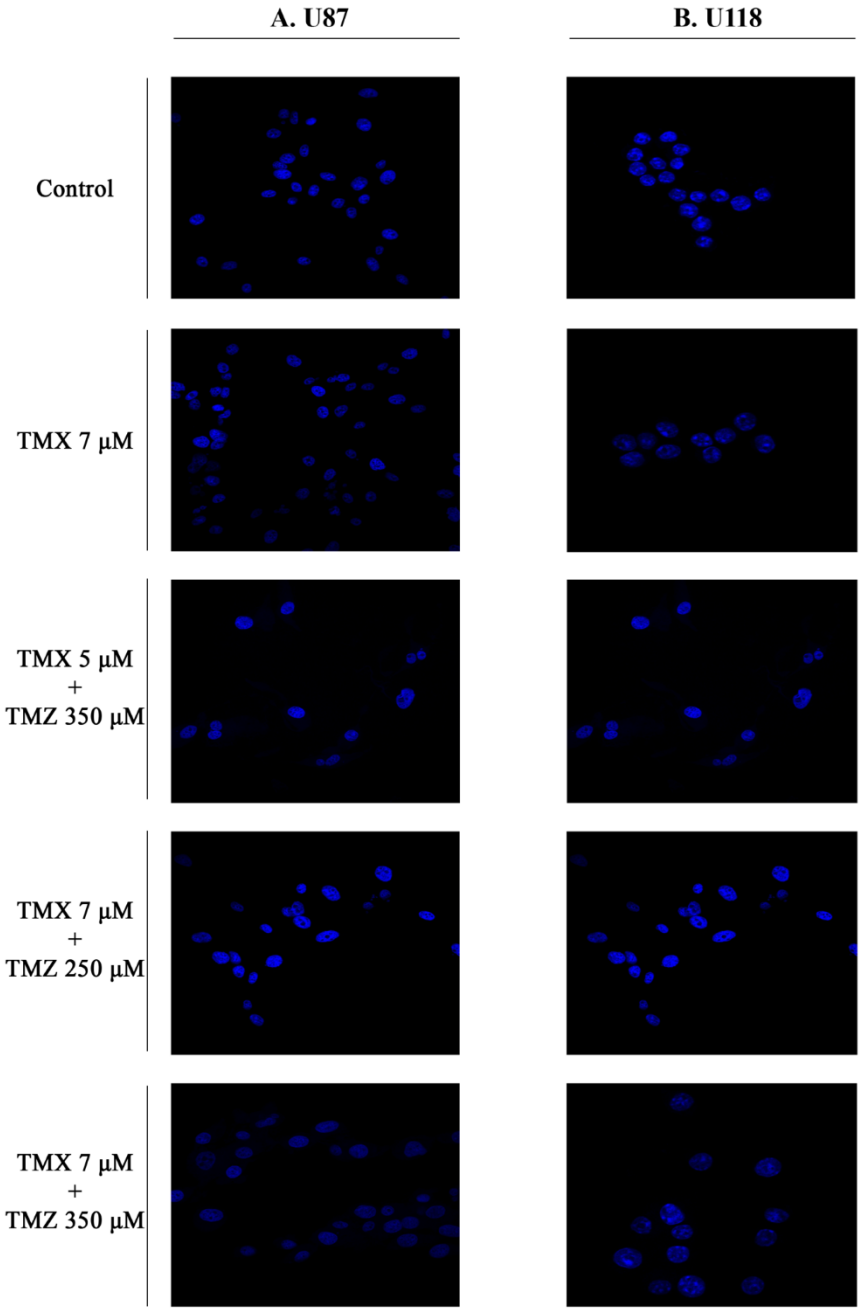

Figure 3.6 Nuclei morphology by *Hoechst 33258* staining. Confocal microscopy analysis of nuclear morphology by *Hoechst 33258* staining of U87 (A) and U118 (B) cells incubated under different conditions for 48 h. Magnification is 10 ×.

3.4.7 Study of cell migration in glioma cells treated with TMZ and/or TMX

To evaluate whether TMZ and/or TMX could regulate the motility of glioma cells, a scratch assay was used according to the method described by Liang *et al.*, (Liang *et al.*,

2007). The results indicated that 6 h after the scratch, the U87 and U118 control cells had the ability to move and to fill the scratch.

U87 cells incubated with TMX alone or in combination with TMZ showed a significantly decrease cell motility (Figure 3.7A). The greatest decrease in cells motility was observed in the presence of 7 μM TMX plus 250 μM TMZ (41.3% ± 8.3) compared to control cells, $p < 0.01$, and to TMX 7 μM alone (12.8%), besides the latest comparation was not statistically significant ($p = 0.06$).

In U118 cells, there was also a significant reduction of the motility with TMX alone and in combination with TMZ. We noticed a decreased in the scratch closure capability of 25.8% ± 5.4 in cells treated with 7 μM TMX alone compared to control cells that was maintained in the combined treatment ($p < 0.01$) (Figure 3.7B).

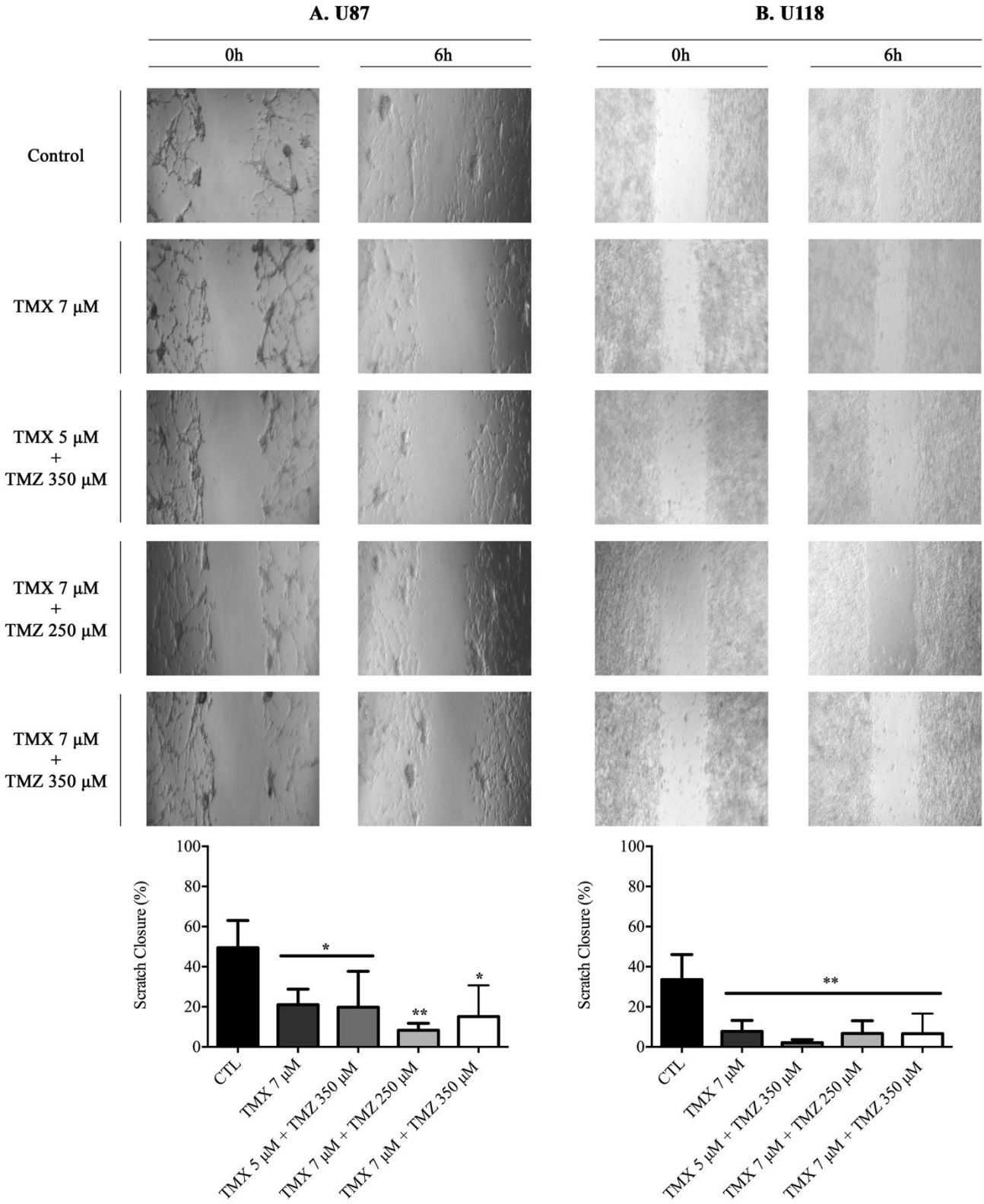

Figure 3.7 Effects of TMX and TMZ on cell migration capability. The images represent photographs of U87 (A) and U118 (B) cells from scratch assay. The scratch closure was measured at various time points (T_0, 2, 4 and - T_6) after the scratch was made in the culture dish. The figure represents the results at 0 h (T_0) and 6 h (T_6) for each condition. Confluent monolayers of control conditions, TMX-treated cells with 7 µM, TMX 5 µM in combination with TMZ 350 µM and TMX

7 μM in combination with TMZ 250 μM and 350 μM were analyzed. Magnification is 10 ×. Statistical analysis was performed in *GraphPad Prism 5* for Windows (version 5.00; GraphPad Software, Inc., San Diego, CA, USA). Each value represents the mean ± SEM from three independent experiments, *p <0.05, **p <0.01.

3.4.8 Evaluation of F-actin filament organization in the presence of TMX and/or TMZ

In order to evaluate if glioma cells acquired a phenotype compatible with the reduction of migration, the effect of TMX and TMZ on the organization of the F-actin filaments was evaluated. For that, cells were stained using Alexa Fluor 568 phalloidin and the circularity parameter according the *ImageJ Software* was determined. Control U87 cells showed a very irregular organization of F-actin filaments which limited the analysis of the results in the presence of TMX and TMZ (Figure 3.8A). However, in U118 cells it was possible to identify several alterations induced by the chemotherapeutic agents. In control cells, F-actin was condensed in the cell body, and the cells were rounded (Figure 3.8B). This organization pattern became slightly disrupted in cells treated with TMX alone and was replaced by a spindle-like pattern (Figure 3.8B). In cells incubated simultaneously with TMX and TMZ, most of the cells showed a F-actin organized in a spindle-pattern, with longer and thicker spindles compared to control or to TMX alone conditions, p <0.001.

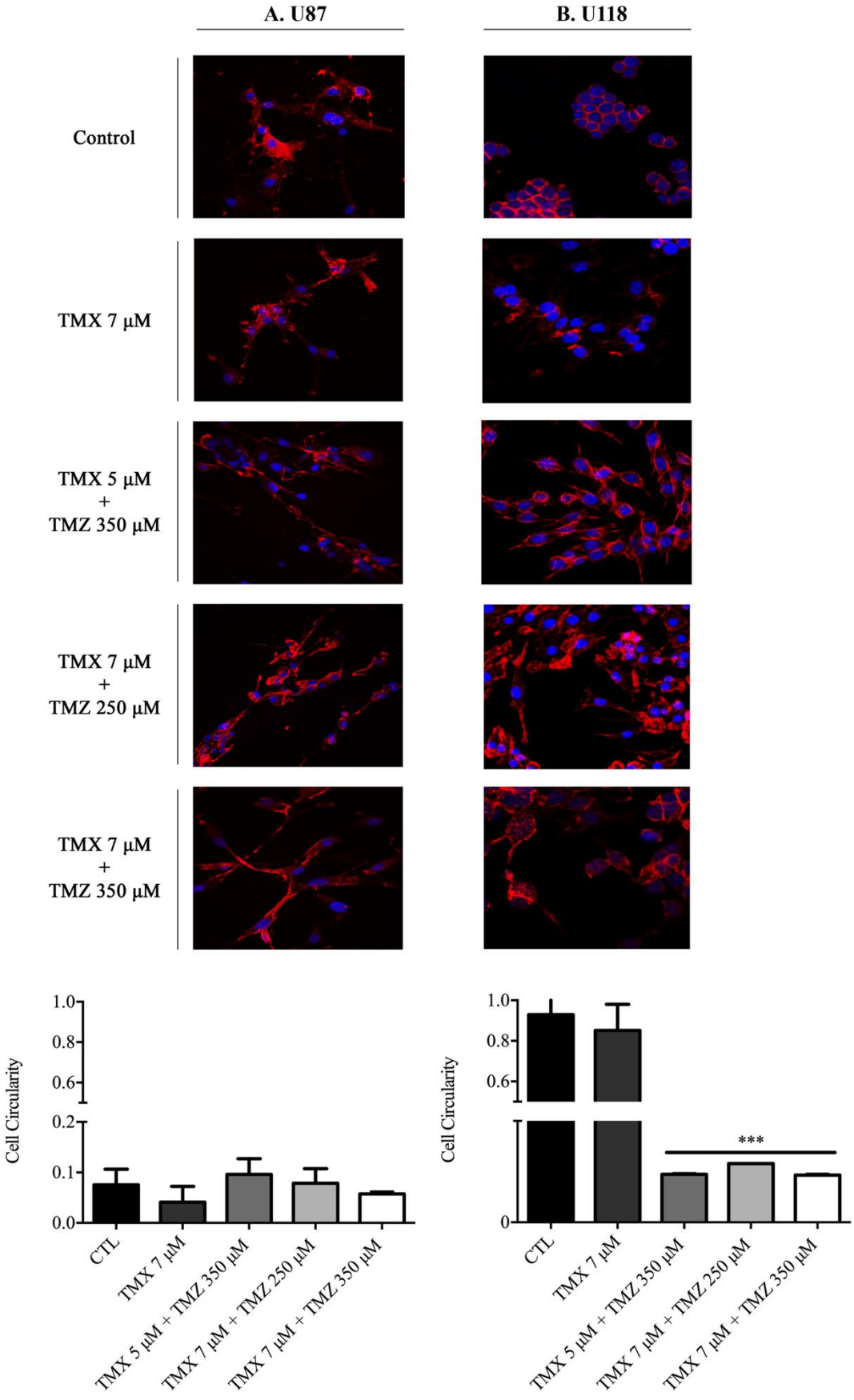

Figure 3.8 Effects of TMX and TMZ on the organization of f-actin filaments. U87 (A)

and U118 (B) cells were incubated for 48 h in the presence of TMZ and/or TMX. Cells were then fixed and F-actin was stained with Alexa Fluor 555 phalloidin. Nuclei were counterstained with DAPI. Red represents F-actin staining and blue represents cell nuclei. Magnification is 10 ×. Statistical analysis was performed in GraphPad Prism 5 for Windows (version 5.00; GraphPad Software, Inc., San Diego, CA, USA). Each value represents the mean ± SEM from three independent experiments, ***p <0.001.

3.5. DISCUSSION

TMZ is considered part of the *gold standard* in GBM treatment, despite of its reduced ability to significantly increase the survival of GBM patients. The antitumor activity of TMZ is based on its ability to introduce DNA adducts and to activate apoptosis. Previous studies reported that the methylation status of the *MGMT* promoter has prognostic value (Hegi *et al.,* 2005; Ueno *et al.,* 2006; Zhang *et al.,* 2012). However, other studies pointed that the TMZ-chemoresistance was also associated to gene mutations and to the constitutive activation of signalling pathways that control survival and proliferation, such as PKC. PKC is one of the most enigmatic signalling pathways since, in tumor cells, according to the isoform, it may promote or inhibit apoptosis and cell survival (Carmo *et al.,* 2013; Mochly-Rosen *et al.,* 2012). Previous studies agree that GBMs are characterized by an increased expression and activity of PKC. However, there is no consensus regarding the PKC contribution to the aggressiveness of glioma cells. This controversy is associated to the existence of isoforms that play different roles and also to the difficulty to obtain PKC inhibitors (Carmo *et al.,* 2013; Cho *et al.,* 1999; da Rocha *et al.,* 1999; O'Brian *et al.,* 1986). In fact, due to the homology of the different isoforms, the developing of specific PKC inhibitor has proven to be difficult.

Tamoxifen is one of PKC inhibitors used in *in vitro* studies with glioma cells and also in clinical trials with GBM patients. The *in vitro* effect of TMX was not completely elucidated and the results of the *in vivo* studies were disappointing since treatment of patients with recurrent malignant glioma with low doses of TMX did not significantly increase the survival rate of the patients (da Rocha *et al.,* 1999; Puchner and Giese, 2000). However, clinical trials using high doses of tamoxifen alone or in combination with other cytotoxic agents have yielded better results (Borowski *et al.,* 2005; Hui *et al.,* 2004; Kamburoğlu *et al.,* 2007; O'Brian *et al.,* 1985; Pollack *et al.,* 1990; Zhang *et al.,* 2000). Since TMX when used in high doses is a non-selective PKC inhibitor, and is associated with an increased toxicity, in this study it was evaluated the effect of the combination of

low doses of TMX with TMZ on the proliferation, survival and migration of two different GBM cell lines (Mochly-Rosen *et al.,* 2012).

In accordance with previous studies, herein we showed that U87 and U118 cells constitutively express the p-PKC-pan. TMX induced a significantly reduction of the p-PKC-pan in both cell lines, confirming that TMX is an inhibitor of the p-PKC. The results also indicated that the expression of p-PKC in U87 cells is more susceptible to TMX, than the p-PKC in the U118 cells. In fact, in the U87 cell line, TMX 7 µM induced a reduction of 39.1% in the amount of p-PKC-pan, while in the U118 cells it just induced a reduction of 28.9%. When cells were incubated with the combination of TMX plus TMZ, the amount of the phosphorylated p-PKC-pan was reduced to approximately 57 and 55% in U87 and U118 cell lines, respectively, indicating that the drug combination is more effective than the drugs alone.

The study of cell viability in the presence of TMX also put in evidence the distinction in susceptibility of the U87 and U118 cell lines to TMX. In the U118 cell line, the IC50 was 7.3 µM and in the U87 cell line the IC50 was 9.1 µM. The differences among cell susceptibility to TMX and TMZ could be due to genetic and molecular alterations that characterize glioma cells (Gupta *et al.,* 2006; Zhong *et al.,* 2001). One of the molecular alterations that may explain the difference of susceptibility of the two cell lines is the constitutive expression of p-ERK1/2 and of PI3k/AKT which according previous studies contribute to the proliferation and resistance to apoptosis of glioma cells. Another alteration that could also contribute to the differences of susceptibility is the expression and activity of P-glycoprotein (PGP). Previous studies indicated that in GBM there is an overexpression of PGP coded by the multidrug resistance 1 gene, which may prevent the accumulation of several chemotherapeutic drugs in glioma cells (Rittierodt and Harada, 2003). Considering that the increase of PGP expression was correlated with a poor response to TMX treatment in several types of cells and also that TMZ may downregulate the expression of glycoprotein P it is possible that the differences among U118 cells and U87 could be due to PGP (Alves *et al.,* 2011; Rittierodt and Harada, 2003).

Considering that previous studies reported that PKC contributes to the increased proliferation it was expected that the reduction of p-PKC by TMX was accompanied by a reduction in cell proliferation. Regarding U118 cells, the proliferation rate was significantly reduced when TMX was combined with TMZ compared to TMX alone condition. However, in U87 cells the proliferation rate was not significantly affected by TMX alone as revealed by the EdU incorporation assay. This observation could be in accordance to a

previous study from Cameron *et al.,* (2008) who sustained that while the activity of PKC is not less than a minimum, it acts as a pro-mitogenic signal (Cameron *et al.,* 2008). In accordance to this hypothesis is the fact that the greatest reduction in U87 cell proliferation was achieved in the presence of TMX (7 µM) plus TMZ (350 µM), which was also the condition that induced the greatest reduction in the phosphorylation status of p-PKC-pan.

Considering that TMX alone or in combination with TMZ induced a reduction in the p-PKC and in cell viability but did not affect the percentage of dividing cells we evaluated the effect of these drugs in cell cycle. In the U87 cell line, TMX alone did not alter the percentage of cells in each cell cycle phase. However, when cells were incubated with TMX and TMZ there was a significantly increase in the percentage of cells in the S and G2/M phases, indicating that the drug combination induced a cell cycle arrest and is in agreement with the results from the proliferation assay. Considering that there is an increased percentage of cells in the S phase, and that in turn the entry of cells in the S phase is associated to cyclin D, which inhibits mitochondrial function, and that the MTT assay depends on the activity of mitochondria to reduce MTT, we may hypothesize that the cell cycle arrest could be associated to a reduction in mitochondrial activity, to a decreased ability of cells to reduce MTT, and consequently to the reduced cell viability detected in the MTT assay.

In the U118 cells the percentage of cells in each cell cycle phase was not affected by TMX or by TMZ. Since the results from the proliferation assay indicated that the combination of TMX plus TMZ significantly decreased the percentage of the incorporated EdU, we hypothesize that not all U118 cells have the same susceptibility to TMZ. Some cells are resistant to TMX and TMZ and maintain the proliferation ability, contributing to the maintenance of the cell cycle characteristics but other cells die when incubated with TMX and TMZ explaining the decreased in cell viability detected by MTT. The variability of susceptibility among cells from a cell line isolated from a human GBM was previously described, reflects the genetic and molecular alterations that characterize GBM and may contribute to the development of chemoresistance (Boyer *et al.,* 2005; Lee *et al.,* 2006). In accordance with this hypothesis the analysis of apoptosis and necrosis revealed that in the U118 cells the combination of TMX plus TMZ induced a significant increase in the percentage of necrotic cells.

In the U87 cells, TMX plus TMZ induced a slight increase in the percentage of apoptotic cells that we hypothesize may result from the cell cycle arrest. Furthermore, since damage cells activate the DNA repair systems, which could be associated to the synthesis

of DNA, it is possible that the incorporated EdU is a consequence of the proliferation and also of the repair systems. Considering that cell cycle arrest in G2, after DNA damage, may activate a process known as cell-cycle adaptation, in which cells reactivate cyclin-dependent kinase 2 complexes and proceed with mitosis, despite the presence of unrepaired damaged DNA, it is possible that U87 cells activate this process justifying the maintenance of the proliferation rate and of the cell cycle (Shen *et al.*, 2013; Syljuåsen, 2007).

Moreover considering that: 1) cell cycle progression is dependent on P21, which plays a critical role in arresting the cell cycle in G1 and G2 after DNA damage (Abbas and Dutta, 2009); 2) the PKC activation upregulates the P21 protein (Besson and Yong, 2000); and that 3) in this study the treatment of U118 cells with TMX plus TMZ significantly reduced the p-PKC-pan expression, it is possible that the reduction of p-PKC-pan is involved in down-regulation of P21 expression, and as a result, the cell cycle progresses normally in some cells.

In addition to the effect of TMX and TMZ on proliferation and cell survival, our results also showed that these drugs reduced the motility of both cell lines, which was accompanied by a reorganization of the F-actin filaments well visible on U118 cell line (Figure 3.8).

Taking altogether, our results emphasize that PKC may play a relevant role in the proliferation, survival and migration of glioma cells. However, its contribution is dependent on the characteristics of the glioma cells, which emphasizes the need to establish a personalized therapy. In fact, the comparison of U118 cell line with U87 cell line showed that both cells have a basal expression of p-PKC. However, the susceptibility of each cell line to TMX and TMZ is different. The U118 cells are more susceptible to TMX than U87 cells, suffering a more significant reduction in cell proliferation and a more significant increase in necrosis when cells were incubated with TMZ plus TMX. On the other hand, U87 cells showed a more significant increase in the percentage of apoptotic cells and a more significant reduction in the motility when cells were incubated with TMX plus TMZ. In conclusion, our results showed that the combination of TMX and TMZ reduces the amount of the phosphorylated PKC-pan and contributes to the reduction of the aggressive behavior of the glioma cells. Together, the results show that PKC could be considered a therapeutic target and emphasize the importance of the combined therapy in the treatment of GBM.

CHAPTER 4

Glioblastoma entities express subtle differences in molecular composition and response to treatment

Joana Balça-Silva, Diana Matias, Anália do Carmo, Luiz Gustavo Dubois, Ana Cristina Gonçalves, Henrique Girão, Nathalia Silva Canedo, Ana Helena Correia, Jorge Marcondes de Souza, Ana Bela Sarmento-Ribeiro, Maria Celeste Lopes, Vivaldo Moura-Neto. 2017

Oncology Reports. 38 (3), 1341-1352.

4.1 ABSTRACT[5]

Glioblastoma (GBM) is a grade IV astrocytoma. GBM patients show resistance to chemotherapy such as temozolomide (TMZ), part of the *gold standard* treatment. In order to simulate the molecular mechanisms behind the different chemotherapeutic responses between GBM patients we aim to compare the cellular heterogeneity and chemotherapeutic resistance mechanisms between different GBM cell lines. We isolate and characterize a human GBM cell line obtained from a recurrent GBM patient, named GBM11. We studied the GBM11 behavior when treated with Tamoxifen (TMX) that, among other functions, is a protein kinase C (PKC) inhibitor, alone and in combination with TMZ in comparation with the responses of U87 and U118 human GBM cell lines. We evaluated cell death, cell cycle arrest, cell proliferation, mainly through PKC expression, by flow cytometry and western blot and, ultimately, cell migration capability and F-actin filaments disorganization by fluorescence microscopy. We demonstrated that the constitutive activation of p-PKC seems to be one of the main metabolic via implicated on GBM malignancy. Despite of its higher resistant behavior, perhaps due to the overexpression of P-glycoprotein and stem-like cell markers, GBM11 cells presented a subtle different chemotherapeutic response compared to U87 and U118 cells. Our GBM11, U87, U118 cell lines show molecular differences, which claim to subtle, but clear, learning about the characterization of GBM heterogeneity, one of the main reasons for tumor resistance. The adding of cellular heterogeneity in molecular behavior constitutes an utmost step closer in the understanding of resistant molecular mechanisms behind GBM and can circumvents the eventual impaired therapy.

Keywords: Glioblastoma; Glioma cancer stem-like cells; Cellular heterogeneity; Chemotherapeutic resistance; Cell motility.

[5] This chapter contains the text and the figures originally published in *Joana Balça-Silva, Diana Matias, Anália do Carmo, Luiz Gustavo Dubois, Ana Cristina Gonçalves, Henrique Girão, Nathalia Silva Canedo, Ana Helena Correia, Jorge Marcondes de Souza, Ana Bela Sarmento-Ribeiro, Maria Celeste Lopes, Vivaldo Moura-Neto. 2017. Oncology Reports. 38(3), 1341-1352.* Copyright permission of Spandidos Publications Ltd.

4.2 INTRODUCTION

Glioblastoma (GBM) is the most common and malignant type of primary brain tumor (Louis *et al.,* 2016; Stupp *et al.,* 2007). The median survival of GBM patients remains approximately 15 months under part of the *gold standard* treatment, temozolomide (TMZ) (Huse *et al.,* 2013; Lima *et al.,* 2012; Louis *et al.,* 2016; Stupp *et al.,* 2005). GBM chemoresistance has been linked to several mechanisms. The presence of stem-like cells, overexpression of efflux proteins, like P-glycoprotein (PGP), the expression of the MGMT protein and the constitutive activation of proliferative signalling pathways, mainly phosphorylated protein kinase C (PKC), have been described as some of the main reasons of GBM chemoresistance, and contribute to the increased proliferation, survival and motility of GBM cells (Balça-Silva *et al.,* 2015; Carmo *et al.,* 2011a; do Carmo *et al.,* 2010; Hattermann and Mentlein, 2013; Safa *et al.,* 2015; Stupp *et al.,* 2009; Thirant *et al.,* 2011; Zhou *et al.,* 2012). We previously reported that the combination of tamoxifen (TMX), a PKC inhibitor, with TMZ can reduce the amount of phosphorylated PKC-pan and contribute to the reduction of aggressive behavior of two GBM cell lines, U87 and U118 (Balça-Silva *et al.,* 2015). In fact, a large spectrum of TMX targets, other than estrogen receptors, have been defined as key mediators of signal pathways activating cell proliferation, determining aggressive course of neoplastic disorders or tumor chemosensitivity, namely in GBM (Bogush *et al.,* 2012). Taking into consideration the genetic and molecular variability in GBM cell lines, we intended to: 1) isolate and characterize a human GBM cell line, henceforth termed GBM11; and 2) compare the effect of TMX and TMZ co-treatment on this GBM cell line with that observed in U87 and U118 cell lines in our previous study (Balça-Silva *et al.,* 2015). The treatment comparison between our GBM11 cell line and the U87 and U118 cell lines with TMX and TMZ as chemotherapeutic compounds and their combinations could reveal distinct cytotoxic effects among GBM cells, indicating an individualized response to therapy.

GBM11 cell line was isolated as previously described from surgical biopsies from a glial tumor diagnosed as recurrent GBM (Faria *et al.,* 2006; Kahn *et al.,* 2012). Next, we characterized the GBM11 considering their stem cell properties, i.e. expression of stem-like cell markers, histopathological features, analysis of GFAP and Nestin expression, properties found in the other established cell lines. To GBM11, U87 and U118 cell lines we also analysed PGP expression. We also tested the sensitivity of GBM11 cells to TMZ treatment alone as a *gold standard* for GBM treatment. We finally evaluated the effect of

TMX and TMZ co-treatment on GBM11 cells by comparing with U87 and U118 cell lines, previously published by our group (Balça-Silva *et al.,* 2015). Principally, our results showed that our GBM11 cells presented a higher resistance to TMX and/ or TMZ treatment compared to that obtained with U87 and U118 cells, probably due to the existence of a stem-like cell population and a higher PGP expression. In fact, the overexpression of PGP at the blood-brain barrier (BBB) is discussed as a major mechanism of pharmacoresistance in cancer, namely in GBM (Linn *et al.,* 1995), but some studies also suggested an intrinsic chemoresistance role of *MRP1* expression in GBM tumor cells, independent of the BBB endothelial transport system (Calatozzolo *et al.,* 2005).

With this study we intended to introduce a new human GBM cell line, GBM11, that could serve as a patient-specific approach to understand the mechanisms underlying chemotherapeutic resistance expanding the resources available for preclinical studies in GBM treatment. We believe that the introduction of this cellular resistant model could provide a potential testing platform to investigate new therapeutic strategies. We consider that our new GBM cell line derived from human tumor cells, came to introduce the variability of a patient-specific response to therapy in a way to reinforce the individually-designed cancer therapy approach and circumvent the eventual impaired therapy.

4.3 MATERIAL AND METHODS

4.3.1 Material

DMEM and fetal bovine serum (FBS) were supplied by Invitrogen (Paisley, UK). The anti-mouse and anti-rabbit antibodies were obtained from GE Healthcare (UK). Protease and phosphatase inhibitors were supplied by Roche (Indianapolis, IN, USA). Antibody for PKC-pan was purchased from Cell Signalling Technology (Beverly, MA, USA). Mouse anti-tubulin and mouse anti-actin antibody were purchased from Boehringer Mannheim (Germany). Temozolomide (TMZ) and Tamoxifen (TMX) were dissolved in dimethylsulfoxide (DMSO) at a stock concentration of 0.133 M and 3 mM, respectively, and diluted in culture medium according to the concentrations used. Both TMZ and TMX were purchased from Sigma Chemicals (St. Louis, MO, USA). 3-(4,5-dimethyl-2-thiazolyl)-2,5-diphenyl-2H-tetrazolium bromide (MTT) was purchased from Sigma Chemicals. Glucose was purchased from Merck (Germany). Fungizone was purchased

from Bristol-Meyers Squibb (Princeton, NJ, USA). Penicillin/streptomycin was purchased from Gibco. Rabbit anti-glial fibrillary acidic protein (GFAP) and Nestin clone 10c2 and PVDF membranes were purchased from Millipore (Billerica, MA, USA). The 5-ethynyl-2'-deoxyuridine (EdU) kit was purchased from Invitrogen. AnnexinV and propidium iodide were purchased from BD-Pharmingen (Biolegends, San Diego, CA, USA). PI/RNase was purchased from Immunostep (Salamanca, Spain). The Phalloidin and the anti-human PGP (fluorescein isothiocyanate (FITC) mouse anti-human P-glycoprotein) were purchased from BD-Pharmingen. NZYDNA Ladder VI (NZYTech, Lisbon). Antibodies for Nanog (#3580), Oct-4A (#2840) and SOX2 (#D6D9), Slug (#9585) were purchased from Cell Signalling Technology (Beverly, MA, USA). Mouse anti-actin antibody was purchased from Boehringer (Mannheim, Germany). PVDF membranes were purchased from Millipore (Billerica, MA, USA). 2x laemmli buffer and ß-mercaptoethanol were purchased from Bio-Rad (São Paulo, Brazil).

4.3.2 Cell line culture conditions

The GBM11 cell line was established and characterized in our laboratory as previously described to other cell lines (Faria *et al.,* 2006; Kahn *et al.,* 2012) using the same protocols to U87 and U118 cell cultures. Briefly, GBM11 cells were obtained by surgical biopsy from a 57-year-old male patient bearing a recurrent glioblastoma previously treated with TMZ concomitantly with radiotherapy, who had given written consent to the study. All procedures were in agreement with the Brazilian Ministry of Health Ethics Committee (CONEP No. 2340). The tumor cells were termed GBM11. The tumor sample was analysed histologically by the Pathology Service of the Federal University of Rio de Janeiro Hospital as previously described (Faria *et al.,* 2006). The biopsy was washed in DMEM medium, mechanically dissociated and then directly plated on a 24 multi-well plate and/or 25 cm^2 tissue culture flasks with Dulbecco's modified Eagle's medium (DMEM) supplemented with 3.5mg/ml glucose, 0.1mg/ml penicillin, 0.14 mg/ml streptomycin and 10% inactivated FBS. Cells were maintained at 37˚C in an atmosphere containing 95% air and 5% CO_2. The medium was changed every 3 days until the culture was near confluence, approximately after 7 days. Then, cell cultures were either fixed and processed for characterization as described in Faria *et al.,* (Faria *et al.,* 2006). Cells were also frozen in FBS and 10% DMSO in cryotubes and conserved in liquid N_2. For the experiments, unsynchronized cells were treated with different concentrations of TMX or TMZ. The

curve for the calculation of each drug concentration necessary to inhibit cell proliferation by 50% was fitted using *GraphPad Prism 5* for Windows (version 5.00; GraphPad Software, Inc., San Diego, CA, USA).

4.3.3 Cell viability evaluation by MTT assay

Metabolically active cells were assessed using the 3-(4,5-dimethylthiazol-2-yl)-2,5-diphenyl tetrazolium bromide (MTT) reduction colorimetric assay, as described by Balça-Silva *et al.,* (Balça-Silva *et al.,* 2015). Briefly, GBM11 cells were plated in 96 multi-well plates and then were incubated with TMX and/ or TMZ at different concentrations for 48 h. After 48 h of incubation, MTT (5 mg/ml) was added to each well at a final concentration of 0.5mg/ml and left for 1h. In order to dissolve the blue formazan crystals, 200µL of DMSO was added. The absorbance was read in a microplate reader at 570 nm. Cytotoxicity was evaluated as the percentage of metabolically active cells in relation to untreated cells. The drug concentration required to reduce the percentage of metabolically active cells by 50% (IC50) was estimated with *GraphPad*.

4.3.4 Histological analysis and immunofluorescence

Haematoxylin was used to stain and counterstain paraffin tumor sections for histopathological analysis. Sections were mounted with Permount™. For immunofluorescence analysis, 10 x 10^4 cells/ml were plated on 24 multi-well plates, as described by Khan *et al.,* (Kahn *et al.,* 2012). Briefly, cells were fixed with 4% PFA in PBS for 15 minutes and then washed with PBS and incubated with 5% BSA/PBS for 30 minutes. Cells were incubated with mouse anti-Nestin (1:200), rabbit anti-GFAP (1:500). Cells were incubated overnight at 4°C with the primary antibodies and then washed with PBS and incubated with secondary antibodies conjugated with Alexa Fluor 488 (goat anti-mouse; 1:250) overnight. The day after, cells were washed with PBS, stained with DAPI, then washed with PBS again and mounted. Negative controls were performed with non-immune rabbit or mouse IgG. Cells were imaged using a DMi8 advanced fluorescence microscope (Leica Microsystems, Germany) equipped with a 63x oil-immersion objective. Imaging processing was performed with the software ImageJ 1.49v.

4.3.5 Analysis of F-actin filament organization

GBM11 cells were incubated with TMZ and/or TMX for 48 h and F-actin filament organization was studied using Alexa Fluor 568 phalloidin staining solution (5 U/ml) as described by Balça-Silva *et al.,* (Balça-Silva *et al.,* 2015). Briefly, cells were fixed with 2.5% paraformaldehyde/ PBS for 20 min. Next, cells were permeabilized with 0.1% Triton X-100/ PBS for 3 min and then incubated for 30 min with the Alexa Fluor 568 phalloidin staining solution (5 U/ml) in PBS containing 1% BSA. Nuclei were stained with DAPI for 2 min. Finally, the coverslips were mounted on glass slides and inspected under a Zeiss LSM 510 Meta confocal microscope at a magnification of 40 x, using a filter set with an excitation filter of 568 nm and a barrier filter of 585 nm. Then, cells were viewed on a Zeiss LSM image browser (Version 4.2.0.121; Carl Zeiss Inc., Germany).

4.3.6 Western blot analysis of protein expression

The PKC-pan expression was analysed by western blot as described by Balça-Silva *et al.,* (Balça-Silva *et al.,* 2015). Also, the expressions of SOX2, Oct-4A and NANOG were also analysed by western blot as originally described by Towbin and adapted by Balça-Silva *et al.,* and Kahn *et al.,* in both the GBM and GBM-serum free (GBM-SF) cell lines (Balça-Silva *et al.,* 2015; Kahn *et al.,* 2012; Towbin *et al.,* 1989). Briefly, cells were centrifuged at 500 xg for 10 min at 4 °C. The supernatants were discarded. Cells were then resuspended in RIPA buffer (50 mM Tris–HCl at pH 8.0, 150 mM NaCl, 1.0% NP-40, 0.5% sodium deoxycholate, 0.1% SDS and 2 mM EDTA, supplemented with protease and phosphatase inhibitors and DTT), and finally sonicated. The samples were denatured with Lämmli buffer 2 x added to each sample at a 1:1 ratio. All the protein extracts were boiled at 95 °C for 5 min before use. 30 µg of protein was run on a 10% SDS-PAGE gel and transferred to a PVDF membrane. Then, it was incubated with a solution of 5% non-fat milk in TBST for 1 h at room temperature. The primary antibodies against p-PKC pan (1:1000), SOX2 (1:1000), Oct-4A (1:1000), and NANOG (1:1000) were diluted in TBST with 1% non-fat milk supplemented with azide. After the incubation period, the immunocomplexes were detected with anti-rabbit antibody (1:1000) and conjugated with horseradish peroxidase. Bands were obtained after exposing the membranes to an X-ray film, and analysed through densitometry scanning. The protein expression was quantified using the software ImageJ 1.49v (Wayne Rasband, National Institutes of Health, USA) with

the expression of ß- Actin used as a loading control. Each experiment was repeated three times separately.

4.3.7 PGP expression by flow cytometry

The expression of PGP in the different GBM cell lines U87, U118 and GBM11 was assessed by flow cytometry using monoclonal antibodies labelled with fluorochromes. For each assay, 10^6 cells were used and data on at least 10,000 events was collected using a FACSCalibur flow cytometer, and analysed using *CellQuest™* software (Becton Dickinson). Since PGP is a membrane protein, cells were centrifuged at 300 xg and incubated for 15 min at room temperature with the monoclonal antibodies: anti-human PGP (fluorescein isothiocyanate (FITC) and mouse anti-human P-glycoprotein (BD Pharmingen).

4.3.8 MGMT methylation pattern analysis

DNA from GBM cell lines U87, U118 and GBM11 was extracted according to standard procedures by the GRS Genomic DNA kit. One microgram of genomic DNA was treated with sodium bisulfite using the EpiTect Bisulfite Kit (Qiagen, Hilden, Germany). Methylation-specific PCRs of *MGMT* gene promoters were carried out as described by Gonçalves *et al.,* (Gonçalves *et al.,* 2015) by the EpiTect PCR control DNA kit (*Qiagen*) according manufactures instructions. PCR products were resolved on 4% agarose gels, stained with ethidium bromide, and observed under UV illumination.

4.3.9 Cell apoptosis analysis by flow cytometry

Cells were collected after 48 h of incubation with TMZ and/or TMX, washed with PBS, resuspended in binding buffer, and incubated with Annexin V (AV) (BD Pharmingen) and Propidium iodide (PI) (BioLegends) for 15 min in the dark as described by Balça-Silva *et al.,* (Balça-Silva *et al.,* 2015). Cells were then diluted in binding buffer and analysed using a FACSCalibur flow cytometer. The experiments were performed in triplicate, and the results were analysed through *CellQuest™* and data analysed by modfif LTMM software.

4.2.10 Cell cycle analysis by flow cytometry

The cell cycle analysis was performed by flow cytometry, using the detection kit PI/RNAse (Immunostep), after the cells were incubated for 48 h with TMZ and/or TMX, as described by Balça-Silva *et al.,* (Balça-Silva *et al.,* 2015). Briefly, after incubation, cells were collected and washed with PBS, and the pellet was resuspended in cold 70% ethanol, during vortex agitation, and finally incubated during 30 min on ice. Cells were incubated in PI/RNAse solution. 20,000 events were acquired, and cells were evaluated through *CellQuest*^{TM} and data analysed by modfif LTMM software. The results are expressed by the percentage of cells in each phase of cell cycle with a mean ± SEM of at least three independent experiments.

4.3.11 Cell proliferation using EdU assay

Cells were plated in six multi-well plates with different TMZ and/or TMX concentrations for 48 h, and the effect on the proliferation rate was assayed using the EdU (5-ethynyl-2'-deoxyuridine) kit, exactly as described by Balça-Silva *et al.,* (Balça-Silva *et al.,* 2015). In the final step, cells were incubated with click-it reaction cocktail (PBS, $CuSO_4$, fluorescent dye azide and reaction buffer additive) working solution for 30 min at 37 °C in a humidified atmosphere (5% CO_2). The incorporation of EdU was analysed by flow cytometry and data were analysed with modfif LTMM software.

4.3.12 Evaluation of cell migration ability

Cell migration was studied according to the method described by Liang *et al.,* (Liang *et al.,* 2007). After the cells incubation with TMZ and/or TMX at different concentrations, for 48 h, and the cell monolayer was scraped in a straight line with a p200 pipette tip, just as described by Balça-Silva *et al.,* (Balça-Silva *et al.,* 2015). The debris were removed by washing the cells with culture medium and new culture medium was added. *ImageJ software* (National Institute of Health, Bethesda, MD, USA) was used to record the coordinates for each scratch location using a computer-controlled stage. The mean scratch width at 6 h was compared to the original scratch width (0 h). Each experiment was repeated three times.

4.3.13 Statistical analysis

Statistical analysis was performed on *GraphPad Prism 5* for Windows, version 5.00. After confirmation of the assumption of normality and homogeneity of variance across groups, the groups were compared by nested design with analysis of variance and post-hoc comparison, with correction of α error according to Bonferroni probabilities to compensate for multiple comparisons. All values were expressed as mean ± SEM, $p < 0.05$.

4.4 RESULTS

4.4.1 Establishment and characterization of GBM11 cell line

Surgical biopsy from a glial tumor diagnosed as a recurrent GBM was used in this study. The diagnose was based on magnetic resonance imaging (MRI), which showed a typical ring-shaped appearance with a hypodense area due to necrosis, peripheral contrast enhancement, and edema that indicates a GBM (Figure 4.1A). Haematoxylin and eosin (H&E) staining revealed hypercellular injury with a fibrillary background and significant atypia, glomeruloid vessels, and extensive areas of necrosis (Figure 4.1B). Also, immunohistochemistry analysis showed GFAP-positive cells (Figure 4.1C) and negativity for cytokeratin pool (AE1 / AE3), TTF-1, chromogranin, synaptophysin, CK7, CK20 and PSA (data not shown).

After tumor removal, cells were isolated and cultured as previously described for other GBM cultures established in our laboratory (Faria *et al.,* 2006). The presence of stem-like cell markers, namely SOX2, OCT-4A and NANOG was also confirmed (Figure 4.1D). We also evaluated the viability of GBM11 cells in the presence of TMX and TMZ, by MTT assay. Treatment with TMZ alone did not induce any alteration in cell viability (Figure 4.1E), whereas treatment with TMX alone induce a reduction of cell viability, with an IC50 of 25.6 µM (Figure 4.1F). On the other hand, the combination of TMX (8.8 µM) plus TMZ (250 µM) induced a reduction of 49.2% in cell viability (Figure 4.1G).

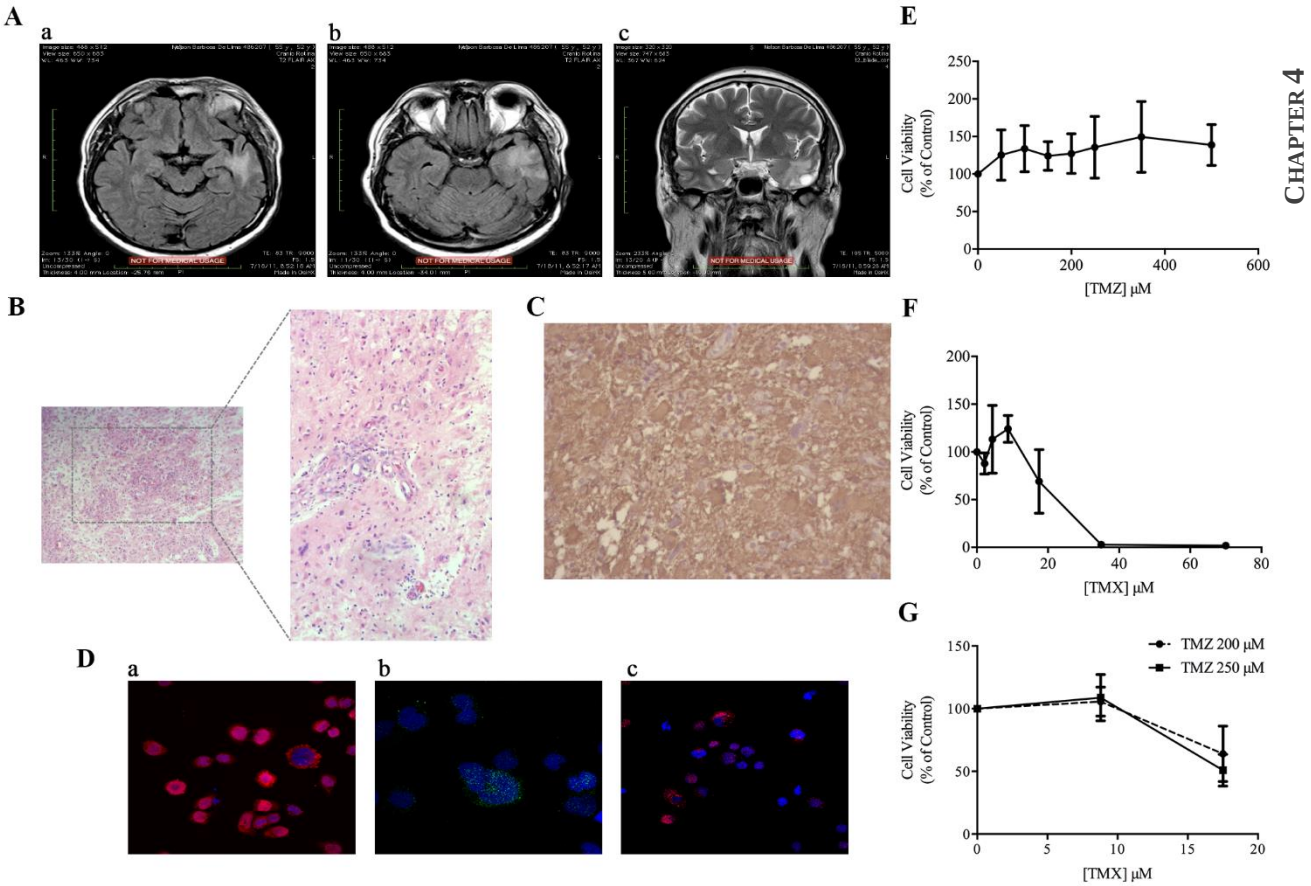

Figure 4.1 GBM cell line isolation and characterization and evaluation of the effect of the TMX and TMZ combination on cell viability. (A) Magnetic resonance image of the patient. a and b: Axial FLAIR are two cuts in different slices, showing the infiltration of brain tissue adjacent to the lesion; c: sequence termed T2 shows the lesion and the surrounding edema with a cyst in its interior, which represents a central necrosis. (B) Haematoxylin–eosin staining of GBM11 cells showing vascular endothelial proliferation, cellular pleomorphism, nuclear atypia and necrosis; left image 100x, right image, 400x magnification. (C) GFAP-positive staining at the time of the diagnosis. (D) Positive stem-like cell markers expression: (a) SOX2, (b) OCT4 and (c) NANOG. The nuclei were counterstained with DAPI. (E) GBM11 cells were treated with TMZ (0 to 500 µM) or (F) TMX alone (0 to 70 µM) and (G) with the combination of two doses above the IC50 of each drug individually, e.g. 8.8 µM TMX plus 200 µM TMZ; 8.8 µM TMX plus 250 µM TMZ; 17.5 µM TMX plus 200 µM TMZ; 17.5 µM TMX plus 250 µM TMZ. Dose–response curves represent the mean ± SEM of 3 independent experiments for each concentration tested, ** $p < 0.01$.

4.4.2 Resistance mechanisms evaluation of different GBM cell lines

The U87 and U118 cell lines, previously studied, and the new GBM11 cell line established in our laboratory revealed a positive staining for Nestin, a neuronal marker; for GFAP, usually overexpressed in GBM cells; as well as a different F-actin organization by phalloidin staining (Figure 4.2A), which suggests a similar origin of these three cell lines. Since the activity of P-glycoprotein (PGP) may prevent the accumulation of several chemotherapeutic drugs in glioma cells, we evaluated the expression of PGP in all GBM

cell lines (Borowski *et al.,* 2005; Linn *et al.,* 1995; Rittierodt and Harada, 2003). The results showed that in GBM11 the PGP expression was 3-fold higher compared with another GBM cells: U87 and U118 (Figure 4.2B).

It is also well known that methylation of the *MGMT* promoter can affect the sensitivity of cells to TMZ (Hegi *et al.,* 2005; Qiu *et al.,* 2014). These findings led us to analyse the methylation status through a methylation-specific PCR in the three GBM cell lines. In U87 and GBM11 cell lines, the *MGMT* proved to be completely methylated and in the U118 cell line the *MGMT* showed to be partially methylated (Figure 4.2C). Regarding the stem-like cell markers expression we noticed that the U87 cell line present a 61.3% ± 11.5 of SOX2; 6.8% ± 3.7 of Oct-4A; and 49.3% ± 20.7 of NANOG. The U118 cell line present 57.9% ±17.3 of SOX2; 16.01% ± 4.2% of OCT4 and 28.0% ± 14.4 of NANOG. Finally, the GBM11 cell line present 76.8% ± 25.8 of SOX2; 7.0% ± 1.5 of Oct-4A; and 38.8% ± 17.4 of NANOG (Figure 4.2D).

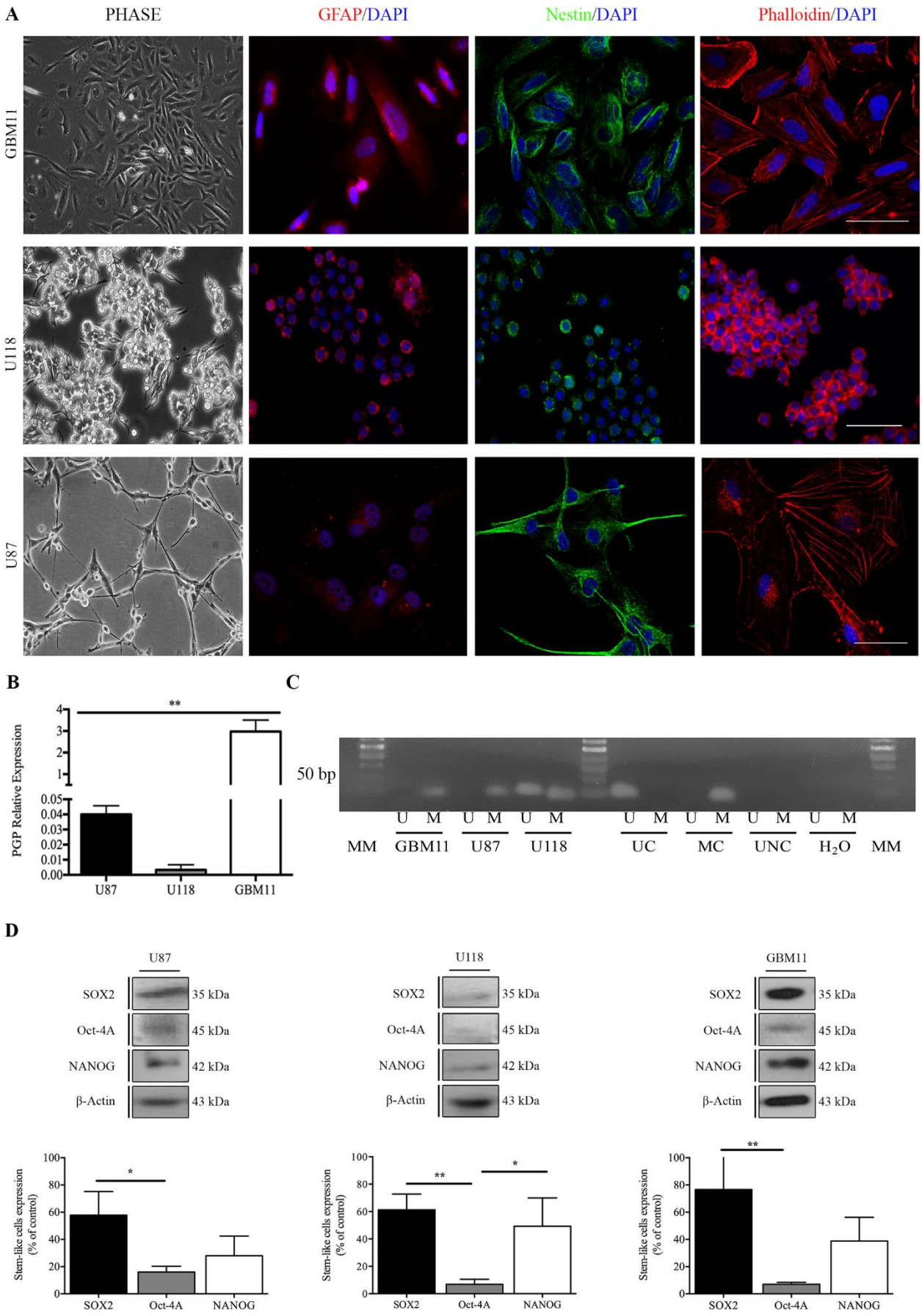

Figure 4.2 Resistance mechanisms evaluation in GBM cell lines. (A) Nestin, Glial fibrillary

acidic protein (GFAP) and Phalloidin positive-staining were analysed for U87, U118 and GBM11 cell lines. (B) PGP expression was quantified in the three GBM cell lines, U87, U118 and GBM11 by flow cytometry analysis in a BD FACSCalibur system. A total of 10,000 events were collected. Relative expression was obtained by PGP expression compared to the respective isotype and corresponds to the % of Gated cells. (C) MGMT methylation pattern was analysed through Methylation-specific PCRs for U87, U118 and GBM11 cells lines. UC - universal unmethylated control (bisulfite converted); MC - universal methylated control (bisulfite converted); UNC - universal not converted unmethylated control (not bisulfite converted); MM – molecular marker of 50 bp. (D) The expression of SOX2, OCT-4A and Nanog in U87, U118 and GBM11 cell lines was quantified by western blot. Statistical analysis was performed in GraphPad Prism 5 for Windows (version 5.00; GraphPad Software, Inc., San Diego, CA, USA). Each value represents the mean ± SEM from three independent experiments, * $p < 0.05$, ** $p < 0.01$.

4.4.3 Evaluation of death and cell cycle in GBM11 cells treated with TMX and TMZ

To evaluate cell death with the combined therapy compared with monotherapy with TMZ, we stained the cells with Annexin V (AV), to analyse apoptotic cells, and with propidium iodide (PI), to analyse necrotic cells, by flow cytometry (Figure 4.3A). TMZ alone did not induce cell death in GBM11 (Figure 4.3B). However, 17.5 µM of TMX induced an increase of 7.5% ± 0.7 in apoptosis and 37.5% ± 21.5 in late apoptosis, respectively, compared to control cells. Combined treatment with 17.5 µM TMX plus 250 µM TMZ induced an increase of 8.1% ± 2.3 in apoptosis and 36.5% ± 23.4 in late apoptosis, $p < 0.001$ (Figure 4.3C). Cell cycle analysis showed an arrest in the G1 phase when TMX was administered alone, $p < 0.001$ (Figure 4.3D).

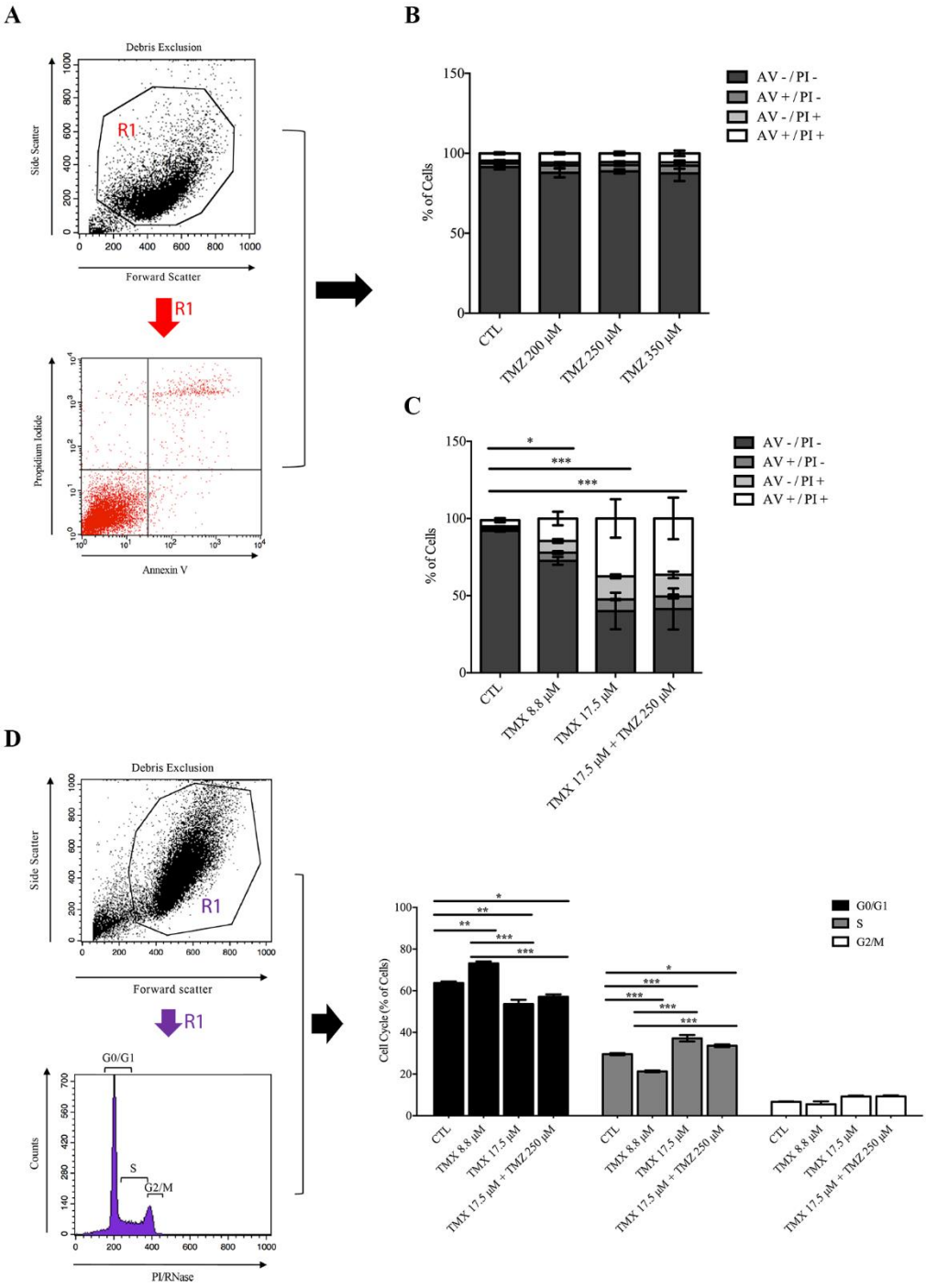

Figure 4.3 Effects of TMX and TMZ combination on cell death and cell cycle of GBM11 cells. Following the incubation of GBM11 cells with TMX and/or TMZ for 48 h, cells were stained with Annexin V (AV) and Propidium Iodide (PI) and analysed by flow cytometry. (A) Debris were removed to obtain the viable cells region, R1. The R1 region was used to analyse AV and PI expression by flow cytometry. The analysis was based on the percentage of gated positive cells. (B) TMZ alone was added to GBM11 cells in different concentrations. (C) TMX and/or in combination with TMZ was added to GBM11 cells in different concentrations. The chosen doses were above the dose that inhibited growth by 50% (IC50) individually. The AV positive cells, PI positive cells, AV and PI double-positive cells and the live cells (double-negative) were immediately analysed by flow cytometry in a BD FACSCalibur system and evaluated in the FL2 and FL1 channel, respectively. A total of 10,000 events were collected. (D) Cell cycle analysis was determined by gating G0/ G1, S and G2/ M on PI-area signal by flow cytometry after the debris were removed to obtain the R1 region.

4.4.4 Evaluation of EdU incorporation and p-PKC-pan regulation in GBM11 cells treated with TMX and TMZ

EdU incorporation in 17.5 µM of TMX and in 17.5 µM TMX plus 250 µM TMZ was reduced by 90.7% ± 8.0 and 96.2% ± 3.4, respectively, compared to control cells, $p < 0.001$ (Figure 4.4A).

We verified that GBM11 cells also express p-PKC-pan. The 17.5 µM of TMX induced a significant reduction of 49.3% ± 30.1 in p-PKC-pan regulation, $p < 0.05$. When combined with TMZ, the reduction of p-PKC-pan was 44.3% ± 29.4 with 17.5 µM TMX plus 250 µM TMZ ($p < 0.01$), and 65.2% ± 20.3 with 17.5 µM TMX plus 350 µM TMZ (Figure 4.4B).

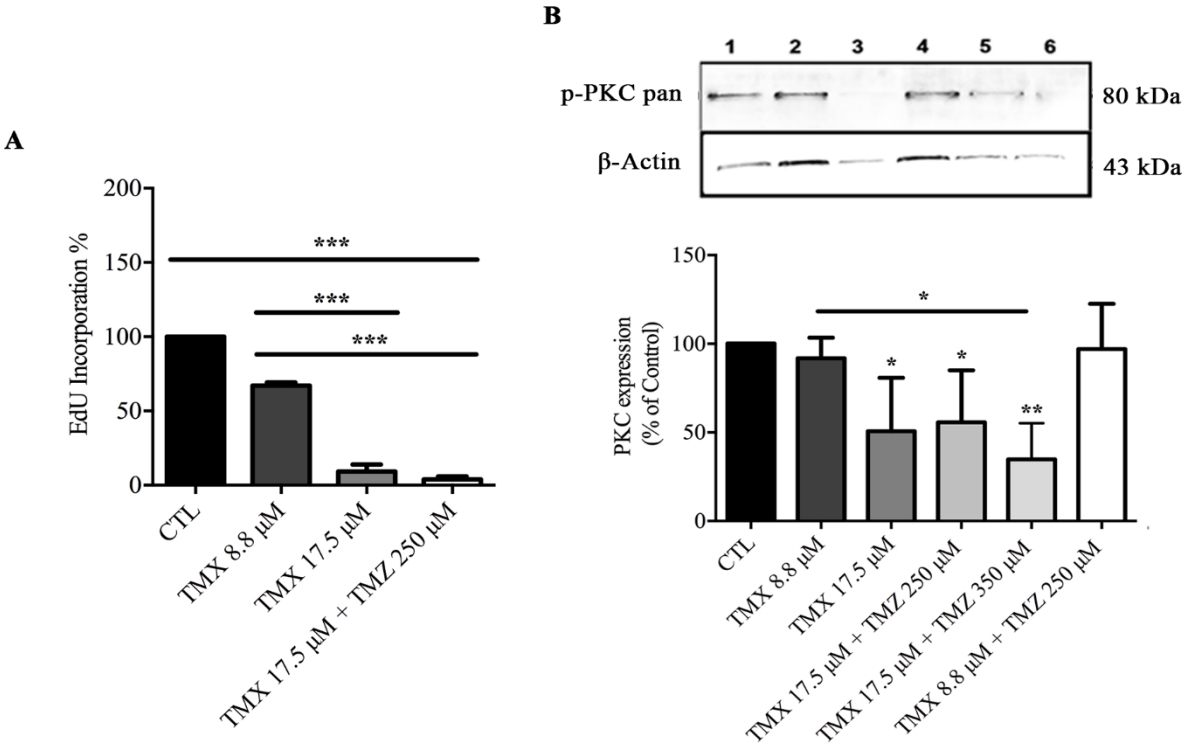

Figure 4.4 Effects of TMX and TMZ combination on EdU incorporation and p-PKC expression of GBM11 cells. (A) The proliferation rate was evaluated by measuring the incorporation of EdU. Analysis were performed with a BD FACSCalibur system evaluated in the FL2 and FL1 channel and a total of 10,000 events were collected. (B) The effect of TMX and/ or TMZ on PKC-pan expression was evaluated by western blot. Loading control was performed with an antibody for β-Actin. The bands numbered from 1 to 6 were in the same order that they appear in the graph. Each value represents the mean ± SEM from three independent experiments, * $p < 0.05$, ** $p < 0.01$, *** $p < 0.001$.

4.4.5 Study of cell migration and organization of F-actin filaments in GBM11 cells treated with TMX and TMZ

To evaluate the effect of TMX and TMZ co-treatment on GBM11cells, we performed the scratch assay. After 6 h, control cells moved and filled the scratch (Figure 4.5A). When cells were incubated with 17.5 µM TMX or with TMX 17.5 µM plus 250 µM TMZ, cell motility was reduced by 80.8% ± 29.1 and 73.9% ± 13.9 compared to control cells, respectively, $p < 0.05$ (Figure 4.5B). Phalloidin staining was performed to evaluate the cytoskeleton organization in the presence of TMX and/or TMZ (Figure 4.5C).

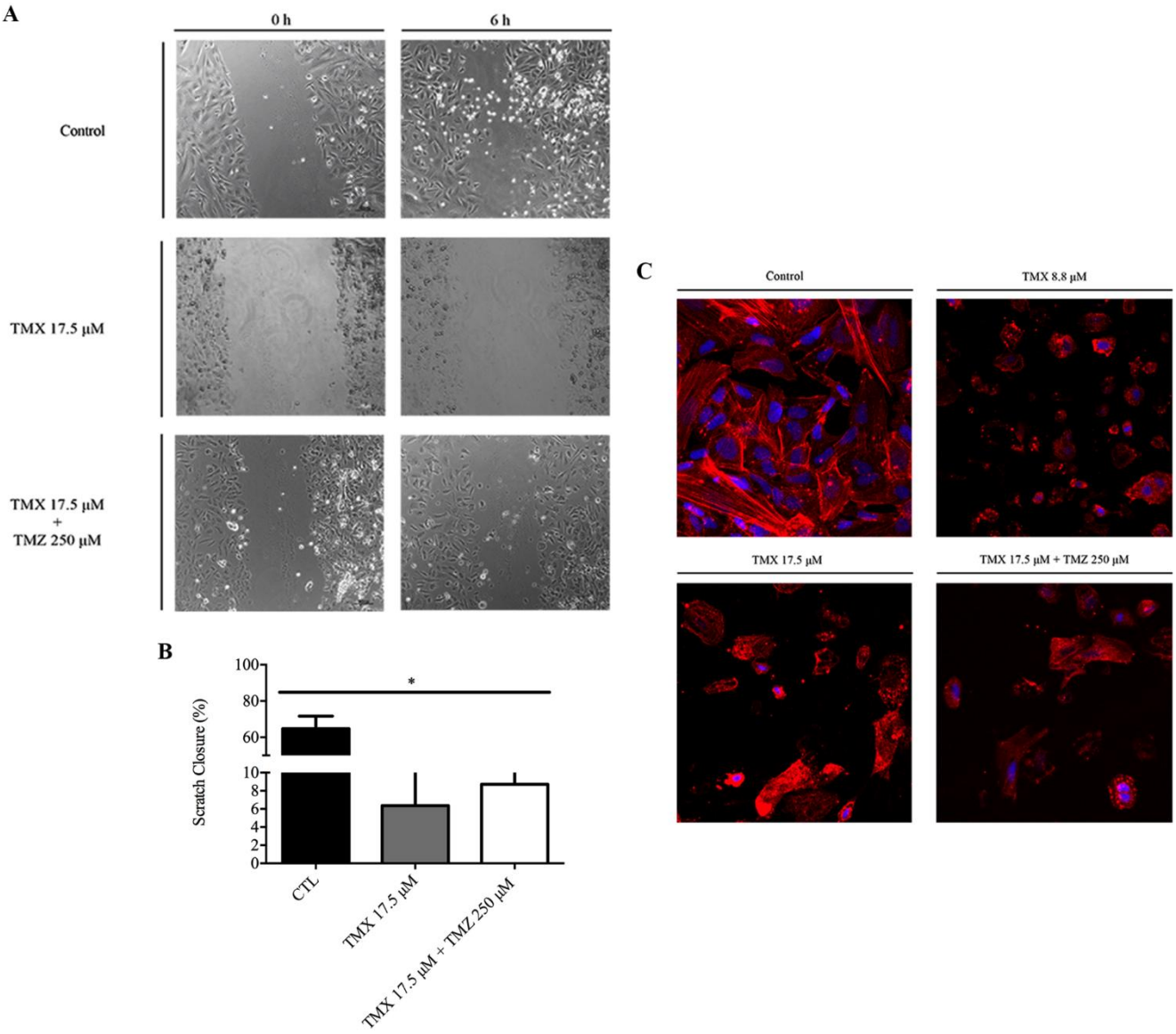

Figure 4.5 Effects of TMX and TMZ combination on cell migration capability and f-actin filament organization of GBM11 cells. (A) The images represent photographs of GBM11 cells from scratch assay. The scratch closure was measured at two time points (T0 and T6) after the scratch was made in the culture dish. Every picture was acquired at the same magnification of 10x (x10/ 0.25 Ph1 N-Plan) (Scale bar = 100 µm) with aDMI3000B light microscope (Leica Germany)

and acquired with Leica Application Suite v 4.3, Switzerland. ImageJ software was used to record the coordinates for each scratch location. (B) Statistical analysis was performed in GraphPad Prism 5. Each value represents the mean ± SEM from three independent experiments, * $p < 0.05$. (C) Cells were fixed and F-actin was stained with Alexa Fluor 555 phalloidin. Nuclei were counterstained with DAPI. Observations were made with a Zeiss LSM 510 Meta confocal microscope at a magnification of 40x, using a filter set with an excitation filter of 568 nm and a barrier filter of 585 nm. Red indicates F-actin staining and blue indicates the nuclei. All the doses chosen were above the one that inhibited growth by 50% (IC50) individually.

4.5 DISCUSSION

Besides the lack of a successful response, temozolomide (TMZ) is still considered part of the *gold-standard* for GBM treatment. Currently, few alternative treatment options for patients with TMZ resistant GBMs are desperately needed (He *et al.,* 2015). Tamoxifen (TMX) is an estrogen receptor (ER) modulator commonly used for the treatment of ER-positive breast cancer recently considered to have many other anti-tumor actions, mainly in the phosphorylated protein kinase C (PKC) regulation when used in higher concentrations (Couldwell *et al.,* 1994; He *et al.,* 2015; Hegi *et al.,* 2005; Zhou *et al.,* 2012). Phosphorylated PKC is one of the most enigmatic signalling pathways that may promote or inhibit apoptosis and cell survival, as previously described (Balça-Silva *et al.,* 2015). TMX is well known to be one of the p-PKC inhibitors used in *in vitro* studies with glioma cells and also in clinical trials with GBM patients. Besides the *in vivo* studies were disappointing since treatment of patients with recurrent malignant glioma with low doses of TMX did not significantly increase the survival rate of the patients, the clinical trials using high doses of TMX alone or in combination with other cytotoxic agents, have yielded better results (Balça-Silva *et al.,* 2015; Hui *et al.,* 2004; Kamburoğlu *et al.,* 2007; O'Brian *et al.,* 1985; Zhang *et al.,* 2000). We recently described the success of TMX and TMZ combination in two GBM cell lines, U87 and U118. In order to study the heterogeneity between GBM cells and the variability in the chemotherapeutic response, similarly to that observed in GBM patients, we established a new GBM cell line in laboratory and compare the mechanisms underlying chemoresistance and the response to treatment with the two cell lines previously studied, the U87 and U118 (Balça-Silva *et al.,* 2015).

As so, a tumor sample from GBM was analysed histologically by the Pathology Service of the Federal University of Rio de Janeiro Hospital, as described by Faria *et al.,* (Faria *et al.,* 2006). Prior to isolation of the GBM cells and at the time of the diagnosis, the tumor was classified as GBM due to the: 1) magnetic resonance diagnosis (Figure 4.1A);

2) histopathological characteristics of GBM by staining with HE in paraffin sections (Figure 4.1B); 3) the positive GFAP immunostaining, which is currently used for diagnosis of GBM (Figure 4.1C) (Deck *et al.,* 1978); and 4) existence of a previous GBM lesion. Subsequently, the tumor cells from the biopsy sample of GBM were isolated and established in culture. GBM is also characterized as an heterogeneous tumor that has a subpopulation of glioma stem-like cells (GSCs), known to be chemo- and radioresistant, properties that are responsible for tumor recurrence (Altaner and Altanerova, 2012; Jackson *et al.,* 2015; Meacham and Morrison, 2013). In fact, our GBM cells also expressed stem-like cell markers, mainly SOX2, OCT-4A and NANOG (Figure 4.1D), probably because these tumor stem-like cells have been selected through the previous TMZ treatment. GBM11 cells could also grow in an *in vivo* animal model (data not shown), as described by Garcia *et al.,* (Garcia *et al.,* 2014). This suggests that the glioma stem-like cells are able to contribute to the tumor growing *in vivo* and that the previous treatment with TMZ may have contributed to the recurrence of a tumor endowed with a higher number of cancer stem-like cells.

Regarding cell cytotoxicity, we noticed an expected resistance of GBM11 to TMZ treatment (Figure 4.1E), similarly to that observed in the U87 and U118 cell lines as well (Balça-Silva *et al.,* 2015), which was in accordance with the low survival rate of GBM patients treated with TMZ (Carmo *et al.,* 2011a; do Carmo *et al.,* 2010; Kahn *et al.,* 2012; Stupp *et al.,* 2007). Regarding cell cytotoxicity of TMX in GBM11 cells we noticed a higher IC50, 25.6 µM, compared, respectively, to 9.1 µM and 7.3 µM from U87 and U118, previously published (Figure 4.1F), which suggests that this new cell line presents a more resistant behavior when compared to U87 and U118. The combined treatment of GBM11 with TMX and TMZ induce a decrease in cell viability until 49.2% using doses below the IC50 of each drug alone. A similar cytotoxicity was observed in U87 cells, about 50.0% in cell viability decrease and a higher one observed in U118 of 90.0% (Figure 4.1G). These results are in accordance with the higher resistance of GBM11 cells and higher sensitivity of U118 to TMX alone.

After the analysis of the GFAP and Nestin positive expression and F-actin filaments staining, confirming a GBM phenotype of all three GBM cells (Figure 4.2A), we analysed the expression of PGP. PGP is expressed by endothelial cells in the brain and in the newly formed blood vessels in glioma. PGP recognizes structurally unrelated chemotherapeutic agents such as Vincristine, Etoposide, Doxorubicin, Taxol and Temozolomide (Calatozzolo *et al.,* 2005; Cordon-Cardo *et al.,* 1989; Schaich *et al.,* 2009; Sun *et al.,*

2003; Tóth *et al.,* 1996). In our study we observed that the PGP expression in GBM11 is significantly higher than compared to U87 and U118. It suggests that PGP expression is enhanced by previous TMZ treatment and may explain the more aggressive phenotype of recurrent gliomas. As so, we considered that, together with the higher IC50 of TMX and lower cell viability of TMX plus TMZ treatment, GBM11 could be used to evaluate the chemoresistance of different therapeutic agents in future studies (Figure 4.2B).

Regarding the mechanisms of chemoresistance of GBM to TMZ, we evaluated the expression of O6-methylguanine-DNA methyltransferase (*MGMT*) (Qiu *et al.,* 2014; Tomaszowski *et al.,* 2015). Accordingly, analysis of the methylation pattern revealed a total methylation of the *MGMT* in GBM11 and U87 cell lines and a partial methylation in U118 cell line, suggesting that the resistance of TMZ is probably not related with the *MGMT* action. In the U118 case, due to a partial methylation pattern of the *MGMT* we could expect a higher resistance to TMZ compared with the other cell lines (Figure 4.2C). Still, *MGMT* alone is not always correlated with resistance to TMZ in GBM, which was apparently the case of these three cell lines (Schaich *et al.,* 2009; Tomaszowski *et al.,* 2015; Tóth *et al.,* 1996). Accordingly, since the glioma stem-like cells are known to be chemo and radioresistant and so responsible for tumor recurrence (Diaz and Leon, 2011; Ortensi *et al.,* 2013; Seymour *et al.,* 2015; Singh *et al.,* 2004), the stem-like cell markers expression evaluation confirmed that the GBM11 could be the more resistant cell line since it presents higher levels of SOX2, which the overexpression has been correlated with poor prognosis in gliomas, compared to U87 and U118 cell lines (Figure 4.2D). In fact, SOX2 levels must be tightly controlled for proper development of the nervous system. Specifically, deregulation of SOX2 levels in chick neural stem cells (NSC) has been shown to disrupt their fate (Cox *et al.,* 2012).

Similarly to the results obtained for the U87 and U118 cell lines, we observed an induction of cell death (Figure 4.3A, B and C) and an induction of cell cycle arrest (Figure 4.3D) in GBM11 cells treated with TMX and TMZ, although the TMX alone treatment induce a similar effect than the combined therapy in this cell line. It may suggest that for recurrent tumors previously treated with TMZ accordingly to Stupp protocol, the best choice of second-line treatment may be only TMX to reduce putative side effects of combined treatment with TMZ. Also, a reduction in cell proliferation (Figure 4.4A) was observed in GBM11 cells, probably due to the decreased expression of p-PKC-pan (Figure 4.4B).

We finally observed a reduction of cell migration (Figure 4.5A and B), which could be explained, not exclusively, but consistently, by the visible disorganization of F-actin filaments (Figure 4.5C).

Altogether, when treated with TMX, our new GBM11 cell line presented a higher IC50 of TMX alone, higher reduction of cell proliferation, probably due to the reduction of p-PKC expression and cell migration capability, and a higher expression of PGP compared to U87 and U118 cell lines previously described (Table 4.1). The increase of PGP expression has been correlated with a poor response to therapy, which may justify the higher resistance of GBM11 cells (Callaghan and Higgins, 1995; Cordon-Cardo *et al.,* 1989; Tomaszowski *et al.,* 2015; Tóth *et al.,* 1996). Also, TMX is known to inhibit drug transport since it interacts with PGP inhibiting PGP-dependent drug transport (Callaghan and Higgins, 1995). GBM11 may be more resistant also due to the previous treatment with TMZ. Nonetheless, the overexpression of PGP and the higher amount of stem-like cells are more likely to be responsible for the GBM11 resistant profile. In this way, the concentration of TMX required to induce an effect would be expected to be higher compared to U87 and U118 cell lines, which is also in accordance with our results.

Table 4.1. Comparation of different GBM cell lines response to treatment.

	Cell viability (μM) (IC50)		p-PKC reduction (%)		EdU incorporation reduction (%)		Cell cycle arrest	Cell death (%)	Cell migration reduction (%)	F-actin filaments disorganization	MGMT methylation	PGP expression (% relative to GBM11)
	TMX	**TMZ**	**TMX**	**TMX + TMZ**	**TMX**	**TMX + TMZ**						
U87	9.1	-	39.1 ± 8.9*[1]	56.9 ± 14.8**[1]	-	-	G0/G1***[1;2]	3.8 ± 0.7**[1] (TMX alone)	41.3 ± 8.3**[1] (TMX + TMZ)	-	M	1.34
U118	7.3	-	28.9 ± 14.0*[1]	55.2 ± 23.1***[1]	-	68.3 ± 2.3***[1;2]	-	37.8 ± 7.3***[1;2] (TMX + TMZ)	25.8 ± 5.4**[1] (TMX alone)	↑	PM	0.11
GBM11	25.6	-	49.3 ± 30.1*[1]	44.3 ± 29.4**[1]	90.7 ± 8.0***[1]	96.2 ± 3.4***[1]	G0/G1***[1]	37.5 ± 21.5**[1] (TMX alone)	73.9 ± 13.9*[1] (TMX alone)	↑	M	100

* p <0.05; ** p <0.01; *** p <0.001; [1] in comparation to control; [2] in comparation to TMX alone; ↑ Increase; M – Methylated; PM – Partial Methylated; - Without alterations.
Note: The U87 and U118 data were previously published by our group (Balça-Silva *et al.,* 2015).

However, and probably due to the higher resistance of this new GBM cell line, the combination of TMX and TMZ had not a synergistic effect as observed in U87 and U118 cell lines. In GBM11 the results between combined or monotherapy are the same, which

could represent action in another receptor site of interaction and would be an alternative chemotherapeutic approach for GBM. Besides TMX can actually be very important on p-PKC regulation, and consequently, interfere with proliferation, survival and migration of glioma cells, the contribution of chemotherapeutic drugs depends on the GBM cells characteristics. In the current study, we evaluated the effect of TMX on TMZ-resistant GBM cell lines, which express different levels of PGP expression and similar *MGMT* activity. The *MGMT* is totally methylated in the GBM11 and U87 cell lines, which may not justify the chemoresistance of these cells to TMZ. However, in the U118 cell line we could see only a partial methylation of *MGMT,* which could explain some of the TMZ resistance behavior but a better response of the combined therapy, since TMX could sensitize cells to TMZ action in this cell line, which is in accordance with our results (Table 4.1). We found that TMX alone significantly inhibited the viability of TMZ-resistant GBM cells with higher expression of PGP, and induced apoptosis of glioma cells *in vitro*. In GBM11 case we noticed no need to TMZ addiction in the chemotherapeutic approach, besides this drug combination with TMX presented a huge advantage in U87 and U118 cells. This response suggests that TMX alone can be used as a second-line therapy in patients bearing recurrent tumors previously treated with TMZ, instead of a combination of TMZ and TMX (DI Cristofori *et al.,* 2013). It also emphasizes the heterogeneity response between GBM cells, which reflects the same variability between different GBM, highlighting the urgent need of the establishment of a personalized therapy (Balça-Silva *et al.,* 2015; Bogush *et al.,* 2012; Kahn *et al.,* 2012).

Our results propose TMX alone treatment as a successful approach in GBM cells that have previously been treated according to the Stupp protocol (Stupp *et al.,* 2009). Since the TMX and TMZ constitutes a beneficial combination for U87 and U118 cells, and since TMZ is still part of the *gold-standard* for GBM treatment, the combination constitutes a therapeutic approach that still reaches a wide range of GBM cells, especially those that still have not been exposed to TMZ. Furthermore, these results open new avenues to recognize different cell responses according to tumor heterogeneity that together might evidence functional differences between gliomas entities.

CHAPTER 5

The expression of connexins and SOX2 reflects the plasticity of glioma stem-like cells

Joana Balça-Silva, Diana Matias, Luiz Gustavo Dubois, Brenno Carneiro, Anália do Carmo, Henrique Girão, Fernanda Ferreira, Valéria Pereira Ferrer, Leila Chimelli, Paulo Niemeyer-Filho, Hermínio Tão, Olinda Rebelo, Marcos Barbosa, Ana Bela Sarmento-Ribeiro, Maria Celeste Lopes, Vivaldo Moura-Neto. 2017

Translational Oncology. 10 (4), 555-569.

5.1 ABSTRACT[6]

Glioblastoma (GBM) is the most malignant primary brain tumor, with an average survival rate of 15 months. GBM is highly refractory to therapy and such unresponsiveness is due, primarily, but not exclusively, to the glioma stem-like cells (GSCs). This subpopulation express stem-like cell markers and is responsible for the heterogeneity of GBM generating multiple differentiated cell phenotypes. However, how GBM maintain the balance between stem and non-stem populations is still poorly understood. We investigated the GBM ability to interconvert between stem and non-stem states through the evaluation of the expression of specific stem cell markers as well as cell communication proteins. We evaluated the molecular and phenotypic characteristics of GSCs derived from differentiated GBM cell lines, by comparing their stem-like cell properties and expression of connexins. We showed that non-GSCs as well as GSCs can undergo successive cycles of gain and loss of stem properties, demonstrating a bidirectional cellular plasticity model that is accompanied by changes on connexins expression. Our findings indicate that the interconversion between non-GSCs and GSCs can be modulated by extracellular factors culminating on differential expression of stem-like cell markers and cell-cell communication proteins. Ultimately, we observed that stem markers are mostly expressed on GBMs rather than on low-grade astrocytomas, suggesting that the presence of GSCs is a feature of high-grade gliomas. Together, our data demonstrate the utmost importance of the understanding of stem cell plasticity properties in a way to a step closer to new strategic approaches to potentially eliminate GSCs and, hopefully, prevent tumor recurrence.

[6] This chapter contains the text and the figures originally published in *Joana Balça-Silva, Diana Matias, Luiz Gustavo Dubois, Brenno Carneiro, Anália do Carmo, Henrique Girão, Fernanda Ferreira, Valéria Pereira Ferrer, Leila Chimelli, Paulo Niemeyer-Filho, Hermínio Tão, Olinda Rebelo, Marcos Barbosa, Ana Bela, Sarmento-Ribeiro, Maria Celeste Lopes, Vivaldo Moura-Neto. 2017. Translational Oncology. 10 (4), 555-569,* with the copyright permission under the terms of the Creative Commons Attribution-NonCommercial-No Derivatives License (CC BY NC ND).

5.2 INTRODUCTION

In the last decade, cancer cells endowed with self-renewal, differentiation and tumor-initiating properties have been isolated from several kinds of malignancies, including central nervous system (CNS) neoplasms. In the brain, glioma stem-like cells (GSCs) have been isolated from primary glioblastomas (GBMs), the most common and malignant primary brain tumor in adults (Louis *et al.,* 2016; Oliveira-Nunes *et al.,* 2016; Singh *et al.,* 2004). On average, patients with GBM survive only about 15 months after diagnosis, even under treatment with temozolomide (TMZ), which is part of the *gold-standard* therapy (Deheeger *et al.,* 2014; Grossman *et al.,* 2010; Huse *et al.,* 2013; Stupp *et al.,* 2005). This unfavourable prognosis is due to the high proliferation rate, resistance to apoptosis, increased migratory ability of the cells, deregulation of important signalling pathways, and the existence of GSCs. In addition to their potential for tumor initiation, GSCs are responsible for cellular heterogeneity and chemo- and radioresistance, classical features of GBM (Singh *et al.,* 2004). This heterogeneity provides several distinct cell populations that differ from each other not only phenotypically, but also genetically (Ding *et al.,* 2012; Nik-Zainal *et al.,* 2012; Schuh *et al.,* 2012; Shah *et al.,* 2012) and physiologically (Garcia *et al.,* 2014). These distinct cell subpopulations produce a rich environment with a sufficient number of cells that can bypass selection pressures to evolve and sustain tumor growth.

The key characteristics of GSCs are suggested to be closely associated with the expression of pluripotency genes, namely the sex-determining region Y-Box (SOX2) (Seymour *et al.,* 2015).

Nonetheless, a growing body of evidence indicates that intercellular communication through gap junctions (ICGJ) could contribute to the coordination of mechanisms involved in cell differentiation (Evans and Martin, 2002; Naus and Laird, 2010; Saez *et al.,* 2003; Todorova *et al.,* 2008). Gap junctions are formed by proteins of the connexin (Cx) family, which may exert both tumor-suppressor and oncogenic functions, specifically connexin 43 (Cx43) and connexin 46 (Cx46) (Orellana *et al.,* 2012; Soares *et al.,* 2015). Since the expression of connexins varies according to the differentiation spectrum of GBM cells, Hitomi and colleagues suggested that Cx expression could be essential for transitions between stem-like and non-stem-like states (Hitomi *et al.,* 2015). Switching between stem states allow cells to reprogram their differentiation status, and contribute to the development of chemoresistance mechanisms (Deheeger *et al.,* 2014; Hitomi *et al.,* 2015;

Liu and Lu, 2012; Safa *et al.,* 2015). However, the mechanisms involved in these cellular transitions and their contributions to GBM chemoresistance, and thus aggressiveness are poorly understood (Chaffer *et al.,* 2011; Easwaran *et al.,* 2014; Meacham and Morrison, 2013; Tata *et al.,* 2013). Here, we hypothesized that this heterogeneity in GBM tumor mass could represent the reversibly transit of GBM cells between different states, such as stem-like and non-stem-like as a demonstration of glioma stem-like cells plasticity.

Therefore, in order to determine if GBM cells are able to switch between stem and non-stem states, we compared the expression of stem-like markers in GBM cell lines, such as SOX2 upon different culture conditions. Moreover, we compared Cxs expression in such conditions. We also investigated whether the differential expression of SOX2 or Cxs can distinguish glioma grades malignancy, through the analysis of human astrocytoma samples. We consider of sublime importance the understanding of stem-like cell state plasticity, which could explain the aggressiveness of GBM and lead us to identify new molecular markers for its treatment.

5.3 MATERIAL AND METHODS

5.3.1 Material

DMEM/F12 Dulbecco's Modified Eagle Medium: Nutrient Mixture F-12 and NS34 NeuroBasal medium were supplied by Gibco®; HEPES was supplied by Life Technologies (São Paulo, Brazil), and fetal bovine serum (FBS) was supplied by Invitrogen (Paisley, UK). The growth factors B27, N2 and G5 were obtained from Thermo Scientific (Waltham, MA, USA). All secondary antibodies conjugated with either Alexa Fluor 488 or Fluor 546 were obtained from Invitrogen-Life Technologies (Carlsbad, CA, USA). Glucose was purchased from Merck (Darmstadt, Germany). Fungizone was purchased from Bristol-Myers Squibb (Princeton, NJ, USA). Penicillin/streptomycin was purchased from Gibco, and rabbit anti-glial fibrillary acidic protein (GFAP) and mouse anti-vimentin clone V9 antibodies were purchased from Dako (Glostrup, Denmark). 4-6-diamino-2-phenylindole (DAPI) was obtained from Sigma (Natick, MA, USA). Protease and phosphatase inhibitors were supplied by Roche (Indianapolis, IN, USA). Antibodies for Nanog (#3580), Oct-4A (#2840) SOX2 (#D6D9) and Slug (#9585) were purchased from Cell Signalling Technology (Beverly, MA, USA). Mouse GAPDH, Anti-Connexin 43 / GJA1 antibody

(Connexin 43) (#ab11370) and Anti-GJA3 antibody (Connexin 46) (#ab176394) were purchased from Abcam. Anti-Vimentin was obtained from Dako (Glostrup, Denmark). Mouse anti-actin antibody was purchased from Boehringer (Mannheim, Germany). Nestin clone 10c2 and PVDF membranes were purchased from Millipore (Billerica, MA, USA). 2x laemmli buffer and ß-mercaptoethanol were purchased from Bio-Rad (São Paulo, Brazil).

5.3.2 Maintenance of cell line cultures

The U87 cell line was acquired from the American Type Culture Collection (ATCC) (Manassas, VA, USA). The human tumor cell lines, GBM02 and GBM11 cells, were established and characterized in our laboratory, and maintained directly in DMEM/F12 supplemented with bovine serum, after collected from a GBM patient biopsy sample, as previously described (Faria *et al.,* 2006; Kahn *et al.,* 2012). The human cell line OB1 was established and characterized by the laboratory of Dr. Hervé Chneiweiss, and maintained in NS34 serum-free medium as described by Thirant *et al.,* (Thirant *et al.,* 2011). Cells were cultured in Dulbecco's modified Eagle's medium (DMEM) supplemented with 3.5 mg/ml glucose, 0.1 mg/ml penicillin, 0.14 mg/ml streptomycin and 10% inactivated FBS, maintained at 37°C in an atmosphere containing 95% air and 5% CO_2 as described by Faria *et al.,* (Faria *et al.,* 2006). The GSC populations were obtained from U87, GBM02 and GBM11 and maintained in NeuroBasal medium (NS34) supplemented with sodium pyruvate, glutamine, B27 supplement, EGF, basic FGF, penicillin and streptomycin, as described by Patru *et al.,* (Patru *et al.,* 2010) and Thirant *et al.,* (Thirant *et al.,* 2011). Since these cells were obtained in the absence of serum (serum-free, SF), they were termed U87-SF, GBM02-SF, GBM11-SF and OB1-SF. Spheres from U87-SF, GBM02-SF, GBM11-SF and OB1-SF were passed by mechanical dissociation through a *p200* pipette and reseeded into NS34 medium, used for stem-like cells at the same density of 0.5 x 10^6 cells/mL to form new spheres.

5.3.3 Clonogenic assay

To determine the ability of GBM cells to form spheres, a single viable cell was transferred to each well of a 96-well plate containing 100 µL of NS34 medium. Fresh stem-cell medium was added every 2 days. Over 4 weeks of culture, by observation under phase contrast microscope, the sphere-positive wells were counted.

5.3.4 Western Blot

The SOX2, OCT-4A, NANOG, Cx43, Cx46, Slug and vimentin proteins were analyzed by western blotting as originally described by Towbin and adapted by Balça-Silva and Kahn in both the GBM and GBM-SF cell lines (Balça-Silva *et al.,* 2015; Kahn *et al.,* 2012; Towbin *et al.,* 1989). Briefly, cells were centrifuged at 500 xg for 10 min at 4 °C. The supernatants were discarded. The cells were resuspended in RIPA buffer (50 mM Tris–HCl at pH 8.0, 150 mM NaCl, 1.0% NP-40, 0.5% sodium deoxycholate, 0.1% SDS and 2 mM EDTA, supplemented with protease and phosphatase inhibitors and DTT), and sonicated. After that, the samples were denatured with Lämmli buffer 2x added to each sample at a 1:1 ratio. Protein extracts were boiled at 95 °C for 5 min before use. 30 µg of protein was run on a 10% SDS-PAGE gel and transferred to a PVDF membrane, and then incubated with a solution of 5% non-fat milk in TBST for 1 h at room temperature. The primary antibodies against SOX2 (1:1000), OCT-4A (1:1000), NANOG (1:1000), Slug (1:1000), vimentin (1:1000), Cx43 (1:1000), and Cx46 (1:100) were diluted in TBST with 1% non-fat milk supplemented with azide. After the incubation period, the immunocomplexes were detected with anti-rabbit antibody (1:1000) and conjugated with horseradish peroxidase. Bands were obtained after exposing the membranes to an X-ray film, and analysed through densitometry scanning. The protein expression was quantified using the software ImageJ 1.49v (Wayne Rasband, National Institutes of Health, USA) with the expression of tubulin or GAPDH used as a loading control. Each experiment was repeated three times.

5.3.5 Immunofluorescence

For immunofluorescence analysis, 10 x 10^4 cells/ml were plated on coverslips placed on a 24 multi-well plate, as previously described (Kahn *et al.,* 2012). Briefly, GSCs and GBM cells were fixed with 4% PFA in PBS for 15 min. Then, cells were washed with PBS and permeabilized with Triton 0.1% for 30 min. Cells were the washed with PBS and incubated with 5% BSA/PBS for 30 min. Cells were incubated with rabbit anti-SOX2 (1:400), rabbit anti-glial fibrillary acidic protein (GFAP) (1:500), rabbit anti-OCT-4A (1:400), rabbit anti-Nanog (1:400), mouse anti-Nestin (1:200), rabbit anti-Cx43 (1:1000) and/or rabbit anti-Cx46 (1:100). Cells were incubated overnight at 4°C with the primary antibodies, then washed again with PBS and incubated overnight with secondary antibodies conjugated with Alexa Fluor 488 (goat anti-mouse; 1:250) and/or Alexa Fluor 488 (goat anti-rabbit; 1:250). Cells were then washed with PBS, stained with DAPI, washed with PBS and mounted in Fluoromount-G®. Negative controls were performed with non-immune rabbit or mouse IgG. Cells were imaged using a DMi8 advanced fluorescence microscope (Leica Microsystems, Germany) equipped with a 63x oil-immersion objective and analysed with Leica LA SAF Lite. Images were processed using the software ImageJ 1.49v (Wayne Rasband, National Institutes of Health, USA).

5.3.6 Real time PCR

Total RNAs were extracted from OB1 and GBM02 cells using PureLink RNA Mini Kit (Thermo Fisher Scientific) following the manufacturer's instructions. One microgram of the total RNA, oligodT(12-18) primer (Thermo Fisher Scientific) and High-Capacity cDNA Reverse Transcription Kit (Applied Biosystems) were used to perform the cDNA synthesis. For quantitative Polymerase Chain Reaction (qPCR) using OB1 cell samples, we utilized 12 ng per well of cDNA, SOX2 and Cx43 Taqman® Probes (Hs01053049_s1 and Hs00748445_s1, respectively) and GAPDH (Hs02786624_g1) as endogenous gene. To calculate the relative fold variation in mRNA expression, we performed the 2-ΔΔCT method. For qPCR from GBM02 cell samples, we designed and used the SOX2 primers (Forward: 5'-AGGGCTGGGAGAAAGAAGAG-3'; Reverse: 5'-GGAGAATAGTTGGGGGGAAG-3'), the Cx43 primers (Forward: 5'-ATGAGCAGTCTGCCTTTCGT-3'; Reverse: 5'-TCTGCTTCAAGTGCATGTCC-3') and

GAPDH (Forward: 5'-GAGTCAACGGATTTGGTCGT-3'; Reverse: 5'-TTGATTTTGGAGGGATCTCG-3') primers. Here, we employed the Power SybrGreen Master Mix (Thermo Fisher Scientific) and the Pfaffl method of Pfaffl to calculate the relative fold variation in mRNA expression. Data were always obtained from three independent experiments and analyzed using student's t-test. Thermal cycling was carried out using the manufacturer's recommended conditions, in a CFX96 Touch Real-Time PCR Detector (BioRad) (Pfaffl, 2001).

5.3.7 In vivo mouse GBM model

Swiss mice were obtained from the Biomedical Sciences Institute (Universidade Federal do Rio de Janeiro – UFRJ, Brazil). This study was approved by the Ethics Committee of the Center for Health Sciences (Centro de Ciências da Saúde - CCS, UFRJ) (Protocol No. DA- HEICB 015) and by the Brazilian Ministry of Health Ethics Committee (CONEP No. 2340), as described by Kahn *et al.,* (Kahn *et al.,* 2012). The Guide for the Care and Use of Laboratory Animals (National Academy of Sciences, National Academy Press, Washington, DC) was strictly followed in all experiments. All efforts were made to minimize the number of animals used and their suffering. 10-14-week-old male Swiss mice weighing 20-25 g were anesthetized with diazepam (5 mg/kg i.m.), ketamine (100 mg/kg i.m.) and xylazine (25 mg/kg i.m.), and then a brain midline incision was made on the scalp, as previously described (Garcia *et al.,* 2014; Kahn *et al.,* 2012). Briefly, a small hole was drilled in the skull and 1 x 10^5 GBM11 cells (or DMEM-F12 – control) were delivered in 3 µL DMEM-F12 at a depth of 3 mm with a Hamilton syringe (Hamilton, Reno, NV, USA) over 30 min at the stereotaxic coordinates: 1 mm posterior to the bregma and + 2 mm mediolateral from the midline. Animals were followed for 7, 14 and 21 days after tumor cell injection.

5.3.8 Magnetic resonance imaging

Magnetic resonance imaging (MRI) was performed 7, 14 and 21 days after the tumor injection, as previously described (Garcia *et al.,* 2014; Kahn *et al.,* 2012). Briefly, mice were anesthetized with ketamine (100 mg/kg i.m.) and xylazine (25 mg/kg i.m.) and

images were acquired with a magnetic resonance scanner (7T/210 horizontal Varian scanner, Agilent Technologies). All images of the brain were obtained using proton density sequences (TR/TE: 10/2000 ms; matrix: 128 x 128, slice thickness: 1 mm; 12 continuous slices with no gap; 16 averages) in the axial (field of view: 25.6 x 25.6 cm), coronal (field of view: 32 x 32 cm) and sagittal (field of view: 25.6 x 25.6 cm) planes. For each dataset, all images were visually inspected for artefacts. Data were processed using Osirix software (www.osirix-viewer.com). Brain morphology and tumor characteristics were evaluated by two experienced researchers.

5.3.9 Mouse tissue processing

Briefly, mice brains were dissected, fixed in 4% PFA for 24 h at 4°C and stored before processing. Then, the tissues were dehydrated in a graded ethanol series (30%, 40%, 50% and 60% for 30 min, next 70%, 80% and 90% for 1 h, and finally 100% twice for 1 h each), followed by xylene overnight at room temperature. Finally, brains were embedded in paraffin for 3 h at 67°C. Coronal sections were cut (5 µm thick) on a microtome. The sections were stained with haematoxylin and eosin and photographed using a DMi8 advanced fluorescence microscope (Leica Microsystems, Germany). For immunofluorescence of GBM11 cells injected in the striatum of immunocompetent mice, mouse anti-human vimentin (hVim) (1:50) was stained at the core of the tumor mass, as shown by cell nuclei atypia (DAPI counterstaining in cyan, inset) and at the border of the tumor mass.

5.3.10 Human tissue processing

A total of 10 human brain samples, of which 6 were astrocytoma grade IV (GBM), 2 astrocytoma grade II, and 2 temporal lobectomy neocortex samples acquired from epilepsy surgery patients with mesial sclerosis were considered as normal brain and used as controls were collected. All patients were admitted to the Neurosurgery Service of the University Hospital of Coimbra (Coimbra, Portugal). The study was approved by the University Hospital of Coimbra Ethics Committee, according to the Declaration of Helsinki protocol and all patients assigned an inform consent for the use of biological material for

research investigation. The GBM, astrocytoma grade II and normal brain tissues were fixed in 4% paraformaldehyde for 12 – 24 h, embedded in paraffin, and cut into 4 μm sections. The brain tissues were prepared for immunohistochemistry by deparaffinising the sections in xylene for 20 min and rehydrating in an ethanol series, using a Vector Laboratories (Burlingame, CA, USA) kit. Then, all sections were incubated for 30 min with 3% H_2O_2. Antigens were retrieved from the samples with citric acid buffer (citric acid 0.1 M and sodium citrate 0.1 M in distilled water) in a microwave (two cycles of 5 min, 400 w) to break the methylene bonds and expose the antigenic sites. After that, the sections were incubated in horse normal serum (Vector Laboratories) at 4°C for 30 min, and then incubated with SOX2 primary antibody (1:100) diluted in TBS (Tris-Buffered Saline) overnight at 4°C. The sections were washed three times with TBS-Tween and next incubated with a 1:100 secondary antibody ImmPress reagent (Vector Laboratories Anti-mouse/rabbit Ig, cat. no. MP-7500) for 30 min at room temperature. Then, all sections were incubated with diaminobenzidine (DAB) (Bios, Beijing, China) for visualizing the positive signal, counterstained with Mayer's haematoxylin, and evaluated and scored by two independent pathologists (with no knowledge of the patients' records). The sections were observed at the same magnification of 10x (x10/ 0.25 PH1 NPLAN) and amplified 40x (x40/ 0.55 CORR PH2) (Scale bar = 100 μm), with a Leica DMI3000B light microscope (Leica, Germany) and acquired with the Leica Application Suite v 4.3 (Leica, Switzerland).

5.3.11 Statistical analysis

Statistical analysis was performed in *GraphPad Prism 5* for Windows, version 5.00 (GraphPad Software, Inc., San Diego, CA, USA). After the assumption of normality and homogeneity of variance across groups was confirmed, the groups were compared using a nested design with analysis of variance and post-hoc comparison, with correction of α error according to Bonferroni probabilities to compensate for multiple comparisons. All values were expressed as mean ± SEM, $p < 0.05$.

5.4.1 GBM Cell Lines Interconversion Between Stem-Like and Non–Stem-Like States

GBM can generate cells that are able to acquire the stem-like state independently of their differentiation state (Safa *et al.,* 2015). Two different GBM cell lines, which were isolated by different methods, were cultured in different media. GBM02 was derived from an adult human patient and isolated directly in medium supplemented with fetal bovine serum (DMEM-F12, 10% FBS). OB1-SF (OB1-serum-free) was isolated from an adult human patient and first cultured in a defined growth media supplemented with growth factors (NS34, which contains DMEM/F12 5 x; Glucose 30%; 200 mM Glutamine; Hepes 3.6%; $NaHCO_3$ 7.5%; Pen/Strep; N2 1 x; B27 1 x and G5 1 x), known for maintaining stem-like properties (Oliveira-Nunes *et al.,* 2016; Thirant *et al.,* 2011). Specifically, the N2 is constituted by human transferrin, human insulin, progesterone, putrescine and sodium selenite and is recommended for the growth and expression of neuroblastomas (Spoerri *et al.,* 1983). The B27 is composed by a cocktail of vitamins, proteins and other components like linoleic acid, linolenic acid, progesterone, selenite sodium, among others. The B27 is used to induce growth and long-term viability of CNS cells (Brewer, 1995). Finally, the G5 is composed by biotin, basic fibroblast growth factor (FGF), epidermal growth factor (EGF), human transferrin, human insulin, among others and is also important to the growth and maintenance of primary and tumor glial cells (Michler-Stuke *et al.,* 1984). To investigate whether the two cell lines can switch between stem-like and non-stem-like states, the expressions of SOX2 and Cxs 43 and 46 were measured by western blot (WB), when the cells were cultured in their respective media, for both GBM02 (Figure 5.1A, T0) and OB1-SF (Figure 5.2A, T0). The expressions of SOX2, Cx43 and 46 were also evaluated by immunofluorescence (IF) (Figures 5.1B and 5.2B) and by qPCR (Figures 5.1C and 5.2C). Two weeks later, cell differentiation was induced in the OB1 cell line by exposing the cells to DMEM-F12 10% FBS; and reacquisition of stem-like properties in GBM02 (GBM02-SF) was induced by exposure to NS34 medium. The expression of markers of the stem-like state was assessed by WB, IF and qPCR (Figures 5.1 and 5.2). At the end of four weeks, the GBM02 cells were transferred back to the DMEM-F12 10% SFB medium, and the OB1-SF cells were transferred back to the NS34 medium (Figures 5.1 and 5.2, T4). Our results showed that after this transfer, in the GBM02 cells (T4), the Cx43 protein amount

was 4.3-fold higher than in the GBM02-SF cells (T2), $p < 0.01$ (Figure 5.1A). However, there was no significant difference among the Cx43 mRNA expression analyzed (Figure 5.1C). The GBM02-SF cells (T2) maintained the ability to form spheres, and the Cx46 protein was 4.0-fold higher than in the GBM02 cells (T0), $p < 0.05$; and 6.0-fold higher than in the GBM02 cells (T4), $p < 0.05$. In addition, the quantity of SOX2 in the GBM02-SF cells (T2) was 3.6-fold higher than in the GBM02 cells (T0), $p < 0.05$, and 2.8-fold higher than in the GBM02 cells (T4), $p < 0.05$ (Figure 5.1A and 5.1B). Corroborating, the qPCR results showed that SOX2 expression was 1.98 higher in the GBM02-SF cells (T2) than in GBM02 cells (T0), $p < 0.05$. In addition, statistically, the same mRNA expression value was found in GBM02 cells (T4) and (T0) (Figure 5.1C).

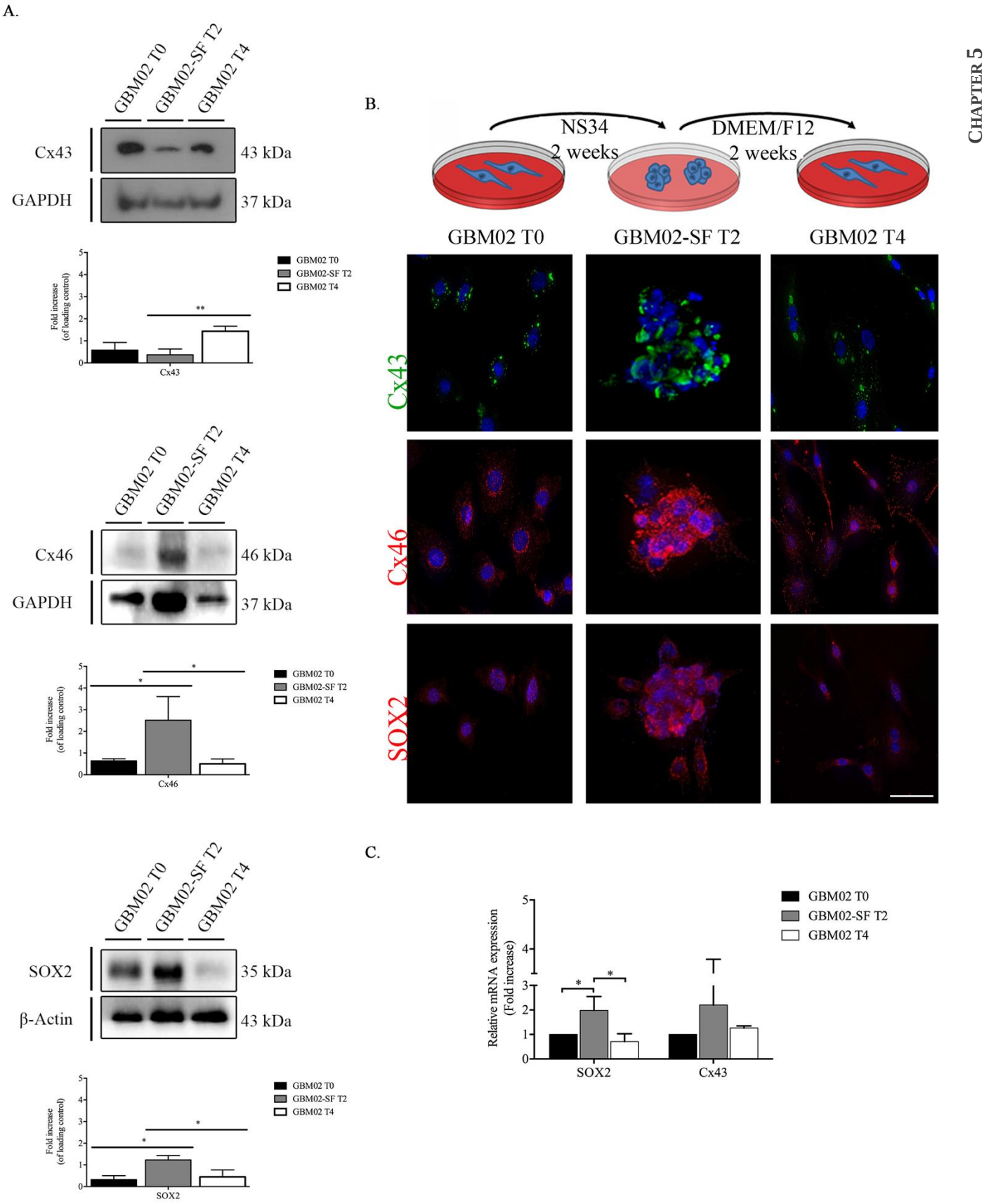

Figure 5.1 GBM stem-like cell plasticity properties in GBM02 and GBM02-SF cells. The expression of Connexin 43, Connexin 46 and SOX2 in the GBM and the respective serum-free cell

lines was evaluated by western blot (A) and immunofluorescence (B). **A.** GBM02 cells were maintained in DMEM-F12 supplemented with serum for 2 weeks (GBM02 T0). At the end of this time, part of the cells was isolated and the other part was maintained in culture with NS34, a serum-free medium, for 2 more weeks (GBM02-SF T2). Next, part of the cells was also isolated and the other part was again maintained in culture with DMEM/F12 supplemented with serum for a further 2 weeks (GBM02 T4). At the end of this time, cells were collected and the expression of Cx43, Cx46 and SOX2 was quantified by western blot as previously described. Statistical analysis was performed in *GraphPad Prism 5* for Windows (version 5.00; GraphPad Software, Inc., San Diego, CA, USA). Each value represents the mean ± SEM from three independent experiments, * $p < 0.05$, ** $p < 0.01$. **B.** Immunofluorescence staining of Cx43, Cx46 and SOX2 was performed in parallel. Cells were imaged using a DMi8 advanced fluorescence microscope (Leica Microsystems, Germany). Scale bar = 50 μM. Images were processed using the software ImageJ 1.49v (Wayne Rasband, National Institutes of Health, USA). **C.** The expression of Connexin 43 and SOX2 in the GBM02 and GBM02-SF cells was evaluated by qPCR. Total RNA was extracted using a PureLink RNA Mini Kit following the manufacturer's instructions. One microgram of total RNA, oligo(dT) primer and High-Capacity cDNA Reverse Transcription Kit were used to perform cDNA synthesis. The qPCR reaction was done in duplicate using SOX2, Cx43 and GAPDH primers and Power SybrGreen Master Mix. To calculate the relative fold variation in mRNA expression, GBM02 cells (T0) were applied as control at the 2-ΔΔCT method. Each value represents the ± SEM, * $p < 0.05$.

In the OB1 cells (T2), the expression of Cx43 was higher than that observed in the OB1-SF cells (T0 and T4). The mRNA expression was more than 3-fold higher in (T2) compared with (T0), $p < 0.05$; and (T4) condition, $p < 0.01$, although the difference was not statistically significant for the protein amount. In the OB1-SF cells (T0), the expression of Cx46 was 3.9-fold higher than in OB1 cells (T2), $p < 0.05$; and in the OB1-SF cells (T4), the expression of Cx46 was 3.8-fold higher than in the OB1 cells (T2), $p < 0.05$. In the OB1-SF cells (T0) the total of SOX2 protein was 4.5-fold higher than in the OB1 cells (T2), $p < 0.05$; and in the OB1-SF cells (T4), SOX2 expression was 3.0-fold higher than in the OB1 cells (T2), although this difference was not statistically significant (Figure 5.2A). Similar results were found for the real-time PCR. SOX2 expression was 9.28 higher in OB1-SF cells (T0) than in OB1 cells (T2), $p < 0.001$; and the transcripts levels increased in OB1-SF cells (T4) compared with OB1 cells (T2), not statistically significant (Figure 5.2C). Also, the OB1 cells formed spheres when cultured in the stem-like serum-free medium (Figure 5.2B).

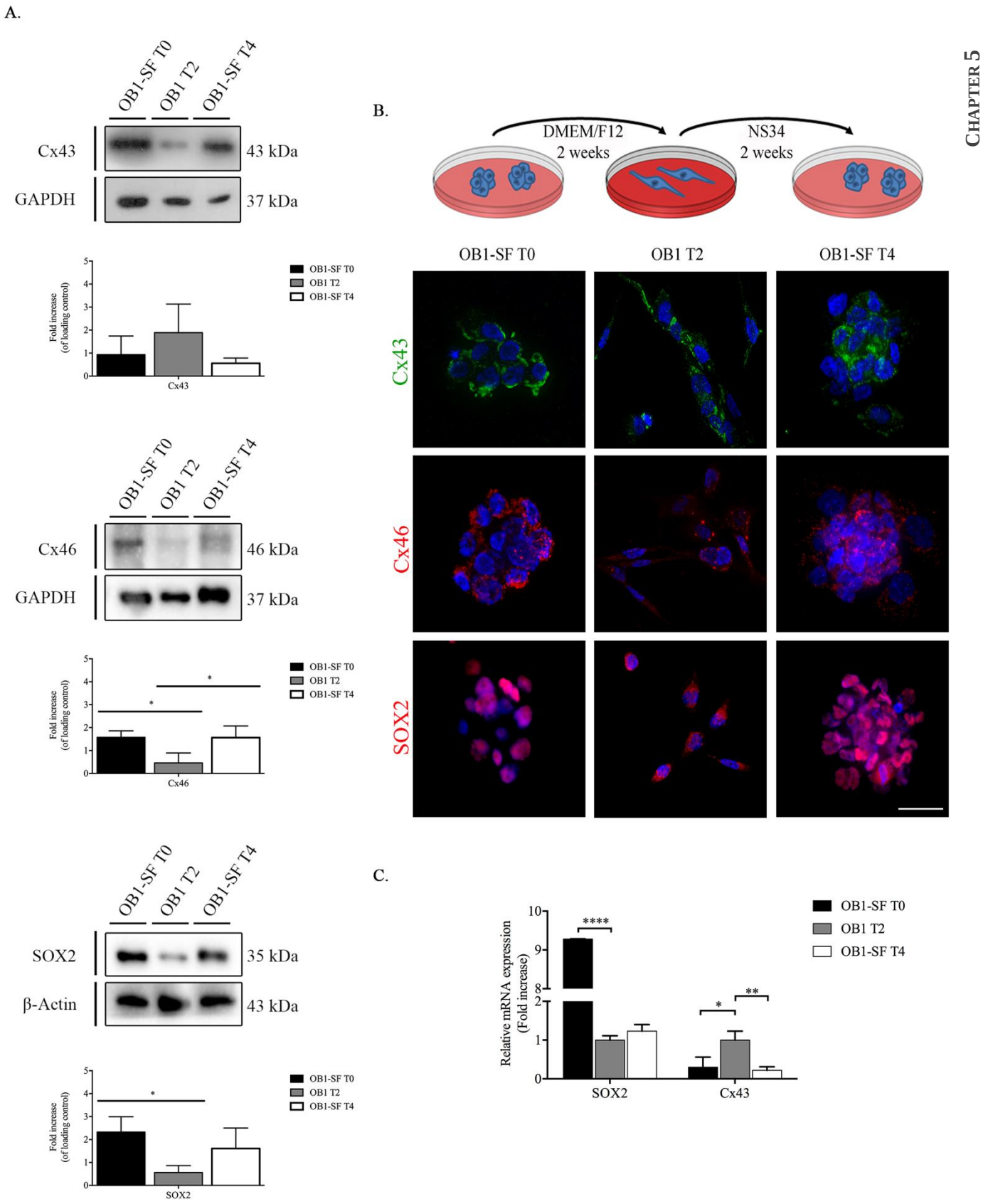

Figure 5.2 GBM stem-like cell plasticity properties in OB1 and OB1-SF cells. The expression of Connexin 43, Connexin 46 and SOX2 expression was analysed in the GBM, and the respective

serum-free cell lines were evaluated by western blot (A) and immunofluorescence (B). **A.** OB1-SF cells were maintained in culture with the serum-free medium NS34 for 2 weeks (OB1-SF T0). At the end of this time, part of the cells was isolated and the other part was maintained in DMEM-F12 supplemented with serum for 2 more weeks (OB1 T2). After this time, part of the cells was also isolated and the other part was again maintained in culture with NS34, a serum-free medium for a further 2 weeks (OB1-SF T4). At the end of this time, cells were collected and the expression of Cx43, Cx46 and SOX2 was quantified by western blot as previously described. Statistical analysis was performed in GraphPad Prism 5 for Windows (version 5.00; GraphPad Software, Inc., San Diego, CA, USA). Each value represents the mean ± SEM from three independent experiments, * $p < 0.05$, ** $p < 0.01$. **B.** Immunofluorescence staining of Cx43, Cx46 and SOX2 was performed in parallel. Cells were imaged using a DMi8 advanced fluorescence microscope (Leica Microsystems, Germany). Scale bar = 50 μM. Images were processed using the software ImageJ 1.49v (Wayne Rasband, National Institutes of Health, USA). **C.** The expression of Connexin 43 and SOX2 in OB1-SF and OB1 cells was evaluated by qPCR. Total RNA was extracted using PureLink RNA Mini Kit following the manufacturer's instructions. One microgram of total RNA, oligo(dT) primer and High-Capacity cDNA Reverse Transcription Kit were used to achieve cDNA synthesis. The qPCR reaction was done in duplicate using SOX2, Cx43 and GAPDH Taqman Probes. To calculate the relative fold variation in mRNA expression, OB1 cells (T2) were used as control at the 2-ΔΔCT method. Each value represents the ± SEM, * $p < 0.05$; ** $p < 0.01$; **** $p < 0.0001$.

Currently, several studies demonstrate that the shifts in the stem-like properties are accompanied by changes in expression of epithelial-mesenchymal transition (EMT) markers (Meacham and Morrison, 2013; Tam and Weinberg, 2013). We investigated the expression of SLUG and Vimentin, two markers of enhanced EMT (Mallini *et al.,* 2014; Tania *et al.,* 2014), on OB1 cells in three different time points (Figure 5.3). SLUG and Vimentin expression was downregulated on cells cultured on differentiation conditions (OB1-T2), when compared to OB1-SF (T0). On the other hand, their expression was restored when the same population of OB1 cells was cultured back on serum-free media (OB1-T4), $p < 0.05$ (Figure 5.3).

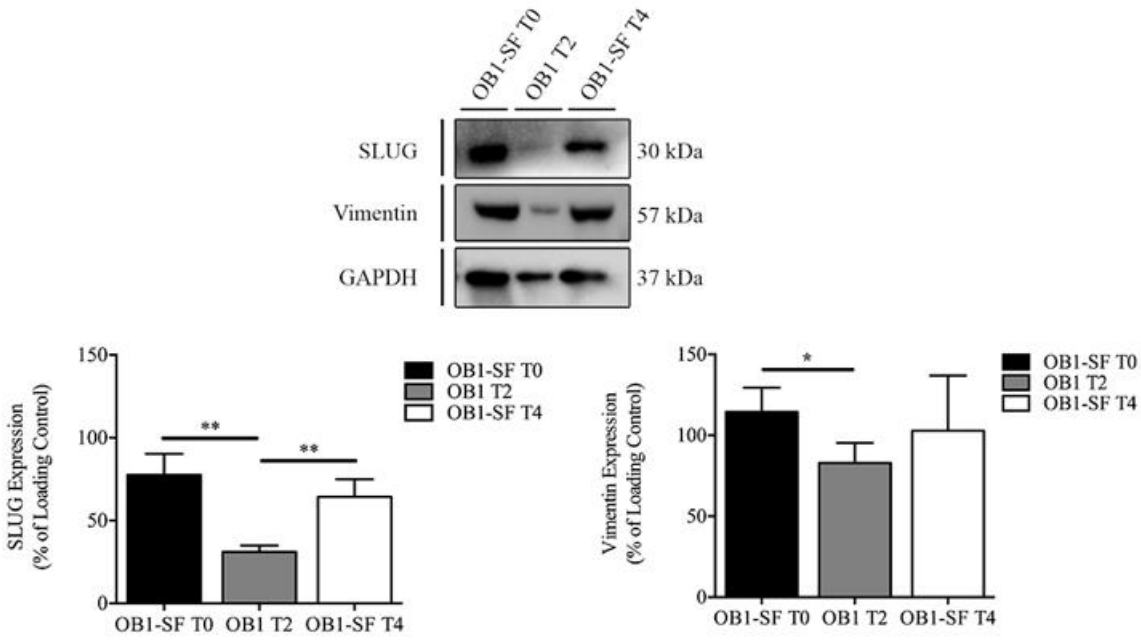

Figure 5.3 Deregulation of Epithelial-mesenchymal transition (EMT) markers in OB1 cells. The SLUG and Vimentin expression was evaluated in OB1 cells in T0, T2 and T4 time points by western blot. There was a significant downregulation in expression of SLUG and vimentin in cells cultured on differentiation conditions (OB1-T2) ($p < 0.05$), when compared to OB1-SF (T0). SLUG and vimentin levels were restored when OB1 cells was cultured back on serum-free media (OB1-T4), $p < 0.05$. However, the Vimentin expression was not statistically significant. Statistical analysis was performed in *GraphPad Prism 5* for Windows (version 5.00; GraphPad Software, Inc., San Diego, CA, USA). Each value represents the mean ± SEM from three independent experiments, * $p < 0.05$.

5.4.2 GSCs Clonogenic Properties

We observed that GBM02 cultured in DMEM/F12 with serum could enhance the expression of stem-like markers after culturing in NS34. This observation prompted us to investigate whether other GBM cell lines previously cultured in serum-supplemented media could acquire stem-like properties when cultured in NS34. The U87, GBM02 and GBM11 cell lines were transferred to the serum-free stem cell medium NS34 (U87-SF; GBM02-SF and GBM11-SF), and their ability to form clones was evaluated. OB1-SF was used as a control, since it was already a GSC cell line. Single cells divided within 3 days, followed the formation of small "oncosphere-like" structures at the end of 1 week. Each sphere contained approximately four cells per sphere. The cells in the U87-SF culture formed spheres containing approximately four cells each, and the GBM02-SF and GBM11-

SF cultures formed spheres containing four to eight cells each. After two weeks of culture, observation with a phase-contrast microscope showed that oncospheres had formed, and these were maintained until they reached the maximum size of 200 µm (Figure 5.4A). The spheres were then dissociated, and 0.5 x 10^6 cells were transferred to a new flask with new NS34 medium in order to evaluate the formation of new spheres, which occurred 1 week later. Serial passage in NS34 medium revealed that the oncospheres maintained the self-renewing ability after at least 4 generations. We then evaluated the ability of stem-like cells to form new clones by clonogenic assay (Figure 5.4B). In a limited-dilution assay, oncospheres were dissociated into a suspension of single cells, and 1 cell was reseeded into each well of 96 multi-well plates. At the end of each week, the number of spheres was quantified. We found that the GBM02-SF culture cells were better able to form tumor spheres than the GBM11-SF (1.3-fold difference; $p = 0.2$), OB1-SF (3.9-fold difference; $p < 0.05$) and U87-SF cells (5.4-fold difference; $p < 0.01$). On other hand, GBM11-SF demonstrated a better ability to form spheres than OB1-SF (2.9-fold difference; $p < 0.01$) and U87-SF (4.0-fold difference; $p < 0.01$). However, the OB1-SF cells were better able to form spheres than the U87-SF cells (1.3-fold difference; $p < 0.01$) (Figure 5.4B). As so, GBM11-SF has a higher capability to form spheres compared to the other cell lines.

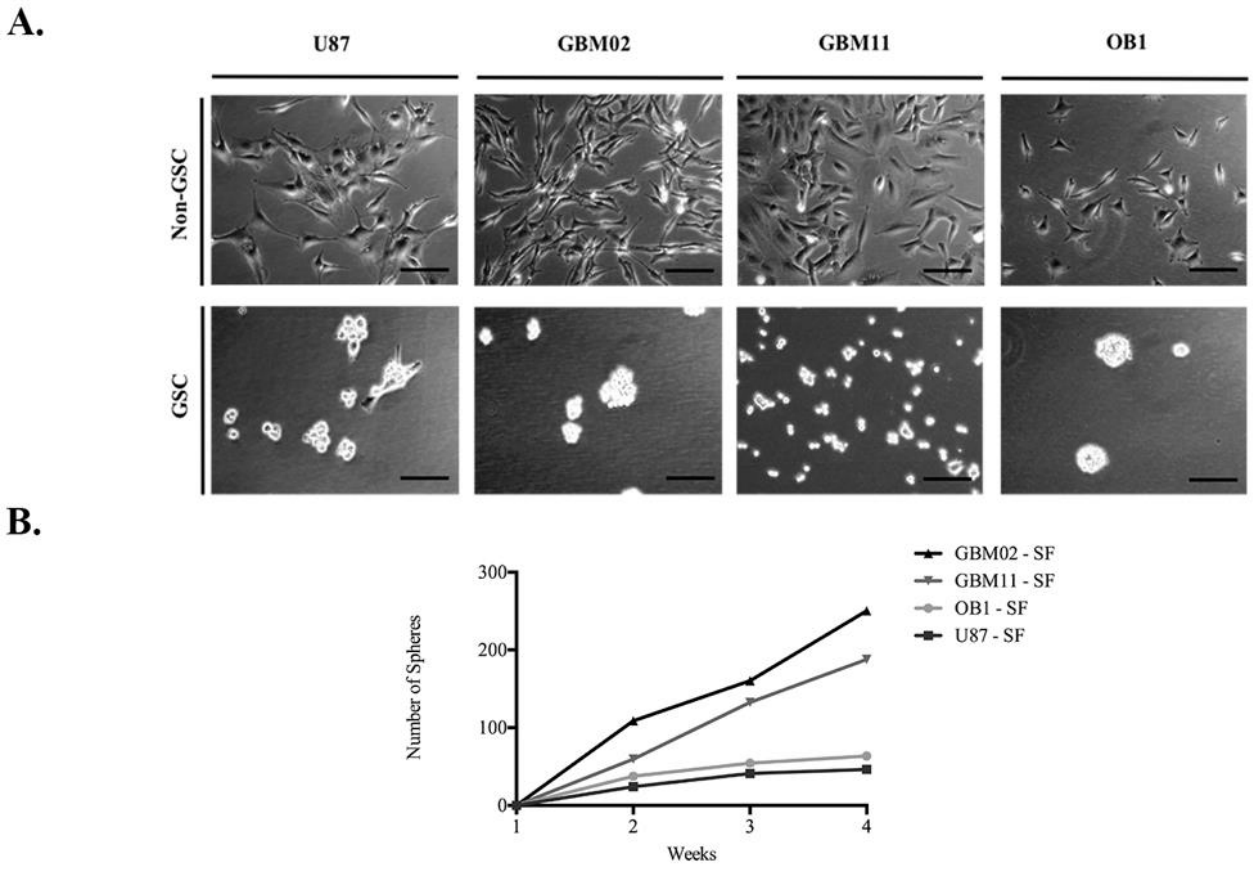

Figure 5.4 The glioblastoma stem-like cells (GSC) maintenance (A) and Clonogenic Assay (B). **A.** The human tumor cell lines were established in our laboratory. The use of patients' surgical specimens for the establishment of cell lines for *in vitro* and *in vivo* studies had written informed consent from the patients, and was approved by the Brazilian Ministry of Health Ethics Committee, under the Institutional Review Board (IRB - Research Ethics Committee of Hospital Universitário Clementino Fraga Filho) consent, CEP-HUCFF No. 002/01. Cells were grown and maintained in DMEM-F12 supplemented with 10% FBS. Culture flasks were maintained at 37°C in a humidified 5% CO_2 and 95% air atmosphere. Glioblastoma stem-like cells (GSCs) were maintained as tumor-sphere cultures in NeuroBasal medium supplemented with sodium pyruvate, glutamine, B27 supplement, EGF, basic FGF, penicillin and streptomycin. The OB1 differentiated cell line was obtained by the removal of EGF and bFGF and the addition of 10% fetal bovine serum. **B.** To estimate stem cell frequency in the cell population, tumor-sphere formation was assayed with 1 cell per well in 96 multi-well plates in NeuroBasal medium supplemented with sodium pyruvate, glutamine, B27 supplement, EGF, basic FGF, penicillin and streptomycin. During 4 weeks of culture, sphere-positive wells were scored by observation under an inverted microscope with phase-contrast optics. The image is representative of three independent experiments. Cells were imaged using a DMi8 advanced fluorescence microscope (Leica Microsystems, Germany). Scale bar = 50 μM. Images were processed using the software ImageJ 1.49v (Wayne Rasband, National Institutes of Health, USA).

5.4.3 GSCs Expression of Stem-Like State Markers

In order to determine whether the ability of GSCs derived from previously serum-cultured GBM cell lines to form spheres was accompanied by an increase in the expression of stem-like markers, the expression of SOX2, OCT-4A and NANOG was evaluated using WB (Figures 5.5A and 5.6A) and immunofluorescence (Figures 5.5B and 5.6B). In parallel, the GFAP and Nestin, a type VI intermediate filament protein that is expressed mostly in precursor of nervous cells, were also evaluated by immunofluorescence analysis (Figures 5.4B and 5.5B). The results showed that in the GBM02-SF cells, the expression of SOX2 was 1.75-fold higher, $p < 0.05$; the expression of OCT-4A was 43-fold higher, $p < 0.01$; and the expression of NANOG was 1.7-fold higher, $p < 0.01$, compared to their expression in the GBM02 cells (Figure 5.5A). In the GBM11-SF cells, the expression of SOX2 was 2.6-fold higher, $p < 0.05$; the expression of OCT-4A was 15.8-fold higher, $p < 0.01$; and the expression of NANOG was 2.6-fold higher, $p < 0.01$, compared to their expression in GBM11 (Figure 5.5A).

A.

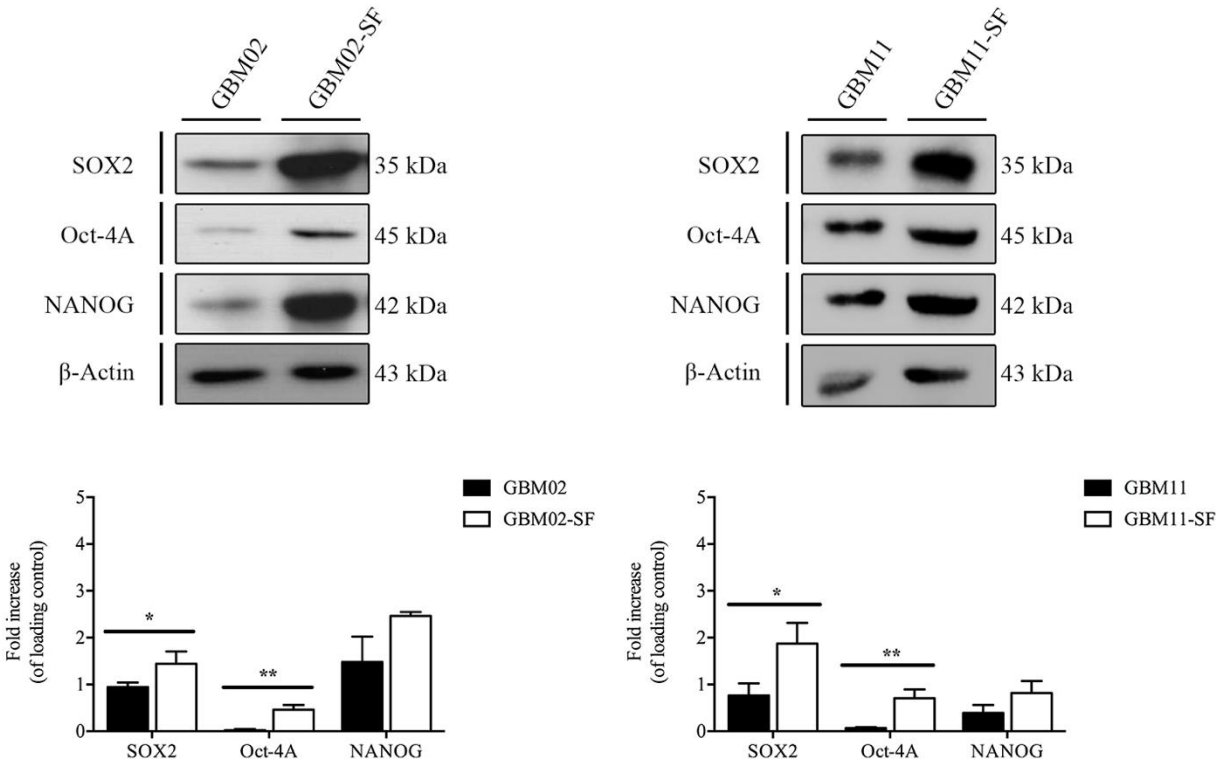
GBM02
GBM02-SF
SOX2
Oct-4A
NANOG
β-Actin
35 kDa
45 kDa
42 kDa
43 kDa
GBM11
GBM11-SF
Fold increase (of loading control)
SOX2
Oct-4A
NANOG

B.

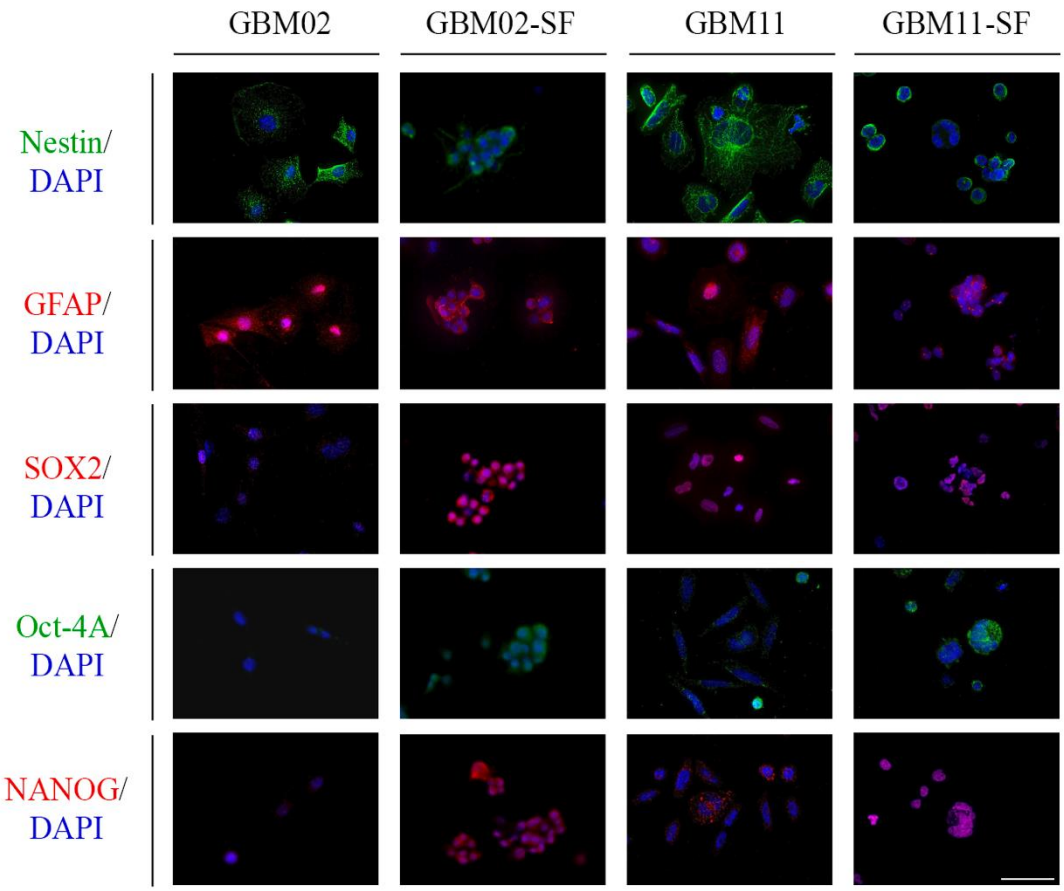
GBM02
GBM02-SF
GBM11
GBM11-SF
Nestin/ DAPI
GFAP/ DAPI
SOX2/ DAPI
Oct-4A/ DAPI
NANOG/ DAPI

Figure 5.5 Stem-like cell marker expression in two GBM cell lines isolated from patients in DMEM/F12 supplemented with serum, by western blot (A) and immunofluorescence (B). A. The expression of SOX2, OCT-4A and Nanog in both the GBM02 and GBM11 cell lines, isolated from GBM diagnosed patients, and the respective serum-free GBM cells, as previously described, was quantified by western blot. Statistical analysis was performed in GraphPad Prism 5 for Windows (version 5.00; GraphPad Software, Inc., San Diego, CA, USA). Each value represents the mean ± SEM from three independent experiments, *p< 0.05, **p<0.01. B. Immunofluorescence staining of SOX2, OCT-4A and Nanog as well as Nestin and GFAP was performed in both the GBM02 and GBM11 cell lines and the respective serum-free GBM cells, GBM02-SF and GBM11-SF. Cells were imaged using a DMi8 advanced fluorescence microscope (Leica Microsystems, Germany). Scale bar = 50 µM. Images were processed using the software ImageJ 1.49v (Wayne Rasband, National Institutes of Health, USA).

In the OB1-SF cells only the expression of SOX2 and NANOG was increased compared to their OB1 cells (2.9-fold higher, $p<0.05$ and 2.5-fold higher, $p<0.01$, respectively) (Figure 5.6A). Finally, in the U87-SF cells, the expressions of SOX2, OCT-4A and NANOG were 2.8-, 5.0- and 3.0-fold higher than in U87 cells ($p<0.05$; $p<0.01$; $p<0.01$), respectively (Figure 5.6A).

A.

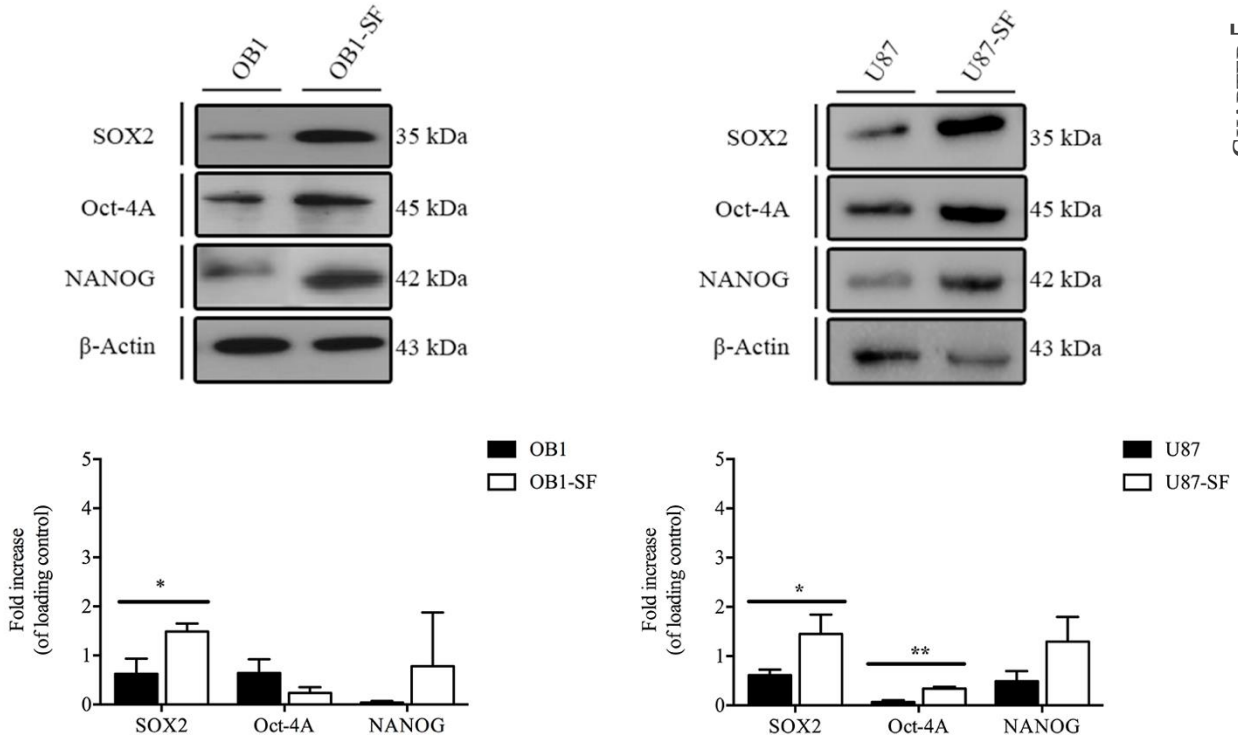
OB1
OB1-SF
SOX2
Oct-4A
NANOG
β-Actin
35 kDa
45 kDa
42 kDa
43 kDa
U87
U87-SF
Fold increase (of loading control)
SOX2
Oct-4A
NANOG

B.

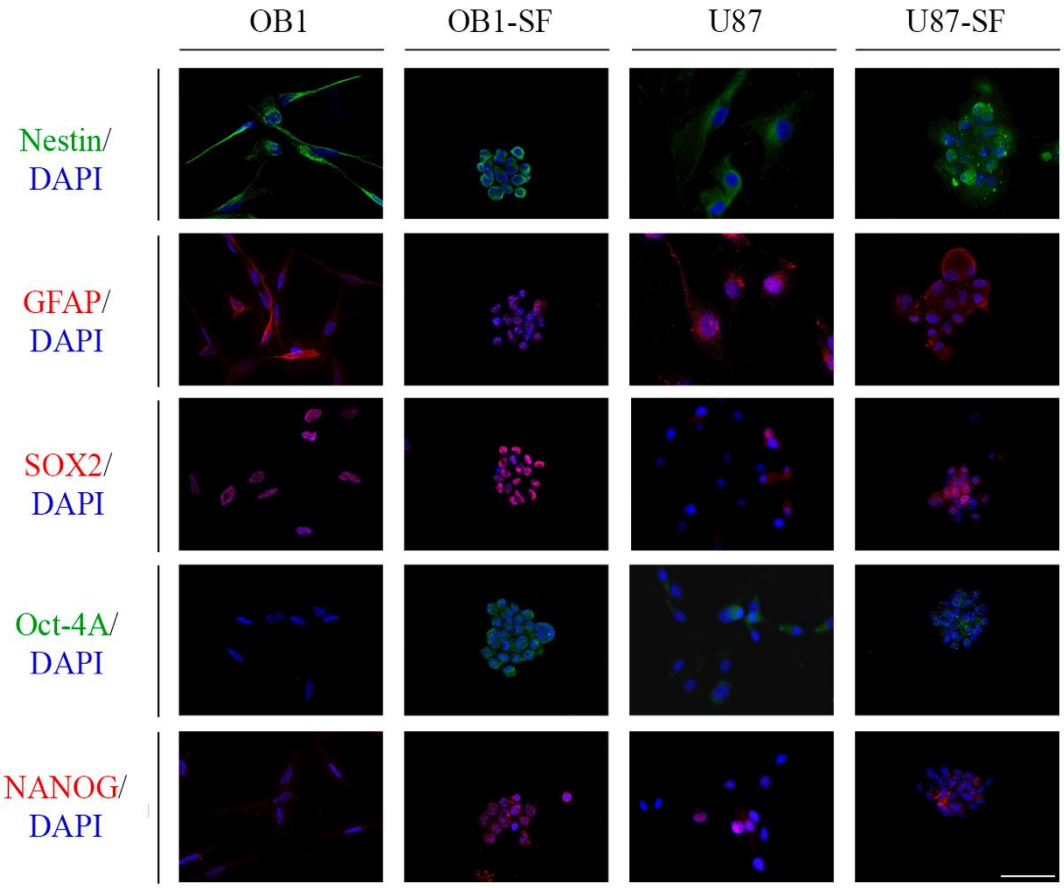
OB1
OB1-SF
U87
U87-SF
Nestin/ DAPI
GFAP/ DAPI
SOX2/ DAPI
Oct-4A/ DAPI
NANOG/ DAPI

Figure 5.6 Stem-like cell marker expression in the U87 ATCC GBM cell line, and the OB1, a GBM cell line isolated from a patient directly in NS34 serum-free medium, by western blot (A) and immunofluorescence (B). A. The expression of SOX2, OCT-4A and Nanog was quantified in both the OB1 cell line isolated from a GBM diagnosed patient directly in NS34 serum-free medium, and in U87, a GBM cell line acquired by ATCC. The respective OB1 differentiated cells were isolated from OB1-SF, and the serum-free GBM cells were isolated from the U87 cell line, U87-SF, as previously described, by western blot. Statistical analysis was performed in *GraphPad Prism 5* for Windows (version 5.00; GraphPad Software, Inc., San Diego, CA, USA). Each value represents the mean ± SEM from three independent experiments, * $p < 0.05$, ** $p < 0.01$. **B.** Immunofluorescence staining of SOX2, OCT-4A and Nanog as well as Nestin and GFAP was performed in both the OB1 and U87 cell lines and the respective serum-free GBM cells, OB1-SF and U87-SF. Cells were imaged using a DMi8 advanced fluorescence microscope (Leica Microsystems, Germany). Scale bar = 50 µM. Images were processed using the software ImageJ 1.49v (Wayne Rasband, National Institutes of Health, USA).

5.4.4 Connexins 43 and 46 Expression During Transition of GBM Cells Between Stem-Like and Non–Stem-Like States

Due to the particular functions of gap junctions in the coordination of many cellular processes, mainly cell proliferation, survival, differentiation and chemoresistance (Soroceanu *et al.,* 2001), we compared the expression of connexins, particularly Cx43 and Cx46, in the DMEM F12 10% SFB or NS34-cultured GBM cell lines, using WB (Figure 5.7A) and IF (Figure 5.7B). Our results showed that in the GBM02 cells, the Cx43 expression was higher than in the GBM02-SF cells; and the Cx46 expression was 12.0-fold higher in the GBM02-SF cells than in the GBM02 cells, $p < 0.001$. In the GBM11 cells, the Cx43 expression was 1.5-fold higher than in the GBM11-SF cells, although with no statistical significance; the Cx46 expression was 4.0-fold higher in the GBM11-SF cells than in the GBM11 cells, $p < 0.05$. In the OB1 cells, the Cx43 expression was 5.3-fold higher than in the OB1-SF cells, $p < 0.01$; and the Cx46 expression was 1.6-fold higher in OB1-SF than in the OB1 cells, although with no statistical significance. Finally, in the U87 cell line, the Cx43 expression was 0.8-fold higher than in the U87-SF cells, with no statistical significance; and the Cx46 expression was 1.3-fold higher in the U87-SF cells than in the U87 cells, with no statistical significance (Figure 5.7A and 5.7B). Overall, accordingly to what is described in literature our results showed, for the first time, that the Cx43 is overexpressed in non-GSCs whereas Cx46 is overexpressed in GSCs (Soroceanu *et al.,* 2001).

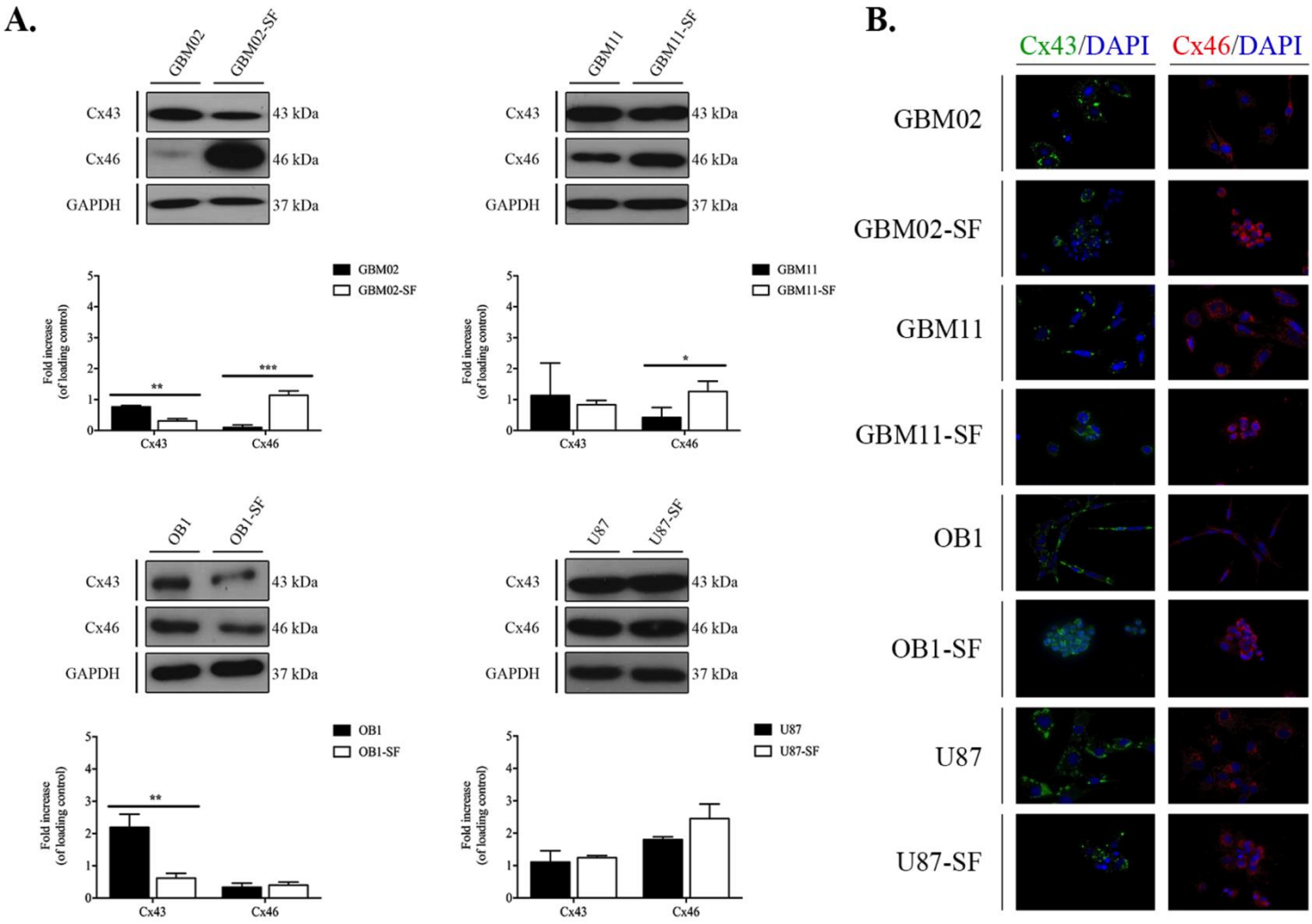

Figure 5.7 Connexin 43 and 46 expression analysis in the GBM and the respective serum-free cell lines (GSCs) by western blot (A) and immunofluorescence (B). A. The expression of Connexin 43 (Cx43) and Connexin 46 (Cx46) in the GBM02, GBM11, OB1 and U87 cell lines and the respective serum-free cells, GBM02-SF, GBM11-SF, OB1-SF and U87-SF, as previously described, was quantified by western blot. Statistical analysis was performed in *GraphPad Prism 5* for Windows (version 5.00; GraphPad Software, Inc., San Diego, CA, USA). Each value represents the mean ± SEM from three independent experiments, * $p < 0.05$, ** $p < 0.01$. **B.** Immunofluorescence staining of Cx43 and Cx46 was also performed in all cell lines. Cells were imaged using a DMi8 advanced fluorescence microscope (Leica Microsystems, Germany). Scale bar = 50 µM. Images were processed using the software ImageJ 1.49v (Wayne Rasband, National Institutes of Health, USA).

5.4.5 Human glioblastoma xenograft growth in immunocompetent mouse brain

A major feature of GSCs is the ability to form a new tumor when xenografted into a mouse brain (Singh *et al.*, 2004). This observation led us to xenograft GBM cell lines

into mouse brains in order to evaluate whether the cells can form new tumors, even when they are not in the stem-like state. GBM11 cells were grafted into the striatum of Swiss mice as previously described (Garcia *et al.,* 2014) (Figure 5.8A). Fourteen days after the tumor cells were injected, MRI was performed to mice brains and mices were subsequently euthanized (Figure 5.8B). The tumor mass was analysed macroscopically, revealing a haemorrhagic and necrotic area in the core of the tumor. The histological examination revealed the existence of a lymphoproliferative infiltrate and the presence of mitotic cells (Figure 5.8C). To confirm that the tumor developed due to the proliferation of the injected human GBM11 cells, infiltrating human cells were identified with a mouse anti-human vimentin antibody derived from V9, which showed positive staining (Figure 5.8D). Finally, to confirm the presence of GSCs in the tumor mass, the cells were stained with SOX2, which revealed SOX2-positive cells (Figure 5.8D). Taken together, this evidence suggests that the stem state is dynamic and can be induced depending on the environment where the tumor cell is immersed.

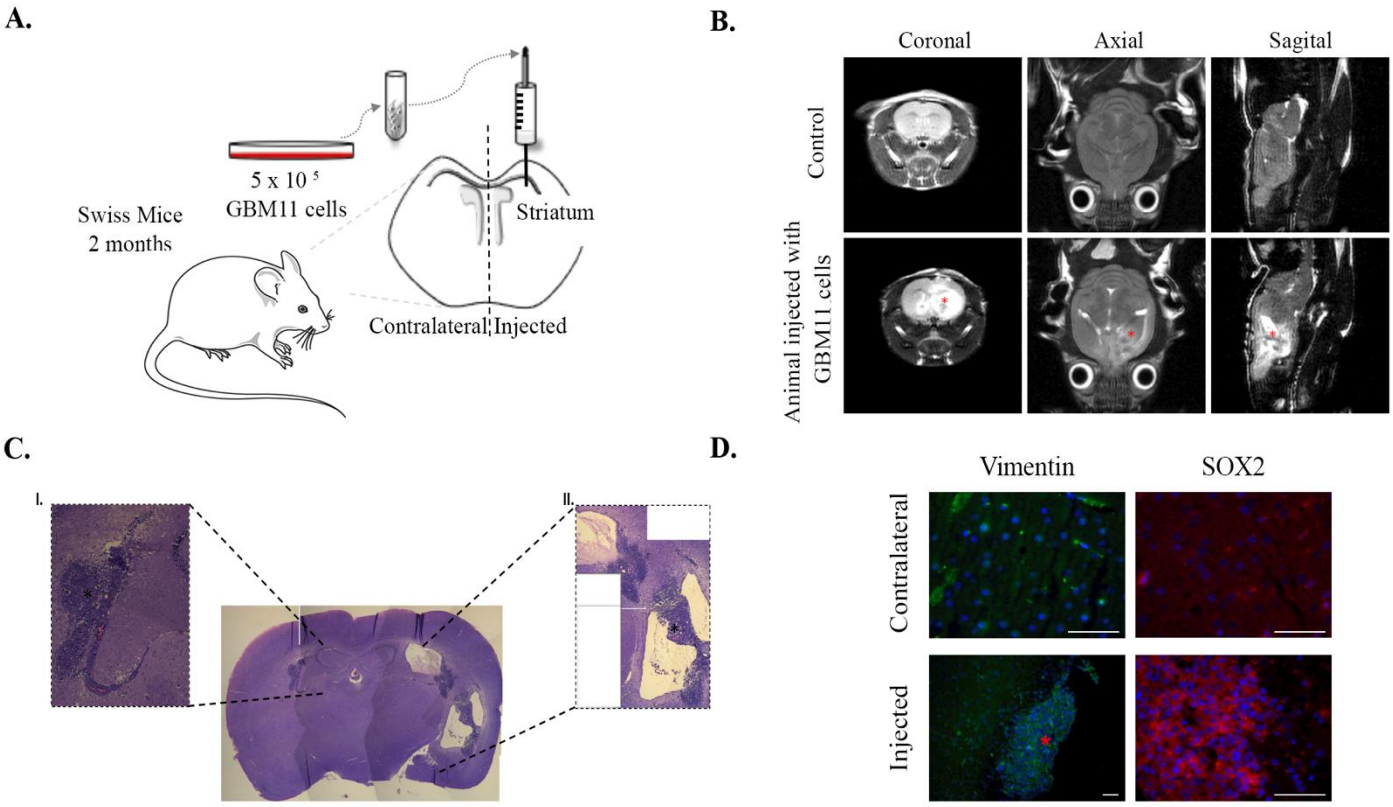

Figure 5.8 Capability of GBM cell lines to form tumors *in vivo*. A. Schematic depiction of GBM11 cells injection in striatum region of immunocompetent Swiss mouse brain. **B.** Magnetic resonance imaging (MRI) 14 days after GBM11 cell transplantation into a representative mouse brain. Coronal, sagittal and axial cuts of tumor site in control and GBM11-injected mice. The asterisk (*) indicates the tumor mass. **C.** Histopathological characteristics of the tumor mass in mouse brain parenchyma 14 days after implantation of GBM11 cells, revealed by haematoxylin-

eosin staining. I: Neoplastic cells forming a circumscribed solid tumor mass in the brain tissue (black asterisk). II: Glomeruloid vessels (black asterisk). Microscopic analysis showed anaplastic cells and tumoral necrosis. **D.** Immunohistochemical characteristics of the tumor revealed the expression of human vimentin (hVim). hVim staining (green) at the core of the tumor mass (red asterisk) and SOX2 (red), depicted by cell nuclei atypia (DAPI counterstaining in cyan blue, inset) and at the border of the tumor mass. Cells were imaged using a DMi8 advanced fluorescence microscope (Leica Microsystems, Germany). Scale bar = 50 µM. Images were processed using the software ImageJ 1.49v (Wayne Rasband, National Institutes of Health, USA).

5.4.6 SOX2 and Cx46 expression in human glioma samples

Since we had determined that the expression of the stem-like cell markers SOX2 and Cx46 mostly changes according to the stem and non-stem state, we next evaluated the expression of SOX2 and Cx46 in tumor sections obtained from a grade II astrocytoma and a grade IV astrocytoma (GBM), comparing with the temporal lobectomy neocortex samples acquired from epilepsy surgery patients with mesial sclerosis considered as normal brain, as described in the material and methods section. Comparing to astrocytoma grade II that presented microcysts and nuclear atypia, in GBM we observed a nuclear atypia, prominent microvasculature proliferation (+) and necrosis (*), which constitutes the essential diagnostic features of GBM (Fig. 5.9A). In the immunohistochemistry analysis the tumor sections obtained from the grade IV astrocytoma showed a higher SOX2 and Cx46 expression than in the tumor sections from the grade II astrocytoma and from normal patients, which suggests that the occurrence of GSCs is linked to the grade of the glioma (Patru *et al.*, 2010; Thirant *et al.*, 2011) (Figure 5.9B and 5.9C).

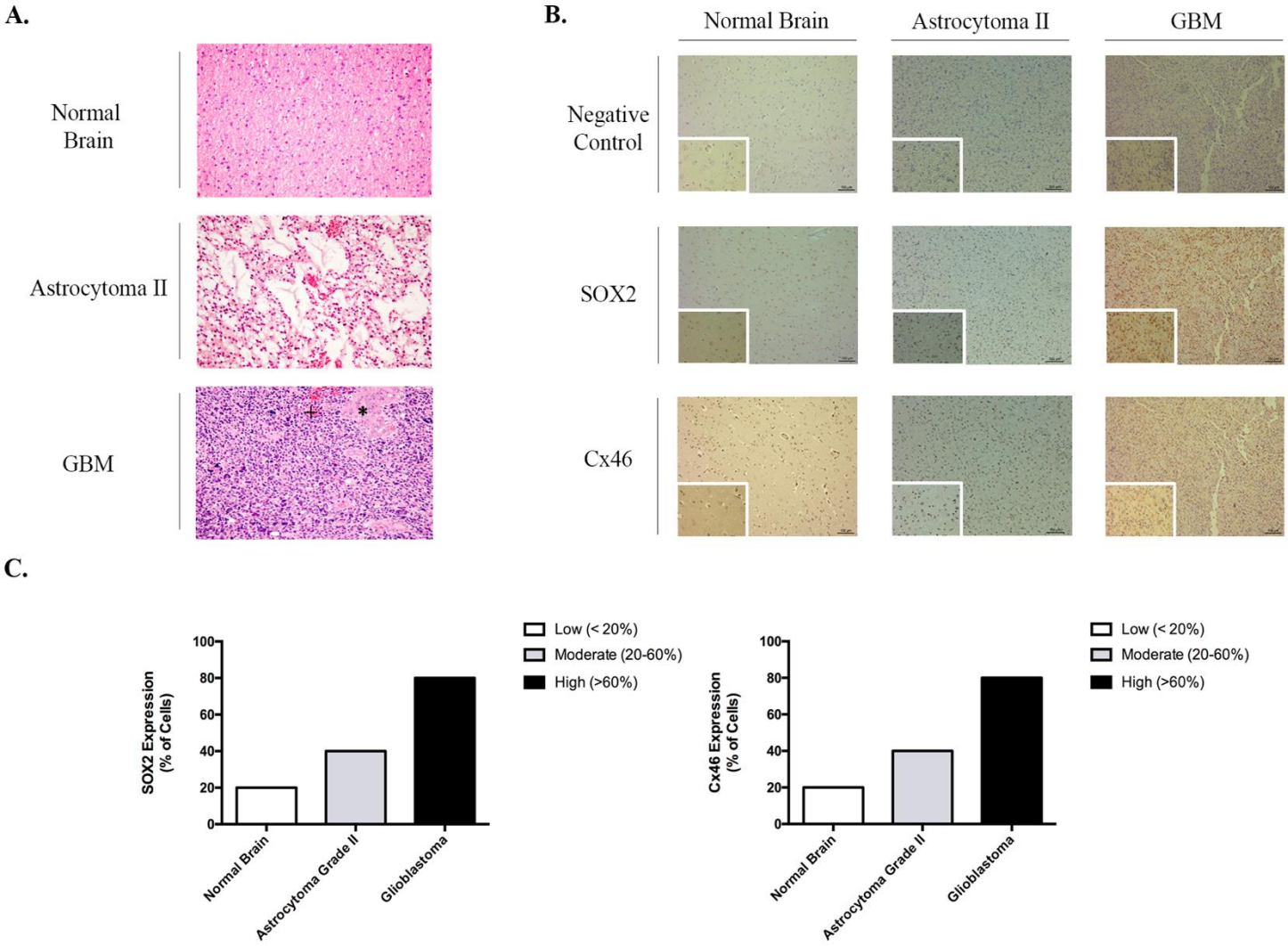

Figure 5.9 Analysis of SOX2 and Cx46 expression in glioblastoma, astrocytoma grade II and in normal human brain tissues by immunohistochemistry (IHC). Patients with clinical evidence of disease, magnetic resonance imaging (MRI) and histologically confirmed diagnosis of astrocytoma grade II and astrocytoma grade IV (GBM) based on the World Health Organization (WHO) 2007 criteria and who gave written informed consent to participate in the study were included. To compare the SOX2 and Cx46 expression, normal brain samples from patients that performed an epilepsy surgery with mesial sclerosis were also analyzed. The study was approved by the University Hospital of Coimbra Ethics Committee, according to the Declaration of Helsinki protocol. **A.** Histopathological characteristics of the tumor mass were evaluated by haematoxylin-eosin staining. The normal brain picture was acquired form the white matter. The astrocytoma grade II showed a nuclear atypia and microcysts and the glioblastoma showed nuclear atypia, microvascular proliferation (+) and necrosis (*). **B.** Immunohistochemistry was performed using the DAB method with haematoxylin counterstaining to evaluate the percentage of cells expressing SOX2 and Cx46. **C.** Tumor samples were ranked for SOX2 or Cx46 expression as high (60% positive cells), moderate (between 20% and 60% positive cells), and low (below 20% cells). Each image was acquired at 10x magnification (x10/ 0.25 PH1 NPLAN) and amplified 40x (x40/ 0.55 CORR PH2) (Scale bar = 100 µm), with a Leica DMI3000B light microscope (Leica, Germany) and acquired with the Leica Application Suite v 4.3 (Leica, Switzerland).

5.5 DISCUSSION

GBM is the most common and fatal type of primary brain tumor (Dubois *et al.,* 2014; Lima *et al.,* 2012; Louis *et al.,* 2016; Stupp *et al.,* 2009). In spite of recent advances, GBM treatment remains palliative, mainly due to the occurrence of chemo- and radioresistant GSCs, which contributes to tumor growth, metastasis and relapse (Diaz and Leon, 2011; Ortensi *et al.,* 2013; Seymour *et al.,* 2015; Singh *et al.,* 2004). As such, GSCs have become a main focus of GBM therapeutic research. Previous studies revealed that GSCs may emerge from the increased self-renewing division of GSCs or from reprogramming of non-GSCs to GSCs, maybe suggesting a plasticity of the stem state in GBM (Safa *et al.,* 2015). We considered that the understanding of GBM stem state plasticity is of utmost importance to identify the mechanisms and factors involved in GSCs resistance to therapy, which may justify tumor recurrence and so, constitute a step forward to the identification of new approaches to treat GBM.

It is well known that GSCs can lose their stem-like properties, giving rise to non-GSCs, but is the reverse true? Previous studies have suggested that GSC plasticity could be dynamic, and that both GSCs and non-GSCs are capable of switching their status (Safa *et al.,* 2015). Moreover, GSC interactions with the surrounding microenvironment could determine GBM heterogeneity and dictate the balance between self-renewal and differentiation properties (Hitomi *et al.,* 2015). Here, using GBM cell lines and patients samples we identified molecular markers that could translate both states in GBM (Figures 5.1 and 5.2). Our results showed that non-GSCs, obtained from culturing in DMEM/F12 with serum-supplemented medium, expressed less SOX2 and Cx46 compared to GSCs as we expected (Figure 5.1), and the reverse in OB1-SF cell line was also observed (Figure 5.2). Precisely, SOX2, an essential transcription factor for the maintenance of embryonic stem cells (ESCs), was overexpressed in GSCs of GBM02-SF and OB1-SF, as we expected.

Our results from the xenotransplant emphasized that the tumor microenvironment plays a critical role in the GBM differentiation status since we could saw a tumor development after GBM cells implantation in brain mices. Accordingly to literature, these interactions between GSCs and their niche dictate the balance between GSCs and non-GSCs through the variation of growth factors, extracellular matrix components, and the ability to communicate with adjacent cells by gap junctions (Hitomi *et al.,* 2015; Liu and Lu, 2012; Visvader and Lindeman, 2012; Wei *et al.,* 2004). Among all these factors, besides the study of stem-like cell markers expression, we assessed the profile expression

of proteins involved in gap junction-mediated intercellular communication, since they can sustain coordinated responses important to tumor growth, differentiation and therapy success. Specifically, we analysed the expression of connexins, Cx43 and Cx46, in GSCs and non-GSCs *in vitro*, in order to understand their expression in the stem cell state (Figure 5.7).

Our results showed that, in all GBM cell lines, Cx43 protein was overexpressed in non-GSC cell lines, whereas Cx46 was upregulated in GSCs (Figure 5.7), which emphasizes our initial hypothesis that GSC maintenance also depends on cell-cell interactions in a connexin-isotype-dependent manner, as proposed in the study of Hitomi et al. (Hitomi *et al.,* 2015).

Here, we also showed that the same cells placed in culture media with different properties, sequentially alter their expression of stem-like cell markers (at times T0, T2 and T4) (Figures 5.1A and 5.2A), together with the phenotype alterations by oncospheres formation, suggesting that "stemness" is actually a state (Figures 5.1B and 5.2B). Our qPCR results endorsed with these ideas (Figures 5.1C and 5.2C). The SOX2 mRNA levels were higher in stem-like conditions, both in GBM02-SF cells (time T2) as in OB1-SF cells (time T0). In OB1-SF cells (T4) there was a tendency of increasing SOX2 transcripts levels but it was not statistically different. In turn, Cx43 mRNA levels were lower in stem-like statements in OB1 cells (time T0 and T4), although was not significant different in GBM02 cells (times T0, T2 and T4). Overall, the mRNA results are in agreement with the protein levels. To confirm this hypothesis, we tested the GSCs for the cardinal properties of stem-like cells, including their clonogenic potential, the expression of transcription factors associated with the stem state, and their ability to form tumors in an orthotopic mouse model. Examined in detail, the GBM cell lines showed differences in clonogenic potential. The GBM02-SF and GBM11-SF cell lines proved to be more capable of forming clones than the OB1-SF and U87-SF cell lines. These differences in the ability to form clones may be related to the intrinsic heterogeneity observed in high-grade gliomas, and perhaps contribute to the different degrees of aggressiveness of GBM cells (Figure 5.3B). Interestingly, in our GSCs, the expression of the stem-like cell markers SOX2, Oct-4A and NANOG was higher than in non-GSCs, as expected. These results accord with the clonogenic capability of each GBM cell line and with previous studies (Altaner and Altanerova, 2012; Jackson *et al.,* 2015; Patru *et al.,* 2010; Safa *et al.,* 2015; Würth *et al.,* 2014).

Since the stem-like properties are known to induce chemoresistance and stem cell state is dynamic, we asked if there would be a possible association between the expression of molecular markers and the aggressiveness of tumors, and their outcome (Figure 5.9). Therefore, we evaluated the expression of SOX2 and Cx46, both overexpressed in GSCs *in vitro*, in samples of normal, astrocytoma grade II and astrocytoma grade IV (GBM) brains from human patients (Figure 5.9A). SOX2 and Cx46 were highly expressed in the GBM compared to the astrocytoma grade II and normal brain samples (Figure 5.9B). We classified the percentage of SOX2 and Cx46 expression in cells as low (< 20% of cells expressing SOX2 or Cx46), moderate (20-60% of cells expressing SOX2 or Cx46) and high (> 60% of cells expressing SOX2 or Cx46), corresponding to the samples from normal, astrocytoma grade II and GBM samples, respectively (Figure 5.9C). These results are in agreement with previous studies that verified a higher expression of SOX2 compared to normal brain tissue samples (Jackson *et al.,* 2015; Soares *et al.,* 2015). These findings suggest that GSCs are more frequent in high-grade gliomas, due to unknown microenvironmental factors that could trigger the switch between stem-like and non-stem-like states in GBM. Our data reinforce the initial proposal that the stem state is a dynamic bidirectional fluctuation that depends not only but also on the microenvironment.

Summarizing, we could for the first time demonstrate the plasticity of the GBM stem-cell state, as represented in Figure 5.10. Briefly, the stem-like cell state is accompanied by the overexpression of markers of stem-like cells, detailed characterized by us, and by downregulation of markers of differentiated cells as expected. However, when the media is changed we observed that the same differentiated cells are accompanied by downregulation of stem-like cell markers and overexpression of differentiated cell markers, which showed that the stem state is not static, definitely established, but dynamic and maybe depending on tumor microenvironment.

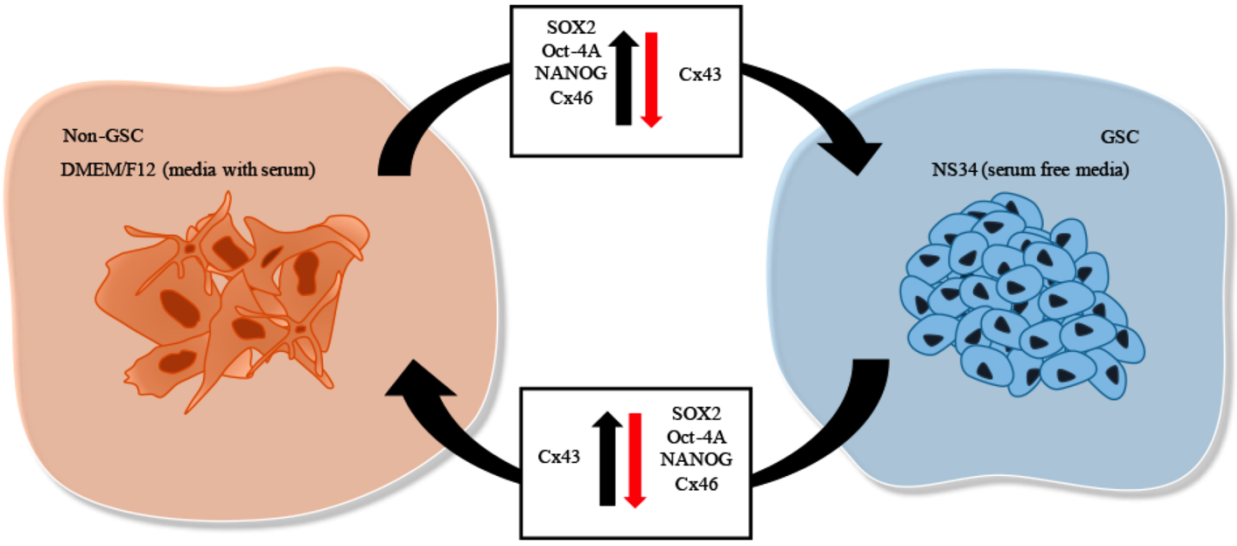

Figure 5.10 Plasticity of GBM stem-like cells. Interactions of GBM cells with the tumor microenvironment can dictate the dynamic balance between self-renewal and differentiation properties, through growth factors present in serum-free stem-like cell medium, NS34, or through bovine-serum supplement in DMEM/F12 medium, respectively. The stem-like cell markers SOX2, OCT-4A and NANOG differ in expression according to the stem cell state. Also the connexins, important for cell-to-cell communication processes, demonstrate the plasticity of stem-like cells. As such, SOX2, OCT-4A, NANOG and Cx46 are overexpressed in GSCs (black arrow), while Cx43 is downregulated (red arrow). In contrast, in non-GSCs, SOX2, OCT-4A, NANOG and Cx46 are downregulated (red arrow); while Cx43 is overexpressed in GSCs (black arrow).

Our results constitute an important advance in the knowledge of stem-like cells behaviour. For the first time we showed that the GBM stem-like cell markers are dynamic and bidirectional, depending on microenvironmental clues. Since GSCs are the most chemoresistant cells in the GBM tumor mass, stem-like cell markers, as SOX2, are more highly expressed in human GBM samples than in lower grades of gliomas, suggesting a direct correlation with the poor prognosis of GBM patients.

Altogether, our *in vitro* and in *vivo* results corroborate our hypothesis. This work highlight to understanding the GSCs and non-GSCs state, which is primary step in comprehension of tumor growth and differentiation processes. Hopefully, this will improve the success of GBM therapy in a way to identify more specific targets to reach GBM.

CHAPTER 6

Nucleolin is expressed in glioblastoma cells and patient-derived samples and enables improved intracellular drug delivery and cytotoxicity

Joana Balça-Silva, Anália do Carmo, Hermínio Tão,
Olinda Rebelo, Marcos Barbosa, Vivaldo Moura-Neto,
Ana Bela Sarmento-Ribeiro, Maria Celeste Lopes,
João Nuno Moreira. 2018

(*To be submitted*)

6.1 ABSTRACT[7]

Glioblastoma (GBM) is the most aggressive type IV astrocytoma. One of the major challenges associated with GBM therapy relates with the existence of a cell population within the tumor mass that presents stem-like cell properties, the glioma stem-like cells (GSCs), known to be related with chemo- and radio-resistance. Cancer stem cells (CSCs) and non-stem cancer cells (non-SCCs) have the ability to interchange, thus emphasizing the importance in glioblastoma of identifying common molecular targets among those cell sub-populations. Nucleolin is a multifunctional protein overexpressed in cancer cells, and it has been recently associated with sub-populations with different stem-like phenotype. Recently we have designed sterically stabilized pH-sensitive liposomes, functionalized with a nucleolin-binding peptide.

The major goal of this work was to evaluate the potential of cell surface nucleolin as a target in GBM cells.

Flow cytometry assays showed that different levels of nucleolin expression resulted in a 3.4-fold higher association of liposomes, functionalized with a nucleolin-binding peptide into bulk U87 cells, relative to GBM11 cells. Moreover, nucleolin may be a potential therapeutic marker in both OCT4- and NANOG-positive GSC, and in the corresponding non-GSC, as well as in SOX2-positive GSC. In cell cytotoxicity assays, DXR delivered by liposomes functionalized with the nucleolin-binding F3 peptide enabled a level of cytotoxicity that was 2.5- or 4.6-fold higher than the one enabled by the delivery of the same drug by non-targeted liposomes or liposomes targeted by a non-specific peptide, respectively. This was further supported by the significant difference of DXR accumulation enabled by the targeted liposomes relative to non-targeted or liposomes targeted by a non-specific peptide. These data along with the marked expression of the protein in more than 60% of cells from patient-derived samples, as compared with less than 20% in normal brain, supported nucleolin as a potential therapeutic target in GBM.

Keywords: Glioblastoma; Glioblastoma stem-like cells; Nucleolin; Therapeutic Target.

[7] This chapter contains the text and the figures to be originally submitted in *Joana Balça-Silva, Anália do Carmo, Hermínio Tão, Olinda Rebelo, Marcos Barbosa, Vivaldo Moura-Neto, Ana Bela Sarmento-Ribeiro, Maria Celeste Lopes, João Nuno Moreira. 2018.*

6.2 INTRODUCTION

Glioblastoma (GBM), the most common and biologically aggressive type IV astrocytoma, is characterized by a highly proliferative index, aggressiveness, invasiveness, and short patient survival. Its current first-line treatment option includes the maximal surgical resection of the tumor followed by radio and chemotherapy with the *gold-standard*, temozolomide (TMZ). Nevertheless, on average the median survival time of GBM patients remains approximately between 12 and 15 months (Furnari *et al.*, 2007; Gladson *et al.*, 2010; Ichimura *et al.*, 2004).

Notwithstanding the important advances on the mechanisms underlying the genetics, biology and clinical behavior of GBM, its pathogenesis is still not completely understood (Dubois *et al.*, 2014; Singh *et al.*, 2004). One of the major challenges associated with GBM therapy relates with the existence of a cell population within the tumor mass that presents stem-like cell properties, usually referred as glioma stem-like cells (GSCs), known to be associated with chemo- and radio-resistance (Abou-Antoun *et al.*, 2017; Bradshaw *et al.*, 2016; Lathia *et al.*, 2015). In a variety of tumors, cancer stem cells (CSC) have also been associated with tumor relapse and poor disease prognosis (Altaner and Altanerova, 2012; Seymour *et al.*, 2015). We have previously demonstrated that the heterogeneity of GBM tumors resulted from the reversible interchange within GBM cells, between stem-like (GSC) and non-stem-like cell phenotypes (non-stem glioblastoma cancer cells, non-GSC), as a consequence of the plasticity associated with glioma stem-like cells (Balça-Silva *et al.*, 2017b). In this respect, the identification of a surface marker expressed in both cancer stem cells (CSCs) and non-stem cancer cells (SCCs) of GBM, aiming at enabling a multicellular therapeutic approach to the tumor niche (Fonseca *et al.*, 2015), is highly relevant in the context of glioblastoma therapy.

Nucleolin is a multifunctional protein (Fonseca *et al.*, 2017, 2015) which besides being overexpressed in cancer cells, such as in breast tumors (Moura *et al.*, 2012), it has been also associated with angiogenesis (Christian *et al.*, 2003) and, more recently, with breast cancer cell sub-populations with different stem-like phenotype (Fonseca *et al.*, 2015). This endows nucleolin as a potential therapeutic target of multiple cell populations within the breast tumors niche, an issue that has not been yet addressed in the context of GBM.

The major goal of this work was to evaluate the potential of cell surface nucleolin as a target in GBM cells. As such, the specific objectives of the work encompassed, at first,

the evaluation of nucleolin expression in different GBM (bulk) cell lines. Moreover, it was also assessed the potential of nucleolin as a target within GBM cells, with stem-like and non-stem like phenotypic characteristics, enabling improved cell cytotoxicity as the result of an active access to the intracellular compartment of a chemotherapeutic drug delivered by a previous developed delivery system, targeting nucleolin (Fonseca *et al.*, 2015, 2014; Moura *et al.*, 2012).

6.3 MATERIAL AND METHODS

6.3.1 Materials

Dulbecco's Modified Eagle Medium: Nutrient Mixture F-12 (DMEM/F-12), fetal bovine serum (FBS) and propidium iodide were supplied from Invitrogen (Paisley, UK). The anti-mouse and anti-rabbit antibodies were obtained from GE Healthcare (UK). The rabbit sex determining region Y-Box (SOX2), octamer-binding transcription factor 4a (OCT-4A), and Nanog homeobox (NANOG) antibodies were obtained from Cell Signalling (MA, USA). Doxorubicin hydrochloride (DXR) was from IdisPharma (UK) and 3-(4,5-dimethyl-2-thiazolyl)-2,5-diphenyl-2H-tetrazolium bromide (MTT), 3β-hydroxy-5-cholestene-3-hemisuccinate (CHEMS) and cholesterol (CHOL) were purchased from Sigma-Aldrich (USA).

The lipids 2-dioleoyl-sn-glycero-3-phosphoethanolamine (DOPE), 1,2-distearoyl-sn-glycero-3-phosphocholine (DSPC), 1,2-distearoyl-snglycero-3-phosphoethanolamine-N-[methoxy(polyethyleneglycol)-2000] (DSPE-PEG2k) and 1,2-distearoyl-sn-glycero-3-phosphoethanolamine-N-[maleimide(polyethyleneglycol)-2000] (DSPE-PEG2kmaleimide) and L-a-Phosphatidylethanolamine-N-(lissaminerhodamine B sulfonyl) (RhoB-PE) were obtained from Avanti Polar Lipids (USA). F3 (KDEPQRRSARLSAKPAPPKPEPKPKKAPAKK) and the non-specific (NS) peptides were custom synthetized by Genecust (Luxemburg). ImmPress reagent was obtained from Vector Laboratories. Diaminobenzidine (DAB) was obtained from Bios (Beijing, China). Fluoromount was obtained from Southern Biotechnology Associates (USA). All other chemicals were of analytical grade purity.

6.3.2 Cell lines

The U87 glioblastoma cell line was acquired from the American Type Culture Collection (ATCC) (Manassas, VA, USA), while the human tumor cell line GBM11 was established and characterized in our laboratory (Balça-Silva *et al.,* 2017a; Faria *et al.,* 2006). These cell lines were cultured as previously described (Balça-Silva *et al.,* 2015) and routinely tested for mycoplasma contamination.

6.3.3 Preparation of liposomes

Sterically stabilized pH-sensitive liposomes were prepared as previously described (Fonseca *et al.,* 2005). Briefly, liposomes were composed of DOPE:CHEMS:DSPC:CHOL:DSPE-PEG2k (4:2:2:2:0.8 molar ratio). Dried lipid films were hydrated at 60°C with ammonium sulfate (pH 8.5) and the resulting liposomes were extruded through 80 nm pore size polycarbonate membranes using a LiposoFast Basic mini extruder (Avestin, Canada). The buffer was exchanged in a Sephadex G-50 gel column (Sigma-Aldrich, USA) equilibrated with Trizma®Base sucrose (10%, w/v, buffered at pH 9.0). Remote encapsulation of DXR was carried out through ammonium sulfate gradient method, upon incubation with liposomes for 1.5 h at 60°C. Nonencapsulated DXR was removed using a Sephadex G-50 gel column equilibrated with 25 mM HEPES, 140 mM NaCl buffer (HBS, pH 7.4). Targeted liposomes, either with the F3 peptide or non-specific peptide, were further prepared by post-insertion of the resulting conjugates into preformed liposomes (Moreira *et al.,* 2002).

Regardless the formulation, resulting liposomes, presented a mean size of 80 nm, with a mean polydispersion index of 0.3 and a 94 – 98% of DXR encapsulation efficiency.

6.3.4 Analysis of expression of cell surface nucleolin

The percentage of U87 and GBM11 cells expressing nucleolin was evaluated by flow cytometry. Cell permeabilization was performed upon slowly adding 0.5 ml of 100% cold methanol, while vortexing and maintained on ice during 30 min. Cells were then washed with incubation buffer (PBS buffer with 1% bovine serum albumin (BSA) (PBS-BSA)). Both permeabilized and non-permeabilized cells were then centrifuged and

incubated with 0.2 µg/µl mouse anti-nucleolin-AlexaFluor 488 antibody (Abcam, UK) or IgG_1 isotype control (Affymetrix, USA), for 30 min at 4ºC in PBS buffer with 1% BSA. Finally, cells were washed, resuspended in 2 µg/ml propidium iodide (PI) and analyzed. Nucleolin and PI were evaluated in the FL1 and FL2 channel, respectively, and a total of 20.000 events were collected by flow cytometry in a BD FACSCalibur system (BD Biosciences, USA). Appropriate controls were used to ensure correct compensation of fluorescence signals in each channel.

6.3.5 Assessment of cellular association of rhodamine-labelled liposomes functionalized with the nucleolin-binding F3 peptide by GBM cells

Half million of GBM (bulk) cells were seeded in 48 multi-well plates. Twenty-four hours later, cells were incubated at 37°C, during 1 h or 4 h with rhodamine-labelled liposomes, either targeted by the F3 peptide or a non-specific peptide or non-targeted liposomes, at 0.4 mM of total lipid as previously described (Gomes-da-Silva *et al.,* 2012b). Following three washing steps with phosphate buffer saline (PBS), pH 7.4, and detachment with trypsin, rhodamine fluorescence was evaluated in the FL2 channel of a FACS Calibur flow cytometer (BD, Biosciences), upon collecting a total of 20,000 events.

In parallel experiments, cells previously incubated with rhodamine-labelled liposomes were immunostained as described in 6.3.6, with anti-SOX2, anti-OCT-4A or anti-NANOG antibodies or IgG1 isotype control, for 1 h at 4°C, in PBS/BSA. The stem-like cells signal and cell-associated rhodamine were immediately analyzed in the FL1 and FL2 channels, respectively, and a total of 20,000 events were collected.

Appropriate controls were used to ensure a correct compensation of fluorescence signals in each channel (Fonseca *et al.,* 2015). Data were analyzed with the *Cell Quest Pro software*.

6.3.6 Analysis of stem-like cell markers expression in GBM cells by flow cytometry and by western blot

U87 and GBM11 cells were fixed for 10 min in PFA/PBS 4%, at 37°C, maintained in ice during 1 min, permeabilized with cold methanol 100%, slowly under vortex, and maintained on ice during 30 min. Cells were further washed in incubation buffer (PBS/BSA), centrifuged and incubated with anti-SOX2 antibody, anti-OCT-4A or anti-

NANOG or IgG1 isotype control, for 1 h at 4°C, in PBS/BSA. Cells were then washed with PBS/BSA and incubated with anti-rabbit Alexa flour 488 reagent for 30 min at room temperature, according to the manufacturer instructions. The stem-like cells signal was immediately analyzed by flow cytometry in the FL1 channel, and a total of 20,000 events were collected. Appropriate controls were used to ensure a correct compensation of fluorescence signals in each channel (Fonseca *et al.,* 2015).

The SOX2, OCT4 and NANOG expression was also analyzed by western blot as previously described (Balça-Silva *et al.,* 2015). Briefly, cells were centrifuged at 500 g for 10 min at 4 °C and further resuspended in RIPA buffer (50 mM Tris–HCl at pH 8.0, 150 mM NaCl, 1.0% NP-40, 0.5% sodium deoxycholate, 0.1% SDS and 2 mM EDTA, supplemented with protease and phosphatase inhibitors and DTT), and sonicated. Proteins were denatured with a TRIS buffer, pH 6.8 (0.5 mM TRIS, pH 6.8; 50% glycerol, 10% SDS, 10% 2β-mercaptoethanol and blue bromophenol), and boiled at 95°C for 5 min before use. For each assay, 30 μg of protein was separated on a 12% SDS–PAGE and then transferred to a PVDF membrane, further incubated with 5% non-fat milk in TRIS Buffered Saline with Tween (200mM TRIS base; 137 mM NaCl; 0.1% Tween 20; pH= 7.6), for 1 h at room temperature. Incubation of anti-SOX2 (diluted at 1:1000, v/v), -OCT-4A (1:1000), or -NANOG (1:1000) primary antibodies was carried out overnight at 4°C, diluted in TRIS Buffered Saline with Tween with 1% milk supplemented with azide. Immunocomplexes were further detected with anti-rabbit secondary antibody (at 1:1000) and conjugated with alkaline phosphatase. An enhanced chemifluorescence detection reagent was used and the protein expression quantified using the software *Image J software 1.49v* (Waine Rasband, National Institutes of Health, USA), having the expression of β-actin as a loading control.

6.3.7 Cell cytotoxicity by liposomes functionalized with the nucleolin-binding F3 peptide and containing DXR

U87 cells were seeded into 96 multi-well plates at 8×10^4 cells/well and incubated for 24 h at 37°C in an atmosphere of 95% humidity and 5% CO_2. Afterwards, cells were incubated with serial dilutions of DXR-containing liposomes, either targeted by the F3 peptide (T) or by a non-specific (NS), or non-targeted (NT), for 1 and 4 h at 37°C and 5% CO_2, after which the cell culture medium was exchanged for fresh one and the experiment extended up to 48 h. Cells were incubated with 0.5 mg/ml 3-(4,5-dimethylthiazol-2-yl)-

2,5-diphenyl tetrazolium bromide (MTT) for 45 min. To dissolve the blue formazan crystals, 0.2 mL of DMSO was added to each well. The absorbance was assessed in a microplate reader at 570 nm. Results were expressed in terms of the drug concentration required to reduce the percentage of metabolically active cells by 50% (IC_{50}), interpolated from dose-response curves.

6.3.8 Cellular association of DXR delivered by liposomes functionalized with the nucleolin binding F3 peptide

U87 cells were incubated with several liposomal formulations, for 4 h at 37ºC as described in the previous section. In the end of the experiment, aiming at removing surface bound liposomes, cells were washed once with 0.12 M NaCl, 0.028 M Na-acetate, pH 3.0 (Kameyama *et al.,* 2007), and then lysed with cold RIPA buffer. In a parallel experiment, cells were washed without the dedicated step with cold acid buffer. Each concentration tested was assessed in triplicate and analyzed with a microplate fluorimeter reader at excitation and emission wavelengths of 485 and 590 nm, respectively, and a cutoff of 570 nm. The amount of DXR was further depicted from a calibration curve. The protein concentrations in the lysates were determined by the BCA assay. Results were expressed as mol of DXR/µg of protein.

6.3.9 Nucleolin expression in human GBM samples

Human-derived tumors (*n*=6) were obtained from patients diagnosed with glioblastomas, while the corresponding control tissue, considered as normal brain, was obtained from 2 temporal lobectomy neocortex samples, from epileptic patients with mesial sclerosis and submitted to surgery. All patients were admitted to the Neurosurgery Service of the University Hospital of Coimbra (Coimbra, Portugal). The study was approved by the University Hospital of Coimbra Ethics Committee, according to the Declaration of Helsinki protocol and all patients assigned an informed consent for the use of biological material for research investigation.

GBM and normal brain tissues were fixed in 4% paraformaldehyde for 12−24 h and embedded into paraffin and cut into 4 µm sections. For immunohistochemistry, the tissue

sections were heated at 60°C for 30 min, deparaffinized in xylene for 20 min and rehydrated in series of ethanol solutions using Vector laboratories (Burlingame, CA 94010). The sections were then incubated for 30 min with 3% H_2O_2, submitted to antigen retrieval and incubated in horse normal serum (Vector laboratories) at 4°C for 30 min. Then, sections were incubated with mouse monoclonal anti-nucleolin primary antibody (Abcam, 5 µg/ml per slice) diluted in TRIS Buffered Saline overnight at 4°C. Upon washing with a solution of TRIS Buffered Saline and Tween (200 mM TRIS base; 137 mM NaCl; 0.1% Tween 20; pH 7.6), cells were further incubated with a secondary anti-mouse/rabbit antibody (ImmunoPress reagent, USA) for 30 min at room temperature and then with diaminobenzidine (DAB). All sections were counterstained with Mayer's haematoxylin and evaluated and scored blindly and independently by two pathologists as previously described (Gregório *et al.,* 2016). Sections were observed at the same magnification of 10x (x10/ 0.25 PH1 NPLAN) and amplified 40x (x40/ 0.55 CORR PH2) (Scale bar = 100 µm) using the *Leica Germany DMI3000B* light microscope and acquired by *Leica Application Suite v 4.3* (Switzerland).

6.3.10 Statistical analysis

All values were expressed as mean ± SEM. After confirmation of the assumption of normality and homogeneity of variance across groups, the groups were compared by nested design, including analysis of variance and post-hoc comparison with correction of α error according to *Bonferroni* probabilities to compensate for multiple comparisons, $p < 0.05$. Also, statistical significance between two groups was assessed by a student's t-test with a significance threshold of $p < 0.05$.

6.4 RESULTS AND DISCUSSION

6.4.1 Expression of cell surface nucleolin and association of liposomes functionalized with the nucleolin-binding F3 peptide by GBM bulk cells

Nucleolin is a multifunctional protein with different roles at different levels of cancer cells, including in the nucleus, cytoplasm and membrane as reviewed by Fonseca et al. (Fonseca *et al.,* 2017), reflected by a pattern of expression that can vary among those

sub-cellular locations. This led herein to the assessment of nucleolin expression in non-permeabilized and permeabilized cells by flow cytometry. Interestingly, the total content of nucleolin was similar among both cell lines permeabilization (Fig. 6.1A). However, the level of cell-surface nucleolin in non-permeabilized U87 cells was 3.7-fold higher than in GBM11 cells ($p < 0.001$), (Fig. 6.1B). These results pointed out a major challenge posed in an oncological setting, which has to do with the tumor heterogeneity among patients (Kleppe and Levine, 2014). In this respect, efficient patient stratification in the context of a targeted therapy plays a major role in the treatment efficacy (Hamburg and Collins, 2010).

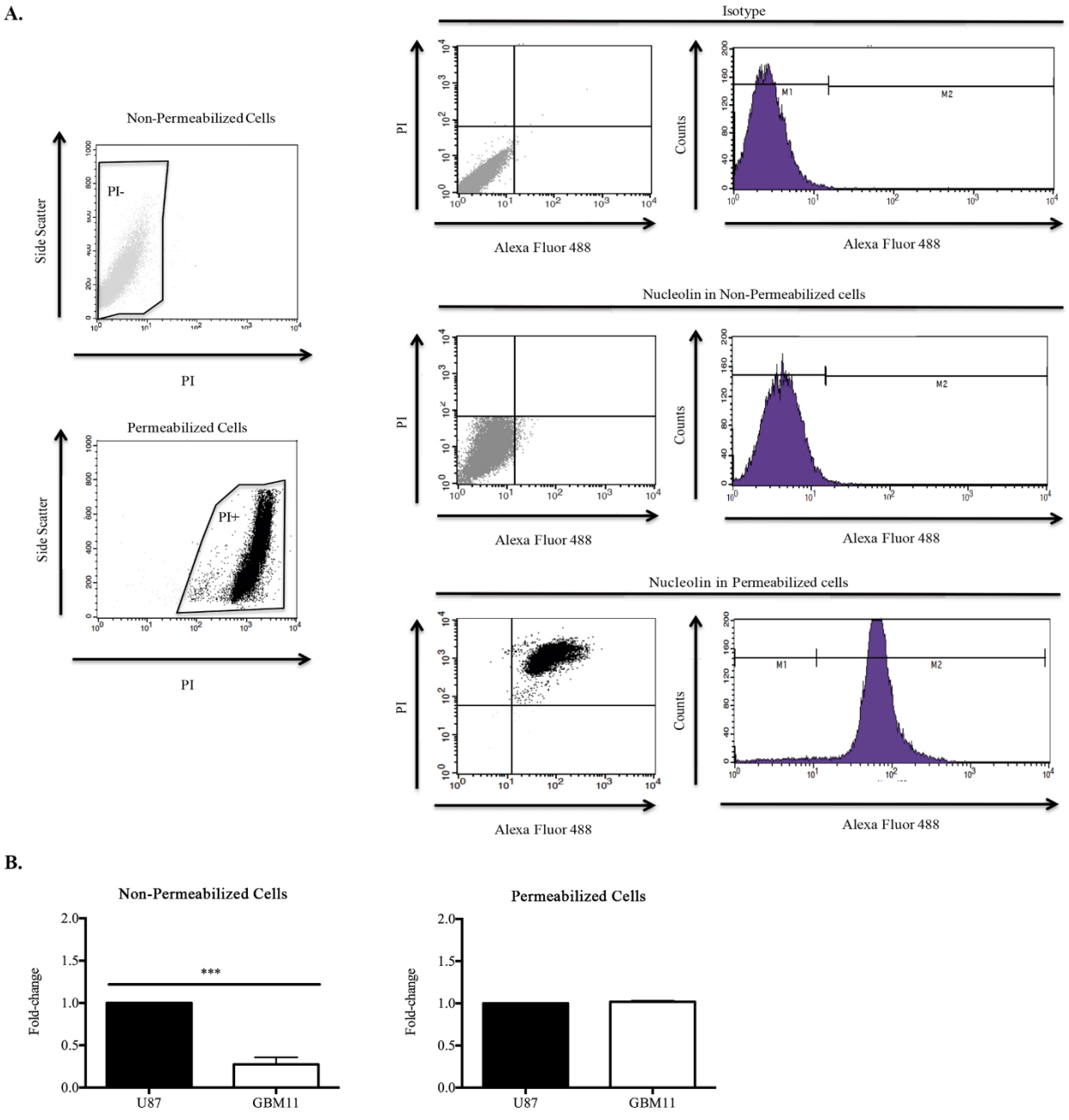

Figure 6.1 Analysis of expression of cell surface nucleolin in GMB cell lines. Nucleolin expression was further assessed by flow cytometry, in propidium iodide–negative (PI-) or –positive (PI+) for non-permeabilized or permeabilized U87 and GBM11 cells, respectively, where M2 region corresponds to nucleolin positive cells, as exemplified in the figure for the former cell line (A). Nucleolin expression levels were normalized to the protein expression of U87 cells (B). All instrumental parameters pertaining to fluorescence detection and images analyses were held constant to allow sample comparison. Data represent the mean ± SEM of three experiments (*t*-student comparison test, *** $p < 0.001$).

Taking advantage of nucleolin overexpression in different cell populations within solid tumors, several targeting strategies have been developed. In the present work, in order to address the question on whether surface nucleolin would enable the access to the intracellular compartment of an agent targeting the referred protein, previously developed sterically stabilized pH-sensitive liposomes, functionalized with the nucleolin-binding 31 amino acid peptide (codenamed F3 peptide), were used. It was previously demonstrated that this targeted system interacts with nucleolin-overexpressing cells in a ligand- (Moura *et al.,* 2012) and cell-specific manner (Gomes-da-Silva *et al.,* 2013a) enabling a significant improvement of activity against nucleolin-overexpressing cells, upon intracellular drug delivery, relative to non-targeted formulations (Fonseca *et al.,* 2014; Gomes-da-Silva *et al.,* 2013a; Moura *et al.,* 2012).

In fact, different levels of nucleolin expression resulted in a 3.4-fold higher association of sterically stabilized pH-sensitive liposomes, functionalized with a nucleolin-binding 31 amino acid peptide (codenamed F3 peptide) (Porkka *et al.,* 2002) into bulk U87 cells, relative to GBM11 cells ($p < 0.01$; Figure 6.2). Within each cell line studied, the extent of association of targeted liposomes by U87 and GBM11 bulk cells was, respectively, 75- and 25-fold higher than the extent of association of non-targeted counterpart (NT) or liposomes targeted by a non-specific peptide (NS). Overall, these results were in accordance with previous studies reporting that the extent of association of the F3 peptide-targeted liposomes is dependent on the levels of nucleolin expression (Fonseca *et al.,* 2015), besides being an interaction that was ligand- and cell-dependent, as demonstrated by the decreased extent of association by (non-neoplastic) fibroblasts *versus* cancer cells (Gomes-da-Silva *et al.,* 2012b).

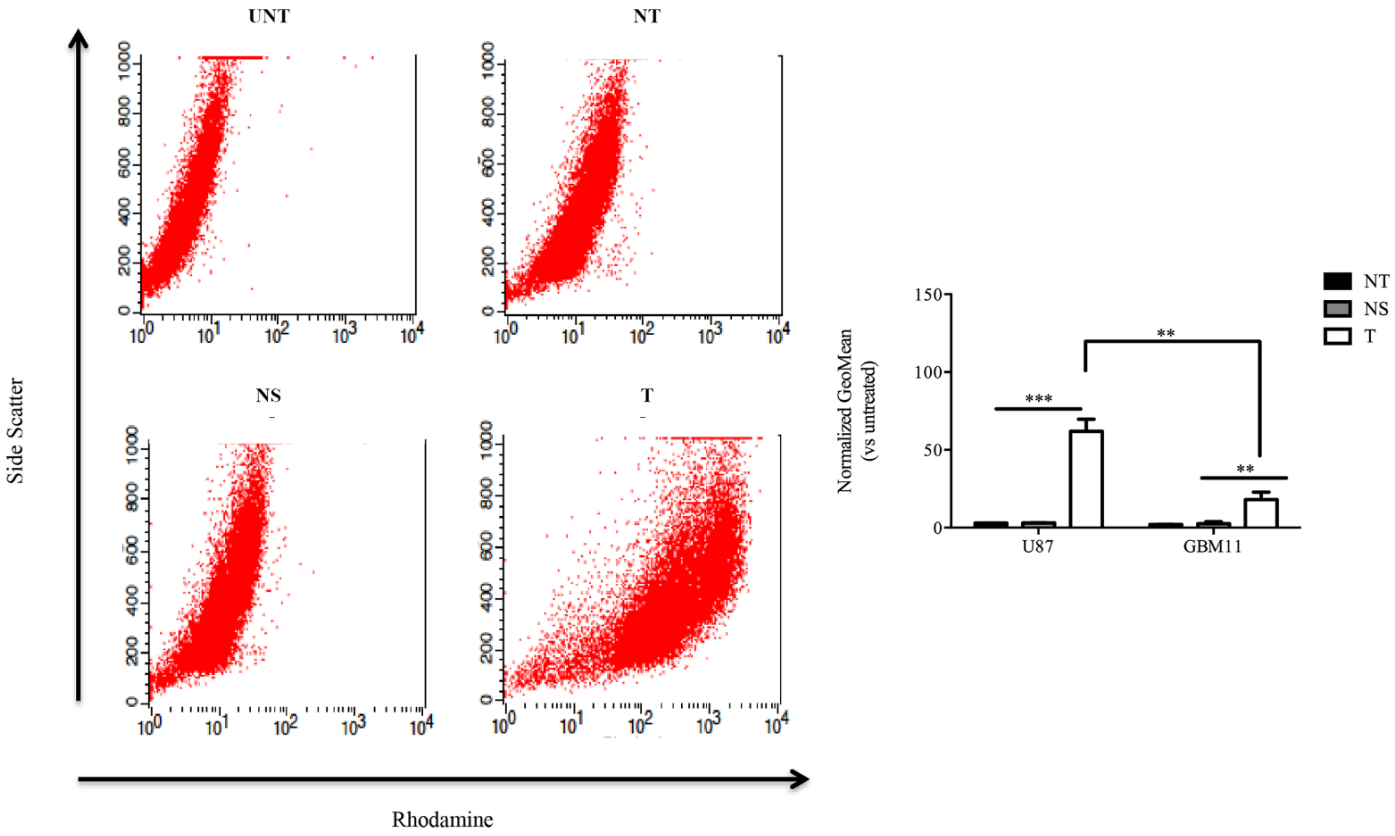

Figure 6.2 Association of rhodamine-labelled liposomes with bulk glioblastoma cell lines. Glioblastoma cell lines (U87 and GBM11) were incubated with rhodamine-labelled liposomes, either targeted by the F3 peptide (T) or a non-specific peptide (NS), or non-targeted (NT), at 0.4 mM of total lipid, for 4 h at 37ºC, and immediately analysed flow cytometry for each tested sample (as exemplified in the figure with the dot plots from the U87 cell line). Results expressed in terms of rhodamine geometric mean fluorescence, were normalized against the respective signal of untreated cells. Data represent mean ± SEM of three independent experiments (two-way ANOVA analysis of variance by Bonferroni's post-test for comparisons between non-targeted and F3 peptide-targeted liposomes; *** $p < 0.0001$ and ** $p < 0.001$).

6.4.2 Association of liposomes functionalized with the nucleolin-binding F3 peptide by glioblastoma stem cells

As previously mentioned, one of the factors that contributes to the aggressiveness of GBM is the presence of a population of glioma stem-like cells (GSCs) that is resistant to radio and chemotherapy, strongly contributing to tumor recurrence (Jackson *et al.*, 2015; Seymour *et al.*, 2015). The expression of several stem cell factors, such as SOX2 (sex determining region Y-box 2), OCT-4A (octamer-binding transcription factor 4), and NANOG (Nanog homeobox) was first assessed in U87 and GBM11 cells. These

transcription factors are stem cell master regulators that may function synergistically to maintain self-renewal and cellular proliferation, contributing to the multilineage potential and heterogeneity of GSCs (Bradshaw *et al.,* 2016; Seymour *et al.,* 2015).

SOX2 is highly expressed in neural stem cells (NSC), and in several tumor types, namely in GBM (Berezovsky *et al.,* 2014). OCT4, namely the OCT-4A, is an octamer motif-binding transcription factor (TF) highly expressed in stem cells, particularly in GSCs (Fang *et al.,* 2011), and is responsible for controlling the transition between pluripotency and differentiation (Radzisheuskaya *et al.,* 2013). NANOG is a homeobox protein that cooperates with SOX2 and OCT4 in the regulation of genes that are also associated with the stemness of GSCs (Seymour *et al.,* 2015).

Specifically, SOX2 was the stem-like cell marker expressed in the highest percentage of the GBM cells studied, in accordance with previous studies (Berezovsky *et al.,* 2014), having GBM11 cells, approximately, twice the percentage of SOX2-positive cells than in U87 cells ($p < 0.01$). In fact, the SOX2-positive cells within GBM11 cells was quite prominent relative to OCT-4A- or NANOG-positive cells ($p < 0.001$), in contrast with the results generated with U87 cells, where no statistical differences were observed among those sub-populations (Figure 6.3A). The assessment of the overall protein content by Western blot revealed that SOX2 was the most expressed stem-like cell marker (Figure 6.3B). These results confirmed the existence of a GSCs population, in agreement with our previous studies (Balça-Silva *et al.,* 2017b), which may justify its association with poor outcome in GBM (Garros-Regulez *et al.,* 2016).

The plasticity associated with CSCs, with the ability to interchange with non-SCCs (Balça-Silva *et al.,* 2017b; Fonseca *et al.,* 2015), poses a major challenge from a therapeutic standpoint. In this respect, the identification of common therapeutic markers between these different sub-populations is highly relevant in the context of glioblastoma. Previous work has demonstrated that nucleolin expression by putative triple-negative breast cancer stem cells and non-stem breast cancer cells was paralleled by OCT4 and NANOG mRNA levels (Fonseca *et al.,* 2015). Moreover, in murine embryonic stem cells, nucleolin mRNA levels and F3 peptide-targeted liposomes association were directly dependent on the stemness *status* (Fonseca *et al.,* 2015). Based on this information, the question on whether liposomes functionalized with the nucleolin-binding F3 peptide associated with both GSC and non-GSC was further addressed.

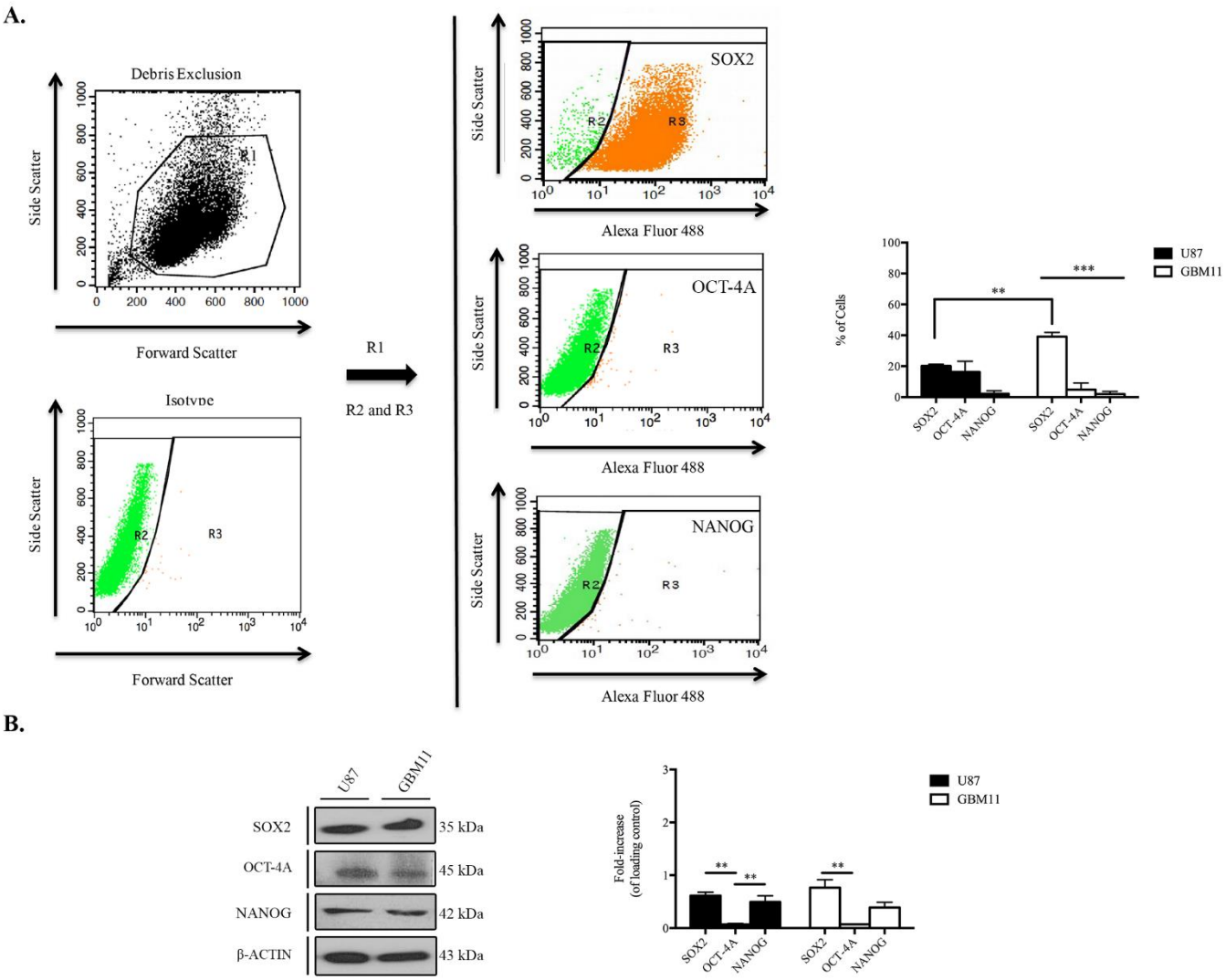

Figure 6.3 Expression of markers in putative cancer stem glioblastoma cells. Percentage of U87 and GBM11 cells positive for SOX2, OCT-4A or NANOG was determined in the R3 region, as exemplified with the dot plots for the former cell line (A). Analysis was further complemented with the determination of total protein content for each stem-like cell marker, relatively to the β-ACTIN expression as the loading control, by western blot (B). Data represent the mean ± SEM from three independent experiments. The student's t-test was used to compare stem-like cells markers between U87 and GBM11 cell lines and two-way ANOVA analysis of variance, with Bonferroni's post-test, was used for comparisons between the stem-like cell markers within each cell line; ** $p < 0.01$; *** $p < 0.001$).

Using rhodamine-labelled liposomes and the gating methodology described in Materials and Methods, association was evaluated in regions R2 and R3, corresponding to non-GSC and GSC, respectively, in both U87 and GBM11 cells (Figure 6.4). Within each

of the cell line studied, F3 peptide-targeted liposomes (T) presented a similar extent of association to non-GSCs and GSC, among each stem cell marker used (Figure 6.4). The only exception was observed with U87 cells, where the extent of association of targeted liposomes to SOX2-overexpressing cells (R3), was 4.3-fold higher than the one to SOX2-negative cells (R2), $p < 0.05$ (Figure 6.4). In fact, SOX2 regulates the expression of key genes and pathways involved in GBM malignancy, and maintains plasticity for bidirectional conversion between the two glioma stem-like and non-stem like cell states, with significant clinical implications (Berezovsky *et al.,* 2014). In tumors of diverse histological origin, high levels of SOX2 have been associated with tumor aggressiveness and worse prognoses, as well as increased plasticity, loss of differentiation markers, and induction of stem cell phenotypes (Berezovsky *et al.,* 2014; Garros-Regulez *et al.,* 2016). Moreover, recent evidences have suggested that nucleolin is associated with malignancy grade in gliomas (Galzio *et al.,* 2012). This could suggest that nucleolin- and SOX2-overexpressing cells could be associated with more aggressive tumor types of GBM. This putative association of expression between nucleolin and SOX2 expression, could support a lower expression of the former in SOX2-negative (U87) cells and thus, the lower extent of association observed of liposomes functionalized with the nucleolin-binding F3 peptide (Figure 6.4).

Important to emphasize that the absolute values of extent of association observed for GSC and non-GSC in GBM11 cells were lower than the ones observed for U87, which is in agreement with the lower expression of nucleolin in the former cells (Figure 6.1). In GSC and non-GSCs, the extent of association of the F3 peptide-targeted liposomes (T) was always significantly higher than that of the non-targeted counterpart (NT), $p < 0.01$ and $p < 0.05$ (Figure 6.4).

These results suggested that nucleolin as a potential therapeutic marker in both OCT4- and NANOG-positive GSC, and in the corresponding non-GSC, as well as in SOX2-positive GSC. Overall, the presented results point nucleolin as a potential therapeutic target to both GSCs and non-GSCs sub-populations, overcoming the difficulties of targeting tumor niche imposed by the plasticity of GBM cells phenotype, namely in the setting of OCT4- and NANOG-positive GSC.

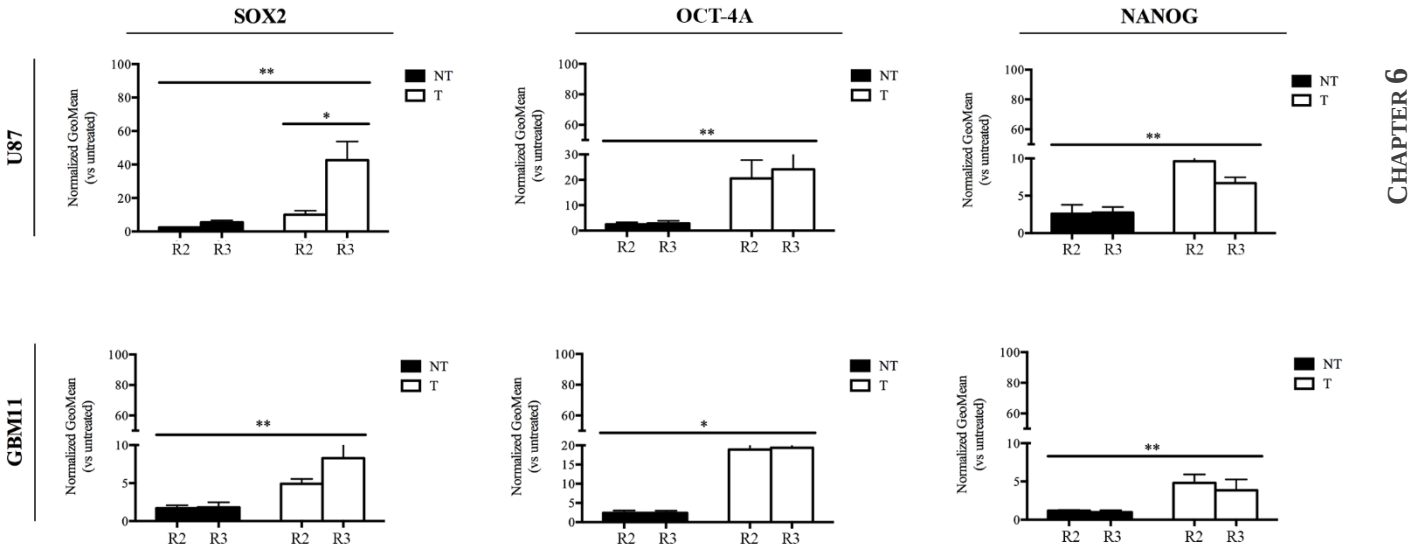

Figure 6.4 Association of several formulations of rhodamine-labelled liposomes with putative cancer stem glioblastoma cells. U87 and GBM11 cells were incubated with rhodamine-labelled liposomes, either targeted by the F3 peptide (T) or non-targeted liposomes (NT), at 0.4 mM of total lipid, for 4 h at 37ºC, and the rhodamine geometric mean fluorescence was determined either in cells enriched in markers of glioblastoma stem-like cells, SOX2, OCT-4A and NANOG, in R3, or in cells negative for the referred markers (gated in R2). Determined values were normalized against the respective signal of the untreated control. Data represent the mean ± SEM from three independent experiments. The student's t-test was applied for comparing R2 and R3 in each formulation, from each stem-like cell marker, and two-way ANOVA analysis of variance, with Bonferroni's post-test, was applied for comparisons between targeted and non-targeted formulations in each stem-like cell marker, in both cell lines (* $p < 0.05$; ** $p < 0.01$).

6.4.3 Cytotoxicity and delivery of liposomal DXR functionalized with the nucleolin-binding F3 peptide

To further reinforce the potential of nucleolin as a path for a therapeutic agent to assess the intracellular compartment of glioblastoma cells, the cytotoxicity of F3 peptide-targeted liposomes containing DXR was assessed in the cell line (U87), which was, among those studied, the one presenting the highest expression of the protein. For 1 h incubation, DXR delivered by liposomes functionalized with the nucleolin-binding F3 peptide enabled a level of cytotoxicity that was 2.5- or 4.6-fold higher than the one enabled by the delivery of the same drug by non-targeted liposomes or liposomes targeted by a non-specific peptide, respectively (Figure 6.5A). Differences of cytotoxicity among those samples were maintained for a 4 h incubation and in the range of 4-fold (Figure 6.5B).

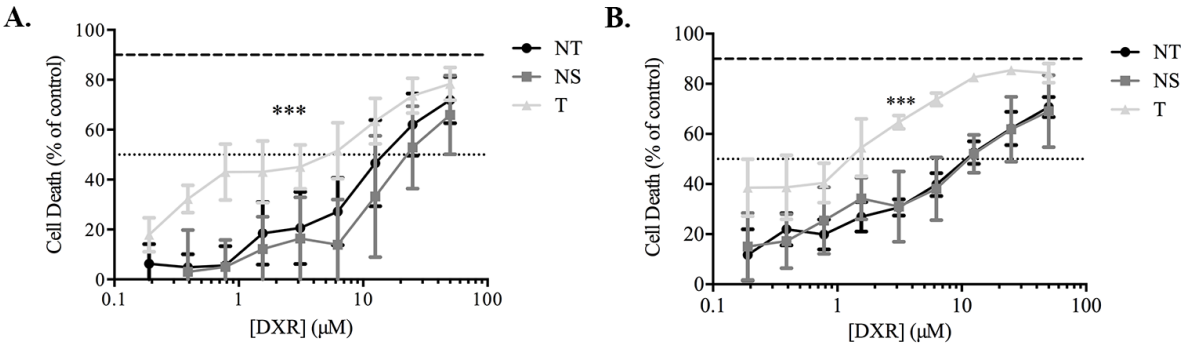

Figure 6.5 Cytotoxicity of different liposomal formulations containing doxorubicin against the U87 glioblastoma cell line. U87 cells were incubated with serially diluted concentrations of different formulations of liposomal doxorubicin (DXR), either non-targeted (NT) or targeted by the F3 peptide (T) or a non-specific peptide (NS), for 1 (A) or 4 h (B) at 37ºC. After the incubation period, cells were maintained in fresh medium during 48 h, after which cell cytotoxicity was assessed by the MTT assay. Dose–response curves represent the mean ± SEM of 3 independent experiments for each concentration tested. The statistical analysis was performed using two-way ANOVA analysis of variance, with Bonferroni's post-test for comparisons between NT, NS and T liposomal formulations in each experience. *** $p < 0.001$.

Based on the previous results, it was then addressed the question on whether this higher extent of cell death enabled by the targeted formulation, would arise from a higher amount of encapsulated drug accessing the intracellular compartment. To address this question, U87 cells, following incubation over 4 h with serially diluted concentrations of the formulations of DXR-containing liposomes previously tested, were washed with cold PBS (Figure 6.6A) or with cold acid buffer (Figure 6.6B). While with the former washing step both intracellular and surface (encapsulated) DXR are assayed, the former removes surface-bound liposomes. Interestingly, at the highest concentrations tested, a maximum of 19 (Figure 6.6B) or 40 (Figure 6.6A) mol DXR/μg protein was achieved upon delivery by liposomes functionalized with the nucleolin-binding F3 peptide. This suggested nucleolin as a path that enables the access to the intracellular compartment of nucleolin-overexpressing glioblastoma cells, of therapeutic agents targeting this protein. This was further supported by the significant difference of DXR accumulation enabled by the targeted liposomes relative to non-targeted or liposomes targeted by a non-specific peptide ($p < 0.0001$ and $p < 0.001$, respectively), with or without removing surface-bound liposomes.

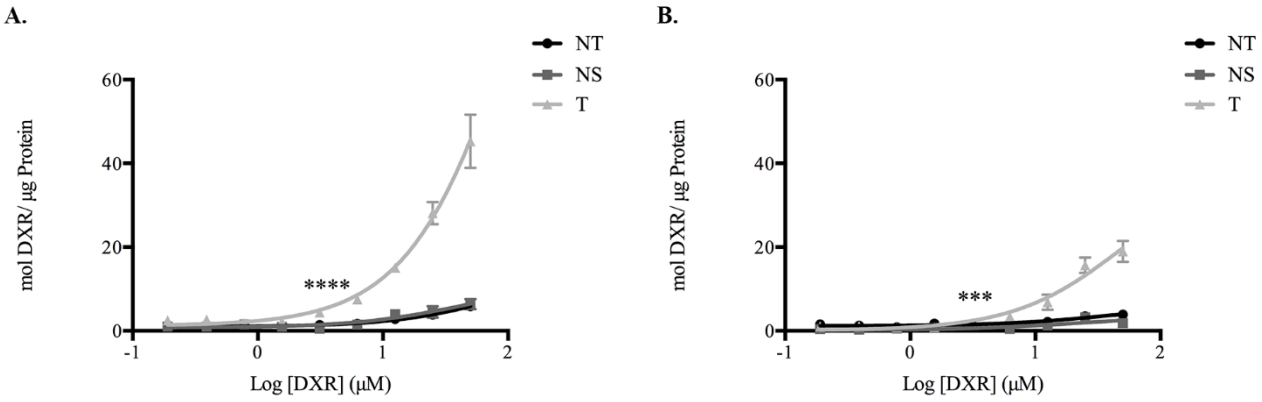

Figure 6.6 Assay of doxorubicin associated with U87 glioblastoma cell line, delivered by several liposomal formulations. U87 cells were incubated with doxorubicin (DXR)-liposomal formulations, either targeted by the F3 peptide (T), non-targeted liposomes (NT), or targeted by a non-specific peptide (NS) for 4 h at 37ºC. Cells were washed with cold PBS (A) or with cold acid buffer (B), and the amount of DXR per µg protein was determined from a calibration curve. Curves represent the mean ± SEM of 3 independent experiments for each concentration tested. The statistical analysis was performed using two-way ANOVA analysis of variance with Bonferroni's post-test for comparisons between NT, NS and T liposomal formulations in each experiment. **** $p < 0.0001$; *** $p < 0.001$.

6.4.4 Nucleolin expression in patient-derived GBM samples

In order to evaluate the clinical potential of nucleolin as a target in GBM, the expression of nucleolin in human GBM samples was compared with human normal brain samples. It was first confirmed by haematoxylin-eosin staining, upon comparison with normal brain, that the selected patient-derived GBM samples presented nuclear atypia, prominent microvasculature proliferation (identified in figure 6.7A with the symbol "*") and necrosis (identified in figure 6.7A with the symbol "+"), which constituted the essential diagnostic features of GBM. Interestingly, patient-derived GBM samples presented a higher expression of nucleolin than normal brain samples (Figure 6.7B), corresponding to more than 60% of cells expressing this protein, while normal brain presented less than 20% (Figure 6.7C). This comes along with the demonstration by other of nucleolin overexpression in GBM brain samples (Galzio *et al.,* 2012; Koutsioumpa *et al.,* 2013; Xu *et al.,* 2012), and related with malignancy grade of gliomas, as previously stated by Galzio *et al.,* (Galzio *et al.,* 2012). Overall, these results complemented the previous ones and suggested nucleolin as a potential target in GBM cells.

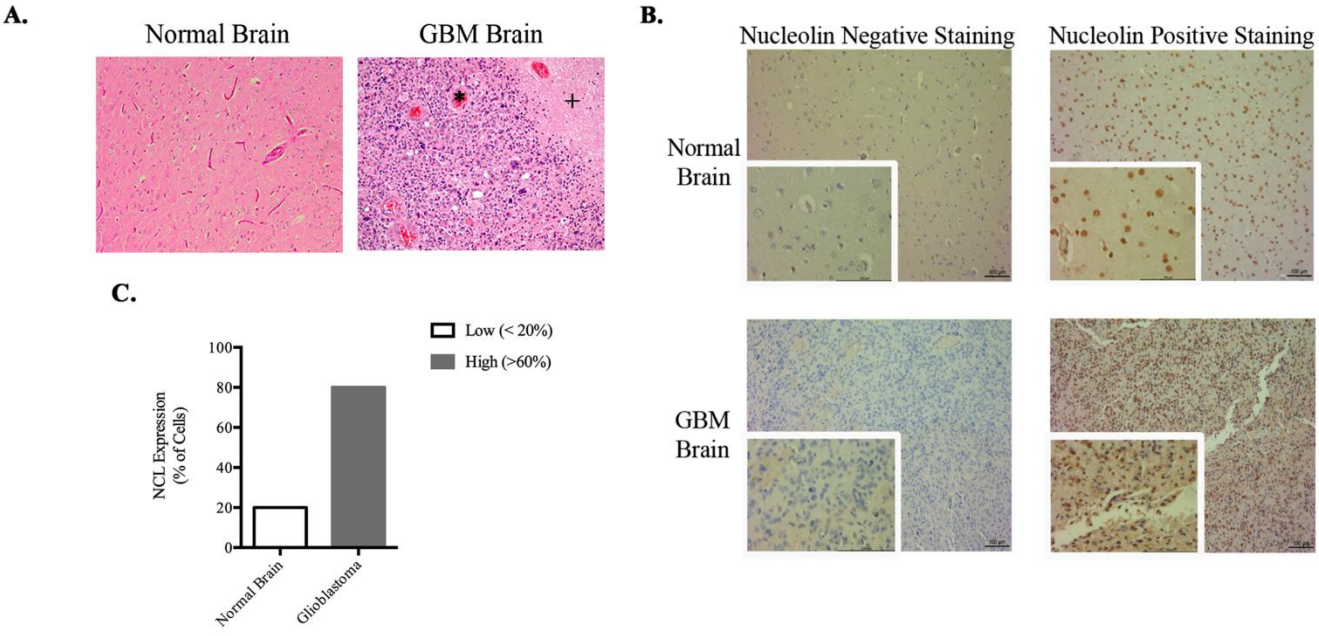

Figure 6.7 Analysis of nucleolin expression in glioblastoma by immunohistochemistry (IHC). Histopathological characteristics of the tumor mass were evaluated by haematoxylin-eosin staining (A). Immunohistochemistry was performed using the DAB method with haematoxylin counterstaining to evaluate the percentage of cells expressing nucleolin (B). Tumor samples were ranked for nucleolin expression as high (60% positive cells), and low (below 20% cells) (n = 6) (C). Each image was acquired at 10 x magnification (x10/ 0.25 PH1 NPLAN) and amplified 40 x (x40/ 0.55 CORR PH2) (Scale bar = 100 µm).

6.5 CONCLUSION

GSCs represent a cell population with stem-like features that are responsible for tumor development, heterogeneity, relapse and drug resistance, and so may constitute a relevant therapeutic target (Rycaj and Tang, 2015; Zong *et al.*, 2015). CSCs and non-SCCs have been demonstrated to be able to interchange by an Epithelial-to-Mesenchymal Transition process (Balça-Silva *et al.*, 2017b; Chaffer *et al.*, 2013; Tam and Weinberg, 2013), thus emphasizing the importance in glioblastoma of identifying common molecular targets among those two cell sub-populations (Fonseca *et al.*, 2015; Visvader and Lindeman, 2012).

Liposomes functionalized with the nucleolin-binding F3 peptide presented similar level of association among OCT4- and NANOG-positive GSC, and the corresponding non-GSC, as well as in SOX2-positive GSC, of both U87 and GBM11 cells. In respect to each stem cell marker assessed, the referred extent of association was higher in the former cell

line relative to the latter, in line with the expression levels of nucleolin assessed in bulk cells. These results suggested nucleolin as a common marker among non-SCC and different sub-populations of GSC. The demonstrated improved cytotoxicity and intracellular delivery of doxorubicin into bulk GBM cells enabled by liposomes functionalized with the nucleolin-binding F3 peptide, suggested nucleolin as functional path towards the cytosolic compartment. These data along with the marked expression of the protein in more than 60% of cells from patient-derived samples, as compared with less than 20% in normal brain, supported nucleolin as a potential therapeutic target in GBM, which deserves to be further explored.

CHAPTER 7

General Discussion & Concluding Remarks

'To me, that's the beauty of science:
to know you will never see everything, but you never stop waiting to;
(...) It's an urge that never dies, a game that never ends.'
Robert Krulwich

Glioblastoma (GBM) is the most common and malignant type of primary brain tumor with a median survival of approximately 15 months under therapy (Huse *et al.,* 2013; Lima *et al.,* 2012; Louis *et al.,* 2016; Stupp *et al.,* 2007, 2005). Temozolomide, an alkylating agent orally administrated, is considered part of the *gold standard* in GBM treatment, although its ability to significantly increase the survival of GBM patients is low. In fact, at least 50% of TMZ treated patients do not respond to TMZ (Lee, 2016). This is due to several factors, such as the overexpression and the methylation status of O^6-methylguanine methyltransferase (*MGMT*) gene, which has, in some cases, a significant increased activity, rendering glioma cells more efficient in repairing TMZ-induced mutations (Jaeckle *et al.,* 1998; Kaina *et al.,* 2007); the deregulation of several molecular signalling pathways, mainly the phosphorylated protein kinase C (PKC), which contributes to increase proliferation, survival and motility of GBM cells (Balça-Silva *et al.,* 2015; Carmo *et al.,* 2011a; do Carmo *et al.,* 2010; Hattermann and Mentlein, 2013; Safa *et al.,* 2015; Stupp *et al.,* 2009; Thirant *et al.,* 2011; Zhou *et al.,* 2012); the existence of a cell subpopulation within the tumor mass known to be chemo and radioresistant and so, responsible for tumor recurrence after therapy, the glioma stem-like cells (GSCs); and also, the inexistence of a recognized specific surface marker, in GSCs and non-GSCs, that could be used in a targeted therapy, in order to establish a more effective delivery of chemotherapeutics with fewer side effects (Wirsching and Weller, 2016).

During the last few years, many studies have been investigating molecular mechanisms underlying GBM's behaviour. Above all, previous studies agree that GBMs are characterized by an increased expression and activity of PKC, when compared with normal astrocytes, which could relate PKC to the tumor proliferative ability (da Rocha *et al.,* 1999; Mochly-Rosen *et al.,* 2012). Tamoxifen (TMX) is a non-steroidal drug mostly used for its anti-estrogen properties against estrogen receptor-positive carcinomas (*i.e.* breast cancer). It has been demonstrated that TMX carries out its action on several pathways, not only acting as an inhibitor of estrogen receptor, but also constitutes an active inhibitor of the phosphorylated protein kinase C (p-PKC). However, there is no consensus regarding the PKC contribution to the aggressiveness of glioma cells (Carmo *et al.,* 2013; Cho *et al.,* 1999; da Rocha *et al.,* 1999; O'Brian *et al.,* 1986), which makes the investigation of this molecular signalling pathway an important point to be elucidate in GBM.

Although some of the signalling mechanisms that are altered in GBM begin to be identified, this type of tumor is characterized by a great cellular heterogeneity, which makes the entire knowledge of the GBM molecular signalling mechanisms still on investigation. In fact, GBM mass is constituted by reactive astrocytes, microglial cells, endothelial cells and tumor stem-like cells. This tumor stem-like cells, also known by glioma stem-like cells (GSCs), constitute one of the major reasons for GBM recurrence after therapy. However, none of the standard chemotherapy protocols is based on directly targeting GSCs. The most important reason to justify the lack of chemotherapeutic approaches for GSCs is precisely the poor knowledge about the factors that influence the stem-like cell state and its plasticity (Safa *et al.,* 2015; Visvader and Lindeman, 2012). For an effective therapy, it is necessary to know and recognize the properties of the stem state and what characterizes them. In this way, it would be possible to associate potential therapeutic targets with strategies of identification of this cellular group, in particular the cells that would predict molecular behaviours taking into account the tumor environment.

The identification of molecular markers overexpressed on the surface of tumor cells and tumor stem-like cells, namely GSCs, gave rise to the development of different therapeutic strategies, like liposomes, designed to specifically target those cells avoiding healthy ones (Fonseca *et al.,* 2015).

In this way, the ultimate goal proposed in our initial project was to clarify the multiple factors that contribute to the malignancy of GBM and, consequently, the failure of the current standard therapy, by the identification of potential therapeutic targets. In order to achieve this goal, we analysed three different perspectives: 1 - the potential of the combined therapy using temozolomide and tamoxifen (TMX), a PKC inhibitor, to inhibit the GBM proliferation capability. We proposed an alternative or adjuvant chemotherapy through the synergistic effect on cell proliferation by the inhibition of p-PKC in different GBM cell lines (Chapter 3 and 4); 2 – understand glioma stem-like cell (GSC) plasticity and identify some of the most important markers that can translate this plasticity (Chapter 5); and 3 - study the potential of a specific target approach to GBM and GSCs (Chapter 6).

In order to address the potential of the combined therapy, TMX and TMZ, on GBM, we incubated different GBM cell lines with doses under the IC50 for each drug alone and we evaluated the cell death, migration capability and proliferation inhibition by p-PKC inhibition activity (Chapter 3).

In fact, TMX is one of the PKC inhibitors used in *in vitro* studies with glioma cells and also in clinical trials with GBM patients. The *in vitro* effect of TMX was not completely elucidated and the results of the *in vivo* studies were disappointing, since treatment of patients with recurrent malignant glioma with low doses of TMX did not significantly increase the survival rate (da Rocha *et al.,* 1999; Puchner and Giese, 2000). However, clinical trials using high doses of TMX alone or in combination with other cytotoxic agents have yielded better results (Borowski *et al.,* 2005; Hui *et al.,* 2004; Kamburoğlu *et al.,* 2007; O'Brian *et al.,* 1985; Pollack *et al.,* 1990; Zhang *et al.,* 2000). Since 1) the expression of PKC in glioma cells is increased; 2) the effect of TMX in glioma cells is not yet fully understood, but it appears to be a non-selective PKC inhibitor and is associated with an increased toxicity when used in such conditions (Mochly-Rosen *et al.,* 2012), and 3) no standardized protocol for the use of tamoxifen in the treatment of high-grade gliomas is available (DI Cristofori *et al.,* 2013), we evaluated the effect of the combination of low doses of TMX with TMZ on the proliferation, survival and migration of two different GBM cell lines (Chapter 3).

In fact, the dose of TMX used in the treatment of breast cancer is in the range 20-40 mg/day. It has been shown that TMX inhibits p-PKC in a dose dependent manner and researchers have been trying to use it to treat brain tumors taking advantage of this property when used in higher doses compared to those used in breast cancer (Chang *et al.,* 2004). William Couldwell administered, for the first time, TMX in anti-estrogen doses (40mg/day) to monitor possible side effects, in a cohort of malignant glioma patients, and noticed that it provided no adverse reactions when dosage was increased to 160mg (female) and 200mg/day (male) (Couldwell *et al.,* 1994). Accordingly, one decade later, another study demonstrated that a subgroup of patients responded to the treatment, or stabilized, with high-dose of TMX administration (Chang *et al.,* 2004).

In turn, our results showed that the combination of TMX and TMZ reduces the amount of the phosphorylated PKC-pan in different GBM cell lines, the U87 and U118, and contributes to the reduction of the aggressive behaviour of the glioma cells, mainly through a reduction of the proliferation and migration capability (Chapter 3). Herein, we could point PKC as an important target to GBM regarding the synergistic response of the combined therapy TMX plus TMZ.

Since our group is focus on studying the combination of new drugs with TMZ, and clarify their effects in GBM cells, the potential of other drugs, mainly Shikonin (SHK), in combination with TMZ, to overcome GBM malignancy was previously studied by us

(Matias *et al.,* 2017). SHK, a naphthoquinone, that has anti-tumor and lipophilic properties, has been used in cancer research including GBM. When combined with TMZ, decreases cell viability in GBM cell lines, namely U118 and GBM02, compared to the effect of each drug in monotherapy (Matias *et al.,* 2017). Accordingly with our previous studies with TMX and TMZ in combination, we also showed that GBM cells proliferation was decreased which was accompanied by the reduction of migration capability and a disorganization of the F-actin filaments and microtubules necessary to cell motility. SHK and TMZ co-treatment suppressed the expression of Glial to mesenchymal-like phenotype (GMT) proteins, such as vimentin and Slug, which was accompanied by a reduction in the phosphorylation of AKT at Ser473, a member of a signalling pathway that is extremely important for the activation of invasion, migration and chemoresistance of tumor cells (Matias *et al.,* 2017). In agreement with our present studies regarding the combination of TMX and TMZ, this combination of SHK and TMZ highlighted the importance of the combined therapies in GBM treatment.

However, it is also well stated that one of the most particular characteristics of GBM is its heterogeneity, which turns out to be one of the major challenges to overcome tumor resistance. In fact, the standard of care approach is generally uniform and does not take into account different molecular signatures of GBM.

Moreover, recurrent GBMs are extremely difficult to treat because they acquire resistance through mechanisms of selection of cells that are able to bypass the effects of chemotherapies, especially cancer stem-like cells (CSCs) (Jackson *et al.,* 2015).

In this sense, we next studied the potential success of TMX plus TMZ in a GBM cell line, established and characterized by us in laboratory, the GBM11, that was previously isolated from a recurrent GBM patient treated with TMZ and radiotherapy, accordingly to the standard protocol established by Stupp and colleagues (Stupp *et al.,* 2005) (Chapter 4).

Our results have demonstrated that TMX in monotherapy can be useful on a recurrent GBM cell line resistant to TMZ, with no need of re-administration of TMZ on a second-line treatment. Indeed, the combinatorial administration of TMX and TMZ appeared to be well-tolerated and potentially effective in increasing the efficacy in some studies, but also still in Phase II clinical trials, due to the contradictory results (He *et al.*, 2015). In our studies, TMX has shown to be efficient to eliminate around 50% of tumor cells *in vitro*, with no need of TMZ concomitant administration and, consequently, reducing the amount of chemotherapeutics given to patients. For the first time, we were able to

highlight the importance of cellular heterogeneity in the response to therapeutics. Probably due to the higher resistance of this new GBM cell line, the combination of TMX and TMZ had not a synergistic effect, as observed in U87 and U118 cell lines. Accordingly, the GBM11 cell line presented a higher IC50 of TMX, higher reduction of cell proliferation, probably due to the reduction of p-PKC expression, a reduction of cell migration capability, a higher expression of PGP and stem-like cell markers compared to U87 and U118 cell lines previously described.

As so, our results obtained with combined or monotherapy exert the same effect in recurrent GBM, which could suggest that TMX alone could be an alternative chemotherapeutic approach for recurrent GBM. Besides TMX can actually be very important on p-PKC regulation, and consequently, interfere with proliferation, survival and migration of glioma cells, the contribution of chemotherapeutic drugs depends on the GBM cells characteristics. Those factors together with the resistance acquired by previous TMZ treatment may be behind the different response to therapeutics between individuals.

Regarding GBM cell's mechanisms of resistance, in fact, P-glycoprotein (PGP) is known to be low expressed in GBM cells compared with other tumors. However, there are some studies that still point that the GBM chemotherapeutic resistance can occur by PGP expression, which is a ATP-dependent drug efflux pump. Studies have proposed an induction of TMZ resistance by increased transcription of *MDR1*, the gene encoding PGP, clarifying how PGP and TMZ interact to gain resistance and, consequently, how increased PGP expression leads to TMZ resistance (Munoz *et al.,* 2015). On the other hand, some studies in literature mentioned the localized expression of MRP1 (encoded by the *ABCC1* gene) within GBM tumor specimens themselves in addition to the tumor vasculature (Calatozzolo *et al.,* 2005). These authors highlighted the role of MRP1 inhibition in improving chemotherapy drug response in both primary and recurrent GBM patient-biopsy derived cell lines, suggesting an intrinsic chemoresistance mediated by MRP1 expression in GBM tumor cells, independent of the BBB endothelial transport system.

Also, TMX is known to inhibit drug transport since it interacts with PGP inhibiting PGP-dependent drug transport (Callaghan and Higgins, 1995). In this way, due to the higher expression of PGP in GBM11 cells, the concentration of TMX needed to cause an effect would be expected to be higher compared to U87 and U118 cell lines, which is also in accordance with our results. Although PGP expression may be relatively small, the chemoresistance shown in the GBM11 cell line relative to the U87 and U118 cells may

also be due to the higher SOX2 expression when compared to U87 and U118 cell lines, corroborating our main conclusions.

Taking altogether, our results in chapter 3 and 4 emphasize that PKC may play a relevant role in the proliferation, survival and migration of glioma cells. However, its contribution is dependent on the characteristics of the glioma cells, which emphasizes the need to establish a personalized therapy, considering PKC as a therapeutic target. Also, our results emphasized the importance of the combined therapy in the treatment of GBM.

Regarding the results included in chapter 3 and 4, we conclude that glioblastoma present subtle differences in response to treatment dependent on the heterogeneity of GBM cells. Also, the use of TMX alone can achieve therapeutic success by inhibiting proliferation, namely through p-PKC reduction. Since standard of care approach in GBM is generally uniform and does not take into account different molecular signatures, we consider this information a truly important step forward to the previous studies already published in literature.

Even the treatment with TMX plus TMZ or TMX alone contribute to the inhibition of the proliferative capability of some GBM cell lines, the truth is that GSCs are still considered the most chemoresistant cells in the GBM tumor mass and consequently responsible for tumor recurrence after therapy. This means that, even if the proliferative capability of GBM cells would be affected with TMX and TMZ treatment, it would not probably be enough to prevent recurrence. The molecular biology of GSCs is still poorly understood and new therapy approaches to achieve GSCs are far from emerging. In this way, it seems of utmost importance the understanding of stem-like cell properties, which raises the question: it is well known that GSCs can lose their stem-like properties, giving rise to non-GSCs, but is the reverse true?

Previous studies revealed that GSCs may emerge from the increased self-renewing division of GSCs or from reprogramming of non-GSCs to GSCs, suggesting a plasticity of the stem state in GBM (Safa *et al.,* 2015). Based on these observations, we considered that the understanding of the plasticity of GBM stem-like state is crucial to the identification of the mechanisms and factors involved in GSCs resistance to therapy, which may be in the base of tumor recurrence, constituting a step forward to the identification of therapeutic targets in GBM. In this sense, we next studied the plasticity of the maintenance of GSC stem-like properties as a dynamic behaviour, implying that both GSCs and non-GSCs are

capable of switching between both states (Chapter 5). We hypothesized that GSC interactions with the surrounding microenvironment could determine GBM heterogeneity and dictate the balance between self-renewal and differentiation properties. Regarding this, the identification of stem-like cell markers directly related with stem state plasticity are crucial to identify new molecular therapies for addressing specifically GSCs.

The key characteristics of GSCs are closely associated with the expression of pluripotency genes, namely the sex-determining region Y-Box (SOX2) (Gangemi *et al.*, 2009). In parallel, a growing body of evidence also indicates that intercellular communication through gap junctions (ICGJ) could contribute to the coordination of mechanisms involved in cell differentiation (Soares *et al.*, 2015; Todorova *et al.*, 2008). These gap junctions, formed by proteins of the connexin (Cx) family, may have tumor-suppressor or oncogenic functions. Specifically, connexin 43 (Cx43) and connexin 46 (Cx46) expression varies according to the differentiation spectrum of GBM cells. Hitomi and colleagues suggested that Cx expression could be essential for transitions between stem-like and non-stem-like states (Hitomi *et al.*, 2015; Safa *et al.*, 2015). However, the plasticity of pluripotent genes and connexin proteins was not explored and clarified so far.

We then studied the stem-like cell markers expression as well as the cell-cell communication proteins and their influence in the plasticity of glioma stem-like cells in GBM cell lines isolated by us in laboratory, namely the previous used U87 and GBM11 cell lines plus GBM02 and OB1 cell lines also established in our laboratory (Chapter 5).

Overall, our results showed that: 1) among all GBM cell lines, the GBM11 together with the GBM02 cells present the higher stem-like phenotype, which is in accordance with the previous chapter characterizing GBM11 as a recurrent GBM cell line, with a more resistant behaviour; 2) in all studied GBM cell lines, the non-GSCs obtained from culturing in DMEM/F12 serum-supplemented medium (GBM02), expressed less SOX2 and Cx46 compared to GSCs (GBM02-SF) and the reverse in OB1-SF cell line, culturing in NS34 serum-free medium, was also observed; 3) Cx43 was overexpressed in non-GSC cell lines, whereas SOX2, an essential transcription factor for the maintenance of embryonic stem cells (ESCs), and Cx46, were upregulated in GSCs, which defends that GSC maintenance also depends on cell-cell interactions in a connexin-isotype-dependent manner, as proposed in the study of Hitomi *et al.* (Hitomi *et al.*, 2015).

Our results showed that the same cells placed in culture media with different properties, sequentially alter their expression of stem-like cell markers together with the phenotype modifications, by oncospheres formation, and also according to the mRNA

expressions, which could lead us to hypothesize that the expression of these stem-like cell markers could be associated with the malignancy of GBM cells.

Together, we observed that SOX2 and Cx46, overexpressed in our GSCs *in vitro*, are also overexpressed in high grade gliomas compared to lower grades and to normal human brain samples. These conclusions suggest that the switch between stem-like and non-stem-like states in GBM accompanies the variation on the expression of these markers, suggesting that the stem-like state is a dynamic bidirectional fluctuation. Moreover, it justifies the high expression of stem-like cell markers in human GBM samples compared to lower grades of gliomas, and is in agreement with the poor prognosis of GBM patients, and so depends on tumor microenvironment.

In fact, WNT signalling has been associated with maintenance of stemness and plasticity of GBM (Binda *et al.,* 2017; Hu *et al.,* 2016). However, the WNT role in tumor microenvironment interactions is still misunderstood. In a parallel study, we have been demonstrated that GBM cells stimulate the activation of WNT/β-catenin signalling in microglial cells by releasing WNT3a. We observed the translocations of β-catenin from cytosol to nuclei and also the induction of expression of WNT target genes, such as Cyclin D1, slug and WNT3a. These findings suggest that WNT3a plays an important role in GBM-microglia-crosstalk and consequently contribute to invasiveness and aggressiveness of GBM cells, highlighting the role of the tumor microenvironment to the tumor malignancy (data not shown).

Ultimately, the present work aimed to understand the GSCs and non-GSCs state, which is the primary step in the comprehension of tumor growth and differentiation processes. Our results suggest that the success of GBM therapy could be related to the identification of more specific targets to reach GBM cells, both GSCs and non-GSCs, which leads us to our final goal.

The previous acknowledgment that CSCs may originate from non-stem cancer cells (non-SCCs) has turned these cell sub-populations into two relevant therapeutic targets. Therefore, to specifically tackle the disease at its roots, we finally intended to find suitable molecular targets that enable simultaneous targeting of both GSC and non-GSC, providing the necessary accessibility to the GSC niche (Chapter 6).

Previous results showed that Nucleolin (NCL) is overexpressed in tumors cells, such as breast cancer cells, compared to normal ones (Christian *et al.,* 2003; Fonseca *et al.,* 2015; Li *et al.,* 2014; Yang *et al.,* 2012). Also, NCL expression was previously

described to be essential for mantainence of embryonic stem cell homeostasis as well as self-renewal, which makes it a potential therapeutic target for both CSCs and non-SCCs (Fonseca *et al.,* 2015; Li *et al.,* 2014; Shi *et al.,* 2007).

Additionally, taking advantage of the NCL overexpression in CSCs and non-CSCs, Moura *et al.,* designed a F3 peptide-targeted sterically stabilized pH-sensitive liposome (SLpH) that upon targeted, the nucleolin receptor was specifically internalized (Fonseca *et al.,* 2015, 2014; Moura *et al.,* 2012). These liposomes were loaded with doxorubicin (DXR), a topoisomerase II inhibitor targeting multiple molecular pathways and that presents a wide range of cytotoxic effects, leading to cell death in a variety of tumors, including GBM (Tacar *et al.,* 2013; Zhao *et al.,* 2016).

Therefore, as a final goal of our work, we assessed the potential of NCL as a target in both non-GSCs and GSCs sub-populations in the U87 and GBM11 cell lines (Chapter 6).

Overall, our results demonstrated the potential of nucleolin as a target within GBM cells, with stem-like and non-stem like phenotypic characteristics, enabling improved cell cytotoxicity, as the result of an active access of a chemotherapeutic drug to the intracellular compartment of GBM cells. This delivery was possible through the previous mentioned liposomes, targeting nucleolin.

Notwithstanding the different responses of U87 and GBM11 cell lines to the liposome target approach, we were able to prove the ability of F3-targeted liposomes, functionalizing with the nucleolin-binding F3 peptide, to target both non-GSCs as well as GSCs. These results suggested nucleolin as a common marker among non-GSCs and different sub-populations of GSC. These findings along with the marked expression of the protein in more than 60% of cells from patient-derived samples, as compared with less than 20% in normal brain, supported nucleolin as a potential therapeutic target in GBM.

Altogether, on the one hand we have been able to propose a therapeutic approach based on a combination of drugs, TMZ plus TMX, that culminate in an inhibition of cell proliferation and migration capability, which are crucial for GBM malignancy, taking into account the heterogeneity characteristic of this type of tumor. In either case, being given orally, these drugs may target malignant cells or healthy ones, which renders the therapy unspecific, and therefore conducive to the known side effects of chemotherapy. On the other hand, we know that this tumor heterogeneity is also due to the existence of stem cells, which are the main cause of tumor chemoresistance and recurrence. Thus, the identification

of markers capable of discerning the stem state could help to delineate a more effective therapeutic approach to these cells, mainly by associating specific markers, such as SOX2 or Cx46, to the stem state. Finally, taking the previous knowledge into account, we could associate a specific therapeutic target not only to tumor cells without stem-like cell phenotypic characteristics but also to stem-like cells. For this, through Nucleolin targeting, overexpressed in glioblastoma, it was possible to present a therapeutic goal that would identify the two sub-populations of cells, GSCs and non-GSCs. In spite of the success of nucleolin overexpression as a potential target in U87 cells, enabling improved cell cytotoxicity, what is certain is that not all cells respond in the same way, like GBM11, a recurrent GBM cell line with a more resistant phenotype and behavior compared to U87 cells. In this sense, the therapeutic approach through drugs, such as tamoxifen, would probably still be the best hypothesis. Overall, the therapeutic response varies in parallel with tumor heterogeneity, although it is possible to associate the expression of certain markers to this response, similar to what can happen with potential prognostic markers. We next illustrated the different hypothesis of GBM therapy that were discussed along this work (Figure 7.1).

Overall, our findings along this dissertation contribute to a better understanding of the molecular basis of glioblastomas, since it allows the identification of chemoresistant mechanisms and potential therapeutic targets, as well as the prediction of disease outcome. We intended to better understand the biology of glioblastoma, through the crosstalk between the deregulated molecular signalling pathways in GBM cells, the plasticity of a glioma stem-like cell population as well as the potential of a specific target approach on the development and progression of glioblastomas.

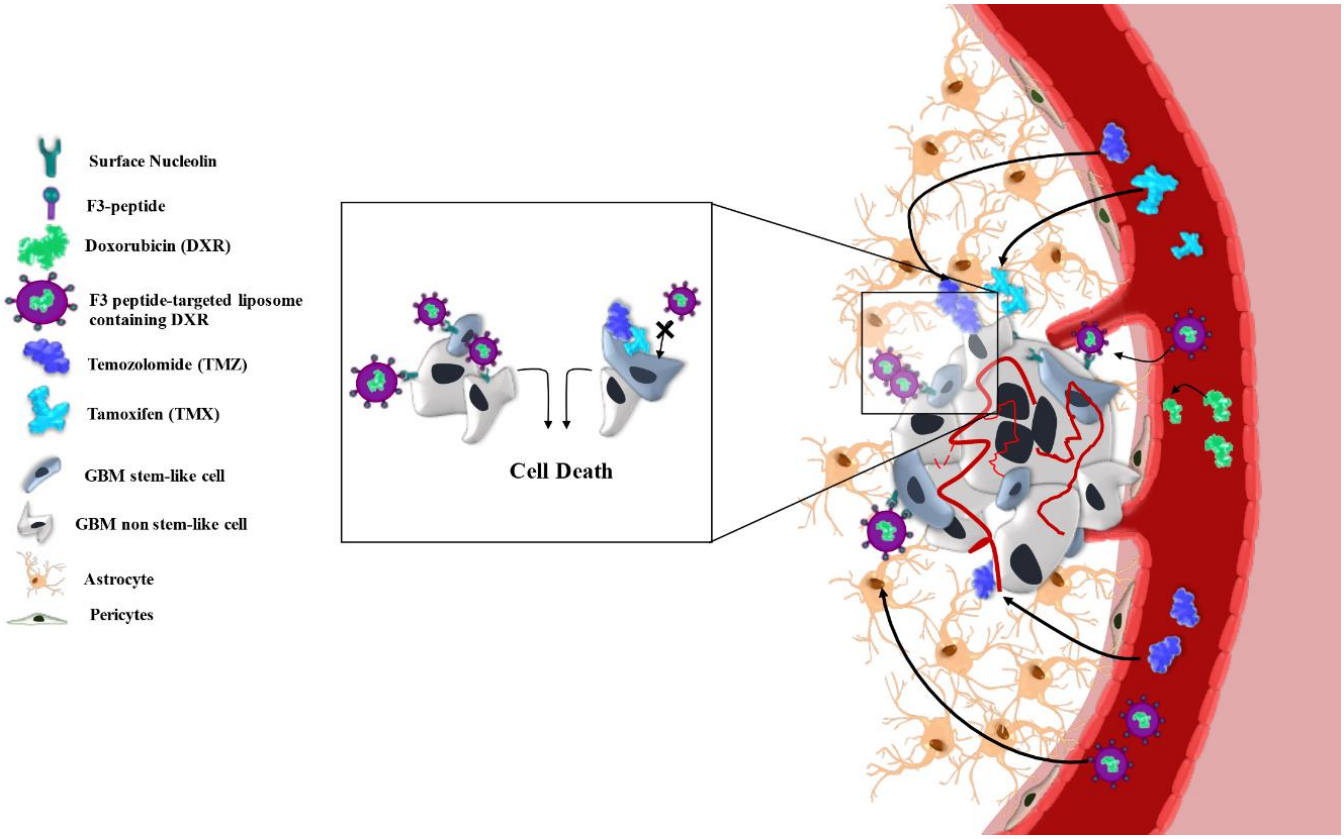

Figure 7.1. Representative illustration of the different molecular therapeutic approaches in GBM. Here we illustrate the different potential therapeutic approaches for GBM addressed in this dissertation. On one way, tamoxifen (TMX), an inhibitor of p-PKC expression, alone or in association with the *gold-standard* temozolomide (TMZ), induced cell death in GBM cells. On the other hand, the F3-targeted liposome strategy, which constitutes a direct tumor-specific approach that depends on the GBM cells expression of specific surface receptors, like nucleolin, also leading to cell death. The multiple targeting through important signalling pathways inhibitors, like TMX, in combination with TMZ, or through cell surface markers overexpression, as nucleolin, as a target for GSCs and non-GSCs, constitute potential options for chemotherapy regarding the heterogeneity among GBM cells.

In summary, the major conclusions obtained from the research work included in this thesis were:

- One of the major reasons of GBM resistance is the deregulation of several molecular signalling pathways involved in cell death, cell proliferation and migration ability, mainly PKC activity. TMX, a PKC inhibitor, combined with TMZ have a synergistic effect in cell proliferation inhibition, in GBM cell lines (Chapter 3);
- Treatment with TMX alone treatment may have an equivalent action as the combination of TMX and TMZ in a GBM cell line of a recurrent GBM resistant to

TMZ, with no need of re-administration of TMZ on a second-line treatment, which highlights the heterogeneity among GBM cells, similar to GBM in human patients, and suggests the need of a more individualized therapy (Chapter 4).

- GSCs, the most chemoresistant population of cells in the tumor mass, are associated with the coordination of mechanisms involved in cell differentiation. The higher expression of Cx46 and SOX2 reflects the plasticity of glioma stem-like cells, which means that GSC interactions with the surrounding microenvironment can determine GBM heterogeneity and dictate the balance between self-renewal and differentiation properties, leading to the understanding of tumor growth and differentiation processes, and hopefully contributing to identify more specific targets to reach GBM (Chapter 5).
- Nucleolin is generally overexpressed in GBM brain samples compared to normal tissues and, through a previously characterized liposome strategy, we could point nucleolin as a potential therapeutic target either for non-GSCs as for GSCs (Chapter 6).

To conclude, the present study reflects the complexity of glioblastomas and emphasizes a possible link between different chemoresistant mechanisms that make GBM the most malignant tumor of the centre nervous system. Besides the relevance in the development and progression of these neoplasms, our study could make a step forward to the identification of new diagnostic or prognostic biomarkers, and new potential therapeutic targets.

CHAPTER 7

CHAPTER 8

References

Abbas, T., Dutta, A., 2009. p21 in cancer: intricate networks and multiple activities. Nature reviews. Cancer 9, 400–14. doi:10.1038/nrc2657

Abbott, N.J., 2013. Blood–brain barrier structure and function and the challenges for CNS drug delivery. Journal of Inherited Metabolic Disease 36, 437–449. doi:10.1007/s10545-013-9608-0

Abedalthagafi, M., Phillips, J.J., Kim, G.E., Mueller, S., Haas-Kogen, D.A., Marshall, R.E., Croul, S.E., Santi, M.R., Cheng, J., Zhou, S., Sullivan, L.M., Martinez-Lage, M., Judkins, A.R., Perry, A., 2013. The alternative lengthening of telomere phenotype is significantly associated with loss of ATRX expression in high-grade pediatric and adult astrocytomas: a multi-institutional study of 214 astrocytomas. Modern pathology : an official journal of the United States and Canadian Academy of Pathology, Inc 26, 1425–32. doi:10.1038/modpathol.2013.90

Abou-Antoun, T.J., Hale, J.S., Lathia, J.D., Dombrowski, S.M., 2017. Brain Cancer Stem Cells in Adults and Children: Cell Biology and Therapeutic Implications. Neurotherapeutics 14, 372–384. doi:10.1007/s13311-017-0524-0

Aeder, S.E., Martin, P.M., Soh, J.-W., Hussaini, I.M., 2004. PKC-η mediates glioblastoma cell proliferation through the Akt and mTOR signaling pathways. Oncogene 23, 9062–9069. doi:10.1038/sj.onc.1208093

Agarwala, S.S., Kirkwood, J.M., 2000. Temozolomide, a novel alkylating agent with activity in the central nervous system, may improve the treatment of advanced metastatic melanoma. The oncologist 5, 144–51.

Agrawal, A., 2009. Butterfly glioma of the corpus callosum. Journal of cancer research and therapeutics 5, 43–5.

Akhavan, D., Cloughesy, T.F., Mischel, P.S., 2010. mTOR signaling in glioblastoma: lessons learned from bench to bedside. Neuro-Oncology 12, 882–889. doi:10.1093/neuonc/noq052

Allard, E., Passirani, C., Benoit, J.-P., 2009. Convection-enhanced delivery of nanocarriers for the treatment of brain tumors. Biomaterials 30, 2302–18. doi:10.1016/j.biomaterials.2009.01.003

Allen, T.M., Sapra, P., Moase, E., Moreira, J., Iden, D., 2002. Adventures in targeting. Journal of liposome research 12, 5–12. doi:10.1081/LPR-120004771

Almutairi, M.M.A., Gong, C., Xu, Y.G., Chang, Y., Shi, H., 2016. Factors controlling permeability of the blood–brain barrier. Cellular and Molecular Life Sciences 73, 57–77. doi:10.1007/s00018-015-2050-8

Altaner, C., Altanerova, V., 2012. Stem cell based glioblastoma gene therapy. Neoplasma 59, 756–60. doi:10.4149/neo_2012_95

Alves, T.R., Lima, F.R.S., Kahn, S.A., Lobo, D., Dubois, L.G.F., Soletti, R., Borges, H., Neto, V.M., 2011. Glioblastoma cells: a heterogeneous and fatal tumor interacting with the parenchyma. Life sciences 89, 532–9. doi:10.1016/j.lfs.2011.04.022

Alyautdin, R., Khalin, I., Nafeeza, M.I., Haron, M.H., Kuznetsov, D., 2014. Nanoscale drug delivery systems and the blood-brain barrier. International journal of nanomedicine 9, 795–811. doi:10.2147/IJN.S52236

Ambegia, E., Ansell, S., Cullis, P., Heyes, J., Palmer, L., MacLachlan, I., 2005. Stabilized plasmid-lipid particles containing PEG-diacylglycerols exhibit extended circulation lifetimes and tumor selective gene expression. Biochimica et biophysica acta 1669, 155–63. doi:10.1016/j.bbamem.2005.02.001

Arko, L., Katsyv, I., Park, G.E., Luan, W.P., Park, J.K., 2010. Experimental approaches for the treatment of malignant gliomas. Pharmacology & Therapeutics 128, 1–36. doi:10.1016/j.pharmthera.2010.04.015

Arora, a, Scholar, E.M., 2005. Role of tyrosine kinase inhibitors in cancer therapy. J Pharmacol Exp Ther 315, 971–979. doi:10.1124/jpet.105.084145.have

Attaphitaya, S., Park, K., Melvin, J.E., 1999. Molecular cloning and functional expression of a rat Na+/H+ exchanger (NHE5) highly expressed in brain. The Journal of biological chemistry 274, 4383–8. doi:10.1074/JBC.274.7.4383

Balça-Silva, J., Matias, D., Do Carmo, A., Dubois, L.G., Gonçalves, A.C., Girão, H., Canedo, N.H.S., Correia, A.H., De Souza, J.M., Sarmento-Ribeiro, A.B., Lopes, M.C., Moura-Neto, V., 2017a. Glioblastoma entities express subtle differences in molecular composition and response to treatment. Oncology Reports 38, 1341–1352.

Balça-Silva, J., Matias, D., Do Carmo, A., Girão, H., Moura-Neto, V., Sarmento-Ribeiro, A.B., Lopes, M.C., 2015. Tamoxifen in combination with temozolomide induce a synergistic inhibition of PKC-pan in GBM cell lines. Biochimica et Biophysica Acta - General Subjects 1850, 722–732. doi:10.1016/j.bbagen.2014.12.022

Balça-Silva, J., Matias, D., Dubois, L.G., Carneiro, B., do Carmo, A., Girão, H., Ferreira, F., Ferrer, V.P., Chimelli, L., Filho, P.N., Tão, H., Rebelo, O., Barbosa, M., Sarmento-Ribeiro, A.B., Lopes, M.C., Moura-Neto, V., 2017b. The Expression of Connexins and SOX2 Reflects the Plasticity of Glioma Stem-Like Cells. Translational Oncology 10, 555–569. doi:10.1016/j.tranon.2017.04.005

Baldwin, R.M., Barrett, G.M., Parolin, D.A., Gillies, J.K., Paget, J.A., Lavictoire, S.J., Gray, D.A., Lorimer, I.A., 2010. Coordination of glioblastoma cell motility by PKCι. Molecular Cancer 9, 233. doi:10.1186/1476-4598-9-233

Bangham, A.D., Horne, R.W., 1964. Negative Staining Of Phospholipids And Their Structural Modification By Surface-Active Agents As Observed In The Electron Microscope. Journal of Molecular Biology 8, 660–8.

Bao, S., Wu, Q., McLendon, R.E., Hao, Y., Shi, Q., Hjelmeland, A.B., Dewhirst, M.W., Bigner, D.D., Rich, J.N., 2006. Glioma stem cells promote radioresistance by preferential activation of the DNA damage response. Nature 444, 756–760. doi:10.1038/nature05236

Bar, E.E., Chaudhry, A., Lin, A., Fan, X., Schreck, K., Matsui, W., Piccirillo, S., Vescovi, A.L., DiMeco, F., Olivi, A., Eberhart, C.G., 2007. Cyclopamine-Mediated Hedgehog Pathway Inhibition Depletes Stem-Like Cancer Cells in Glioblastoma. Stem Cells 25, 2524–2533. doi:10.1634/stemcells.2007-0166

Baselga, J., 2006. Targeting Tyrosine Kinases in Cancer: The Second Wave. Science 312, 1175–1178. doi:10.1126/science.1125951

Basu, A., Sivaprasad, U., 2007. Protein kinase Cε makes the life and death decision. Cellular Signalling 19, 1633–1642. doi:10.1016/j.cellsig.2007.04.008

Beier, D., Hau, P., Proescholdt, M., Lohmeier, A., Wischhusen, J., Oefner, P.J., Aigner, L., Brawanski, A., Bogdahn, U., Beier, C.P., 2007. CD133+ and CD133- Glioblastoma-Derived Cancer Stem Cells Show Differential Growth Characteristics and Molecular Profiles. Cancer Research 67, 4010–4015. doi:10.1158/0008-5472.CAN-06-4180

Berezovsky, A.D., Poisson, L.M., Cherba, D., Webb, C.P., Transou, A.D., Lemke, N.W., Hong, X., Hasselbach, L.A., Irtenkauf, S.M., Mikkelsen, T., de Carvalho, A.C., deCarvalho, A.C., 2014. Sox2 promotes malignancy in glioblastoma by regulating plasticity and astrocytic differentiation. Neoplasia

(United States) 16, 193–206. doi:10.1016/j.neo.2014.03.006

Bertossi, M., Virgintino, D., Maiorano, E., Occhiogrosso, M., Roncali, L., 1997. Ultrastructural and Morphometric Investigation of Human Brain Capillaries in Normal and Peritumoral Tissues. Ultrastructural Pathology 21, 41–49. doi:10.3109/01913129709023246

Besson, A., Yong, V.W., 2000. Involvement of p21(Waf1/Cip1) in protein kinase C alpha-induced cell cycle progression. Molecular and cellular biology 20, 4580–90.

Beyer, S., von Bueren, A.O., Klautke, G., Guckenberger, M., Kortmann, R.-D., Pietschmann, S., Müller, K., 2016. A Systematic Review on the Characteristics, Treatments and Outcomes of the Patients with Primary Spinal Glioblastomas or Gliosarcomas Reported in Literature until March 2015. PloS one 11, e0148312. doi:10.1371/journal.pone.0148312

Bhowmik, A., Khan, R., Ghosh, M.K., 2015. Blood Brain Barrier: A Challenge for Effectual Therapy of Brain Tumors. BioMed Research International 2015, 1–20. doi:10.1155/2015/320941

Bianco, R., Rosa, R., Damiano, V., Daniele, G., Gelardi, T., Garofalo, S., Tarallo, V., De Falco, S., Melisi, D., Benelli, R., Albini, A., Ryan, A., Ciardiello, F., Tortora, G., 2008. Vascular Endothelial Growth Factor Receptor-1 Contributes to Resistance to Anti-Epidermal Growth Factor Receptor Drugs in Human Cancer Cells. Clinical Cancer Research 14, 5069–5080. doi:10.1158/1078-0432.CCR-07-4905

Binda, E., Visioli, A., Giani, F., Trivieri, N., Palumbo, O., Restelli, S., Dezi, F., Mazza, T., Fusilli, C., Legnani, F., Carella, M., Di Meco, F., Duggal, R., Vescovi, A.L., 2017. Wnt5a Drives an Invasive Phenotype in Human Glioblastoma Stem-like Cells. Cancer Research 77, 996–1007. doi:10.1158/0008-5472.CAN-16-1693

Blakeley, J., 2008. Drug Delivery to Brain Tumors. Current Neurology and Neuroscience Reports 8, 235–241.

Bogush, T., Dudko, E., Bogush, E., Polotsky, B., Tjulandin, S., Davydov, M., 2012. Tamoxifen non-estrogen receptor mediated molecular targets. Oncology reviews 6, e15. doi:10.4081/oncol.2012.e15

Borlongan, C. V, Emerich, D.F., 2003. Facilitation of drug entry into the CNS via transient permeation of blood brain barrier: laboratory and preliminary clinical evidence from bradykinin receptor agonist, Cereport. Brain research bulletin 60, 297–306.

Borovski, T., De Sousa E Melo, F., Vermeulen, L., Medema, J.P., 2011. Cancer stem cell niche: the place to be. Cancer research 71, 634–9. doi:10.1158/0008-5472.CAN-10-3220

Borowski, E., Bontemps-Gracz, M.M., Piwkowska, A., 2005. Strategies for overcoming ABC-transporters-mediated multidrug resistance (MDR) of tumor cells. Acta biochimica Polonica 52, 609–27.

Boyer, L.A., Lee, T.I., Cole, M.F., Johnstone, S.E., Levine, S.S., Zucker, J.P., Guenther, M.G., Kumar, R.M., Murray, H.L., Jenner, R.G., Gifford, D.K., Melton, D.A., Jaenisch, R., Young, R.A., 2005. Core Transcriptional Regulatory Circuitry in Human Embryonic Stem Cells. Cell 122, 947–956. doi:10.1016/j.cell.2005.08.020

Bradshaw, A., Wickremesekera, A., Brasch, H.D., Chibnall, A.M., Davis, P.F., Tan, S.T., Itinteang, T., 2016. Cancer Stem Cells in Glioblastoma Multiforme. Frontiers in Surgery 3, 48. doi:10.3389/fsurg.2016.00048

Brandes, A.A., Ermani, M., Turazzi, S., Scelzi, E., Berti, F., Amistà, P., Rotilio, A., Licata, C., Fiorentino, M. V, 1999. Procarbazine and high-dose tamoxifen as a second-line regimen in recurrent high-grade

gliomas: a phase II study. Journal of clinical oncology : official journal of the American Society of Clinical Oncology 17, 645–50. doi:10.1200/jco.1999.17.2.645

Brat, D.J., Van Meir, E.G., 2004. Vaso-occlusive and prothrombotic mechanisms associated with tumor hypoxia, necrosis, and accelerated growth in glioblastoma. Laboratory investigation; a journal of technical methods and pathology 84, 397–405. doi:10.1038/labinvest.3700070

Brem, H., Mahaley, M.S., Vick, N.A., Black, K.L., Schold, S.C., Burger, P.C., Friedman, A.H., Ciric, I.S., Eller, T.W., Cozzens, J.W., Kenealy, J.N., 1991. Interstitial chemotherapy with drug polymer implants for the treatment of recurrent gliomas. Journal of neurosurgery 74, 441–6. doi:10.3171/jns.1991.74.3.0441

Brennan, C., Momota, H., Hambardzumyan, D., Ozawa, T., Tandon, A., Pedraza, A., Holland, E., 2009. Glioblastoma subclasses can be defined by activity among signal transduction pathways and associated genomic alterations. PloS one 4, e7752. doi:10.1371/journal.pone.0007752

Brenner, A. V, Linet, M.S., Fine, H.A., Shapiro, W.R., Selker, R.G., Black, P.M., Inskip, P.D., 2002. History of allergies and autoimmune diseases and risk of brain tumors in adults. International journal of cancer 99, 252–9. doi:10.1002/ijc.10320

Brewer, G.J., 1995. Serum-free B27/neurobasal medium supports differentiated growth of neurons from the striatum, substantia nigra, septum, cerebral cortex, cerebellum, and dentate gyrus. Journal of Neuroscience Research 42, 674–683. doi:10.1002/jnr.490420510

Buonerba, C., Di Lorenzo, G., Marinelli, A., Federico, P., Palmieri, G., Imbimbo, M., Conti, P., Peluso, G., De Placido, S., Sampson, J.H., 2011. A comprehensive outlook on intracerebral therapy of malignant gliomas. Critical reviews in oncology/hematology 80, 54–68. doi:10.1016/j.critrevonc.2010.09.001

Calatozzolo, C., Gelati, M., Ciusani, E., Sciacca, F.L., Pollo, B., Cajola, L., Marras, C., Silvani, A., Vitellaro-Zuccarello, L., Croci, D., Boiardi, A., Salmaggi, A., 2005. Expression of Drug Resistance Proteins Pgp, MRP1, MRP3, MRP5 AND GST-π in Human Glioma. Journal of Neuro-Oncology 74, 113–121. doi:10.1007/s11060-004-6152-7

Calixto, G., Bernegossi, J., Fonseca-Santos, B., Chorilli, M., 2014. Nanotechnology-based drug delivery systems for treatment of oral cancer: a review. International journal of nanomedicine 9, 3719–35. doi:10.2147/IJN.S61670

Callaghan, R., Higgins, C., 1995. Interaction of tamoxifen with the multidrug resistance P-glycoprotein 71, 94–299.

Cameron, A.J., Procyk, K.J., Leitges, M., Parker, P.J., 2008. PKC alpha protein but not kinase activity is critical for glioma cell proliferation and survival. International Journal of Cancer 123, 769–779. doi:10.1002/ijc.23560

Cancer Genome Atlas Research Network, 2008. Comprehensive genomic characterization defines human glioblastoma genes and core pathways. Nature 455, 1061–8. doi:10.1038/nature07385

Carico, C., Nuño, M., Mukherjee, D., Elramsisy, A., Dantis, J., Hu, J., Rudnick, J., Yu, J.S., Black, K.L., Bannykh, S.I., Patil, C.G., 2012. Loss of PTEN Is Not Associated with Poor Survival in Newly Diagnosed Glioblastoma Patients of the Temozolomide Era. PLoS ONE 7, e33684. doi:10.1371/journal.pone.0033684

Carmo, A., Balça-Silva, J., Matias, D., Lopes, M.C., 2013. PKC signaling in glioblastoma. Cancer Biology

and Therapy 14, 1–8. doi:10.4161/cbt.23615

Carmo, A., Carvalheiro, H., Crespo, I., Nunes, I., Lopes, M.C., 2011a. Effect of temozolomide on the U-118 glioma cell line. Oncology letters 2, 1165–1170. doi:10.3892/ol.2011.406

Carmo, A., Crespo, I., Celeste, M., 2011b. Genetics and Biology of Glioblastoma Multiforme. Molecular Targets of CNS Tumors. doi:10.5772/23479

Castro, M.G., Candolfi, M., Kroeger, K., King, G.D., Curtin, J.F., Yagiz, K., Mineharu, Y., Assi, H., Wibowo, M., Ghulam Muhammad, A.K.M., Foulad, D., Puntel, M., Lowenstein, P.R., 2011. Gene therapy and targeted toxins for glioma. Current gene therapy 11, 155–80.

Cerna, T., Stiborova, M., Adam, V., Kizek, R., Eckschlager, T., 2016. Nanocarrier drugs in the treatment of brain tumors. Journal of Cancer Metastasis and Treatment 2, 407. doi:10.20517/2394-4722.2015.95

Chaffer, C.L., Brueckmann, I., Scheel, C., Kaestli, A.J., Wiggins, P.A., Rodrigues, L.O., Brooks, M., Reinhardt, F., Su, Y., Polyak, K., Arendt, L.M., Kuperwasser, C., Bierie, B., Weinberg, R.A., 2011. Normal and neoplastic nonstem cells can spontaneously convert to a stem-like state. Proceedings of the National Academy of Sciences of the United States of America 108, 7950–5. doi:10.1073/pnas.1102454108

Chaffer, C.L., Marjanovic, N.D., Lee, T., Bell, G., Kleer, C.G., Reinhardt, F., D'Alessio, A.C., Young, R.A., Weinberg, R.A., 2013. Poised Chromatin at the ZEB1 Promoter Enables Breast Cancer Cell Plasticity and Enhances Tumorigenicity. Cell 154, 61–74. doi:10.1016/j.cell.2013.06.005

Chakroun, R.W., Zhang, P., Lin, R., Schiapparelli, P., Quinones-Hinojosa, A., Cui, H., 2017. Nanotherapeutic systems for local treatment of brain tumors. Wiley Interdisciplinary Reviews: Nanomedicine and Nanobiotechnology e1479. doi:10.1002/wnan.1479

Chamberlain, M.C., Cloughsey, T., Reardon, D. a, Wen, P.Y., 2012. A novel treatment for glioblastoma: integrin inhibition. Expert review of neurotherapeutics 12, 421–35. doi:10.1586/ern.11.188

Chang, J.E., Khuntia, D., Robins, H.I., Mehta, M.P., 2007. Radiotherapy and radiosensitizers in the treatment of glioblastoma multiforme. Clinical advances in hematology & oncology : H&O 5, 894–902, 907–15.

Chang, S.M., Lamborn, K.R., Malec, M., Rabbitt, J., Page, M., Prados, M.D., 2004. Phase II study of salvage therapy with high-dose tamoxifen and oral etoposide for recurrent malignant glioma. Therapy 1, 53–60.

Cho, K.K., Mikkelsen, T., Lee, Y.J., Jiang, F., Chopp, M., Rosenblum, M.L., 1999. The role of protein kinase Calpha in U-87 glioma invasion. International journal of developmental neuroscience : the official journal of the International Society for Developmental Neuroscience 17, 447–61.

Christian, S., Pilch, J., Akerman, M.E., Porkka, K., Laakkonen, P., Ruoslahti, E., 2003. Nucleolin expressed at the cell surface is a marker of endothelial cells in angiogenic blood vessels. Journal of Cell Biology 163, 871–878. doi:10.1083/jcb.200304132

Cohen, A.L., Holmen, S.L., Colman, H., 2013. IDH1 and IDH2 mutations in gliomas. Current neurology and neuroscience reports 13, 345. doi:10.1007/s11910-013-0345-4

Combs, S.E., Debus, J., Schulz-Ertner, D., 2007. Radiotherapeutic alternatives for previously irradiated recurrent gliomas. BMC cancer 7, 167. doi:10.1186/1471-2407-7-167

Combs, S.E., Heeger, S., Haselmann, R., Edler, L., Debus, J., Schulz-Ertner, D., 2006. Treatment of primary glioblastoma multiforme with cetuximab, radiotherapy and temozolomide (GERT)--phase I/II trial:

study protocol. BMC cancer 6, 133. doi:10.1186/1471-2407-6-133

Cong, D., Zhu, W., Kuo, J.S., Hu, S., Sun, D., 2015. Ion transporters in brain tumors. Current medicinal chemistry 22, 1171–81.

Cordon-Cardo, C., O'Brien, J.P., Casals, D., Rittman-Grauer, L., Biedler, J.L., Melamed, M.R., Bertino, J.R., 1989. Multidrug-resistance gene (P-glycoprotein) is expressed by endothelial cells at blood-brain barrier sites. Proceedings of the National Academy of Sciences of the United States of America 86, 695–8.

Couldwell, W.T., Hinton, D.R., He, S., Chen, T.C., Sebat, I., Weiss, M.H., Law, R.E., 1994. Protein kinase C inhibitors induce apoptosis in human malignant glioma cell lines. FEBS letters 345, 43–46. doi:0014-5793(94)00415-3 [pii]

Cox, J.L., Wilder, P.J., Desler, M., Rizzino, A., 2012. Elevating SOX2 levels deleteriously affects the growth of medulloblastoma and glioblastoma cells. PloS one 7, e44087. doi:10.1371/journal.pone.0044087

Crespo, I., Vital, A.L., Gonzalez-Tablas, M., Patino, M.D.C., Otero, A., Lopes, M.C., De Oliveira, C., Domingues, P., Orfao, A., Tabernero, M.D., 2015. Molecular and Genomic Alterations in Glioblastoma Multiforme. American Journal of Pathology 185, 1820–1833. doi:10.1016/j.ajpath.2015.02.023

da Rocha, A.B., Mans, D.R.A., Regner, A., Schwartsmann, G., 2002. Targeting protein kinase C: new therapeutic opportunities against high-grade malignant gliomas? The Oncologist 7, 17–33. doi:10.1634/THEONCOLOGIST.7-1-17

da Rocha, A.B., Mans, D.R., Bernard, E.A., Ruschel, C., Logullo, A.F., Wetmore, L.A., Leyva, A., Schwartsmann, G., 1999. Tamoxifen inhibits particulate-associated protein kinase C activity, and sensitises cultured human glioblastoma cells not to etoposide but to gamma-radiation and BCNU. European journal of cancer (Oxford, England : 1990) 35, 833–9.

Dasari, V.R., Kaur, K., Velpula, K.K., Gujrati, M., Fassett, D., Klopfenstein, J.D., Dinh, D.H., Rao, J.S., 2010. Upregulation of PTEN in Glioma Cells by Cord Blood Mesenchymal Stem Cells Inhibits Migration via Downregulation of the PI3K/Akt Pathway. PLoS ONE 5, e10350. doi:10.1371/journal.pone.0010350

Daumas-Duport, C., Varlet, P., 2003. [Dysembryoplastic neuroepithelial tumors]. Revue neurologique 159, 622–36.

de Vries, N.A., Buckle, T., Zhao, J., Beijnen, J.H., Schellens, J.H.M., van Tellingen, O., 2012. Restricted brain penetration of the tyrosine kinase inhibitor erlotinib due to the drug transporters P-gp and BCRP. Investigational New Drugs 30, 443–449. doi:10.1007/s10637-010-9569-1

Deck, J.H., Eng, L.F., Bigbee, J., Woodcock, S.M., 1978. The role of glial fibrillary acidic protein in the diagnosis of central nervous system tumors. Acta neuropathologica 42, 183–90.

Deeken, J.F., Loscher, W., 2007. The Blood-Brain Barrier and Cancer: Transporters, Treatment, and Trojan Horses. Clinical Cancer Research 13, 1663–1674. doi:10.1158/1078-0432.CCR-06-2854

Deheeger, M., Lesniak, M.S., Ahmed, A.U., 2014. Cellular plasticity regulated cancer stem cell niche: a possible new mechanism of chemoresistance. Cancer cell & microenvironment 1. doi:10.14800/ccm.295

Deltour, I., Auvinen, A., Feychting, M., Johansen, C., Klaeboe, L., Sankila, R., Schüz, J., 2012. Mobile phone use and incidence of glioma in the Nordic countries 1979-2008: consistency check. Epidemiology

(Cambridge, Mass.) 23, 301–7. doi:10.1097/EDE.0b013e3182448295

Di Cristofano, A., Pandolfi, P.P., 2000. The multiple roles of PTEN in tumor suppression. Cell 100, 387–90.

DI Cristofori, A., Carrabba, G., Lanfranchi, G., Menghetti, C., Rampini, P., Caroli, M., 2013. Continuous tamoxifen and dose-dense temozolomide in recurrent glioblastoma. Anticancer research 33, 3383–9.

Diaz, A., Leon, K., 2011. Therapeutic approaches to target cancer stem cells. Cancers 3, 3331–3352. doi:10.3390/cancers3033331

Ding, L., Ley, T.J., Larson, D.E., Miller, C.A., Koboldt, D.C., Welch, J.S., Ritchey, J.K., Young, M.A., Lamprecht, T., McLellan, M.D., McMichael, J.F., Wallis, J.W., Lu, C., Shen, D., Harris, C.C., Dooling, D.J., Fulton, R.S., Fulton, L.L., Chen, K., Schmidt, H., Kalicki-Veizer, J., Magrini, V.J., Cook, L., McGrath, S.D., Vickery, T.L., Wendl, M.C., Heath, S., Watson, M.A., Link, D.C., Tomasson, M.H., Shannon, W.D., Payton, J.E., Kulkarni, S., Westervelt, P., Walter, M.J., Graubert, T.A., Mardis, E.R., Wilson, R.K., DiPersio, J.F., 2012. Clonal evolution in relapsed acute myeloid leukaemia revealed by whole-genome sequencing. Nature 481, 506–10. doi:10.1038/nature10738

do Carmo, A., Patricio, I., Cruz, M.T., Carvalheiro, H., Oliveira, C.R., Lopes, M.C., 2010. CXCL12/CXCR4 promotes motility and proliferation of glioma cells. Cancer biology & therapy 9, 56–65.

Doetsch, F., Petreanu, L., Caille, I., Garcia-Verdugo, J.M., Alvarez-Buylla, A., 2002. EGF converts transit-amplifying neurogenic precursors in the adult brain into multipotent stem cells. Neuron 36, 1021–34.

Dohan, F.C., Kornblith, P.L., Wellum, G.R., Pfeiffer, S.E., Levine, L., 1977. S-100 protein and 2',3'-cyclic nucleotide 3'-phosphohydrolase in human brain tumors. Acta neuropathologica 40, 123–8.

Dolecek, T.A., Propp, J.M., Stroup, N.E., Kruchko, C., 2012. CBTRUS statistical report: primary brain and central nervous system tumors diagnosed in the United States in 2005-2009. Neuro-oncology 14 Suppl 5, v1-49. doi:10.1093/neuonc/nos218

Drappatz, J., Brenner, A., Wong, E.T., Eichler, A., Schiff, D., Groves, M.D., Mikkelsen, T., Rosenfeld, S., Sarantopoulos, J., Meyers, C.A., Fielding, R.M., Elian, K., Wang, X., Lawrence, B., Shing, M., Kelsey, S., Castaigne, J.P., Wen, P.Y., 2013. Phase I Study of GRN1005 in Recurrent Malignant Glioma. Clinical Cancer Research 19, 1567–1576. doi:10.1158/1078-0432.CCR-12-2481

Du, Z., Jia, D., Liu, S., Wang, F., Li, G., Zhang, Y., Cao, X., Ling, E.-A., Hao, A., 2009. Oct4 is expressed in human gliomas and promotes colony formation in glioma cells. Glia 57, 724–733. doi:10.1002/glia.20800

Dubois, L.G., Campanati, L., Righy, C., D'Andrea-Meira, I., Spohr, T.C.L. de S.E., Porto-Carreiro, I., Pereira, C.M., Balça-Silva, J., Kahn, S.A., DosSantos, M., Oliveira, M. de A.R., Ximenes-da-Silva, A., Lopes, M.C., Faveret, E., Gasparetto, E.L., Moura-Neto, V., 2014. Gliomas and the vascular fragility of the blood brain barrier. Frontiers in cellular neuroscience 8, 418. doi:10.3389/fncel.2014.00418

Dunn, G.P., Rinne, M.L., Wykosky, J., Genovese, G., Quayle, S.N., Dunn, I.F., Agarwalla, P.K., Chheda, M.G., Campos, B., Wang, A., Brennan, C., Ligon, K.L., Furnari, F., Cavenee, W.K., Depinho, R.A., Chin, L., Hahn, W.C., 2012. Emerging insights into the molecular and cellular basis of glioblastoma. Genes & development 26, 756–84. doi:10.1101/gad.187922.112

Easwaran, H., Tsai, H.-C., Baylin, S.B., 2014. Cancer epigenetics: tumor heterogeneity, plasticity of stem-like states, and drug resistance. Molecular cell 54, 716–27. doi:10.1016/j.molcel.2014.05.015

Evans, W.H., Martin, P.E.M., 2002. Gap junctions: structure and function (Review). Molecular membrane

biology 19, 121–36. doi:10.1080/09687680210139839

Fabel, K., Dietrich, J., Hau, P., Wismeth, C., Winner, B., Przywara, S., Steinbrecher, A., Ullrich, W., Bogdahn, U., 2001. Long-term stabilization in patients with malignant glioma after treatment with liposomal doxorubicin. Cancer 92, 1936–1942. doi:10.1002/1097-0142(20011001)92:7<1936::AID-CNCR1712>3.0.CO;2-H

Fang, X., Zhang, W., Zhao, N., Yu, W., Ding, D., Hong, X., Li, L., Zhang, H., Zheng, S., Lin, B., 2011. Genome-wide analysis of OCT4 binding sites in glioblastoma cancer cells. Journal of Zhejiang University. Science. B 12, 812–9. doi:10.1631/jzus.B1100059

Faria, J., Romão, L., Martins, S., Alves, T., Mendes, F.A., De Faria, G.P., Hollanda, R., Takiya, C., Chimelli, L., Morandi, V., De Souza, J.M., Abreu, J.G., Neto, V.M., 2006. Interactive properties of human glioblastoma cells with brain neurons in culture and neuronal modulation of glial laminin organization. Differentiation 74, 562–572. doi:10.1111/j.1432-0436.2006.00090.x

Favaro, R., Appolloni, I., Pellegatta, S., Sanga, A.B., Pagella, P., Gambini, E., Pisati, F., Ottolenghi, S., Foti, M., Finocchiaro, G., Malatesta, P., Nicolis, S.K., 2014. Sox2 is required to maintain cancer stem cells in a mouse model of high-grade oligodendroglioma. Cancer Research 74, 1833–1844. doi:10.1158/0008-5472.CAN-13-1942

Feldkamp, M.M., Lala, P., Lau, N., Roncari, L., Guha, A., 1999. Expression of activated epidermal growth factor receptors, Ras-guanosine triphosphate, and mitogen-activated protein kinase in human glioblastoma multiforme specimens. Neurosurgery 45, 1442–53.

Fonseca, C., Moreira, J.N., Ciudad, C.J., Pedroso De Lima, M.C., Simões, S., 2005. Targeting of sterically stabilised pH-sensitive liposomes to human T-leukaemia cells. European Journal of Pharmaceutics and Biopharmaceutics 59, 359–366. doi:10.1016/j.ejpb.2004.08.012

Fonseca, N.A., Cruz, A.F., Moura, V., Simões, S., Moreira, J.N., 2017. The cancer stem cell phenotype as a determinant factor of the heterotypic nature of breast tumors. Critical Reviews in Oncology/Hematology 113, 111–121. doi:10.1016/j.critrevonc.2017.03.016

Fonseca, N.A., Gomes-Da-Silva, L.C., Moura, V., Simões, S., Moreira, J.N., 2014. Simultaneous active intracellular delivery of doxorubicin and C6-ceramide shifts the additive/antagonistic drug interaction of non-encapsulated combination. Journal of Controlled Release 196, 122–131. doi:10.1016/j.jconrel.2014.09.024

Fonseca, N.A., Rodrigues, A.S., Rodrigues-Santos, P., Alves, V., Gregório, A.C., Valério-Fernandes, Â., Gomes-da-Silva, L.C., Rosa, M.S., Moura, V., Ramalho-Santos, J., Simões, S., Moreira, J.N., 2015. Nucleolin overexpression in breast cancer cell sub-populations with different stem-like phenotype enables targeted intracellular delivery of synergistic drug combination. Biomaterials 69, 76–88. doi:10.1016/j.biomaterials.2015.08.007

Ford, J., Osborn, C., Barton, T., Bleehen, N.M., 1998. A phase I study of intravenous RMP-7 with carboplatin in patients with progression of malignant glioma. European journal of cancer (Oxford, England : 1990) 34, 1807–11.

Francisco, V., Figueirinha, A., Neves, B.M., García-Rodríguez, C., Lopes, M.C., Cruz, M.T., Batista, M.T., 2011. Cymbopogon citratus as source of new and safe anti-inflammatory drugs: bio-guided assay using lipopolysaccharide-stimulated macrophages. Journal of ethnopharmacology 133, 818–27.

doi:10.1016/j.jep.2010.11.018

Friedman, H.S., Kerby, T., Calvert, H., 2000. Temozolomide and treatment of malignant glioma. Clinical cancer research : an official journal of the American Association for Cancer Research 6, 2585–97.

Friedmann-Morvinski, D., Verma, I.M., 2014. Dedifferentiation and reprogramming: Origins of cancer stem cells. EMBO Reports 15, 244–253. doi:10.1002/embr.201338254

Fujisawa, H., Reis, R.M., Nakamura, M., Colella, S., Yonekawa, Y., Kleihues, P., Ohgaki, H., 2000. Loss of heterozygosity on chromosome 10 is more extensive in primary (de novo) than in secondary glioblastomas. Laboratory investigation; a journal of technical methods and pathology 80, 65–72.

Furnari, F.B., Fenton, T., Bachoo, R.M., Mukasa, A., Stommel, J.M., Stegh, A., Hahn, W.C., Ligon, K.L., Louis, D.N., Brennan, C., Chin, L., DePinho, R.A., Cavenee, W.K., 2007. Malignant astrocytic glioma: genetics, biology, and paths to treatment. Genes & development 21, 2683–710. doi:10.1101/gad.1596707

Gabathuler, R., 2010. Approaches to transport therapeutic drugs across the blood-brain barrier to treat brain diseases. Neurobiology of disease 37, 48–57. doi:10.1016/j.nbd.2009.07.028

Gaiano, N., Fishell, G., 2002. The role of notch in promoting glial and neural stem cell fates. Annual review of neuroscience 25, 471–90. doi:10.1146/annurev.neuro.25.030702.130823

Galzio, R., Rosati, F., Benedetti, E., Cristiano, L., Aldi, S., Mei, S., D'Angelo, B., Gentile, R., Laurenti, G., Cifone, M.G., Giordano, A., Cimini, A., 2012. Glycosilated nucleolin as marker for human gliomas. Journal of Cellular Biochemistry 113, 571–579. doi:10.1002/jcb.23381

Gan, H.K., Cvrljevic, A.N., Johns, T.G., 2013. The epidermal growth factor receptor variant III (EGFRvIII): Where wild things are altered. FEBS Journal 280, 5350–5370. doi:10.1111/febs.12393

Gangemi, R.M., Griffero, F., Marubbi, D., Perera, M., Capra, M.C., Malatesta, P., Ravetti, G.L., Zona, G.L., Daga, A., Corte, G., 2009. SOX2 silencing in glioblastoma tumor-initiating cells causes stop of proliferation and loss of tumorigenicity. Stem Cells 27. doi:10.1634/stemcells.2008-0493

Garcia, C., Dubois, L., Xavier, A., Geraldo, L., da Fonseca, A.C., Correia, A., Meirelles, F., Ventura, G., Romão, L., Canedo, N.H., de Souza, J., de Menezes, J.R., Moura-Neto, V., Tovar-Moll, F., Lima, F.R., 2014. The orthotopic xenotransplant of human glioblastoma successfully recapitulates glioblastoma-microenvironment interactions in a non-immunosuppressed mouse model. BMC Cancer 14, 923. doi:10.1186/1471-2407-14-923

Garros-Regulez, L., Garcia, I., Carrasco-Garcia, E., Lantero, A., Aldaz, P., Moreno-Cugnon, L., Arrizabalaga, O., Undabeitia, J., Torres-Bayona, S., Villanua, J., Ruiz, I., Egaña, L., Sampron, N., Matheu, A., 2016. Targeting SOX2 as a Therapeutic Strategy in Glioblastoma. Frontiers in oncology 6, 222. doi:10.3389/fonc.2016.00222

Gerstner, E.R., Eichler, A.F., Plotkin, S.R., Drappatz, J., Doyle, C.L., Xu, L., Duda, D.G., Wen, P.Y., Jain, R.K., Batchelor, T.T., 2011. Phase I trial with biomarker studies of vatalanib (PTK787) in patients with newly diagnosed glioblastoma treated with enzyme inducing anti-epileptic drugs and standard radiation and temozolomide. Journal of Neuro-Oncology 103, 325–332. doi:10.1007/s11060-010-0390-7

Ghosal, G., Chen, J., 2013. DNA damage tolerance: a double-edged sword guarding the genome. Translational cancer research 2, 107–129. doi:10.3978/j.issn.2218-676X.2013.04.01

Gilbert, M.R., Dignam, J.J., Armstrong, T.S., Wefel, J.S., Blumenthal, D.T., Vogelbaum, M.A., Colman, H.,

Chakravarti, A., Pugh, S., Won, M., Jeraj, R., Brown, P.D., Jaeckle, K.A., Schiff, D., Stieber, V.W., Brachman, D.G., Werner-Wasik, M., Tremont-Lukats, I.W., Sulman, E.P., Aldape, K.D., Curran, W.J., Mehta, M.P., 2014. A Randomized Trial of Bevacizumab for Newly Diagnosed Glioblastoma. New England Journal of Medicine 370, 699–708. doi:10.1056/NEJMoa1308573

Gilbert, M.R., Kuhn, J., Lamborn, K.R., Lieberman, F., Wen, P.Y., Mehta, M., Cloughesy, T., Lassman, A.B., DeAngelis, L.M., Chang, S., Prados, M., 2012. Cilengitide in patients with recurrent glioblastoma: the results of NABTC 03-02, a phase II trial with measures of treatment delivery. Journal of Neuro-Oncology 106, 147–153. doi:10.1007/s11060-011-0650-1

Gladson, C.L., Prayson, R.A., Liu, W.M., 2010. The pathobiology of glioma tumors. Annual review of pathology 5, 33–50. doi:10.1146/annurev-pathol-121808-102109

Glunde, K., Düssmann, H., Juretschke, H.-P., Leibfritz, D., 2002. Na(+)/H(+) exchange subtype 1 inhibition during extracellular acidification and hypoxia in glioma cells. Journal of neurochemistry 80, 36–44.

Goldhoff, P., Clarke, J., Smirnov, I., Berger, M.S., Prados, M.D., James, C.D., Perry, A., Phillips, J.J., 2012. Clinical stratification of glioblastoma based on alterations in retinoblastoma tumor suppressor protein (RB1) and association with the proneural subtype. Journal of neuropathology and experimental neurology 71, 83–9. doi:10.1097/NEN.0b013e31823fe8f1

Goldmann, E.E., 1909. Die äussere und innere Sekretion des gesunden und kranken Organismus im Lichte der vitalen Färbung. [WWW Document]. URL http://www.eurobuch.com/buch/nr/739ef8acb1a11c81ea61b06ffe9873d8.html

Gomes-da-Silva, L.C., Fernández, Y., Abasolo, I., Schwartz, S., Ramalho, J.S., Pedroso de Lima, M.C., Simões, S., Moreira, J.N., 2013a. Efficient intracellular delivery of siRNA with a safe multitargeted lipid-based nanoplatform. Nanomedicine 8, 1397–1413. doi:10.2217/nnm.12.174

Gomes-da-Silva, L.C., Fonseca, N.A., Moura, V., Pedroso De Lima, M.C., Simões, S., Moreira, J.N., 2012a. Lipid-based nanoparticles for siRNA delivery in cancer therapy: Paradigms and challenges. Accounts of Chemical Research 45, 1163–1171. doi:10.1021/ar300048p

Gomes-da-Silva, L.C., Ramalho, J.S., Pedroso De Lima, M.C., Simões, S., Moreira, J.N., 2013b. Impact of anti-PLK1 siRNA-containing F3-targeted liposomes on the viability of both cancer and endothelial cells. European Journal of Pharmaceutics and Biopharmaceutics 85, 356–364. doi:10.1016/j.ejpb.2013.04.007

Gomes-da-Silva, L.C., Santos, A.O., Bimbo, L.M., Moura, V., Ramalho, J.S., Pedroso de Lima, M.C., Simões, S., Moreira, J.N., 2012b. Toward a siRNA-containing nanoparticle targeted to breast cancer cells and the tumor microenvironment. International journal of pharmaceutics 434, 9–19. doi:10.1016/j.ijpharm.2012.05.018

Gonçalves, A.C., Cortesão, E., Oliveiros, B., Alves, V., Espadana, A.I., Rito, L., Magalhães, E., Lobão, M.J., Pereira, A., Nascimento Costa, J.M., Mota-Vieira, L., Sarmento-Ribeiro, A.B., 2015. Oxidative stress and mitochondrial dysfunction play a role in myelodysplastic syndrome development, diagnosis, and prognosis: A pilot study. Free radical research 49, 1081–94. doi:10.3109/10715762.2015.1035268

Graff, J.R., McNulty, A.M., Hanna, K.R., Konicek, B.W., Lynch, R.L., Bailey, S.N., Banks, C., Capen, A., Goode, R., Lewis, J.E., Sams, L., Huss, K.L., Campbell, R.M., Iversen, P.W., Neubauer, B.L., Brown, T.J., Musib, L., Geeganage, S., Thornton, D., 2005. The Protein Kinase C -Selective Inhibitor,

Enzastaurin (LY317615.HCl), Suppresses Signaling through the AKT Pathway, Induces Apoptosis, and Suppresses Growth of Human Colon Cancer and Glioblastoma Xenografts. Cancer Research 65, 7462–7469. doi:10.1158/0008-5472.CAN-05-0071

Grahn, A.Y., Bankiewicz, K.S., Dugich-Djordjevic, M., Bringas, J.R., Hadaczek, P., Johnson, G.A., Eastman, S., Luz, M., 2009. Non-PEGylated liposomes for convection-enhanced delivery of topotecan and gadodiamide in malignant glioma: initial experience. Journal of Neuro-Oncology 95, 185–197. doi:10.1007/s11060-009-9917-1

Gregório, A.C., Fonseca, N.A., Moura, V., Lacerda, M., Figueiredo, P., Simões, S., Dias, S., Moreira, J.N., 2016. Inoculated Cell Density as a Determinant Factor of the Growth Dynamics and Metastatic Efficiency of a Breast Cancer Murine Model. PLOS ONE 11, e0165817. doi:10.1371/journal.pone.0165817

Griner, E.M., Kazanietz, M.G., 2007. Protein kinase C and other diacylglycerol effectors in cancer. Nature Reviews Cancer 7, 281–294. doi:10.1038/nrc2110

Gromnicova, R., Davies, H.A., Sreekanthreddy, P., Romero, I.A., Lund, T., Roitt, I.M., Phillips, J.B., Male, D.K., 2013. Glucose-Coated Gold Nanoparticles Transfer across Human Brain Endothelium and Enter Astrocytes In Vitro. PLoS ONE 8, e81043. doi:10.1371/journal.pone.0081043

Grossman, S.A., Ye, X., Piantadosi, S., Desideri, S., Nabors, L.B., Rosenfeld, M., Fisher, J., NABTT CNS Consortium, 2010. Survival of patients with newly diagnosed glioblastoma treated with radiation and temozolomide in research studies in the United States. Clinical cancer research : an official journal of the American Association for Cancer Research 16, 2443–9. doi:10.1158/1078-0432.CCR-09-3106

Gruber, W., Scheidt, T., Aberger, F., Huber, C.G., 2017. Understanding cell signaling in cancer stem cells for targeted therapy - can phosphoproteomics help to reveal the secrets? Cell communication and signaling : CCS 15, 12. doi:10.1186/s12964-017-0166-1

Gupta, V., Su, Y.S., Wang, W., Kardosh, A., Liebes, L.F., Hofman, F.M., Schönthal, A.H., Chen, T.C., 2006. Enhancement of glioblastoma cell killing by combination treatment with temozolomide and tamoxifen or hypericin. Neurosurgical Focus 20, E20. doi:10.3171/foc.2006.20.4.13

Haar, C.P., Hebbar, P., Iv, G.C.W., Das, A., William, A., Iii, V., Smith, J.A., Giglio, P., Patel, S.J., Ray, S.K., Banik, N.L., 2015. HHS Public Access 37, 1192–1200. doi:10.1007/s11064-011-0701-1.Drug

Haar, C.P., Hebbar, P., Wallace, G.C., Das, A., Vandergrift, W.A., Smith, J.A., Giglio, P., Patel, S.J., Ray, S.K., Banik, N.L., 2012. Drug Resistance in Glioblastoma: A Mini Review. Neurochemical Research 37, 1192–1200. doi:10.1007/s11064-011-0701-1

Hadjipanayis, C.G., Van Meir, E.G., 2009. Brain cancer propagating cells: biology, genetics and targeted therapies. Trends in molecular medicine 15, 519–30. doi:10.1016/j.molmed.2009.09.003

Hamada, H., Tsuruo, T., 1988. Purification of the 170- to 180-kilodalton membrane glycoprotein associated with multidrug resistance. 170- to 180-kilodalton membrane glycoprotein is an ATPase. The Journal of biological chemistry 263, 1454–8.

Hamburg, M.A., Collins, F.S., 2010. The Path to Personalized Medicine. New England Journal of Medicine 363, 301–304. doi:10.1056/NEJMp1006304

Han Bae, Y., Park, K., 2011. Targeted drug delivery to tumors: Myths, reality and possibility. Journal of Controlled Release 153, 198–205. doi:10.1016/j.jconrel.2011.06.001

Haque, A., Banik, N.L., Ray, S.K., 2011. Molecular alterations in glioblastoma: potential targets for immunotherapy. Progress in molecular biology and translational science 98, 187–234. doi:10.1016/B978-0-12-385506-0.00005-3

Harbour, J.W., Dean, D.C., 2000. The Rb/E2F pathway: expanding roles and emerging paradigms. Genes & development 14, 2393–409. doi:10.1101/GAD.813200

Hartz, A.M.S., Bauer, B., 2011. ABC transporters in the CNS - an inventory. Current pharmaceutical biotechnology 12, 656–73.

Hatanpaa, K.J., Burma, S., Zhao, D., Habib, A.A., 2010. Epidermal growth factor receptor in glioma: signal transduction, neuropathology, imaging, and radioresistance. Neoplasia (New York, N.Y.) 12, 675–84.

Hattermann, K., Mentlein, R., 2013. An infernal trio: the chemokine CXCL12 and its receptors CXCR4 and CXCR7 in tumor biology. Annals of Anatomy 195, 103–10. doi:10.1016/j.aanat.2012.10.013

Hau, P., Fabel, K., Baumgart, U., Rümmele, P., Grauer, O., Bock, A., Dietmaier, C., Dietmaier, W., Dietrich, J., Dudel, C., Hübner, F., Jauch, T., Drechsel, E., Kleiter, I., Wismeth, C., Zellner, A., Brawanski, A., Steinbrecher, A., Marienhagen, J., Bogdahn, U., 2004. Pegylated liposomal doxorubicin-efficacy in patients with recurrent high-grade glioma. Cancer 100, 1199–1207. doi:10.1002/cncr.20073

He, W., Liu, R., Yang, S.-H., Yuan, F., 2015. Chemotherapeutic effect of tamoxifen on temozolomide-resistant gliomas. Anti-cancer drugs 26, 293–300. doi:10.1097/CAD.0000000000000197

Hegi, M.E., Diserens, A.-C., Gorlia, T., Hamou, M.-F., de Tribolet, N., Weller, M., Kros, J.M., Hainfellner, J.A., Mason, W., Mariani, L., Bromberg, J.E.C., Hau, P., Mirimanoff, R.O., Cairncross, J.G., Janzer, R.C., Stupp, R., 2005. MGMT gene silencing and benefit from temozolomide in glioblastoma. The New England journal of medicine 352, 997–1003. doi:10.1056/NEJMoa043331

Herrmann, A., Cherryholmes, G., Schroeder, A., Phallen, J., Alizadeh, D., Xin, H., Wang, T., Lee, H., Lahtz, C., Swiderski, P., Armstrong, B., Kowolik, C., Gallia, G.L., Lim, M., Brown, C., Badie, B., Forman, S., Kortylewski, M., Jove, R., Yu, H., 2014. TLR9 Is Critical for Glioma Stem Cell Maintenance and Targeting. Cancer Research 74, 5218–5228. doi:10.1158/0008-5472.CAN-14-1151

Hide, T., Makino, K., Nakamura, H., Yano, S., Anai, S., Takezaki, T., Kuroda, J., Shinojima, N., Ueda, Y., Kuratsu, J., 2013. New Treatment Strategies to Eradicate Cancer Stem Cells and Niches in Glioblastoma. Neurologia medico-chirurgica 53, 764–772. doi:10.2176/nmc.ra2013-0207

Hirose, Y., Katayama, M., Mirzoeva, O.K., Berger, M.S., Pieper, R.O., 2005. Akt activation suppresses Chk2-mediated, methylating agent-induced G2 arrest and protects from temozolomide-induced mitotic catastrophe and cellular senescence. Cancer research 65, 4861–9. doi:10.1158/0008-5472.CAN-04-2633

Hitomi, M., Deleyrolle, L.P., Mulkearns-Hubert, E.E., Jarrar, A., Li, M., Sinyuk, M., Otvos, B., Brunet, S., Flavahan, W.A., Hubert, C.G., Goan, W., Hale, J.S., Alvarado, A.G., Zhang, A., Rohaus, M., Oli, M., Vedam-Mai, V., Fortin, J.M., Futch, H.S., Griffith, B., Wu, Q., Xia, C.-H., Gong, X., Ahluwalia, M.S., Rich, J.N., Reynolds, B.A., Lathia, J.D., 2015. Differential connexin function enhances self-renewal in glioblastoma. Cell reports 11, 1031–42. doi:10.1016/j.celrep.2015.04.021

Hong, M., Zhu, S., Jiang, Y., Tang, G., Pei, Y., 2009. Efficient tumor targeting of hydroxycamptothecin loaded PEGylated niosomes modified with transferrin. Journal of Controlled Release 133, 96–102. doi:10.1016/j.jconrel.2008.09.005

Hsu, J.Y., Wakelee, H.A., 2009. Monoclonal Antibodies Targeting Vascular Endothelial Growth Factor. BioDrugs 23, 289–304. doi:10.2165/11317600-000000000-00000

Hu, B., Wang, Q., Wang, Y.A., Hua, S., Sauv?, C.-E.G., Ong, D., Lan, Z.D., Chang, Q., Ho, Y.W., Monasterio, M.M., Lu, X., Zhong, Y., Zhang, J., Deng, P., Tan, Z., Wang, G., Liao, W.-T., Corley, L.J., Yan, H., Zhang, J., You, Y., Liu, N., Cai, L., Finocchiaro, G., Phillips, J.J., Berger, M.S., Spring, D.J., Hu, J., Sulman, E.P., Fuller, G.N., Chin, L., Verhaak, R.G.W., DePinho, R.A., 2016. Epigenetic Activation of WNT5A Drives Glioblastoma Stem Cell Differentiation and Invasive Growth. Cell 167, 1281–1295.e18. doi:10.1016/j.cell.2016.10.039

Huang, L., Fu, L., 2015. Mechanisms of resistance to EGFR tyrosine kinase inhibitors. Acta Pharmaceutica Sinica B 5, 390–401. doi:10.1016/j.apsb.2015.07.001

Hubensack, M., Müller, C., Höcherl, P., Fellner, S., Spruss, T., Bernhardt, G., Buschauer, A., 2008. Effect of the ABCB1 modulators elacridar and tariquidar on the distribution of paclitaxel in nude mice. Journal of Cancer Research and Clinical Oncology 134, 597–607. doi:10.1007/s00432-007-0323-9

Hui, A.-M., Zhang, W., Chen, W., Xi, D., Purow, B., Friedman, G.C., Fine, H.A., 2004. Agents with selective estrogen receptor (ER) modulator activity induce apoptosis in vitro and in vivo in ER-negative glioma cells. Cancer research 64, 9115–23. doi:10.1158/0008-5472.CAN-04-2740

Humphries, J.D., 2006. Integrin ligands at a glance. Journal of Cell Science 119, 3901–3903. doi:10.1242/jcs.03098

Huse, J.T., Holland, E., DeAngelis, L.M., 2013. Glioblastoma: molecular analysis and clinical implications. Annual review of medicine 64, 59–70. doi:10.1146/annurev-med-100711-143028

Huwyler, J., Wu, D., Pardridge, W.M., 1996. Brain drug delivery of small molecules using immunoliposomes. Proceedings of the National Academy of Sciences of the United States of America 93, 14164–9. doi:10.1073/pnas.93.24.14164

Hynes, R.O., 2002. Integrins: bidirectional, allosteric signaling machines. Cell 110, 673–87.

Ichimura, K., Ohgaki, H., Kleihues, P., Collins, V.P., 2004. Molecular pathogenesis of astrocytic tumours. Journal of neuro-oncology 70, 137–60. doi:10.1007/s11060-004-2747-2

Ikushima, H., Todo, T., Ino, Y., Takahashi, M., Miyazawa, K., Miyazono, K., 2009. Autocrine TGF-β Signaling Maintains Tumorigenicity of Glioma-Initiating Cells through Sry-Related HMG-Box Factors. Cell Stem Cell 5, 504–514. doi:10.1016/j.stem.2009.08.018

Inda, M. -d.-M., Bonavia, R., Mukasa, A., Narita, Y., Sah, D.W.Y., Vandenberg, S., Brennan, C., Johns, T.G., Bachoo, R., Hadwiger, P., Tan, P., DePinho, R.A., Cavenee, W., Furnari, F., 2010. Tumor heterogeneity is an active process maintained by a mutant EGFR-induced cytokine circuit in glioblastoma. Genes & Development 24, 1731–1745. doi:10.1101/gad.1890510

Izumoto, S., Ohnishi, T., Arita, N., Hiraga, S., Taki, T., Hayakawa, T., 1996. Gene expression of neural cell adhesion molecule L1 in malignant gliomas and biological significance of L1 in glioma invasion. Cancer research 56, 1440–4.

Jackson, M., Hassiotou, F., Nowak, A., 2015. Glioblastoma stem-like cells: at the root of tumor recurrence and a therapeutic target. Carcinogenesis 36, 177–85. doi:10.1093/carcin/bgu243

Jaeckle, K.A., Eyre, H.J., Townsend, J.J., Schulman, S., Knudson, H.M., Belanich, M., Yarosh, D.B., Bearman, S.I., Giroux, D.J., Schold, S.C., 1998. Correlation of tumor O6 methylguanine-DNA

methyltransferase levels with survival of malignant astrocytoma patients treated with bis-chloroethylnitrosourea: a Southwest Oncology Group study. Journal of clinical oncology : official journal of the American Society of Clinical Oncology 16, 3310–5.

Jhanwar-Uniyal, M., Labagnara, M., Friedman, M., Kwasnicki, A., Murali, R., 2015. Glioblastoma: Molecular pathways, stem cells and therapeutic targets. Cancers 7, 538–555. doi:10.3390/cancers7020538

Jiao, Y., Killela, P.J., Reitman, Z.J., Rasheed, B.A., Heaphy, C.M., de Wilde, R.F., Rodriguez, F.J., Rosemberg, S., Obashinjo, S.M., Nagahashi Marie, S.K., Bettegowda, C., Agrawal, N., Lipp, E., Pirozzi, C., Lopez, G., He, Y., Friedman, H., Friedman, A.H., Riggins, G.J., Holdhoff, M., Burger, P., McLendon, R., Bigner, D.D., Vogelstein, B., Meeker, A.K., Kinzler, K.W., Papadopoulos, N., Diaz, Jr., L.A., Yan, H., 2012. Frequent ATRX, CIC, FUBP1 and IDH1 mutations refine the classification of malignant gliomas. Oncotarget 3, 709–722. doi:10.18632/oncotarget.588

Johannessen, T.-C.A., Bjerkvig, R., Tysnes, B.B., 2008. DNA repair and cancer stem-like cells – Potential partners in glioma drug resistance? Cancer Treatment Reviews 34, 558–567. doi:10.1016/j.ctrv.2008.03.125

Jue, T.R., McDonald, K.L., 2016. The challenges associated with molecular targeted therapies for glioblastoma. Journal of Neuro-Oncology 127, 427–434. doi:10.1007/s11060-016-2080-6

Jung, T.-Y., Jung, S., Moon, K.-S., Kim, I.-Y., Kang, S.-S., Kim, Y.-H., Park, C.-S., Lee, K.-H., 2010. Changes of the O6-methylguanine-DNA methyltransferase promoter methylation and MGMT protein expression after adjuvant treatment in glioblastoma. Oncology reports 23, 1269–76.

Kahn, S.A., Biasoli, D., Garcia, C., Geraldo, L.H., Pontes, B., Sobrinho, M., Frauches, A.C., Romao, L., Soletti, R.C., Assuncao Fdos, S., Tovar-Moll, F., de Souza, J.M., Lima, F.R., Anderluh, G., Moura-Neto, V., 2012. Equinatoxin II potentiates temozolomide- and etoposide-induced glioblastoma cell death. Curr Top Med Chem 12, 2082–2093.

Kaina, B., Christmann, M., Naumann, S., Roos, W.P., 2007. MGMT: key node in the battle against genotoxicity, carcinogenicity and apoptosis induced by alkylating agents. DNA repair 6, 1079–99. doi:10.1016/j.dnarep.2007.03.008

Kamburoğlu, G., Kiratli, H., Söylemezoğlu, F., Bilgiç, S., 2007. Clinicopathological parameters and expression of P-glycoprotein and MRP-1 in retinoblastoma. Ophthalmic research 39, 191–7. doi:10.1159/000104680

Kameyama, S., Horie, M., Kikuchi, T., Omura, T., Tadokoro, A., Takeuchi, T., Nakase, I., Sugiura, Y., Futaki, S., 2007. Acid wash in determining cellular uptake of Fab/cell-permeating peptide conjugates. Biopolymers 88, 98–107. doi:10.1002/bip.20689

Kanzawa, T., Germano, I.M., Komata, T., Ito, H., Kondo, Y., Kondo, S., 2004. Role of autophagy in temozolomide-induced cytotoxicity for malignant glioma cells. Cell Death and Differentiation 11, 448–457. doi:10.1038/sj.cdd.4401359

Kao, H.W., Chiang, S.W., Chung, H.W., Tsai, F.Y., Chen, C.Y., 2013. Advanced MR imaging of gliomas: An update. BioMed Research International 2013. doi:10.1155/2013/970586

Karim, R., Palazzo, C., Evrard, B., Piel, G., 2016. Nanocarriers for the treatment of glioblastoma multiforme: Current state-of-the-art. Journal of controlled release : official journal of the Controlled Release Society

227, 23–37. doi:10.1016/j.jconrel.2016.02.026

Karkkainen, M.J., Petrova, T. V, 2000. Vascular endothelial growth factor receptors in the regulation of angiogenesis and lymphangiogenesis. Oncogene 19, 5598–5605. doi:10.1038/sj.onc.1203855

Karoubi, G., Cortes-Dericks, L., Gugger, M., Galetta, D., Spaggiari, L., Schmid, R.A., 2010. Atypical expression and distribution of embryonic stem cell marker, OCT4, in human lung adenocarcinoma. Journal of Surgical Oncology 102, 689–698. doi:10.1002/jso.21665

Kato, T., Natsume, A., Toda, H., Iwamizu, H., Sugita, T., Hachisu, R., Watanabe, R., Yuki, K., Motomura, K., Bankiewicz, K., Wakabayashi, T., 2010. Efficient delivery of liposome-mediated MGMT-siRNA reinforces the cytotoxity of temozolomide in GBM-initiating cells. Gene Therapy 17, 1363–1371. doi:10.1038/gt.2010.88

Kemper, E.M., van Zandbergen, A.E., Cleypool, C., Mos, H.A., Boogerd, W., Beijnen, J.H., van Tellingen, O., 2003. Increased penetration of paclitaxel into the brain by inhibition of P-Glycoprotein. Clinical cancer research : an official journal of the American Association for Cancer Research 9, 2849–55.

Khosla, D., 2016. Concurrent therapy to enhance radiotherapeutic outcomes in glioblastoma. Ann Transl Med 4, 54. doi:10.3978/j.issn.2305-5839.2016.01.25

Kim, M.-J., Lee, J.-H., Kim, Y.-K., Myoung, H., Yun, P.-Y., 2007. The role of tamoxifen in combination with cisplatin on oral squamous cell carcinoma cell lines. Cancer Letters 245, 284–292. doi:10.1016/j.canlet.2006.01.017

Kitahara, C.M., Wang, S.S., Melin, B.S., Wang, Z., Braganza, M., Inskip, P.D., Albanes, D., Andersson, U., Beane Freeman, L.E., Buring, J.E., Carreón, T., Feychting, M., Gapstur, S.M., Gaziano, J.M., Giles, G.G., Hallmans, G., Hankinson, S.E., Henriksson, R., Hsing, A.W., Johansen, C., Linet, M.S., McKean-Cowdin, R., Michaud, D.S., Peters, U., Purdue, M.P., Rothman, N., Ruder, A.M., Sesso, H.D., Severi, G., Shu, X.-O., Stevens, V.L., Visvanathan, K., Waters, M.A., White, E., Wolk, A., Zeleniuch-Jacquotte, A., Zheng, W., Hoover, R., Fraumeni, J.F., Chatterjee, N., Yeager, M., Chanock, S.J., Hartge, P., Rajaraman, P., 2012. Association between adult height, genetic susceptibility and risk of glioma. International journal of epidemiology 41, 1075–85. doi:10.1093/ije/dys114

Kleihues, P., Louis, D.N., Scheithauer, B.W., Rorke, L.B., Reifenberger, G., Burger, P.C., Cavenee, W.K., 2002. The WHO classification of tumors of the nervous system. Journal of neuropathology and experimental neurology 61, 215-25–9.

Kleppe, M., Levine, R.L., 2014. Tumor Heterogeneity Confounds and Illuminates: Assessing the implications. Nat Med 20, 342–344.

Knudsen, E.S., Wang, J.Y.J., 2010. Targeting the RB-pathway in Cancer Therapy. Clinical Cancer Research 16, 1094–1099. doi:10.1158/1078-0432.CCR-09-0787

Koo, Y.-E.L., Reddy, G.R., Bhojani, M., Schneider, R., Philbert, M.A., Rehemtulla, A., Ross, B.D., Kopelman, R., 2006. Brain cancer diagnosis and therapy with nanoplatforms. Advanced drug delivery reviews 58, 1556–77. doi:10.1016/j.addr.2006.09.012

Koukourakis, M.I., Koukouraki, S., Fezoulidis, I., Kelekis, N., Kyrias, G., Archimandritis, S., Karkavitsas, K., 2000. High intratumoural accumulation of stealth liposomal doxorubicin (Caelyx) in glioblastomas and in metastatic brain tumours. British Journal of Cancer 83, 1281–1286. doi:10.1054/bjoc.2000.1459

Koutsioumpa, M., Polytarchou, C., Courty, J., Zhang, Y., Kieffer, N., Mikelis, C., Skandalis, S.S., Hellman,

U., Iliopoulos, D., Papadimitriou, E., 2013. Interplay between v 3 Integrin and Nucleolin Regulates Human Endothelial and Glioma Cell Migration. Journal of Biological Chemistry 288, 343–354. doi:10.1074/jbc.M112.387076

Lachance, D.H., Yang, P., Johnson, D.R., Decker, P.A., Kollmeyer, T.M., McCoy, L.S., Rice, T., Xiao, Y., Ali-Osman, F., Wang, F., Stoddard, S.M., Sprau, D.J., Kosel, M.L., Wiencke, J.K., Wiemels, J.L., Patoka, J.S., Davis, F., McCarthy, B., Rynearson, A.L., Worra, J.B., Fridley, B.L., O'Neill, B.P., Buckner, J.C., Il'yasova, D., Jenkins, R.B., Wrensch, M.R., 2011. Associations of high-grade glioma with glioma risk alleles and histories of allergy and smoking. American journal of epidemiology 174, 574–81. doi:10.1093/aje/kwr124

Lakhal, S., Wood, M.J.A., 2011. Exosome nanotechnology: An emerging paradigm shift in drug delivery. BioEssays 33, 737–741. doi:10.1002/bies.201100076

Lakhan, S.E., Harle, L., Guillamo, J., Monjour, A., Taillandier, L., Devaux, B., Varlet, P., Haie-Meder, C., Defer, G., Maison, P., Mazeron, J., Cornu, P., Delattre, J., Albright, A., Albright, A., Freeman, C., Perilongo, G., Epstein, F., Constantini, S., Nadvi, S., Ebrahim, F., Corr, P., Kwon, J., Kim, I., Cheon, J., Kim, W., Moon, S., Kim, T., Chi, J., Wang, K., Chung, J., Yeon, K., Ikeda, T., Yamakawa, Y., Ochiai, H., Yamanaka, H., Yano, T., Hayashi, T., Shuangshoti, S., Wolff, R., Zimmermann, M., Marquardt, G., Lanfermann, H., Nafe, R., Seifert, V., Badhe, P., Chauhan, P., Mehta, N., Mantravadi, R., Phatak, R., Bellur, S., Liebner, E., Haas, R., 2009. Difficult diagnosis of brainstem glioblastoma multiforme in a woman: a case report and review of the literature. Journal of Medical Case Reports 3, 87. doi:10.1186/1752-1947-3-87

Lathia, J.D., Mack, S.C., Mulkearns-Hubert, E.E., Valentim, C.L.L., Rich, J.N., 2015. Cancer stem cells in glioblastoma. Genes & development 29, 1203–17. doi:10.1101/gad.261982.115

Lau, D., Magill, S.T., Aghi, M.K., 2014. Molecularly targeted therapies for recurrent glioblastoma: current and future targets. Neurosurgical Focus 37, E15. doi:10.3171/2014.9.FOCUS14519

Lee, E.J., Ahn, K.J., Lee, E.K., Lee, Y.S., Kim, D.B., 2013. Potential role of advanced MRI techniques for the peritumoural region in differentiating glioblastoma multiforme and solitary metastatic lesions. Clinical radiology 68, e689-97. doi:10.1016/j.crad.2013.06.021

Lee, E.Q., Kuhn, J., Lamborn, K.R., Abrey, L., DeAngelis, L.M., Lieberman, F., Robins, H.I., Chang, S.M., Yung, W.K.A., Drappatz, J., Mehta, M.P., Levin, V.A., Aldape, K., Dancey, J.E., Wright, J.J., Prados, M.D., Cloughesy, T.F., Gilbert, M.R., Wen, P.Y., 2012. Phase I/II study of sorafenib in combination with temsirolimus for recurrent glioblastoma or gliosarcoma: North American Brain Tumor Consortium study 05-02. Neuro-oncology 14, 1511–8. doi:10.1093/neuonc/nos264

Lee, J., Kotliarova, S., Kotliarov, Y., Li, A., Su, Q., Donin, N.M., Pastorino, S., Purow, B.W., Christopher, N., Zhang, W., Park, J.K., Fine, H.A., 2006. Tumor stem cells derived from glioblastomas cultured in bFGF and EGF more closely mirror the phenotype and genotype of primary tumors than do serum-cultured cell lines. Cancer cell 9, 391–403. doi:10.1016/j.ccr.2006.03.030

Lee, S.Y., 2016. Temozolomide resistance in glioblastoma multiforme. Genes & Diseases 3, 198–210. doi:10.1016/j.gendis.2016.04.007

Leite, E.A., Souza, C.M., Carvalho-Júnior, A.D., Coelho, L.G. V, Lana, A.M.Q., Cassali, G.D., Oliveira, M.C., 2012. Encapsulation of cisplatin in long-circulating and pH-sensitive liposomes improves its

antitumor effect and reduces acute toxicity. International journal of nanomedicine 7, 5259–69. doi:10.2147/IJN.S34652

Li, L., Hou, J., Liu, X., Guo, Y., Wu, Y., Zhang, L., Yang, Z., 2014. Nucleolin-targeting liposomes guided by aptamer AS1411 for the delivery of siRNA for the treatment of malignant melanomas. Biomaterials 35, 3840–3850. doi:10.1016/j.biomaterials.2014.01.019

Li, W.-B., Tang, K., Chen, Q., Li, S., Qiu, X.-G., Li, S.-W., Jiang, T., 2012. Li et al. MRI Manifestions Correlate with Survival of GBM Patients 120 MRI Manifestions Correlate with Survival of Glioblastoma Multiforme Patients. doi:10.3969/j.issn.2095-3941.2012.02.007

Li, X., Wu, C., Chen, N., Gu, H., Yen, A., Cao, L., Wang, E., Wang, L., 2016. PI3K/Akt/mTOR signaling pathway and targeted therapy for glioblastoma. Oncotarget 7, 33440–50. doi:10.18632/oncotarget.7961

Liang, C.-C., Park, A.Y., Guan, J.-L., 2007. In vitro scratch assay: a convenient and inexpensive method for analysis of cell migration in vitro. Nature protocols 2, 329–33. doi:10.1038/nprot.2007.30

Lidar, Z., Mardor, Y., Jonas, T., Pfeffer, R., Faibel, M., Nass, D., Hadani, M., Ram, Z., 2004. Convection-enhanced delivery of paclitaxel for the treatment of recurrent malignant glioma: a phase I/II clinical study. Journal of neurosurgery 100, 472–9. doi:10.3171/jns.2004.100.3.0472

Liebelt, B.D., Shingu, T., Zhou, X., Ren, J., Shin, S.A., Hu, J., 2016. Glioma Stem Cells: Signaling, Microenvironment, and Therapy. Stem Cells International 2016. doi:10.1155/2016/7849890

Lima, F.R.S., Kahn, S.A., Soletti, R.C., Biasoli, D., Alves, T., da Fonseca, A.C.C., Garcia, C., Romão, L., Brito, J., Holanda-Afonso, R., Faria, J., Borges, H., Moura-Neto, V., 2012. Glioblastoma: therapeutic challenges, what lies ahead. Biochimica et Biophysica Acta 1826, 338–49. doi:10.1016/j.bbcan.2012.05.004

Lin, G.G., Scott, J.G., 2012. NIH Public Access 100, 130–134. doi:10.1016/j.pestbp.2011.02.012.Investigations

Linkous, A.G., Yazlovitskaya, E.M., 2011. Angiogenesis in glioblastoma multiforme: navigating the maze. Anti-cancer agents in medicinal chemistry 11, 712–8.

Linn, S.C., Giaccone, G., van Diest, P.J., Blokhuis, W.M., van der Valk, P., van Kalken, C.K., Kuiper, C.M., Pinedo, H.M., Baak, J.P., 1995. Prognostic relevance of P-glycoprotein expression in breast cancer. Annals of oncology : official journal of the European Society for Medical Oncology / ESMO 6, 679–685.

Litzinger, D.C., Buiting, A.M., van Rooijen, N., Huang, L., 1994. Effect of liposome size on the circulation time and intraorgan distribution of amphipathic poly(ethylene glycol)-containing liposomes. Biochimica et biophysica acta 1190, 99–107.

Liu, A., Hou, C., Chen, H., Zong, X., Zong, P., 2016. Genetics and Epigenetics of Glioblastoma: Applications and Overall Incidence of IDH1 Mutation. Frontiers in oncology 6, 16. doi:10.3389/fonc.2016.00016

Liu, H.-L., Hua, M.-Y., Chen, P.-Y., Chu, P.-C., Pan, C.-H., Yang, H.-W., Huang, C.-Y., Wang, J.-J., Yen, T.-C., Wei, K.-C., 2010. Blood-Brain Barrier Disruption with Focused Ultrasound Enhances Delivery of Chemotherapeutic Drugs for Glioblastoma Treatment. Radiology 255, 415–425. doi:10.1148/radiol.10090699

Liu, Y., Lu, W., 2012. Recent advances in brain tumor-targeted nano-drug delivery systems. Expert opinion on drug delivery 9, 671–86. doi:10.1517/17425247.2012.682726

Loh, Y.-H., Wu, Q., Chew, J.-L., Vega, V.B., Zhang, W., Chen, X., Bourque, G., George, J., Leong, B., Liu, J., Wong, K.-Y., Sung, K.W., Lee, C.W.H., Zhao, X.-D., Chiu, K.-P., Lipovich, L., Kuznetsov, V.A., Robson, P., Stanton, L.W., Wei, C.-L., Ruan, Y., Lim, B., Ng, H.-H., 2006. The Oct4 and Nanog transcription network regulates pluripotency in mouse embryonic stem cells. Nature Genetics 38, 431–440. doi:10.1038/ng1760

Louis, D.N., 1994. The p53 gene and protein in human brain tumors. Journal of neuropathology and experimental neurology 53, 11–21.

Louis, D.N., Perry, A., Reifenberger, G., von Deimling, A., Figarella-Branger, D., Cavenee, W.K., Ohgaki, H., Wiestler, O.D., Kleihues, P., Ellison, D.W., 2016. The 2016 World Health Organization Classification of Tumors of the Central Nervous System: a summary. Acta Neuropathologica 1–18. doi:10.1007/s00401-016-1545-1

Mabray, M.C., Barajas, R.F., Cha, S., Cha, S., 2015. Modern brain tumor imaging. Brain tumor research and treatment 3, 8–23. doi:10.14791/btrt.2015.3.1.8

Maeda, H., Ueda, M., Morinaga, T., Matsumoto, T., 1985. Conjugation of poly(styrene-co-maleic acid) derivatives to the antitumor protein neocarzinostatin: pronounced improvements in pharmacological properties. Journal of medicinal chemistry 28, 455–61.

Mahvash, M., Hugo, H.-H., Maslehaty, H., Mehdorn, H.M., Stark, A.M., 2011. Glioblastoma multiforme in children: report of 13 cases and review of the literature. Pediatric neurology 45, 178–80. doi:10.1016/j.pediatrneurol.2011.05.004

Mallini, P., Lennard, T., Kirby, J., Meeson, A., 2014. Epithelial-to-mesenchymal transition: what is the impact on breast cancer stem cells and drug resistance. Cancer treatment reviews 40, 341–8. doi:10.1016/j.ctrv.2013.09.008

Mao, H., LeBrun, D.G., Yang, J., Zhu, V.F., Li, M., 2012. Deregulated Signaling Pathways in Glioblastoma Multiforme: Molecular Mechanisms and Therapeutic Targets. Cancer Investigation 30, 48–56. doi:10.3109/07357907.2011.630050

Martiny-Baron, G., Fabbro, D., 2007. Classical PKC isoforms in cancer. Pharmacological research 55, 477–86. doi:10.1016/j.phrs.2007.04.001

Martuscello, R.T., Reynolds, B.A., Kesari, S., 2016. Glioma Stem Cells. Translational Neuroscience 335–356. doi:10.1007/978-1-4899-7654-3_18

Massarweh, S., Osborne, C.K., Creighton, C.J., Qin, L., Tsimelzon, A., Huang, S., Weiss, H., Rimawi, M., Schiff, R., 2008. Tamoxifen Resistance in Breast Tumors Is Driven by Growth Factor Receptor Signaling with Repression of Classic Estrogen Receptor Genomic Function. Cancer Research 68, 826–833. doi:10.1158/0008-5472.CAN-07-2707

Matias, D., Balça-Silva, J., Dubois, L.G., Pontes, B., Ferrer, V.P., Rosário, L., do Carmo, A., Echevarria-Lima, J., Sarmento-Ribeiro, A.B., Lopes, M.C., Moura-Neto, V., 2017. Dual treatment with shikonin and temozolomide reduces glioblastoma tumor growth, migration and glial-to-mesenchymal transition. Cellular Oncology. doi:10.1007/s13402-017-0320-1

Matsui, W.H., 2016. Cancer stem cell signaling pathways. Medicine 95, S8–S19. doi:10.1097/MD.0000000000004765

Mayo, L.D., Dixon, J.E., Durden, D.L., Tonks, N.K., Donner, D.B., 2002. PTEN Protects p53 from Mdm2

and Sensitizes Cancer Cells to Chemotherapy. Journal of Biological Chemistry 277, 5484–5489. doi:10.1074/jbc.M108302200

McLendon, R., Friedman, A., Bigner, D., Van Meir, E.G., Brat, D.J., M. Mastrogianakis, G., Olson, J.J., Mikkelsen, T., Lehman, N., Aldape, K., Alfred Yung, W.K., Bogler, O., VandenBerg, S., Berger, M., Prados, M., Muzny, D., Morgan, M., Scherer, S., Sabo, A., Nazareth, L., Lewis, L., Hall, O., Zhu, Y., Ren, Y., Alvi, O., Yao, J., Hawes, A., Jhangiani, S., Fowler, G., San Lucas, A., Kovar, C., Cree, A., Dinh, H., Santibanez, J., Joshi, V., Gonzalez-Garay, M.L., Miller, C.A., Milosavljevic, A., Donehower, L., Wheeler, D.A., Gibbs, R.A., Cibulskis, K., Sougnez, C., Fennell, T., Mahan, S., Wilkinson, J., Ziaugra, L., Onofrio, R., Bloom, T., Nicol, R., Ardlie, K., Baldwin, J., Gabriel, S., Lander, E.S., Ding, L., Fulton, R.S., McLellan, M.D., Wallis, J., Larson, D.E., Shi, X., Abbott, R., Fulton, L., Chen, K., Koboldt, D.C., Wendl, M.C., Meyer, R., Tang, Y., Lin, L., Osborne, J.R., Dunford-Shore, B.H., Miner, T.L., Delehaunty, K., Markovic, C., Swift, G., Courtney, W., Pohl, C., Abbott, S., Hawkins, A., Leong, S., Haipek, C., Schmidt, H., Wiechert, M., Vickery, T., Scott, S., Dooling, D.J., Chinwalla, A., Weinstock, G.M., Mardis, E.R., Wilson, R.K., Getz, G., Winckler, W., Verhaak, R.G.W., Lawrence, M.S., O'Kelly, M., Robinson, J., Alexe, G., Beroukhim, R., Carter, S., Chiang, D., Gould, J., Gupta, S., Korn, J., Mermel, C., Mesirov, J., Monti, S., Nguyen, H., Parkin, M., Reich, M., Stransky, N., Weir, B.A., Garraway, L., Golub, T., Meyerson, M., Chin, L., Protopopov, A., Zhang, J., Perna, I., Aronson, S., Sathiamoorthy, N., Ren, G., Yao, J., Wiedemeyer, W.R., Kim, H., Won Kong, S., Xiao, Y., Kohane, I.S., Seidman, J., Park, P.J., Kucherlapati, R., Laird, P.W., Cope, L., Herman, J.G., Weisenberger, D.J., Pan, F., Van Den Berg, D., Van Neste, L., Mi Yi, J., Schuebel, K.E., Baylin, S.B., Absher, D.M., Li, J.Z., Southwick, A., Brady, S., Aggarwal, A., Chung, T., Sherlock, G., Brooks, J.D., Myers, R.M., Spellman, P.T., Purdom, E., Jakkula, L.R., Lapuk, A. V., Marr, H., Dorton, S., Gi Choi, Y., Han, J., Ray, A., Wang, V., Durinck, S., Robinson, M., Wang, N.J., Vranizan, K., Peng, V., Van Name, E., Fontenay, G. V., Ngai, J., Conboy, J.G., Parvin, B., Feiler, H.S., Speed, T.P., Gray, J.W., Brennan, C., Socci, N.D., Olshen, A., Taylor, B.S., Lash, A., Schultz, N., Reva, B., Antipin, Y., Stukalov, A., Gross, B., Cerami, E., Qing Wang, W., Qin, L.-X., Seshan, V.E., Villafania, L., Cavatore, M., Borsu, L., Viale, A., Gerald, W., Sander, C., Ladanyi, M., Perou, C.M., Neil Hayes, D., Topal, M.D., Hoadley, K.A., Qi, Y., Balu, S., Shi, Y., Wu, J., Penny, R., Bittner, M., Shelton, T., Lenkiewicz, E., Morris, S., Beasley, D., Sanders, S., Kahn, A., Sfeir, R., Chen, J., Nassau, D., Feng, L., Hickey, E., Zhang, J., Weinstein, J.N., Barker, A., Gerhard, D.S., Vockley, J., Compton, C., Vaught, J., Fielding, P., Ferguson, M.L., Schaefer, C., Madhavan, S., Buetow, K.H., Collins, F., Good, P., Guyer, M., Ozenberger, B., Peterson, J., Thomson, E., 2008. Comprehensive genomic characterization defines human glioblastoma genes and core pathways. Nature 455, 1061–1068. doi:10.1038/nature07385

Meacham, C.E., Morrison, S.J., 2013. Tumour heterogeneity and cancer cell plasticity. Nature 501, 328–37. doi:10.1038/nature12624

Meir, E.G. Van, Hadjipanayis, C.G., Norden, A.D., Shu, H., Wen, P.Y., Olson, J.J., 2010. NIH Public Access. Cancer Journal, The 60, 166–193. doi:10.3322/caac.20069.Exciting

Mellinghoff, I.K., Wang, M.Y., Vivanco, I., Haas-Kogan, D.A., Zhu, S., Dia, E.Q., Lu, K. V., Yoshimoto, K., Huang, J.H.Y., Chute, D.J., Riggs, B.L., Horvath, S., Liau, L.M., Cavenee, W.K., Rao, P.N., Beroukhim, R., Peck, T.C., Lee, J.C., Sellers, W.R., Stokoe, D., Prados, M., Cloughesy, T.F., Sawyers,

C.L., Mischel, P.S., 2005. Molecular Determinants of the Response of Glioblastomas to EGFR Kinase Inhibitors. New England Journal of Medicine 353, 2012–2024. doi:10.1056/NEJMoa051918

Messing, A., Brenner, M., 2003. GFAP: functional implications gleaned from studies of genetically engineered mice. Glia 43, 87–90. doi:10.1002/glia.10219

Michler-Stuke, A., Wolff, J.R., Bottenstein, J.E., 1984. Factors influencing astrocyte growth and development in defined media. International Journal of Developmental Neuroscience 2, 575–584. doi:10.1016/0736-5748(84)90035-2

Milinkovic, V., Bankovic, J., Rakic, M., Milosevic, N., Stankovic, T., Jokovic, M., Milosevic, Z., Skender-Gazibara, M., Podolski-Renic, A., Pesic, M., Ruzdijic, S., Tanic, N., 2012. Genomic instability and p53 alterations in patients with malignant glioma. Experimental and Molecular Pathology 93, 200–206. doi:10.1016/j.yexmp.2012.05.010

Miller, D.H., Rudge, P., Johnson, G., Kendall, B.E., Macmanus, D.G., Moseley, I.F., Barnes, D., McDonald, W.I., 1988. Serial gadolinium enhanced magnetic resonance imaging in multiple sclerosis. Brain : a journal of neurology 927–39.

Miller, D.S., 2015. Regulation of ABC transporters blood-brain barrier: the good, the bad, and the ugly. Advances in cancer research 125, 43–70. doi:10.1016/bs.acr.2014.10.002

Millward, M.J., Cantwell, B.M., Lien, E.A., Carmichael, J., Harris, A.L., 1992. Intermittent high-dose tamoxifen as a potential modifier of multidrug resistance. European journal of cancer (Oxford, England : 1990) 28A, 805–10. doi:10.1016/0959-8049(92)90119-M

Mochly-Rosen, D., Das, K., Grimes, K. V., 2012. Protein kinase C, an elusive therapeutic target? Nature Reviews Drug Discovery 11, 937–957. doi:10.1038/nrd3871

Moiyadi, A. V, Shetty, P.M., 2012. Perioperative outcomes following surgery for brain tumors: Objective assessment and risk factor evaluation. Journal of neurosciences in rural practice 3, 28–35. doi:10.4103/0976-3147.91927

Molnár, J., Engi, H., Hohmann, J., Molnár, P., Deli, J., Wesolowska, O., Michalak, K., Wang, Q., 2010. Reversal of multidrug resitance by natural substances from plants. Current topics in medicinal chemistry 10, 1757–68.

Momekova, D., Rangelov, S., Lambov, N., 2010. Long-circulating, pH-sensitive liposomes. Methods in molecular biology (Clifton, N.J.) 605, 527–44. doi:10.1007/978-1-60327-360-2_35

Morandi, L., Franceschi, E., de Biase, D., Marucci, G., Tosoni, A., Ermani, M., Pession, A., Tallini, G., Brandes, A., 2010. Promoter methylation analysis of O6-methylguanine-DNA methyltransferase in glioblastoma: detection by locked nucleic acid based quantitative PCR using an imprinted gene (SNURF) as a reference. BMC Cancer 10, 48. doi:10.1186/1471-2407-10-48

Moreira, J.N., Ishida, T., Gaspar, R., Allen, T.M., 2002. Use of the post-insertion technique to insert peptide ligands into pre-formed stealth liposomes with retention of binding activity and cytotoxicity. Pharmaceutical Research 19, 265–269. doi:10.1023/A:1014434732752

Moura-Neto, V., Campanati, L., Matias, D., Pereira, C.M., Freitas, C., Coelho-Aguiar, J.M., Leite de Sampaio e Spohr, T.C., Tavares-Gomes, A.L., Pinheiro-Aguiar, D., Kahn, S.A., Silva-Balça, J., Pontes, B., Porto-Carreiro, I., Faria, J., Martins, R.A.P., Lima-Costa, S., Dias-Costa, M. de F., Lopes, M.C., Souza Lima, F.R., 2014. Glioblastomas and the Special Role of Adhesion Molecules in Their Invasion, in:

Glioma Cell Biology. Springer Vienna, Vienna, pp. 293–315. doi:10.1007/978-3-7091-1431-5_11

Moura, V., Lacerda, M., Figueiredo, P., Corvo, M.L., Cruz, M.E.M., Soares, R., de Lima, M.C.P., Simões, S., Moreira, J.N., 2012. Targeted and intracellular triggered delivery of therapeutics to cancer cells and the tumor microenvironment: impact on the treatment of breast cancer. Breast cancer research and treatment 133, 61–73. doi:10.1007/s10549-011-1688-7

Mukhopadhyay, A., Mukhopadhyay, B., Basu, S.K., 1995. Circumvention of multidrug resistance in neoplastic cells through scavenger receptor mediated drug delivery. FEBS letters 376, 95–8.

Munoz, J.L., Walker, N.D., Scotto, K.W., Rameshwar, P., 2015. Temozolomide competes for P-glycoprotein and contributes to chemoresistance in glioblastoma cells. Cancer Letters 367, 69–75. doi:10.1016/j.canlet.2015.07.013

Naidu, M.D., Mason, J.M., Pica, R. V, Fung, H., Peña, L.A., 2010. Radiation resistance in glioma cells determined by DNA damage repair activity of Ape1/Ref-1. Journal of radiation research 51, 393–404.

Naito, M., Tsuruo, T., 1989. Competitive inhibition by verapamil of ATP-dependent high affinity vincristine binding to the plasma membrane of multidrug-resistant K562 cells without calcium ion involvement. Cancer research 49, 1452–5.

Nakada, M., Nambu, E., Furuyama, N., Yoshida, Y., Takino, T., Hayashi, Y., Sato, H., Sai, Y., Tsuji, T., Miyamoto, K., Hirao, a, Hamada, J., 2013. Integrin α3 is overexpressed in glioma stem-like cells and promotes invasion. British journal of cancer 108, 2516–24. doi:10.1038/bjc.2013.218

Naus, C.C., Giaume, C., 2016. Bridging the gap to therapeutic strategies based on connexin/pannexin biology. Journal of translational medicine 14, 330. doi:10.1186/s12967-016-1089-0

Naus, C.C., Laird, D.W., 2010. Implications and challenges of connexin connections to cancer. Nature reviews. Cancer 10, 435–41. doi:10.1038/nrc2841

Newlands, E.S., Stevens, M.F., Wedge, S.R., Wheelhouse, R.T., Brock, C., 1997. Temozolomide: a review of its discovery, chemical properties, pre-clinical development and clinical trials. Cancer treatment reviews 23, 35–61.

Nik-Zainal, S., Van Loo, P., Wedge, D.C., Alexandrov, L.B., Greenman, C.D., Lau, K.W., Raine, K., Jones, D., Marshall, J., Ramakrishna, M., Shlien, A., Cooke, S.L., Hinton, J., Menzies, A., Stebbings, L.A., Leroy, C., Jia, M., Rance, R., Mudie, L.J., Gamble, S.J., Stephens, P.J., McLaren, S., Tarpey, P.S., Papaemmanuil, E., Davies, H.R., Varela, I., McBride, D.J., Bignell, G.R., Leung, K., Butler, A.P., Teague, J.W., Martin, S., Jönsson, G., Mariani, O., Boyault, S., Miron, P., Fatima, A., Langerød, A., Aparicio, S.A.J.R., Tutt, A., Sieuwerts, A.M., Borg, Å., Thomas, G., Salomon, A.V., Richardson, A.L., Børresen-Dale, A.-L., Futreal, P.A., Stratton, M.R., Campbell, P.J., Breast Cancer Working Group of the International Cancer Genome Consortium, 2012. The life history of 21 breast cancers. Cell 149, 994–1007. doi:10.1016/j.cell.2012.04.023

Niu, C.S., Li, D.X., Liu, Y.H., Fu, X.M., Tang, S.F., Li, J., 2011. Expression of NANOG in human gliomas and its relationship with undifferentiated glioma cells. Oncology Reports 26, 593–601. doi:10.3892/or.2011.1308

Noell, S., Ritz, R., Wolburg-Buchholz, K., Wolburg, H., Fallier-Becker, P., Moe, S., Sorbo, J., Sogaard, R., Zeuthen, T., Petter, O., Silberstein, C., Bouley, R., Huang, Y., Fang, P., Pastor-Soler, N., Wolburg, H., Wolburg-Buchholz, K., Fallier-Becker, P., Noell, S., Mack, A., Dermietzel, R., Furman, C., Gorelick-

Feldman, D., Davidson, K., Yasumura, T., Neely, J., Noell, S., Fallier-Becker, P., Beyer, C., Kroger, S., Mack, A., Noell, S., Fallier-Becker, P., Deutsch, U., Mack, A., Wolburg, H., Fallier-Becker, P., Sperveslage, J., Wolburg, H., Noell, S., McMahan, U., Tsen, G., Halfter, W., Kroger, S., Cole, G., Bezakova, G., Ruegg, M., Barber, A., Lieth, E., Rohlmann, A., Gocht, A., Wolburg, H., Verkman, A., Saadoun, S., Papadopoulos, M., Davies, D., Krishna, S., Bell, B., Warth, A., Mittelbronn, M., Wolburg, H., Manley, G., Fujimura, M., Ma, T., Noshita, N., Filiz, F., Vajda, Z., Promeneur, D., Doczi, T., Sulyok, E., Frokiaer, J., Ke, C., Poon, W., Ng, H., Pang, J., Chan, Y., Amiry-Moghaddam, M., Otsuka, T., Hurn, P., Traystman, R., Haug, F., Papadopoulos, M., Manley, G., Krishna, S., Verkman, A., Wolburg, H., Noell, S., Fallier-Becker, P., Mack, A., Wolburg-Buchholz, K., Zelenina, M., Solenov, E., Ivanova, L., Zelenina, M., Solenov, E., Ivanova, L., Sontheimer, H., Engelhorn, T., Savaskan, N., Schwarz, M., Kreutzer, J., Meyer, E., McCoy, E., Haas, B., Sontheimer, H., Pandita, A., Aldape, K., Zadeh, G., Guha, A., James, C., Lee, J., Lund-Smith, C., Borboa, A., Gonzalez, A., Baird, A., McCoy, E., Sontheimer, H., Rascher, G., Fischmann, A., Kroger, S., Duffner, F., Grote, E., Warth, A., Kroger, S., Wolburg, H., Engel, A., Fujiyoshi, Y., Gonen, T., Walz, T., Hiroaki, Y., Tani, K., Kamegawa, A., Gyobu, N., Nishikawa, K., Zhang, H., Verkman, A., Giannini, C., Sarkaria, J., Saito, A., Uhm, J., Galanis, E., Benda, P., Lightbody, J., Sato, G., Levine, L., Sweet, W., Aas, A., Brun, A., Blennow, C., Stromblad, S., Salford, L., Serano, R., Pegram, C., Bigner, D., Neely, J., Christensen, B., Nielsen, S., Agre, P., Bradford, M., Ivanova, T., Mendez, P., Carcia-Segura, L., Beyer, C., Frericks, M., Esser, C., 2012. An Allograft Glioma Model Reveals the Dependence of Aquaporin-4 Expression on the Brain Microenvironment. PLoS ONE 7, e36555. doi:10.1371/journal.pone.0036555

Nonoguchi, N., Ohta, T., Oh, J.-E., Kim, Y.-H., Kleihues, P., Ohgaki, H., 2013. TERT promoter mutations in primary and secondary glioblastomas. Acta Neuropathologica 126, 931–937. doi:10.1007/s00401-013-1163-0

O'Brian, C.A., Liskamp, R.M., Solomon, D.H., Weinstein, I.B., 1986. Triphenylethylenes: a new class of protein kinase C inhibitors. Journal of the National Cancer Institute 76, 1243–6.

O'Brian, C.A., Liskamp, R.M., Solomon, D.H., Weinstein, I.B., 1985. Inhibition of Protein Kinase C by Tamoxifen. Cancer Research 45.

Ogden, A.T., Waziri, A.E., Lochhead, R.A., Fusco, D., Lopez, K., Ellis, J.A., Kang, J., Assanah, M., McKhann, G.M., Sisti, M.B., McCormick, P.C., Canoll, P., Bruce, J.N., 2008. Identification of A2B5+CD133- tumor-initiating cells in adult human gliomas. Neurosurgery 62, 505-14–5. doi:10.1227/01.neu.0000316019.28421.95

Ohgaki, H., Kleihues, P., 2007. Genetic pathways to primary and secondary glioblastoma. The American journal of pathology 170, 1445–53. doi:10.2353/ajpath.2007.070011

Ohgaki, H., Kleihues, P., 2005. Epidemiology and etiology of gliomas. Acta neuropathologica 109, 93–108. doi:10.1007/s00401-005-0991-y

Okhrimenko, H., Lu, W., Xiang, C., Hamburger, N., Kazimirsky, G., Brodie, C., 2005. Protein Kinase C- Regulates the Apoptosis and Survival of Glioma Cells. Cancer Research 65, 7301–7309. doi:10.1158/0008-5472.CAN-05-1064

Oliveira-Nunes, M.C., Assad Kahn, S., de Oliveira Barbeitas, A.L., E Spohr, T.C.L. de S., Dubois, L.G.F., Ventura Matioszek, G.M., Querido, W., Campanati, L., de Brito Neto, J.M., Lima, F.R.S., Moura-Neto,

V., Carneiro, K., 2016. The availability of the embryonic TGF-β protein Nodal is dynamically regulated during glioblastoma multiforme tumorigenesis. Cancer cell international 16, 46. doi:10.1186/s12935-016-0324-3

Onishi, M., Kurozumi, K., Ichikawa, T., Date, I., 2013. Mechanisms of Tumor Development and Anti-angiogenic Therapy in Glioblastoma Multiforme. Neurol Med Chir (Tokyo) 53, 755–763. doi:DN/JST.JSTAGE/nmc/ra2013-0200 [pii]

Orellana, J.A., von Bernhardi, R., Giaume, C., Sáez, J.C., 2012. Glial hemichannels and their involvement in aging and neurodegenerative diseases. Reviews in the neurosciences 23, 163–77. doi:10.1515/revneuro-2011-0065

Orringer, D.A., Golby, A., Jolesz, F., 2012. Neuronavigation in the surgical management of brain tumors: current and future trends. Expert review of medical devices 9, 491–500. doi:10.1586/erd.12.42

Ortensi, B., Setti, M., Osti, D., Pelicci, G., 2013. Cancer stem cell contribution to glioblastoma invasiveness. Stem cell research & therapy 4, 18. doi:10.1186/scrt166

Ostermann, S., Csajka, C., Buclin, T., Leyvraz, S., Lejeune, F., Decosterd, L.A., Stupp, R., 2004. Plasma and cerebrospinal fluid population pharmacokinetics of temozolomide in malignant glioma patients. Clin Cancer Res 10, 3728–3736. doi:10.1158/1078-0432.CCR-03-0807

Ostrom, Q.T., Gittleman, H., Liao, P., Rouse, C., Chen, Y., Dowling, J., Wolinsky, Y., Kruchko, C., Barnholtz-Sloan, J., 2014. CBTRUS statistical report: primary brain and central nervous system tumors diagnosed in the United States in 2007-2011. Neuro-oncology 16 Suppl 4, iv1-63. doi:10.1093/neuonc/nou223

Owonikoko, T.K., Arbiser, J., Zelnak, A., Shu, H.-K.G., Shim, H., Robin, A.M., Kalkanis, S.N., Whitsett, T.G., Salhia, B., Tran, N.L., Ryken, T., Moore, M.K., Egan, K.M., Olson, J.J., 2014. Current approaches to the treatment of metastatic brain tumours. Nature Reviews Clinical Oncology 11, 203–222. doi:10.1038/nrclinonc.2014.25

Paff, M., Alexandru-Abrams, D., Hsu, F.P.K., Bota, D.A., 2014. The evolution of the EGFRvIII (rindopepimut) immunotherapy for glioblastoma multiforme patients. Human Vaccines & Immunotherapeutics 10, 3322–3331. doi:10.4161/21645515.2014.983002

Pardridge, W.M., 2012. Drug Transport across the Blood–Brain Barrier. Journal of Cerebral Blood Flow & Metabolism 32, 1959–1972. doi:10.1038/jcbfm.2012.126

Pardridge, W.M., 2003. Blood-brain barrier drug targeting: the future of brain drug development. Molecular interventions 3, 90–105, 51. doi:10.1124/mi.3.2.90

Pardridge, W.M., 2002. Drug and gene delivery to the brain: the vascular route. Neuron 36, 555–8.

Parsons, D.W., Jones, S., Zhang, X., Lin, J.C.-H., Leary, R.J., Angenendt, P., Mankoo, P., Carter, H., Siu, I.-M., Gallia, G.L., Olivi, A., McLendon, R., Rasheed, B.A., Keir, S., Nikolskaya, T., Nikolsky, Y., Busam, D.A., Tekleab, H., Diaz, L.A., Hartigan, J., Smith, D.R., Strausberg, R.L., Marie, S.K.N., Shinjo, S.M.O., Yan, H., Riggins, G.J., Bigner, D.D., Karchin, R., Papadopoulos, N., Parmigiani, G., Vogelstein, B., Velculescu, V.E., Kinzler, K.W., 2008. An integrated genomic analysis of human glioblastoma multiforme. Science (New York, N.Y.) 321, 1807–12. doi:10.1126/science.1164382

Patel, S., DiBiase, S., Meisenberg, B., Flannery, T., Patel, A., Dhople, A., Cheston, S., Amin, P., 2012. Phase I clinical trial assessing temozolomide and tamoxifen with concomitant radiotherapy for treatment of

high-grade glioma. International journal of radiation oncology, biology, physics 82, 739–42. doi:10.1016/j.ijrobp.2010.12.053

Patru, C., Romao, L., Varlet, P., Coulombel, L., Raponi, E., Cadusseau, J., Renault-Mihara, F., Thirant, C., Leonard, N., Berhneim, A., Mihalescu-Maingot, M., Haiech, J., Bièche, I., Moura-Neto, V., Daumas-Duport, C., Junier, M.-P., Chneiweiss, H., 2010. CD133, CD15/SSEA-1, CD34 or side populations do not resume tumor-initiating properties of long-term cultured cancer stem cells from human malignant glio-neuronal tumors. BMC cancer 10, 66. doi:10.1186/1471-2407-10-66

Pelloski, C.E., Gilbert, M.R., 2007. Current Treatment Options in Adult Glioblastoma. Oncology & Hematology Review (US) 105. doi:10.17925/OHR.2007.00.2.105

Pfaffl, M.W., 2001. A new mathematical model for relative quantification in real-time RT-PCR. Nucleic acids research 29, e45.

Phuphanich, S., Supko, J.G., Carson, K.A., Grossman, S.A., Burt Nabors, L., Mikkelsen, T., Lesser, G., Rosenfeld, S., Desideri, S., Olson, J.J., 2010. Phase 1 clinical trial of bortezomib in adults with recurrent malignant glioma. Journal of Neuro-Oncology 100, 95–103. doi:10.1007/s11060-010-0143-7

Piccirillo, S.G.M., Binda, E., Fiocco, R., Vescovi, A.L., Shah, K., 2009. Brain cancer stem cells. Journal of Molecular Medicine 87, 1087–1095. doi:10.1007/s00109-009-0535-3

Pistollato, F., Chen, H.-L., Rood, B.R., Zhang, H.-Z., D'Avella, D., Denaro, L., Gardiman, M., te Kronnie, G., Schwartz, P.H., Favaro, E., Indraccolo, S., Basso, G., Panchision, D.M., 2009. Hypoxia and HIF1α Repress the Differentiative Effects of BMPs in High-Grade Glioma. Stem Cells 27, 7–17. doi:10.1634/stemcells.2008-0402

Pollack, I.F., Randall, M.S., Kristofik, M.P., Kelly, R.H., Selker, R.G., Vertosick, F.T., 1990. Effect of tamoxifen on DNA synthesis and proliferation of human malignant glioma lines in vitro. Cancer research 50, 7134–8.

Popescu, A.M., Purcaru, S.O., Alexandru, O., Dricu, A., 2016. New perspectives in glioblastoma antiangiogenic therapy. Contemporary oncology (Poznan, Poland) 20, 109–18. doi:10.5114/wo.2015.56122

Porkka, K., Laakkonen, P., Hoffman, J.A., Bernasconi, M., Ruoslahti, E., 2002. A fragment of the HMGN2 protein homes to the nuclei of tumor cells and tumor endothelial cells in vivo. Proceedings of the National Academy of Sciences of the United States of America 99, 7444–9. doi:10.1073/pnas.062189599

Portnow, J., Badie, B., Chen, M., Liu, A., Blanchard, S., Synold, T.W., 2009. The neuropharmacokinetics of temozolomide in patients with resectable brain tumors: potential implications for the current approach to chemoradiation. Clinical cancer research : an official journal of the American Association for Cancer Research 15, 7092–8. doi:10.1158/1078-0432.CCR-09-1349

Primon, M., Huszthy, P.C., Motaln, H., Talasila, K.M., Torkar, A., Bjerkvig, R., Lah Turnšek, T., 2013. Cathepsin L silencing enhances arsenic trioxide mediated in vitro cytotoxicity and apoptosis in glioblastoma U87MG spheroids. Experimental Cell Research 319, 2637–2648. doi:10.1016/j.yexcr.2013.08.011

Puchner, M.J., Giese, A., 2000. Tamoxifen-resistant glioma-cell sub-populations are characterized by increased migration and proliferation. International Journal of Cancer 86, 468–73.

Qiu, Z.-K., Shen, D., Chen, Y.-S., Yang, Q.-Y., Guo, C.-C., Feng, B.-H., Chen, Z.-P., 2014. Enhanced MGMT expression contributes to temozolomide resistance in glioma stem-like cells. Chinese journal of cancer 33, 115–22. doi:10.5732/cjc.012.10236

Radzisheuskaya, A., Chia, G.L. Bin, dos Santos, R.L., Theunissen, T.W., Castro, L.F.C., Nichols, J., Silva, J.C.R., 2013. A defined Oct4 level governs cell state transitions of pluripotency entry and differentiation into all embryonic lineages. Nature cell biology 15, 579–90. doi:10.1038/ncb2742

Raizer, J.J., Abrey, L.E., Lassman, A.B., Chang, S.M., Lamborn, K.R., Kuhn, J.G., Yung, W.K.A., Gilbert, M.R., Aldape, K.A., Wen, P.Y., Fine, H.A., Mehta, M., DeAngelis, L.M., Lieberman, F., Cloughesy, T.F., Robins, H.I., Dancey, J., Prados, M.D., North American Brain Tumor Consortium, 2010. A phase II trial of erlotinib in patients with recurrent malignant gliomas and nonprogressive glioblastoma multiforme postradiation therapy. Neuro-Oncology 12, 95–103. doi:10.1093/neuonc/nop015

Ramirez, Y.P., Weatherbee, J.L., Wheelhouse, R.T., Ross, A.H., 2013. Glioblastoma multiforme therapy and mechanisms of resistance. Pharmaceuticals (Basel, Switzerland) 6, 1475–506. doi:10.3390/ph6121475

Ranjit, M., Motomura, K., Ohka, F., Wakabayashi, T., Natsume, A., 2015. Applicable advances in the molecular pathology of glioblastoma. Brain tumor pathology 32, 153–62. doi:10.1007/s10014-015-0224-6

Reardon, D.A., Desjardins, A., Vredenburgh, J.J., Gururangan, S., Friedman, A.H., Herndon, J.E., Marcello, J., Norfleet, J.A., McLendon, R.E., Sampson, J.H., Friedman, H.S., Friedman, H.S., 2010. Phase 2 trial of erlotinib plus sirolimus in adults with recurrent glioblastoma. Journal of neuro-oncology 96, 219–30. doi:10.1007/s11060-009-9950-0

Redjal, N., Chan, J.A., Segal, R.A., Kung, A.L., 2006. CXCR4 inhibition synergizes with cytotoxic chemotherapy in gliomas. Clinical cancer research : an official journal of the American Association for Cancer Research 12, 6765–71. doi:10.1158/1078-0432.CCR-06-1372

Redzic, Z.B., Preston, J.E., Duncan, J.A., Chodobski, A., Szmydynger-Chodobska, J., 2005. The Choroid Plexus-Cerebrospinal Fluid System: From Development to Aging. pp. 1–52. doi:10.1016/S0070-2153(05)71001-2

Reitman, Z.J., Pirozzi, C.J., Yan, H., 2013. Promoting a new brain tumor mutation: TERT promoter mutations in CNS tumors. Acta neuropathologica 126, 789–92. doi:10.1007/s00401-013-1207-5

Reshkin, S.J., Bellizzi, A., Caldeira, S., Albarani, V., Malanchi, I., Poignee, M., Alunni-Fabbroni, M., Casavola, V., Tommasino, M., 2000. Na+/H+ exchanger-dependent intracellular alkalinization is an early event in malignant transformation and plays an essential role in the development of subsequent transformation-associated phenotypes. FASEB journal : official publication of the Federation of American Societies for Experimental Biology 14, 2185–97. doi:10.1096/fj.00-0029com

Riemenschneider, M.J., Mueller, W., Betensky, R.A., Mohapatra, G., Louis, D.N., 2005. In Situ Analysis of Integrin and Growth Factor Receptor Signaling Pathways in Human Glioblastomas Suggests Overlapping Relationships with Focal Adhesion Kinase Activation. The American Journal of Pathology 167, 1379–1387. doi:10.1016/S0002-9440(10)61225-4

Ringertz, N., 1950. Grading of gliomas. Acta pathologica et microbiologica Scandinavica 27, 51–64.

Rittierodt, M., Harada, K., 2003. Repetitive doxorubicin treatment of glioblastoma enhances the PGP expression--a special role for endothelial cells. Experimental and toxicologic pathology : official

journal of the Gesellschaft für Toxikologische Pathologie 55, 39–44. doi:10.1078/0940-2993-00287

Robert, M., Wastie, M., 2008. Glioblastoma multiforme: a rare manifestation of extensive liver and bone metastases. Biomedical imaging and intervention journal 4, e3. doi:10.2349/biij.4.1.e3

Robins, H.I., Won, M., Seiferheld, W.F., Schultz, C.J., Choucair, A.K., Brachman, D.G., Demas, W.F., Mehta, M.P., 2006. Phase 2 trial of radiation plus high-dose tamoxifen for glioblastoma multiforme: RTOG protocol BR-0021. Neuro-oncology 8, 47–52. doi:10.1215/S1522851705000311

Romão, L.F., Sousa, V. de O., Neto, V.M., Gomes, F.C.A., 2008. Glutamate activates GFAP gene promoter from cultured astrocytes through TGF-beta1 pathways. Journal of neurochemistry 106, 746–56. doi:10.1111/j.1471-4159.2008.05428.x

Russell, J.M., 2000. Sodium-potassium-chloride cotransport. Physiological reviews 80, 211–76.

Rycaj, K., Tang, D.G., 2015. Cell-of-Origin of Cancer versus Cancer Stem Cells: Assays and Interpretations. Cancer Research 75, 4003–4011. doi:10.1158/0008-5472.CAN-15-0798

Ryu, S., Buatti, J.M., Morris, A., Kalkanis, S.N., Ryken, T.C., Olson, J.J., AANS/CNS Joint Guidelines Committee, 2014. The role of radiotherapy in the management of progressive glioblastoma : a systematic review and evidence-based clinical practice guideline. Journal of neuro-oncology 118, 489–99. doi:10.1007/s11060-013-1337-6

Saez, J.C., Berthoud, V.M., Branes, M.C., Martinez, A.D., Beyer, E.C., 2003. Plasma membrane channels formed by connexins: their regulation and functions. Physiological reviews 83, 1359–400. doi:10.1152/physrev.00007.2003

Safa, A.R., Saadatzadeh, M.R., Cohen-Gadol, A.A., Pollok, K.E., Bijangi-Vishehsaraei, K., 2015. Glioblastoma stem cells (GSCs) epigenetic plasticity and interconversion between differentiated non-GSCs and GSCs. Genes and Diseases 2, 152–163. doi:10.1016/j.gendis.2015.02.001

Sage, M.R., Wilson, A.J., 1994. The blood-brain barrier: an important concept in neuroimaging. AJNR. American journal of neuroradiology 15, 601–22.

Sanchez-Martin, M., 2008. Brain tumour stem cells: implications for cancer therapy and regenerative medicine. Current stem cell research & therapy 3, 197–207.

Sarin, H., Kanevsky, A.S., Wu, H., Brimacombe, K.R., Fung, S.H., Sousa, A.A., Auh, S., Wilson, C.M., Sharma, K., Aronova, M.A., Leapman, R.D., Griffiths, G.L., Hall, M.D., 2008. Effective transvascular delivery of nanoparticles across the blood-brain tumor barrier into malignant glioma cells. Journal of translational medicine 6, 80. doi:10.1186/1479-5876-6-80

Sarkaria, J.N., Kitange, G.J., James, C.D., Plummer, R., Calvert, H., Weller, M., Wick, W., 2008. Mechanisms of Chemoresistance to Alkylating Agents in Malignant Glioma. Clinical Cancer Research 14, 2900–2908. doi:10.1158/1078-0432.CCR-07-1719

Sathornsumetee, S., Reardon, D.A., Desjardins, A., Quinn, J.A., Vredenburgh, J.J., Rich, J.N., 2007. Molecularly targeted therapy for malignant glioma. Cancer 110, 12–24. doi:10.1002/cncr.22741

Sato, W., Fukazawa, N., Nakanishi, O., Baba, M., Suzuki, T., Yano, O., Naito, M., Tsuruo, T., 1995. Reversal of multidrug resistance by a novel quinoline derivative, MS-209. Cancer Chemotherapy and Pharmacology 35, 271–277. doi:10.1007/BF00689444

Sayegh, E.T., Kaur, G., Bloch, O., Parsa, A.T., 2014. Systematic Review of Protein Biomarkers of Invasive Behavior in Glioblastoma. Molecular Neurobiology 49, 1212–1244. doi:10.1007/s12035-013-8593-5

Scaltriti, M., Baselga, J., 2006. The epidermal growth factor receptor pathway: a model for targeted therapy. Clinical cancer research : an official journal of the American Association for Cancer Research 12, 5268–72. doi:10.1158/1078-0432.CCR-05-1554

Scambia, G., Lovergine, S., Masciullo, V., 2006. RB family members as predictive and prognostic factors in human cancer. Oncogene 25, 5302–5308. doi:10.1038/sj.onc.1209620

Schaich, M., Kestel, L., Pfirrmann, M., Robel, K., Illmer, T., Kramer, M., Dill, C., Ehninger, G., Schackert, G., Krex, D., 2009. A MDR1 (ABCB1) gene single nucleotide polymorphism predicts outcome of temozolomide treatment in glioblastoma patients. Annals of oncology : official journal of the European Society for Medical Oncology 20, 175–81. doi:10.1093/annonc/mdn548

Scheurer, M.E., Amirian, E.S., Davlin, S.L., Rice, T., Wrensch, M., Bondy, M.L., 2011. Effects of antihistamine and anti-inflammatory medication use on risk of specific glioma histologies. International journal of cancer 129, 2290–6. doi:10.1002/ijc.25883

Schittenhelm, J., Schwab, E.I., Sperveslage, J., Tatagiba, M., Meyermann, R., Fend, F., Goodman, S.L., Sipos, B., 2013. Longitudinal expression analysis of αv integrins in human gliomas reveals upregulation of integrin αvβ3 as a negative prognostic factor. Journal of neuropathology and experimental neurology 72, 194–210. doi:10.1097/NEN.0b013e3182851019

Schuh, A., Becq, J., Humphray, S., Alexa, A., Burns, A., Clifford, R., Feller, S.M., Grocock, R., Henderson, S., Khrebtukova, I., Kingsbury, Z., Luo, S., McBride, D., Murray, L., Menju, T., Timbs, A., Ross, M., Taylor, J., Bentley, D., 2012. Monitoring chronic lymphocytic leukemia progression by whole genome sequencing reveals heterogeneous clonal evolution patterns. Blood 120, 4191–6. doi:10.1182/blood-2012-05-433540

Schultz, S., Pinsky, G.S., Wu, N.C., Chamberlain, M.C., Rodrigo, A.S., Martin, S.E., 2005. Fine needle aspiration diagnosis of extracranial glioblastoma multiforme: Case report and review of the literature. CytoJournal 2, 19. doi:10.1186/1742-6413-2-19

Schwartzbaum, J.A., Fisher, J.L., Aldape, K.D., Wrensch, M., 2006. Epidemiology and molecular pathology of glioma. Nature clinical practice. Neurology 2, 494–503; quiz 1 p following 516. doi:10.1038/ncpneuro0289

Seymour, T., Nowak, A., Kakulas, F., 2015. Targeting Aggressive Cancer Stem Cells in Glioblastoma. Frontiers in oncology 5, 159. doi:10.3389/fonc.2015.00159

Seystahl, K., Wiestler, B., Hundsberger, T., Happold, C., Wick, W., Weller, M., Wick, A., 2013. Bevacizumab Alone or in Combination with Irinotecan in Recurrent WHO Grade II and Grade III Gliomas. European Neurology 69, 95–101. doi:10.1159/000343811

Shah, S.P., Roth, A., Goya, R., Oloumi, A., Ha, G., Zhao, Y., Turashvili, G., Ding, J., Tse, K., Haffari, G., Bashashati, A., Prentice, L.M., Khattra, J., Burleigh, A., Yap, D., Bernard, V., McPherson, A., Shumansky, K., Crisan, A., Giuliany, R., Heravi-Moussavi, A., Rosner, J., Lai, D., Birol, I., Varhol, R., Tam, A., Dhalla, N., Zeng, T., Ma, K., Chan, S.K., Griffith, M., Moradian, A., Cheng, S.-W.G., Morin, G.B., Watson, P., Gelmon, K., Chia, S., Chin, S.-F., Curtis, C., Rueda, O.M., Pharoah, P.D., Damaraju, S., Mackey, J., Hoon, K., Harkins, T., Tadigotla, V., Sigaroudinia, M., Gascard, P., Tlsty, T., Costello, J.F., Meyer, I.M., Eaves, C.J., Wasserman, W.W., Jones, S., Huntsman, D., Hirst, M., Caldas, C., Marra, M.A., Aparicio, S., 2012. The clonal and mutational evolution spectrum of primary

triple-negative breast cancers. Nature 486, 395–9. doi:10.1038/nature10933

Shangary, S., Wang, S., 2009. Small-Molecule Inhibitors of the MDM2-p53 Protein-Protein Interaction to Reactivate p53 Function: A Novel Approach for Cancer Therapy. Annual Review of Pharmacology and Toxicology 49, 223–241. doi:10.1146/annurev.pharmtox.48.113006.094723

Sharif, T.R., Sharif, M., 1999. Overexpression of protein kinase C epsilon in astroglial brain tumor derived cell lines and primary tumor samples. International journal of oncology 15, 237–43.

Sharom, F.J., 2011. The P-glycoprotein multidrug transporter. Essays in biochemistry 50, 161–78. doi:10.1042/bse0500161

Sheehy, R.M., Kuder, C.H., Bachman, Z., Hohl, R.J., 2015. Calcium and P-glycoprotein independent synergism between schweinfurthins and verapamil. Cancer Biology and Therapy 16, 1259–1268. doi:10.1080/15384047.2015.1056420

Shen, H., Perez, R.E., Davaadelger, B., Maki, C.G., 2013. Two 4N cell-cycle arrests contribute to cisplatin-resistance. PloS one 8, e59848. doi:10.1371/journal.pone.0059848

Shi, H., Huang, Y., Zhou, H., Song, X., Yuan, S., Fu, Y., Luo, Y., 2007. Nucleolin is a receptor that mediates antiangiogenic and antitumor activity of endostatin. Blood 110, 2899–906. doi:10.1182/blood-2007-01-064428

Shinojima, N., Tada, K., Shiraishi, S., Kamiryo, T., Kochi, M., Nakamura, H., Makino, K., Saya, H., Hirano, H., Kuratsu, J.-I., Oka, K., Ishimaru, Y., Ushio, Y., 2003. Prognostic value of epidermal growth factor receptor in patients with glioblastoma multiforme. Cancer research 63, 6962–70.

Siegal, T., 2013. Which drug or drug delivery system can change clinical practice for brain tumor therapy? Neuro-oncology 15, 656–669. doi:10.1093/neuonc/not016

Sikic, B.I., Fisher, G.A., Lum, B.L., Halsey, J., Beketic-Oreskovic, L., Chen, G., 1997. Modulation and prevention of multidrug resistance by inhibitors of P-glycoprotein. Cancer Chemotherapy and Pharmacology 40, S13–S19. doi:10.1007/s002800051055

Simões, S., Moreira, J.N., Fonseca, C., Düzgüneş, N., de Lima, M.C.P., 2004. On the formulation of pH-sensitive liposomes with long circulation times. Advanced drug delivery reviews 56, 947–65. doi:10.1016/j.addr.2003.10.038

Singh, S.K., Hawkins, C., Clarke, I.D., Squire, J.A., Bayani, J., Hide, T., Henkelman, R.M., Cusimano, M.D., Dirks, P.B., 2004. Identification of human brain tumour initiating cells. Nature 432, 396–401. doi:10.1038/nature03031.1.

Soares, A.R., Martins-Marques, T., Ribeiro-Rodrigues, T., Ferreira, J.V., Catarino, S., Pinho, M.J., Zuzarte, M., Isabel Anjo, S., Manadas, B., P.G. Sluijter, J., Pereira, P., Girao, H., 2015. Gap junctional protein Cx43 is involved in the communication between extracellular vesicles and mammalian cells. Scientific Reports 5, 13243. doi:10.1038/srep13243

Soffietti, R., Trevisan, E., Rudà, R., 2014. What have we learned from trials on antiangiogenic agents in glioblastoma? Expert review of neurotherapeutics 14, 1–3. doi:10.1586/14737175.2014.873277

Soroceanu, L., Manning, T.J., Sontheimer, H., 2001. Reduced expression of connexin-43 and functional gap junction coupling in human gliomas. Glia 33, 107–17.

Spiegl-Kreinecker, S., Pirker, C., Filipits, M., Lotsch, D., Buchroithner, J., Pichler, J., Silye, R., Weis, S., Micksche, M., Fischer, J., Berger, W., 2010. O6-Methylguanine DNA methyltransferase protein

expression in tumor cells predicts outcome of temozolomide therapy in glioblastoma patients. Neuro-Oncology 12, 28–36. doi:10.1093/neuonc/nop003

Spoerri, P.E., Heyder, H., Eins, S., 1983. Growth of mouse neuroblastoma cell line in a defined medium. Neuroscience letters 37, 313–8.

Srivenugopal, K.S., Shou, J., Mullapudi, S.R., Lang, F.F., Rao, J.S., Ali-Osman, F., 2001. Enforced expression of wild-type p53 curtails the transcription of the O(6)-methylguanine-DNA methyltransferase gene in human tumor cells and enhances their sensitivity to alkylating agents. Clinical cancer research : an official journal of the American Association for Cancer Research 7, 1398–409.

Stavrovskaya, A.A., Shushanov, S.S., Rybalkina, E.Y., 2016. Problems of Glioblastoma Multiforme Drug Resistance. Biochemistry. Biokhimiia 81, 91–100. doi:10.1134/S0006297916020036

Steinberg, S.F., 2008. Structural Basis of Protein Kinase C Isoform Function. Physiological Reviews 88, 1341–1378. doi:10.1152/physrev.00034.2007

Stupp, R., Hegi, M.E., Gilbert, M.R., Chakravarti, A., 2007. Chemoradiotherapy in malignant glioma: standard of care and future directions. Journal of clinical oncology : official journal of the American Society of Clinical Oncology 25, 4127–36. doi:10.1200/JCO.2007.11.8554

Stupp, R., Hegi, M.E., Mason, W.P., van den Bent, M.J., Taphoorn, M.J.B., Janzer, R.C., Ludwin, S.K., Allgeier, A., Fisher, B., Belanger, K., Hau, P., Brandes, A.A., Gijtenbeek, J., Marosi, C., Vecht, C.J., Mokhtari, K., Wesseling, P., Villa, S., Eisenhauer, E., Gorlia, T., Weller, M., Lacombe, D., Cairncross, J.G., Mirimanoff, R.-O., European Organisation for Research and Treatment of Cancer Brain Tumour and Radiation Oncology Groups, National Cancer Institute of Canada Clinical Trials Group, 2009. Effects of radiotherapy with concomitant and adjuvant temozolomide versus radiotherapy alone on survival in glioblastoma in a randomised phase III study: 5-year analysis of the EORTC-NCIC trial. The Lancet. Oncology 10, 459–66. doi:10.1016/S1470-2045(09)70025-7

Stupp, R., Mason, W.P., van den Bent, M.J., Weller, M., Fisher, B., Taphoorn, M.J.B., Belanger, K., Brandes, A.A., Marosi, C., Bogdahn, U., Curschmann, J., Janzer, R.C., Ludwin, S.K., Gorlia, T., Allgeier, A., Lacombe, D., Cairncross, J.G., Eisenhauer, E., Mirimanoff, R.O., European Organisation for Research and Treatment of Cancer Brain Tumor and Radiotherapy Groups, National Cancer Institute of Canada Clinical Trials Group, 2005. Radiotherapy plus concomitant and adjuvant temozolomide for glioblastoma. The New England journal of medicine 352, 987–96. doi:10.1056/NEJMoa043330

Su, G., Kintner, D.B., Flagella, M., Shull, G.E., Sun, D., 2002. Astrocytes from Na+-K+-Cl- cotransporter-null mice exhibit absence of swelling and decrease in EAA release. AJP: Cell Physiology 282, C1147–C1160. doi:10.1152/ajpcell.00538.2001

Sul, J., Fine, H.A., 2010. Malignant Gliomas: New Translational Therapies. Mount Sinai Journal of Medicine: A Journal of Translational and Personalized Medicine 77, 655–666. doi:10.1002/msj.20223

Sun, H., Dai, H., Shaik, N., Elmquist, W.F., 2003. Drug efflux transporters in the CNS. Advanced drug delivery reviews 55, 83–105.

Susan Chang, et al, 2011. Principles & Practice of Neuro-Oncology: A Multidisciplinary Approach - Google Livros. Demos Medical Publishing.

Svolos, P., Kousi, E., Kapsalaki, E., Theodorou, K., Fezoulidis, I., Kappas, C., Tsougos, I., 2014. The role of

diffusion and perfusion weighted imaging in the differential diagnosis of cerebral tumors: a review and future perspectives. Cancer imaging : the official publication of the International Cancer Imaging Society 14, 20. doi:10.1186/1470-7330-14-20

Syljuåsen, R.G., 2007. Checkpoint adaptation in human cells. Oncogene 26, 5833–5839. doi:10.1038/sj.onc.1210402

Tacar, O., Sriamornsak, P., Dass, C.R., 2013. Doxorubicin: an update on anticancer molecular action, toxicity and novel drug delivery systems. The Journal of pharmacy and pharmacology 65, 157–70. doi:10.1111/j.2042-7158.2012.01567.x

Tam, W.L., Weinberg, R.A., 2013. The epigenetics of epithelial-mesenchymal plasticity in cancer. Nature medicine 19, 1438–49. doi:10.1038/nm.3336

Tania, M., Khan, M.A., Fu, J., 2014. Epithelial to mesenchymal transition inducing transcription factors and metastatic cancer. Tumour biology : the journal of the International Society for Oncodevelopmental Biology and Medicine 35, 7335–42. doi:10.1007/s13277-014-2163-y

Tata, P.R., Mou, H., Pardo-Saganta, A., Zhao, R., Prabhu, M., Law, B.M., Vinarsky, V., Cho, J.L., Breton, S., Sahay, A., Medoff, B.D., Rajagopal, J., 2013. Dedifferentiation of committed epithelial cells into stem cells in vivo. Nature 503, 218–23. doi:10.1038/nature12777

Thakkar, J.P., Dolecek, T.A., Horbinski, C., Ostrom, Q.T., Lightner, D.D., Barnholtz-Sloan, J.S., Villano, J.L., 2014. Epidemiologic and molecular prognostic review of glioblastoma. Cancer epidemiology, biomarkers & prevention : a publication of the American Association for Cancer Research, cosponsored by the American Society of Preventive Oncology 23, 1985–96. doi:10.1158/1055-9965.EPI-14-0275

Theeler, B.J., Gilbert, M.R., Ostrom, Q., Gittleman, H., Liao, P., Rouse, C., Chen, Y., Dowling, J., Johnson, D., O'Neill, B., Curran, W., Scott, C., Horton, J., Nelson, J., Weinstein, A., Fischbach, A., Lacroix, M., Abi-Said, D., Fourney, D., Gokaslan, Z., Shi, W., DeMonte, F., Walker, M., Green, S., Byar, D., Alexander, E., Batzdorf, U., Brooks, W., Stewart, L., Yung, W., Albright, R., Olson, J., Fredericks, R., Fink, K., Prados, M., Stupp, R., Mason, W., Bent, M., Weller, M., Fisher, B., Taphoorn, M., Stupp, R., Hegi, M., Mason, W., Bent, M., Taphoorn, M., Janzer, R., Batchelor, T., Mulholland, P., Neyns, B., Nabors, L., Campone, M., Wick, A., Friedman, H., Prados, M., Wen, P., Mikkelsen, T., Schiff, D., Abrey, L., Stupp, R., Wong, E., Kanner, A., Steinberg, D., Engelhard, H., Heidecke, V., Cohen, M., Shen, Y., Keegan, P., Pazdur, R., Ohgaki, H., Dessen, P., Jourde, B., Horstmann, S., Nishikawa, T., Patre, P., Weller, M., Stupp, R., Reifenberger, G., Brandes, A., Bent, M., Wick, W., Hegi, M., Diserens, A., Gorlia, T., Hamou, M., Tribolet, N., Weller, M., Rivera, A., Pelloski, C., Gilbert, M., Colman, H., Cruz, C., Sulman, E., Tolcher, A., Gerson, S., Denis, L., Geyer, C., Hammond, L., Patnaik, A., Gilbert, M., Wang, M., Aldape, K., Stupp, R., Hegi, M., Jaeckle, K., Barker, C., Chang, M., Chou, J., Zhang, Z., Beal, K., Gutin, P., Lombardi, G., Pace, A., Pasqualetti, F., Rizzato, S., Faedi, M., Anghileri, E., Malmström, A., Grønberg, B., Marosi, C., Stupp, R., Frappaz, D., Schultz, H., Perez-Larraya, J.G., Ducray, F., Chinot, O., Catry-Thomas, I., Taillandier, L., Guillamo, J., Wick, W., Platten, M., Meisner, C., Felsberg, J., Tabatabai, G., Simon, M., Parsons, D., Jones, S., Zhang, X., Lin, J., Leary, R., Angenendt, P., Yan, H., Parsons, D., Jin, G., McLendon, R., Rasheed, B., Yuan, W., Lai, A., Kharbanda, S., Pope, W., Tran, A., Solis, O., Peale, F., Choi, C., Ganji, S., Deberardinis, R., Hatanpaa, K., Rakheja, D., Kovacs, Z., Elkhaled, A., Jalbert, L., Phillips, J., Yoshihara, H., Parvataneni, R.,

Srinivasan, R., Nobusawa, S., Watanabe, T., Kleihues, P., Ohgaki, H., Theeler, B., Yung, W., Fuller, G., Groot, J., Hartmann, C., Hentschel, B., Wick, W., Capper, D., Felsberg, J., Simon, M., Wick, W., Meisner, C., Hentschel, B., Platten, M., Schilling, A., Wiestler, B., Molenaar, R., Verbaan, D., Lamba, S., Zanon, C., Jeuken, J., Boots-Sprenger, S., Phillips, H., Kharbanda, S., Chen, R., Forrest, W., Soriano, R., Wu, T., Verhaak, R., Hoadley, K., Purdom, E., Wang, V., Qi, Y., Wilkerson, M., Noushmehr, H., Weisenberger, D., Diefes, K., Phillips, H., Pujara, K., Berman, B., Aldape, K., Zadeh, G., Mansouri, S., Reifenberger, G., Deimling, A., Liu, X., Gerges, N., Korshunov, A., Sabha, N., Khuong-Quang, D., Fontebasso, A., Killela, P., Reitman, Z., Jiao, Y., Bettegowda, C., Agrawal, N., Diaz, L., Liu, X., Wu, G., Shan, Y., Hartmann, C., Deimling, A., Xing, M., Labussière, M., Boisselier, B., Mokhtari, K., Stefano, A., Rahimian, A., Rossetto, M., Schindler, G., Capper, D., Meyer, J., Janzarik, W., Omran, H., Herold-Mende, C., Hyman, D., Puzanov, I., Subbiah, V., Faris, J., Chau, I., Blay, J., Singh, D., Chan, J., Zoppoli, P., Niola, F., Sullivan, R., Castano, A., Olar, A., Wani, K., Alfaro-Munoz, K., Heathcock, L., Thuijl, H., Gilbert, M., Grossman, S., Ye, X., Piantadosi, S., Desideri, S., Nabors, L., Rosenfeld, M., Clarke, J., Iwamoto, F., Sul, J., Panageas, K., Lassman, A., DeAngelis, L., Vredenburgh, J., Desjardins, A., Reardon, D., Peters, K., Herndon, J., Marcello, J., Nabors, L., Fink, K., Mikkelsen, T., Grujicic, D., Tarnawski, R., Nam, D., Stupp, R., Hegi, M., Gorlia, T., Erridge, S., Perry, J., Hong, Y., Lai, A., Tran, A., Nghiemphu, P., Pope, W., Solis, O., Selch, M., Chinot, O., Wick, W., Mason, W., Henriksson, R., Saran, F., Nishikawa, R., Gilbert, M., Dignam, J., Armstrong, T., Wefel, J., Blumenthal, D., Vogelbaum, M., Colman, H., Zhang, L., Sulman, E., McDonald, J., Shooshtari, N., Rivera, A., Sandmann, T., Bourgon, R., Garcia, J., Li, C., Cloughesy, T., Chinot, O., Cahill, D., Levine, K., Betensky, R., Codd, P., Romany, C., Reavie, L., Johnson, B., Mazor, T., Hong, C., Barnes, M., Aihara, K., McLean, C., Fecci, P., Heimberger, A., Sampson, J., Weathers, S., Gilbert, M., Grossman, S., Ye, X., Lesser, G., Sloan, A., Carraway, H., Desideri, S., Sampson, J., Aldape, K., Archer, G., Coan, A., Desjardins, A., Friedman, A., Ishikawa, E., Muragaki, Y., Yamamoto, T., Maruyama, T., Tsuboi, K., Ikuta, S., Prins, R., Soto, H., Konkankit, V., Odesa, S., Eskin, A., Yong, W., Phuphanich, S., Wheeler, C., Rudnick, J., Mazer, M., Wang, H., Nuño, M., Fong, B., Jin, R., Wang, X., Safaee, M., Lisiero, D., Yang, I., Mitchell, D., Batich, K., Gunn, M., Huang, M., Sanchez-Perez, L., Nair, S., Patel, M., Kim, J., Ruzevick, J., Li, G., Lim, M., Schumacher, T., Bunse, L., Pusch, S., Sahm, F., Wiestler, B., Quandt, J., Humphrey, P., Wong, A., Vogelstein, B., Zalutsky, M., Fuller, G., Archer, G., Schuster, J., Lai, R., Recht, L., Reardon, D., Paleologos, N., Groves, M., Rhun, E., Rhun, E., Taillibert, S., Chamberlain, M., Sampson, J., Heimberger, A., Archer, G., Aldape, K., Friedman, A., Friedman, H., Hodi, F., O'Day, S., McDermott, D., Weber, R., Sosman, J., Haanen, J., Margolin, K., Ernstoff, M., Hamid, O., Lawrence, D., McDermott, D., Puzanov, I., Robert, C., Schachter, J., Long, G., Arance, A., Grob, J., Mortier, L., Wolchok, J., Kluger, H., Callahan, M., Postow, M., Rizvi, N., Lesokhin, A., Robert, C., Thomas, L., Bondarenko, I., O'Day, S., Weber, J., Garbe, C., Postow, M., Chesney, J., Pavlick, A., Robert, C., Grossmann, K., McDermott, D., Berghoff, A., Kiesel, B., Widhalm, G., Rajky, O., Ricken, G., Wöhrer, A., Liao, B., Shroff, S., Kamiya-Matsuoka, C., Tummala, S., Mandel, J., Olar, A., Aldape, K., Tremont-Lukats, I., Fink, J., Born, D., Chamberlain, M., Young, R., Gupta, A., Shah, A., Graber, J., Zhang, Z., Shi, W., Melguizo-Gavilanes, I., Bruner, J., Guha-Thakurta, N., Hess, K., Puduvalli, V., Ellingson, B., Wen, P., Bent, M., Cloughesy, T., Gerber, N.,

Young, R., Barker, C., Wolchok, J., Chan, T., Yamada, Y., Wen, P., Macdonald, D., Reardon, D., Cloughesy, T., Sorensen, A., Galanis, E., Reardon, D., Okada, H., 2015. Advances in the treatment of newly diagnosed glioblastoma. BMC Medicine 13, 293. doi:10.1186/s12916-015-0536-8

Thiebaut, F., Tsuruo, T., Hamada, H., Gottesman, M.M., Pastan, I., Willingham, M.C., 1987. Cellular localization of the multidrug-resistance gene product P-glycoprotein in normal human tissues. Proceedings of the National Academy of Sciences of the United States of America 84, 7735–8.

Thirant, C., Bessette, B., Varlet, P., Puget, S., Cadusseau, J., Tavares, S.D.R., Studler, J.-M., Silvestre, D.C., Susini, A., Villa, C., Miquel, C., Bogeas, A., Surena, A.-L., Dias-Morais, A., Léonard, N., Pflumio, F., Bièche, I., Boussin, F.D., Sainte-Rose, C., Grill, J., Daumas-Duport, C., Chneiweiss, H., Junier, M.-P., 2011. Clinical relevance of tumor cells with stem-like properties in pediatric brain tumors. PloS one 6, e16375. doi:10.1371/journal.pone.0016375

Thirant, C., Galan-Moya, E.-M., Dubois, L.G., Pinte, S., Chafey, P., Broussard, C., Varlet, P., Devaux, B., Soncin, F., Gavard, J., Junier, M.-P., Chneiweiss, H., 2012. Differential proteomic analysis of human glioblastoma and neural stem cells reveals HDGF as a novel angiogenic secreted factor. Stem cells (Dayton, Ohio) 30, 845–53. doi:10.1002/stem.1062

Todorova, M.G., Soria, B., Quesada, I., 2008. Gap junctional intercellular communication is required to maintain embryonic stem cells in a non-differentiated and proliferative state. Journal of cellular physiology 214, 354–62. doi:10.1002/jcp.21203

Tomaszowski, K.-H., Schirrmacher, R., Kaina, B., 2015. Multidrug Efflux Pumps Attenuate the Effect of MGMT Inhibitors. Molecular Pharmaceutics 12, 3924–3934. doi:10.1021/acs.molpharmaceut.5b00341

Tóth, K., Vaughan, M.M., Peress, N.S., Slocum, H.K., Rustum, Y.M., 1996. MDR1 P-glycoprotein is expressed by endothelial cells of newly formed capillaries in human gliomas but is not expressed in the neovasculature of other primary tumors. The American journal of pathology 149, 853–8.

Totoń, E., Ignatowicz, E., Skrzeczkowska, K., Rybczyńska, M., 2011. Protein kinase Cε as a cancer marker and target for anticancer therapy. Pharmacological reports : PR 63, 19–29.

Towbin, H., Staehelin, T., Gordon, J., 1989. Immunoblotting in the clinical laboratory. Journal of clinical chemistry and clinical biochemistry. Zeitschrift fur klinische Chemie und klinische Biochemie 27, 495–501.

Tsuruo, T., Naito, M., Tomida, A., Fujita, N., Mashima, T., Sakamoto, H., Haga, N., 2003. resistance , apoptosis and survival signal 94, 15–21.

Ueno, T., Ko, S.H., Grubbs, E., Yoshimoto, Y., Augustine, C., Abdel-Wahab, Z., Cheng, T.-Y., Abdel-Wahab, O.I., Pruitt, S.K., Friedman, H.S., Tyler, D.S., 2006. Modulation of chemotherapy resistance in regional therapy: a novel therapeutic approach to advanced extremity melanoma using intra-arterial temozolomide in combination with systemic O6-benzylguanine. Molecular cancer therapeutics 5, 732–8. doi:10.1158/1535-7163.MCT-05-0098

Uhm, J.H., Ballman, K. V., Wu, W., Giannini, C., Krauss, J.C., Buckner, J.C., James, C.D., Scheithauer, B.W., Behrens, R.J., Flynn, P.J., Schaefer, P.L., Dakhill, S.R., Jaeckle, K.A., 2011. Phase II Evaluation of Gefitinib in Patients With Newly Diagnosed Grade 4 Astrocytoma: Mayo/North Central Cancer Treatment Group Study N0074. International Journal of Radiation Oncology*Biology*Physics 80, 347–353. doi:10.1016/j.ijrobp.2010.01.070

Uhm, J.H., Dooley, N.P., Villemure, J.G., Yong, V.W., 1997. Mechanisms of glioma invasion: role of matrix-metalloproteinases. The Canadian journal of neurological sciences. Le journal canadien des sciences neurologiques 24, 3–15.

Uht, R.M., Amos, S., Martin, P.M., Riggan, A.E., Hussaini, I.M., 2007. The protein kinase C-η isoform induces proliferation in glioblastoma cell lines through an ERK/Elk-1 pathway. Oncogene 26, 2885–2893. doi:10.1038/sj.onc.1210090

Urbańska, K., Sokołowska, J., Szmidt, M., Sysa, P., 2014. Glioblastoma multiforme - an overview. Contemporary oncology (Poznan, Poland) 18, 307–12. doi:10.5114/wo.2014.40559

Van Tellingen, O., Yetkin-Arik, B., De Gooijer, M.C., Wesseling, P., Wurdinger, T., de Vries, H.E., 2015. Overcoming the blood-brain tumor barrier for effective glioblastoma treatment. Drug Resistance Updates 19, 1–12. doi:10.1016/j.drup.2015.02.002

Visvader, J.E., Lindeman, G.J., 2012. Cancer stem cells: current status and evolving complexities. Cell stem cell 10, 717–28. doi:10.1016/j.stem.2012.05.007

Vlachostergios, P.J., Hatzidaki, E., Stathakis, N.E., Koukoulis, G.K., Papandreou, C.N., 2013. Bortezomib Downregulates MGMT Expression in T98G Glioblastoma Cells. Cellular and Molecular Neurobiology 33, 313–318. doi:10.1007/s10571-013-9910-2

Wait, S.D., Prabhu, R.S., Burri, S.H., Atkins, T.G., Asher, A.L., 2015. Polymeric drug delivery for the treatment of glioblastoma. Neuro-oncology 17 Suppl 2, ii9-ii23. doi:10.1093/neuonc/nou360

Wang, X., Dai, J., 2010. Concise review: Isoforms of OCT4 contribute to the confusing diversity in stem cell biology. Stem Cells 28, 885–893. doi:10.1002/stem.419

Watkins, S., Robel, S., Kimbrough, I.F., Robert, S.M., Ellis-Davies, G., Sontheimer, H., Kimelberg, H.K., Nedergaard, M., Mathiisen, T.M., Lehre, K.P., Danbolt, N.C., Ottersen, O.P., Winkler, E.A., Bell, R.D., Zlokovic, B. V., Abbott, N.J., Patabendige, A.A., Dolman, D.E., Yusof, S.R., Begley, D.J., Abbott, N.J., Ronnback, L., Hansson, E., Wolburg, H., Noell, S., Mack, A., Wolburg-Buchholz, K., Fallier-Becker, P., Attwell, D., Filosa, J.A., Girouard, H., Gordon, G.R., Mulligan, S.J., MacVicar, B.A., Mulligan, S.J., MacVicar, B.A., Scherer, H.D., Farin, A., Montana, V., Sontheimer, H., Giese, A., Rief, M.D., Loo, M.A., Berens, M.E., Holash, J., Plate, K.H., Breier, G., Weich, H.A., Risau, W., Zagzag, D., Nagano, N., Sasaki, H., Aoyagi, M., Hirakawa, K., Winkler, F., Fischer, I., Gagner, J.P., Law, M., Newcomb, E.W., Zagzag, D., Giannini, C., Iadecola, C., Nedergaard, M., Takano, T., Shen, Z., Lu, Z., Chhatbar, P.Y., O'Herron, P., Kara, P., Iliff, J.J., Yang, B., Alonso, M., Tamasdan, C., Miller, D.C., Newcomb, E.W., Nakazawa, E., Ishikawa, H., Armulik, A., Daneman, R., Zhou, L., Kebede, A.A., Barres, B.A., Abbott, N.J., Machein, M.R., Kullmer, J., Fiebich, B.L., Plate, K.H., Warnke, P.C., Gordon, G.R., Choi, H.B., Rungta, R.L., Ellis-Davies, G.C., MacVicar, B.A., Zonta, M., Ellis-Davies, G.C., Barsotti, R.J., Blanco, V.M., Stern, J.E., Filosa, J.A., Dorn, G.W., Becker, M.W., Edwards, R., Trizna, W., Narumiya, S., Sugimoto, Y., Ushikubi, F., Junge, C.E., Macfarlane, S.R., Seatter, M.J., Kanke, T., Hunter, G.D., Plevin, R., Cuddapah, V.A., Turner, K.L., Seifert, S., Sontheimer, H., Weaver, A.K., Bomben, V.C., Sontheimer, H., Watkins, S., Sontheimer, H., Buckingham, S.C., Chung, W.J., Jain, R.K., Liebner, S., Wolburg, H., Noell, S., Fallier-Becker, P., Mack, A.F., Wolburg-Buchholz, K., Bell, R.D., Bell, R.D., Akella, N.S., Pellerin, L., Rancillac, A., Geoffroy, H., Rossier, J., Takano, T., Han, X., Deane, R., Zlokovic, B., Nedergaard, M., Kazama, K., Wang, G., Frys, K., Anrather, J.,

Iadecola, C., Mishra, A., Newman, E.A., Suo, Z., Citron, B.A., Festoff, B.W., Maruyama, C., 2014. Disruption of astrocyte–vascular coupling and the blood–brain barrier by invading glioma cells. Nature Communications 5, 338–353. doi:10.1038/ncomms5196

Weathers, S.-P., de Groot, J., 2015. VEGF Manipulation in Glioblastoma. Oncology (Williston Park, N.Y.) 29, 720–7.

Weaver, M., Laske, D.W., 2003. Transferrin receptor ligand-targeted toxin conjugate (Tf-CRM107) for therapy of malignant gliomas. Journal of neuro-oncology 65, 3–13.

Wei, C.-J., Xu, X., Lo, C.W., 2004. Connexins and cell signaling in development and disease. Annual review of cell and developmental biology 20, 811–38. doi:10.1146/annurev.cellbio.19.111301.144309

Wei, X., Chen, X., Ying, M., Lu, W., 2014. Brain tumor-targeted drug delivery strategies. Acta Pharmaceutica Sinica B 4, 193–201. doi:10.1016/j.apsb.2014.03.001

Weigmann, A., Corbeil, D., Hellwig, A., Huttner, W.B., 1997. Prominin, a novel microvilli-specific polytopic membrane protein of the apical surface of epithelial cells, is targeted to plasmalemmal protrusions of non-epithelial cells. Proceedings of the National Academy of Sciences of the United States of America 94, 12425–30.

Weissenberger, J., Loeffler, S., Kappeler, A., Kopf, M., Lukes, A., Afanasieva, T.A., Aguzzi, A., Weis, J., 2004. IL-6 is required for glioma development in a mouse model. Oncogene 23, 3308–3316. doi:10.1038/sj.onc.1207455

Westphal, M., Ram, Z., Riddle, V., Hilt, D., Bortey, E., Executive Committee of the Gliadel Study Group, 2006. Gliadel wafer in initial surgery for malignant glioma: long-term follow-up of a multicenter controlled trial. Acta Neurochir (Wien). 148, 269–75. doi:10.1007/s00701-005-0707-z

Wick, W., Platten, M., Weller, M., 2009. New (alternative) temozolomide regimens for the treatment of glioma. Neuro-oncology 11, 69–79. doi:10.1215/15228517-2008-078

Wick, W., Puduvalli, V.K., Chamberlain, M.C., van den Bent, M.J., Carpentier, A.F., Cher, L.M., Mason, W., Weller, M., Hong, S., Musib, L., Liepa, A.M., Thornton, D.E., Fine, H.A., 2010. Phase III Study of Enzastaurin Compared With Lomustine in the Treatment of Recurrent Intracranial Glioblastoma. Journal of Clinical Oncology 28, 1168–1174. doi:10.1200/JCO.2009.23.2595

Wick, W., Steinbach, J.P., Platten, M., Hartmann, C., Wenz, F., von Deimling, A., Shei, P., Moreau-Donnet, V., Stoffregen, C., Combs, S.E., 2013. Enzastaurin before and concomitant with radiation therapy, followed by enzastaurin maintenance therapy, in patients with newly diagnosed glioblastoma without MGMT promoter hypermethylation. Neuro-oncology 15, 1405–12. doi:10.1093/neuonc/not100

Wilhelmsson, U., Eliasson, C., Bjerkvig, R., Pekny, M., 2003. Loss of GFAP expression in high-grade astrocytomas does not contribute to tumor development or progression. Oncogene 22, 3407–11. doi:10.1038/sj.onc.1206372

Wirsching, H.-G., Weller, M., 2016. The Role of Molecular Diagnostics in the Management of Patients with Gliomas. Current Treatment Options in Oncology 17, 51. doi:10.1007/s11864-016-0430-4

Wrensch, M., Jenkins, R.B., Chang, J.S., Yeh, R.-F., Xiao, Y., Decker, P.A., Ballman, K. V, Berger, M., Buckner, J.C., Chang, S., Giannini, C., Halder, C., Kollmeyer, T.M., Kosel, M.L., LaChance, D.H., McCoy, L., O'Neill, B.P., Patoka, J., Pico, A.R., Prados, M., Quesenberry, C., Rice, T., Rynearson, A.L., Smirnov, I., Tihan, T., Wiemels, J., Yang, P., Wiencke, J.K., 2009. Variants in the CDKN2B and

RTEL1 regions are associated with high-grade glioma susceptibility. Nature Genetics 41, 905–908. doi:10.1038/ng.408

Wullschleger, S., Loewith, R., Hall, M.N., 2006. TOR Signaling in Growth and Metabolism. Cell 124, 471–484. doi:10.1016/j.cell.2006.01.016

Würth, R., Barbieri, F., Florio, T., 2014. New molecules and old drugs as emerging approaches to selectively target human glioblastoma cancer stem cells. BioMed research international 2014, 126586. doi:10.1155/2014/126586

Xu, Z., Joshi, N., Agarwal, A., Dahiya, S., Bittner, P., Smith, E., Taylor, S., Piwnica-Worms, D., Weber, J., Leonard, J.R., 2012. Knocking down nucleolin expression in gliomas inhibits tumor growth and induces cell cycle arrest. Journal of Neuro-Oncology 108, 59–67. doi:10.1007/s11060-012-0827-2

Yan, H., Parsons, D.W., Jin, G., McLendon, R., Rasheed, B.A., Yuan, W., Kos, I., Batinic-Haberle, I., Jones, S., Riggins, G.J., Friedman, H., Friedman, A., Reardon, D., Herndon, J., Kinzler, K.W., Velculescu, V.E., Vogelstein, B., Bigner, D.D., 2009. IDH1 and IDH2 mutations in gliomas. The New England journal of medicine 360, 765–73. doi:10.1056/NEJMoa0808710

Yang, Z.-Z., Li, J.-Q., Wang, Z.-Z., Dong, D.-W., Qi, X.-R., Yang, Y., Yan, Z., Wei, D., Zhong, J., Liu, L., Zhang, L., Wang, F., Wei, X., Xie, C., Lu, W., He, D., Xu, Z., Joshi, N., Agarwal, A., Dahiya, S., Bittner, P., Smith, E., Taylor, S., Piwnica-Worms, D., Weber, J., Leonard, J.R., 2012. Knocking down nucleolin expression in gliomas inhibits tumor growth and induces cell cycle arrest. Journal of Neuro-Oncology 108, 59–67. doi:10.1007/s11060-012-0827-2

Young, R.M., Jamshidi, A., Davis, G., Sherman, J.H., 2015. Current trends in the surgical management and treatment of adult glioblastoma. Annals of translational medicine 3, 121. doi:10.3978/j.issn.2305-5839.2015.05.10

Yuan, F., Leunig, M., Huang, S.K., Berk, D.A., Papahadjopoulos, D., Jain, R.K., 1994. Microvascular permeability and interstitial penetration of sterically stabilized (stealth) liposomes in a human tumor xenograft. Cancer research 54, 3352–6.

Yung, W.K., Albright, R.E., Olson, J., Fredericks, R., Fink, K., Prados, M.D., Brada, M., Spence, A., Hohl, R.J., Shapiro, W., Glantz, M., Greenberg, H., Selker, R.G., Vick, N.A., Rampling, R., Friedman, H., Phillips, P., Bruner, J., Yue, N., Osoba, D., Zaknoen, S., Levin, V.A., 2000. A phase II study of temozolomide vs. procarbazine in patients with glioblastoma multiforme at first relapse. British journal of cancer 83, 588–93. doi:10.1054/bjoc.2000.1316

Zawlik, I., Vaccarella, S., Kita, D., Mittelbronn, M., Franceschi, S., Ohgaki, H., 2009. Promoter Methylation and Polymorphisms of the<i> MGMT</i> Gene in Glioblastomas: A Population-Based Study. Neuroepidemiology 32, 21–29. doi:10.1159/000170088

Zeng, T., Cui, D., Gao, L., 2015. Glioma: an overview of current classifications, characteristics, molecular biology and target therapies. Frontiers in bioscience (Landmark edition) 20, 1104–15.

Zhang, F., Xu, C.-L., Liu, C.-M., 2015. Drug delivery strategies to enhance the permeability of the blood-brain barrier for treatment of glioma. Drug design, development and therapy 9, 2089–100. doi:10.2147/DDDT.S79592

Zhang, J., Stevens, M.F.G., Bradshaw, T.D., 2012. Temozolomide: mechanisms of action, repair and resistance. Current molecular pharmacology 5, 102–14.

Zhang, W., Couldwell, W.T., Song, H., Takano, T., Lin, J.H., Nedergaard, M., 2000. Tamoxifen-induced enhancement of calcium signaling in glioma and MCF-7 breast cancer cells. Cancer research 60, 5395–400.

Zhang, Y., Jeong Lee, H., Boado, R.J., Pardridge, W.M., 2002. Receptor-mediated delivery of an antisense gene to human brain cancer cells. The journal of gene medicine 4, 183–94.

Zhao, Y., Ren, W., Zhong, T., Zhang, S., Huang, D., Guo, Y., Yao, X., Wang, C., Zhang, W.-Q., Zhang, X., Zhang, Q., 2016. Tumor-specific pH-responsive peptide-modified pH-sensitive liposomes containing doxorubicin for enhancing glioma targeting and anti-tumor activity. Journal of controlled release : official journal of the Controlled Release Society 222, 56–66. doi:10.1016/j.jconrel.2015.12.006

Zhong, M., Lu, Z., Abbas, T., Hornia, A., Chatakondu, K., Barile, N., Kaplan, P., Foster, D.A., 2001. Novel tumor-promoting property of tamoxifen. Cell growth & differentiation : the molecular biology journal of the American Association for Cancer Research 12, 187–92.

Zhou, J., Atsina, K.-B., Himes, B.T., Strohbehn, G.W., Saltzman, W.M., 2012. Novel delivery strategies for glioblastoma. Cancer journal (Sudbury, Mass.) 18, 89–99. doi:10.1097/PPO.0b013e318244d8ae

Zhou, J., Tryggestad, E., Wen, Z., Lal, B., Zhou, T., Grossman, R., Wang, S., Yan, K., Fu, D.-X., Ford, E., Tyler, B., Blakeley, J., Laterra, J., van Zijl, P.C.M., 2011. Differentiation between glioma and radiation necrosis using molecular magnetic resonance imaging of endogenous proteins and peptides. Nature Medicine 17, 130–134. doi:10.1038/nm.2268

Zong, H., Parada, L.F., Baker, S.J., 2015. Cell of Origin for Malignant Gliomas and Its Implication in Therapeutic Development. Cold Spring Harbor Perspectives in Biology 7, 1–13. doi:10.1101/CSHPERSPECT.A020610